PRODUCTION, ISOLATION AND CHARACTERISATION OF POLYSACCHARIDES FROM PROBIOTIC BACTERIA

HAFIZ IBRAHIM AHMED

A THESIS SUBMITTED TO THE DEPARTMENT OF CHEMICAL SCIENCES, UNIVERSITY OF HUDDERSFIELD, IN PARTIAL FULFILMENT FOR THE AWARD OF DOCTOR OF PHILOSOPHY

OCTOBER 2019

Abstract

The bacterial species *L. fermentum, L. salivarius,* and *L. mucosae* have received considerable attention due to their probiotic properties and exopolysaccharide (EPS) production. This research aims to isolate and purify the EPSs synthesised by these probiotic strains with a view to assessing their biological activity.

Under optimised conditions, the bacterial strain *L. fermentum* LF2 synthesises a mixture of polysaccharides, up to 2 gL^{-1}, during growth. Analysis of the polysaccharide mixture by ^{1}H-NMR spectroscopy and SEC-MALLS analysis indicated the presence of more than one polysaccharide with two populations of molecular masses: high molecular mass (HMw) of 1.23 x 10^{6} $gmol^{-1}$ and medium molecular mass (MMw) of 8.80 x 10^{4} $gmol^{-1}$. The first population containing the HMw polysaccharide was successfully isolated from the mixture by employing preparative size exclusion chromatography using a Sephacryl S-500 HR column. Monomer, linkage analysis and NMR spectroscopy revealed that the HMw EPS is a β-D-glucan with a trisaccharide-repeating unit having a terminal glucose, a 1,3-linked glucose in the main chain and a 1,2,3-linked glucose in the main chain bearing the side chain. Interpretation of ROESY and HMBC NMR spectra confirmed the HMw polysaccharide to possess a trisaccharide-repeating unit with the sequence: →3)-β-D-Glc*p*-(1→3)-[β-D-Glc*p*-(1→2)]-β-D-Glc*p*-(1→

The combined results of the ^{1}H-NMR and SEC-MALLS analysis of the second population containing the MMw polysaccharides suggested the presence of two MMw polysaccharides accounting for more than 75 % of the EPS mixture by weight, with average weight molecular mass of 8.80 x 10^{4} $gmol^{-1}$. The structures of the two MMw polysaccharides were investigated by subjecting the MMw polysaccharide mixture to Smith degradation. The combined results of the NMR, monomer and linkage analysis of the Smith degraded products identified one of the MMw polysaccharides (MMwa) as having a repeating unit with the sequence: →3)-β-D-Glc*p*-(1→3)-β-D-Ara*f*-(1→6)-β-D-Gal*f*-(1→, whereas the other MMw polysaccharide (MMwb) was identified as having a repeating unit comprising of 1,6-linked-β-D-galactofuranosides. Analysis of the native EPS mixture revealed the structure of the repeating unit contained in MMwa to be →3)-β-D-Glc*p*-(1→3)-β-D-Gal*f*-(1→6)-[α-D-Glc*p*-(1→2)]-β-D-Gal*f*-(1→, and that of MMwb to be →6)-β-D-Gal*f*-(1→6)-[α-D-Glc*p*-(1→2)]-β-D-Gal*f*-(1→. The extent to which the 1,6-linked-β-D-galactofuranoside in MMwb is substituted at the 2-position was very dependent on fermentation conditions. Under optimized fermentation conditions, the 1,6-linked-β-D-galactofuranoside was found to greater than 80% be substituted at the 2-position.

The novel probiotic bacterial strain, *L. mucosae* VG1, isolated at University of Huddersfield, produces 62 mg/L of EPS, whose weight average molecular mass was determined to be 1.51 × 10^{4} $gmol^{-1}$. Monomer, linkage and absolute configuration analysis revealed that the EPS is a D-galactan having a non-reducing terminal galactopyranose, a 1,3-linked galactopyranose, a 1,6-linked galactopyranose, a 1,6-linked galactopyranose and a 1,3,6-linked galactopyranose. ^{1}H-NMR spectra recorded for the native EPS revealed it contains a hexasaccharide repeating unit. Further analysis by 2D-NMR spectroscopy revealed the presence of three possible structures for the *L. mucosae* VG1-EPS. The three similar structures obtained were differentiated by subjecting the *L. mucosae* VG1-EPS to Smith degradation. Monomer, linkage and NMR analysis of the Smith degraded products eliminated all but one out of the three possible structures and therefore the structure of the *L. mucosae* VG1-EPS was found to have a repeating unit containing →6)-β-D-Gal*p*-(1→6)-β-D-Gal*f*-(1→3)-[α-D-Gal*p*-(1→6)]-β-D-Gal*p*-(1→6)-β-D-Gal*f*-(1→3)-α-D-Gal*p*(1→

The growth of the strain *L. salivarius* 702343 was monitored in Huddersfield Broth Media and was found to produce 34 mgL^{-1} of a capsular polysaccharides (CPSs) composed of repeating unit of a 1,4-linked D-glucose (bacterial glycogen). The low yield 19 mgL^{-1} of EPS synthesised by the strain was determined to contain more than one polysaccharide. Unfortunately, use of mild acid hydrolysis, preparative size exclusion chromatography (Sephacryl S500 HR column) and Smith degradation, could not separate the polysaccharides present in the EPS mixture. However, monomer analysis performed on the EPS mixture revealed that the repeating units are composed of glucose and galactose residues. Linkage analysis of the EPS mixture revealed the presence of a non-reducing terminal glucose, a non-reducing terminal galactose, a 1,2-linked hexopyranose, a 1,4-linked hexopyarose, a 1,5-linked hexofuranose, a 1,6-linked hexofuranose, 1,6-linked hexopyranose and a 1,2,6-linked hexofuranose.

Acknowledgements

In the name of Allah, the most gracious, the most merciful. All praise be to Him, for the successful completion of my PhD program.

I would firstly like to thank my supervisor, Prof. Andrew Laws, whose expertise has been and will forever be invaluable in both my research and my future aspirations. Words cannot express how grateful I am, I could not have asked for more. Thank you, Andy!

I would like to acknowledge my second supervisor, Prof. Paul Humphreys, and the post-doctoral researcher, Dr. Sohaib Sadiq, for their guidance, help and wonderful assistance towards the successful completion of this thesis.

I would particularly like to single out Dr. Neil Mclay, for his excellent co-operation and all the opportunities given to me to conduct NMR experiments. Besides, I would like to thank Dr. Ana Vitlic, Dr. Richard Hughes, Dr. Simon Rout and Felix Owusu-Kwarteng for their valuable guidance, training and provision of all the tools that I required during my research.

I would also like to thank my sponsors, the University of Huddersfield and Petroleum Technology Development Fund (PTDF), for providing me with all the financial support that I needed, and Facultad de Ingenieria Quimica (UNL), Instituto de Lactologia Industrial (UNL-CONICET), Santiago del Estero, Santa Fe, Argentina, for their collaboration.

My deepest appreciation goes to my Dad, Justice Ibrahim Bature Ahmed, my Uncle, Senator Abu Ibrahim, my brothers, Abdulhamid and Muhammad, my sisters, Ruqayya, Fati, Hauwa'u and Asma'u, and my dear wife, Ummukhulthum Sadisu for all the support, prayers and advice.

And lastly, to my loving and caring mother. Mum, I want to thank you for… .....EVERYTHING. May Allah in his infinite mercy forgive you, bestow mercy upon you, pardon you, accord you a noble provision and make your grave spacious. I love you!

Table of contents

List of figures

List of Tables

Glossary

Chemical terms

Ac	Acetyl
ADP	Adenosine diphosphate
ATP	Adenosine triphosphate
B.	Bifidobacteria
CCUG	Culture Collection, University of Göteborg
CDM	Chemically Defined Medium
$CHCl_3$	Chloroform
CPS	Capsular polysaccharide
DMSO	Dimethyl Sulfoxide
DNA	Deoxyribonucleic acid
e-DNA	Extracellular-Deoxyribonucleic acid
D_2O	Deuterated water
EPS	Exopolysaccharide
f	Furanose
FDA	Food and Drug Administration
Gal	Galactose
GalNAc	*N*-acetyl-galactosamine
Gal-1-P	Galactose-1-phosphate
Gal-6-P	Galactose-6-phosphate
GIT	Gastrointestinal tract
Glc	Glucose
GlcNAc	*N*-acetyl-glucosamine
GlcNAc-1P	*N*-acetylglucosamine-1-phosphate
Glc-1-P	Glucose-1-phosphate
Glc-6-P	Glucose-6-phosphate
GRAS	Generally regarded as safe
Gro	Glycerol
GroP	Glycerol-Phosphate
GT	Glycosyltransferase
HBM	Huddersfield Broth Media

Hep	Heptose
IL	Interleukin
IUPAC	International Union of Pure and Applied Chemistry
JCM	Japanese Collection of Microorganisms
KDO	2-keto-3-deoxyoctonoic acid
LAB	Lactic acid bacteria
L.	Lactobacillus
LBP	Lipid binding protein
LPS	Lipopolysaccharide
LTA	Lipoteichoic acid
ManNAc	*N*-acetylmannosamine
Me	Methyl
MeI	Methyl iodide
MRD	Maximum recovery diluent
MRS	de Man, Rogosa and Sharpe growth media
MurNAc	*N*-acetylmuramic acid
$NaBD_4$	Sodium borodeuteride
$NaBD_4$	Sodium borohydride
$NaIO_4$	Sodium periodate
NaOH	Sodium hydroxide
NCIMB	National Collection of Industrial, Marine and Food Bacteria
NGal	Galactosamine
NGlc	Glucosamine
OMe	Methoxy
p	Pyranose
PEP	Phosphoenolpyruvate
PG	Peptidoglycan
PRRs	Pattern Recognition Receptors
PTS	Phosphoenolpyruvate transport system
RboP	Ribitol-Phosphate
RCM	Reinforced Clostridial Media
Rha	Rhamnose
SCFAs	Short-chain fatty acids
SDM	Semi-defined medium

TCA	Trichloroacetic acid
TFA	Trifluoroacetic acid
TLR	Toll-like receptor
TNF	Tumor necrosis factor
UDP	Uridine diphosphate
Und-P	Undecaprenylphosphate
UTP	Uridine triphosphate
WTA	Wall teichoic acids
YNB	Yeast nitrogen base

Experimental terms

1D	One dimensional
2D	Two-dimensional
AEC	Anion exchange chromatography
atm	Atmosphere
COSY	Correlated spectroscopy
CZE	Capillary zone electrophoresis
DEPT	Distortionless enhancement by polarization transfer
DP	Degree of polymerisation
dn/dc	Refractive index increment
GC	Gas chromatography
GC-MS	Gas chromatography – mass spectrometry
GPC/GFC	Gel permeation chromatography/ Gel filtration chromatography
HMBC	Heteronuclear multiple bond correlation
HP-AEC-PAD	High performance–anion exchange chromatography–pulsed amperometric detection
HPLC	High Pressure Liquid Chromatography
HSQC	Heteronuclear single quantum coherence
HSQC-TOCSY	Heteronuclear single quantum coherence – total correlation spectroscopy
Hz	Hertz
RI	Refractive index
LALS	Low angle laser light scattering
LC	Liquid chromatography
LC-MS	Liquid chromatography coupled to mass spectrometer
MALLS	Multi-angle laser light scattering
MS	Mass spectrometer
Mw	Weight-average molecular mass
Mn	Number-average molecular mass
NMR	Nuclear magnetic resonance
NOE	Nuclear overhauser effect/enhancement
ppm	parts per million
RI	Refractive Index
SEC	Size exclusion chromatography
TEM	Transmission Electron Microscopy

TOCSY	Total correlation spectroscopy
UV	Ultraviolet

1 Introduction

Polysaccharides secreted by *Gram positive* bacteria are of interest to many research groups because of their potential biological activity. Apart from their use as biothickners, emulsifiers and stabilisers in the dairy industry, it has been suggested that polysaccharides synthesised by probiotic bacteria may confer health benefits to consumers. However, for these studies to be effective, a highly pure polysaccharide is needed. A combination of factors determine the yield and purity level of the polysaccharide, these include: the choice of growth media, growth conditions, isolation procedures, purification techniques, as well as characterisation procedures and techniques involved (Luc De Vuyst & Degeest, 1999; Looijesteijn, Boels, Kleerebezem, & Hugenholtz, 1999; Tallon, Bressollier, & Urdaci, 2003; Welman & Maddox, 2003). Many research groups have demonstrated interest in determining and structurally characterising polysaccharides from novel bacterial strains with a view to understanding their biological activity for potential industrial applications (Looijesteijn, Van Casteren, Tuinier, Doeswijk-Voragen, & Hugenholtz, 2000; Yuksekdag, & Aslim, 2008). However, there is still a lack of understanding of the relationship between the structure and biological activity of polysaccharides synthesised by probiotic bacteria.

This research will focus on optimisation of production, isolation and characterisation of highly pure polysaccharides from novel probiotic strains and, where appropriate, determination of their biological activity.

1.1 Bacteria

Bacteria are *prokaryotic* organisms of which many are heterotrophic. Some make their own food by photosynthesis and grow autographically or may use other synthetic processes (Betsy & Keogh, 2005; Heritage, Evans, & Killington, 1996; Postgate, 2000). Bacteria are unicellular organisms that depend on their cell wall for protection, importation of nutrients, exportation of wastes, shape and rigidity amongst others. The bacterial cell wall is made up of a major component that is unique to bacteria and is responsible for its rigidity; *peptidoglycan*. Peptidoglycan is a high molecular weight polymer composed of *N*-acetylglucosamine, *N*-acetylmuramic acid and a short peptide chain (Hogg, 2013).

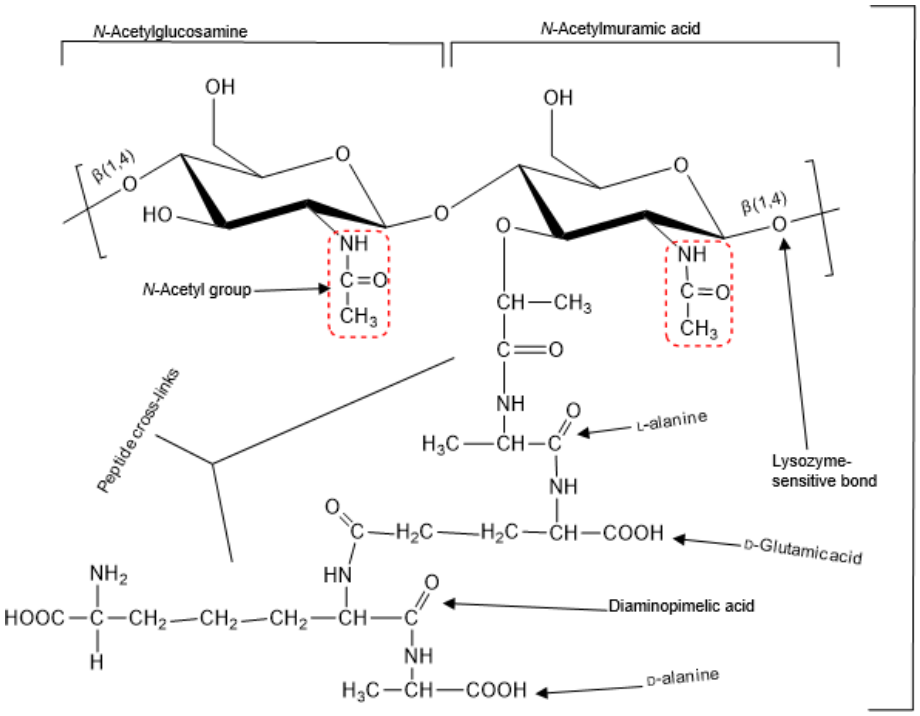

Figure 1.1: Structure of the repeating unit in peptidoglycan, adapted from (Madigan, Martinko, & Parker, 2017).

Based on the structure of their cell wall, bacteria can be categorised into two distinct structural types: *Gram-positive* and *Gram-negative.* The *Gram* stain, a rapid staining technique developed by Danish microbiologist Christian Gram, is used to differentiate between *Gram-positive* and *Gram-negative*. The *Gram* stain depends on the ability of

certain bacteria to retain a complex of a purple dye and iodine after a brief alcohol wash which is dependent on the cell wall structural composition (Hogg, 2013; Schaechter, Ingraham, & Neidhardt, 2006).

1.1.1 Cell wall of *Gram-positive* bacteria

The cell walls of *Gram-positive* bacteria are made up of several layers of peptidoglycan connected to each other via cross-linkages, which makes it thick and strong, strong enough to withstand ~ 200 atm of tugor pressure, and gives it the ability to retain the complex of a purple dye and iodine after *Gram* staining. Apart from the peptidoglycan, the *Gram-positive* bacterial cell wall is also composed of other important polymers that are involved in cell division. These polymers are called teichoic acids, and are essential for cell shape maintenance in rod-shaped bacteria (Brown, Santa Maria Jr, & Walker, 2013; Heritage *et al*., 1996; Hogg, 2013; Schaechter *et al*., 2006).

Teichoic acids were first discovered by Armstrong and co-authors in 1958 and are comprised of cell surface glycopolymers containing phosphodiester-linked polyol repeat units; which include both lipoteichoic acids (LTA) and wall teichoic acids (WTA). In the *Gram-positive* cell wall (Fig 1.11), LTA are attached directly to the membrane, their structure does not exceed beyond the peptidoglycan layer. WTA are covalently attached to peptidoglycan and extend beyond the peptidoglycan layer, which are more likely to be isolated alongside structures loosely attached to the *Gram-positive* cell wall. WTA comprise of up to 60 % of the cell wall mass of *Gram-positive* bacteria (Brown *et al*., 2013).

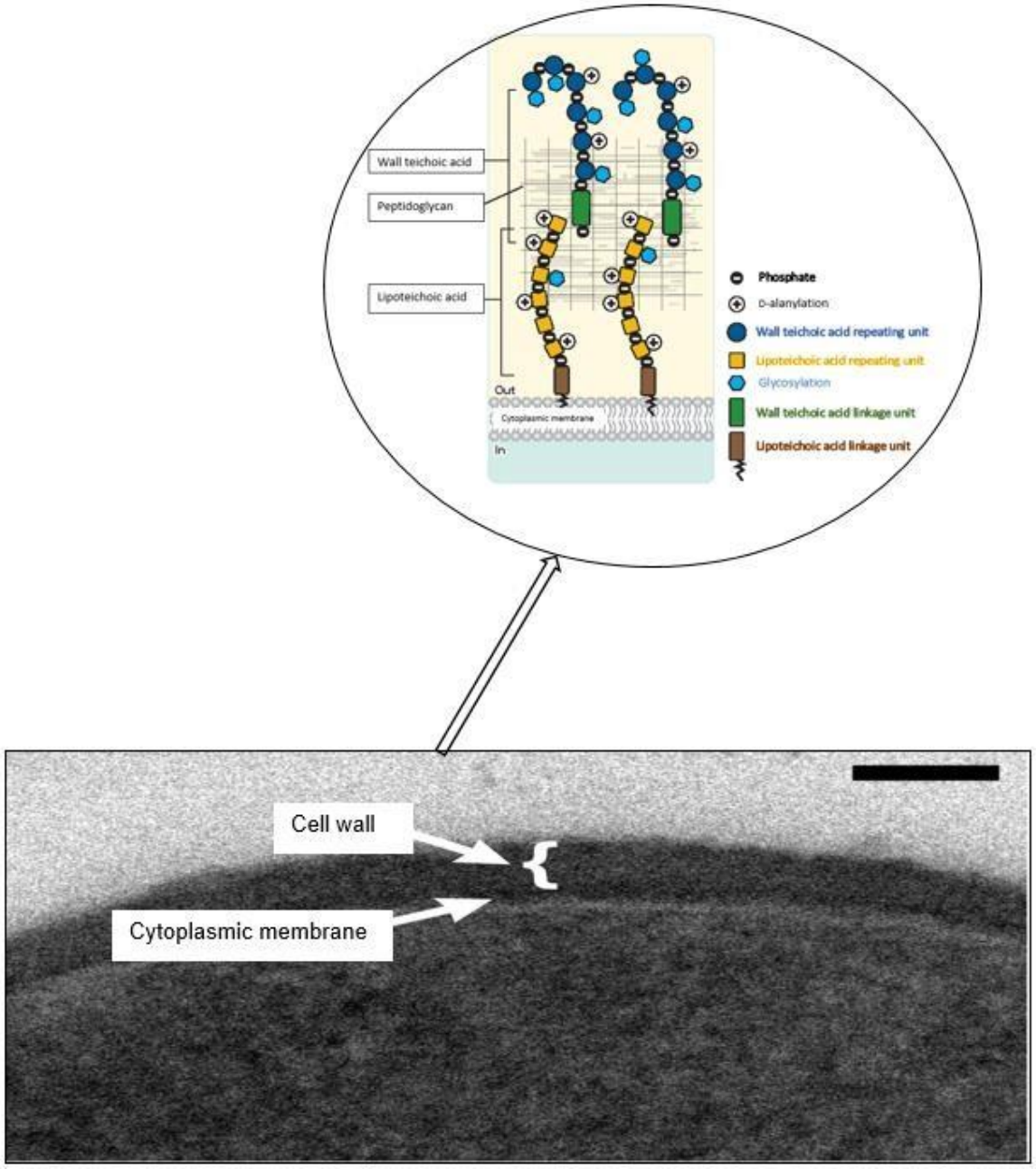

Figure 1.2: Structure of the cell wall of *Gram-positive* bacterium, adapted from (Brown *et al*., 2013; Matias & Beveridge, 2006)

1.1.1.1 Structure of wall teichoic acid

As the most abundant in mass, the structure of WTA usually contains a chain length of about 30-40 repeating units. The monomers that form these repeating units can be highly diverse, despite their diversity, all WTA share common functions. All WTA have a universal negatively charged anionic backbone comprising of *N*-acetylmannosamine

β(1→4) linked to *N*-acetylglucosamine-1-phosphate (ManNAc β(1→4) GlcNAc-1P) with one or two glycerol-phosphate (GroP) units attached to the C-4 oxygen of ManNAc. The *N*-acetylglucosamine-1-phosphate is covalently linked to the C-6 hydroxyl of *N*-acetylmuramic acid of the peptidoglycan via its anomeric phosphate, whereas the phosphodiester linked polyol repeats extends from the glycerol-phosphate end (Brown *et al*., 2013; Poxton, 2015).

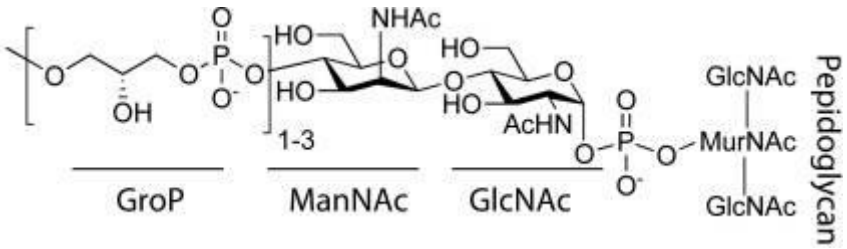

Figure 1.3: Structural backbone of all wall teichoic acids (Brown *et al*., 2013).

Based on the differences in their phosphodiester linked polyol repeats that extends from the glycerol-phosphate end, wall teichoic acids found in *Gram-positive* bacteria have been divided into four different types (I,II,III and IV) (Fig 1.4)

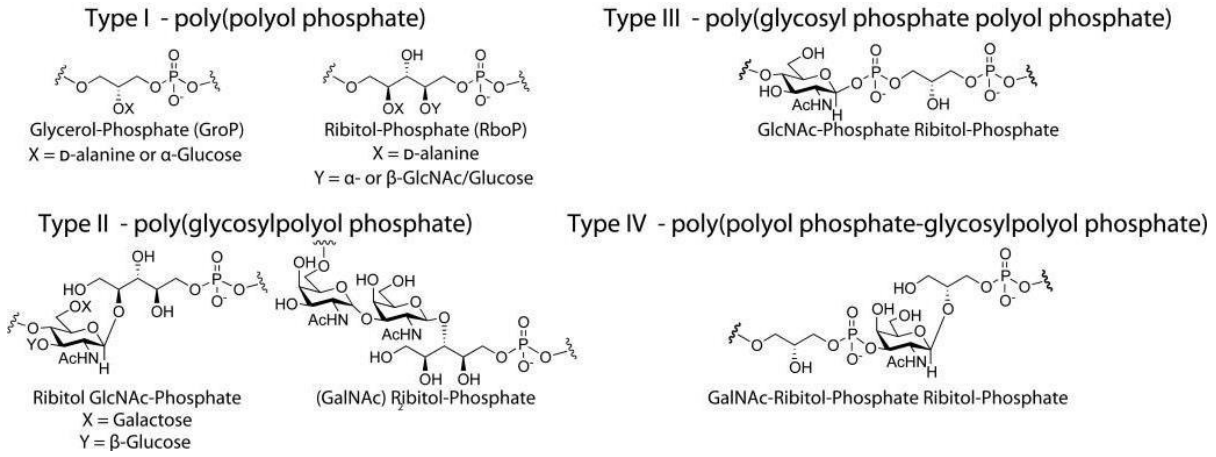

Figure 1.4: Four different types of wall teichoic acid repeat units found in Gram-positive bacteria (Brown *et al*., 2013).

1.1.2 Cell wall of *Gram-negative* bacteria

The structure of the cell wall of a *Gram-negative* bacterium is made up of a much thinner layer of peptidoglycan, making the membrane less thick, less strong (withstands ~3 atm of turgor pressure) and not able to retain the complex of a purple dye and iodine after *Gram* staining (Beveridge, 1999). However, the structure of the *Gram-negative* cell wall is more complex than that of *Gram-positive* bacteria. In the *Gram-negative* cell wall, an outer membrane that is made up of proteins, phospholipids and lipopolysaccharides (LPSs) is situated above the thin peptidoglycan layer contained in a concentrated gel-like matrix (the periplasm) and separates the periplasm from the external environment. The outer membrane is porous to certain substances, as it allows removal of waste and intake of nutrients via diffusion, but not too porous to allow passage of larger periplasmic constituents needed for cell's survival. (Beveridge, 1999; Heritage *et al*., 1996; Hogg, 2013).

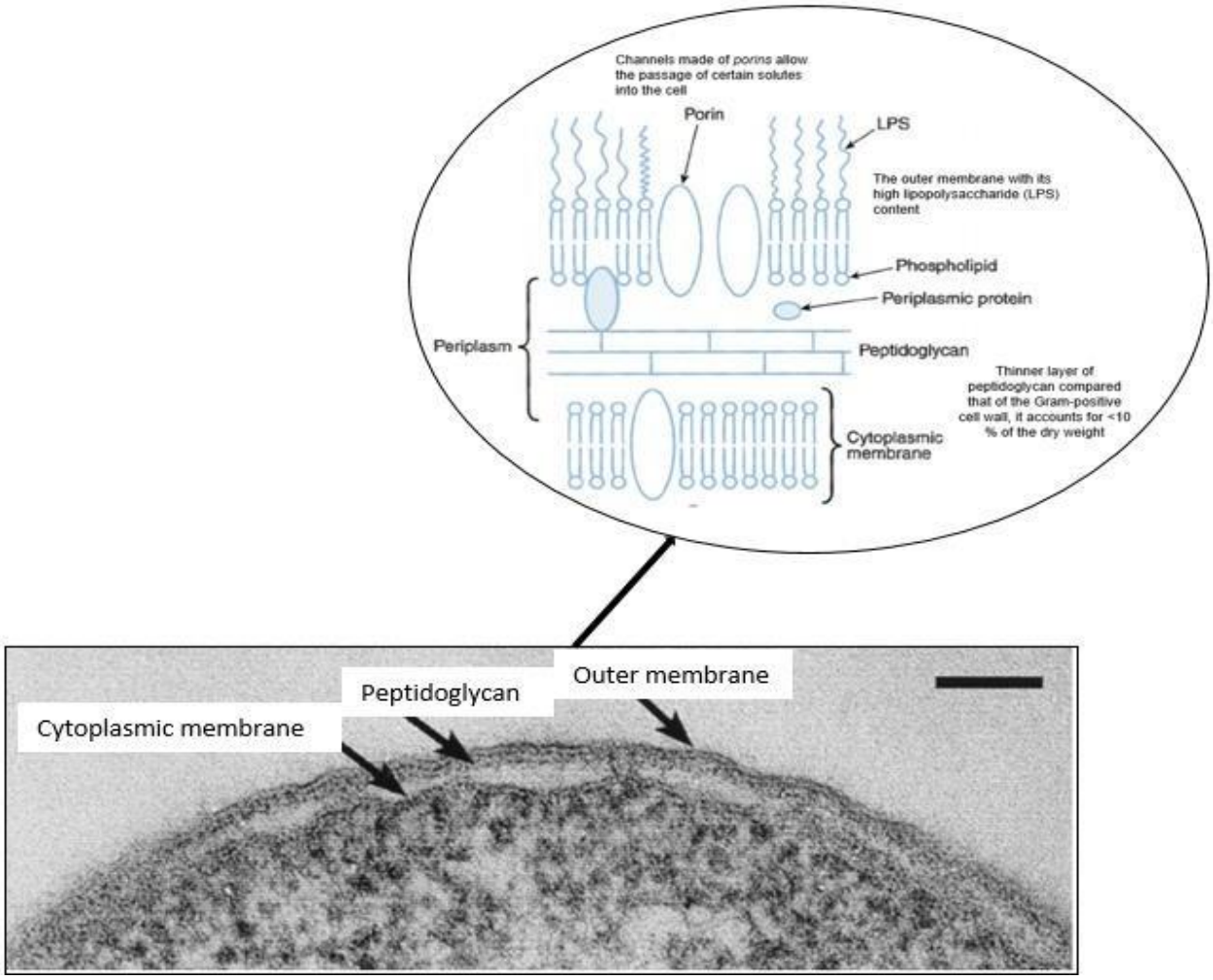

Figure 1.5: The Gram-negative cell wall, adapted from (Beveridge, 1999; Hogg, 2013)

1.1.2.1 Lipopolysaccharide

In *Gram-negative* bacteria, the major constituents of their outer membrane is LPS. LPSs are cell-associated toxins (endotoxins); they are known to stimulate immune response in low amounts and in high amounts they lead to septic shock in animals. LPSs are heat stable toxic substances (withstands boiling for up to 30 min) and have an average weight molecular mass $>1.0 \times 10^5$ $gmol^{-1}$. The structure of LPS is composed of two major components that are responsible for its biological activity: a hydrophilic lipid component (lipid A) that is associated with their toxicity and a hydrophilic polysaccharide (*O*-region) that is non-toxic but is associated with immunogenicity. The hydrophilic lipid A consists of 6 or 7 saturated fatty acids either directly attached to a phosphorylated *N*-acetyl glucosamine dimer or esterified to the 3-hydroxy fatty acids present, whereas the *O*-region consists of repeating oligosaccharide subunits that are made up of 3 to 5 sugars (varying chain lengths ranging up to 40 repeat units) attached to the core polysaccharide. The core polysaccharide (R polysaccharide) consists of a short chain of sugars attached to one of the phosphorylated *N*-acetylglucosamine, in the R polysaccharide, two unusual sugars; 2-keto-3-deoxyoctonoic acid (KDO) and heptoses are usually present with a combination of other monomeric units. KDO has been the most unique and has also been invariably present in LPS, as such, is used as a determining factor when analysing the presence of LPS (Cipolla, Gabrielli, Bini, Russo, & Shaikh, 2010; Sampath, 2018).

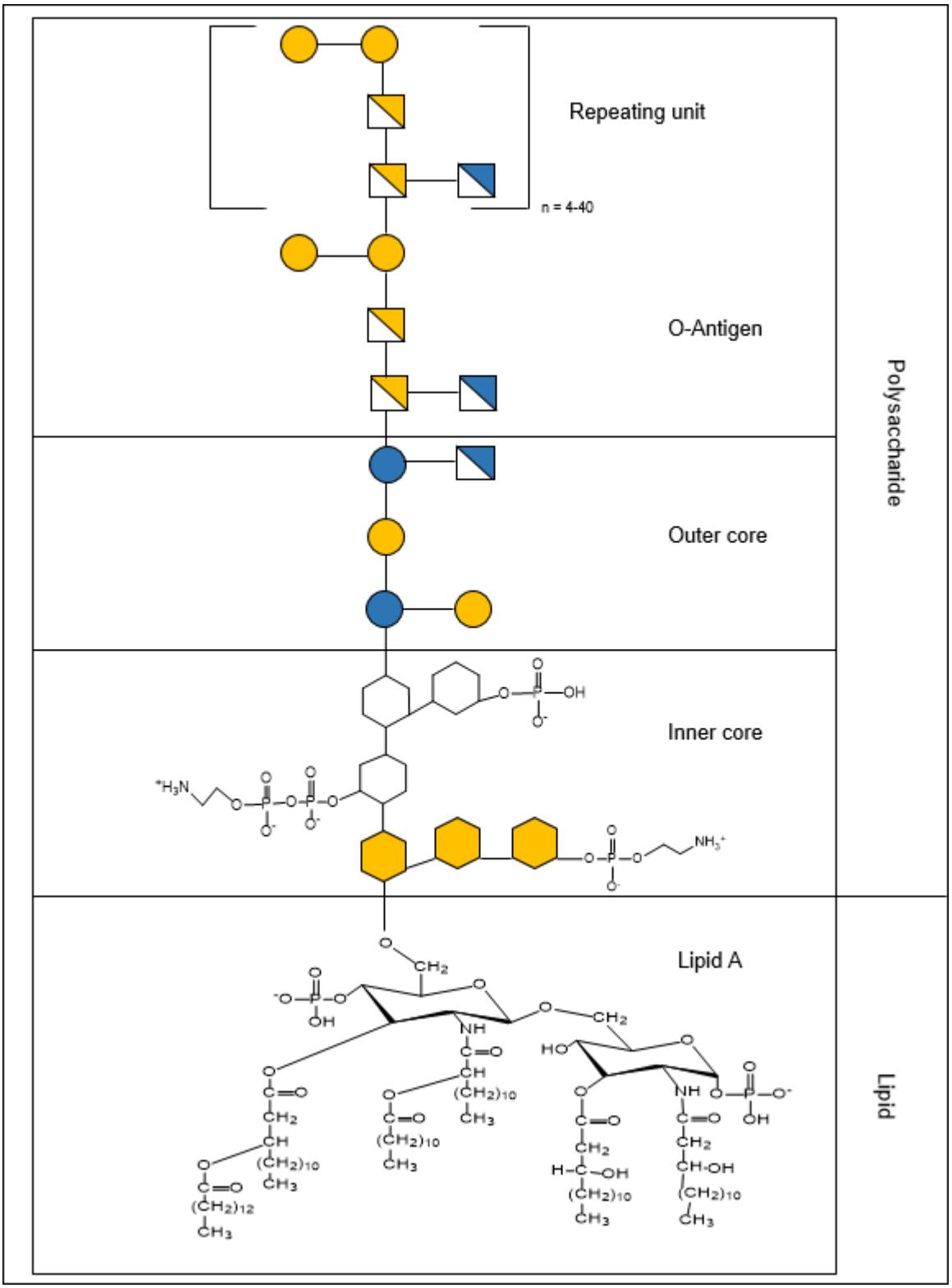

Figure 1.6: General structure for bacterial lipopolysaccharides. Adapted from (https://www.sigmaaldrich.com/technical-documents/articles/biology/glycobiology/lipopolysaccharides.html#ref.

1.1.2.1.1 Biological activity of lipopolysaccharide

The immune system is well equipped with defence mechanisms that detects and fights foreign and native substances that have the potential to cause harm, thereby protecting multicellular organisms, which is a threat to their survival. Lipid A and O-region are the major components in the structure of LPS as highlighted in (Fig 1.6) and are both important for stimulating the mammalian immune system. Of all the defence mechanisms in mammals, the inflammatory response may be the most effective in dealing with microbial infections (Todar, 2006). When a purified LPS is injected into experimental animals, it causes reactions such as fever, changes in white blood cells count, coagulation, hypotension, shock and death, depending on the dose. The mechanism by which the mammalian immune system reacts to LPS is complex, however, in humans, detection of microbes by the innate immune system is mediated by specialised proteins known as Pattern Recognition Receptors (PRRs). One of the best studied PRRs is the toll-like receptor 4 (TLR4); a mammalian receptor for bacterial LPS that is responsible for controlling bacterial infections but also the key player in abnormal inflammation that leads to fatal sepsis (Rosadini & Kagan, 2017; Sampath, 2018).

TLR 4 is a transmembrane receptor located on the cell surface, it is primarily known for binding LPS. The recognition and binding involve other collaborating proteins (see Fig. 1.7) such as LPS binding protein (LBP), cluster of differentiation 14 (CD14) and lymphocyte antigen 96 (Myeloid differentiation; MD-2). LPS binds to LBP in the blood, thereby transferring it to the co-receptor, CD14, located on the cell membrane. CD14 in turn transfers it to MD-2 which serves as a link between LPS signalling and TLR4. When complexed with CD14 and MD-2, TLR4 then triggers endothelial cells to secrete pro-inflammatory mediators such as tumour necrosis factor alpha (TNF-α); a molecule used for cell communication during the inflammatory process and a main driver that causes inflammatory bowel diseases such as Crohn's disease and ulcerative colitis as a result of dysregulated, abnormal immune response (Sanchez-Muñoz, Dominguez-Lopez, & Yamamoto-Furusho, 2008; Todar, 2006; Yamamoto *et al*., 2011).

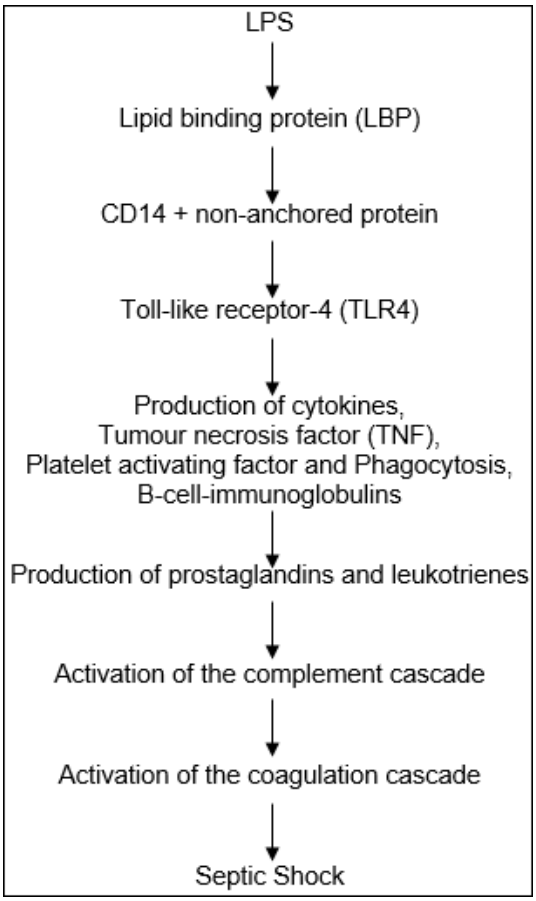

Figure 1.7: Lipopolysaccharide signalling and immune activation mechanism in humans (Sampath, 2018)

In an ideal situation, the first contact of the inflammatory system with LPS in a normal immune system should eradicate the endotoxin and quickly return the host to its stable and relatively constant internal environment (homeostasis). However, in scenarios where there is inappropriate regulation of these normal reactions, LPS can induce massive production of pro-inflammatory cytokines such as TNF-α and interleukin 6 (IL-6) alongside prostaglandins and leukotrienes (lipid mediators), thereby resulting in inflammatory tissue injury. The coagulation system and the inflammatory response system are closely tied, and synergy between the two systems leads to abnormal blood coagulation. Abnormal blood coagulation produces large clots inside the blood vessels, which leads to blockage of blood flow and finally multi-organ failure, the clinical trademark of septic shock (Stearns-Kurosawa, Osuchowski, Valentine, Kurosawa, & Remick, 2011; Yamamoto *et al*., 2011).

Apart from LPS, wall teichoic acids and other cell wall components, some bacteria produce other materials beyond the cell wall during growth, which helps the bacteria to adhere to surfaces, provide protection and helps the bacteria to survive within harsh environments.

1.1.3 Cell surface structures containing glycans

Many bacteria produce structures beyond the cell wall, which have a variety of functions. Many of these structures are composed of polysaccharides that help the bacteria in its attachment to solid surfaces, acts as receptor sites for bacteriophages (viruses that infect bacteria), prevent desiccation or nutrient loss and protect the bacteria against harsh environmental conditions (Heritage *et al*., 1996; Hidalgo-Cantabrana *et al*., 2014; Madigan, Clark, Stahl, & Martinko, 2010). These polysaccharides produced by bacteria are extracellular polymeric substances that are of high molecular weight, they are produced through metabolic pathway. Some bacteria produce these polysaccharides as a mixture with proteins, glycolipids, and in some cases, they are accompanied by extracellular DNA (e-DNA) (Di *et al*., 2017; Flemming, Neu, & Wozniak, 2007; Heritage *et al*., 1996; Mishra & Jha, 2013). Their production was first reported in the 1880s (Whitfield, 1988).

The long-chain polysaccharides that bacteria secrete into their surroundings during growth that are not permanently attached to the surface of the microbial cell are called exopolysaccharides (EPSs). Whereas, those that are permanently attached to the cell surface, thus not excreted as slime, like EPS, are termed as capsular polysaccharides (CPSs) (Luc De Vuyst & Degeest, 1999).

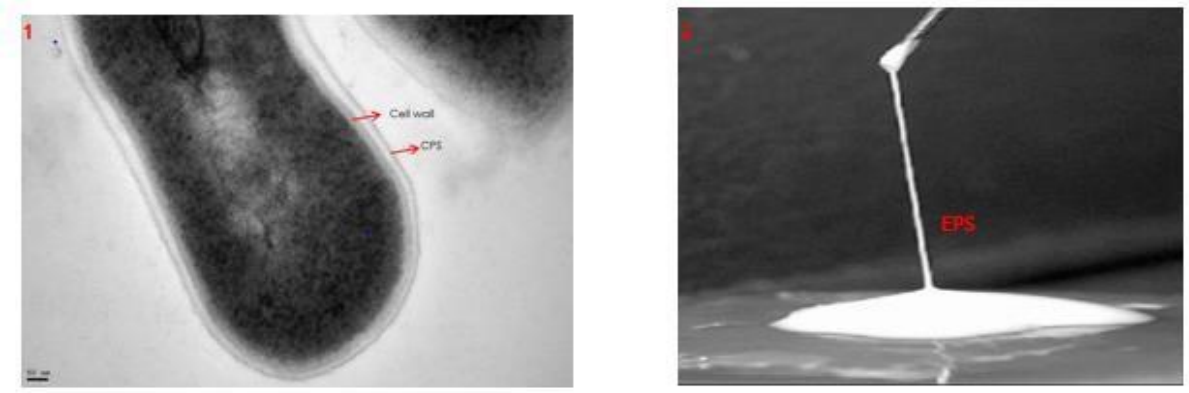

Figure 1.8: 1; Transmission Electron Microscopy (TEM) image showing the capsular polysaccharide attached to the cell surface of a bacterium and 2; a cellular mass of an EPS producing strain, showing the ropy nature of the slime EPS, adapted from (Ruas-Madiedo & De Los Reyes-Gavilán, 2005).

Amongst bacteria, lactic acid bacteria (LAB) are particularly good at converting substantial amounts of fermentable sugars towards the biosynthesis of functional polysaccharides.

1.1.4 Lactic acid bacteria (LAB)

Lactic acid bacteria (LAB) are a group of Gram-positive, anaerobic (sometimes aero tolerant anaerobes), acid tolerant, non-spore forming, coccus and rod shaped microorganisms that produces lactic acid as the major end product during fermentation of carbohydrates (Axelsson & Ahrné, 2000; Halász, 2009). Although many bacteria produce lactic acid as their primary or secondary end-product during fermentation of sugars, the term LAB has historically been reserved for the representative genera of *Lactobacillus*, *Leuconostoc*, *Pediococcus*, *Lactococcus* and *Streptococcus* (Halász, 2009). Other genera such as *Carnobacterium*, *Enterococcus*, *Oenococcus*, *Testragenococcus*, *Vagococcus* and *Weisella* are also considered as LAB. Amongst all the genera included in LAB, the genus *Lactobacillus* is by far the largest with over 70 recognised species. Amongst LAB, the most prominent EPS producers belongs to the genera *Streptococcus, Lactobacillus, Lactococcus, Leuconostoc,* and *Pediococcus* (Cescutti, 2009; Luc De Vuyst, De Vin, Vaningelgem, & Degeest, 2001; Mozzi *et al*., 2006)

LAB is a group that comprises of both pathogenic and non-pathogenic bacteria, the main emphasis of this research is on bacteria that are normally associated with positive health benefits. However, it is equally important to note that, a small number of LAB species, particularly members of genus *Streptococcus* are pathogenic to animals e.g. *Streptococcus pneumonia* that causes disease such as pneumonia and meningitis. Members of the genus *Carnobacterium* are normal inhabitants in meat but are also pathogenic to fish (Salminen & Von Wright, 2004; Todar, 2006). LAB can be found in soil, water, manure, sewage, milk and milk products, and in decaying plant materials. They are the normal inhabitants of the gastrointestinal tract (GIT) and the vagina, where they play a beneficial role (Holzapfel, Haberer, Geisen, Björkroth, & Schillinger, 2001).

1.1.4.1 The human gut microbiota

The human GIT is a home to LAB and other microorganisms i.e. they are present in the normal gut microbiota. The gut microbiota comprises of up to $10^{14}/\mathrm{mL}$ colonies of different species of bacteria, ranging from a sparsely populated stomach ($10^{2}/\mathrm{mL}$) to a densely populated colon (10^{11} to $10^{12}/\mathrm{mL}$). The human GIT is colonised by bacteria right from birth, the complexity and diversity of the colonies increases from infants to adults and reduces in old age. Many environmental factors play significant roles in the composition of the microbiota, the most significant ones being diet, method of delivery (natural vs C-section), use of antibiotics and ageing (Castro-Bravo, Wells, Margolles, & Ruas-Madiedo, 2018; Salazar, Gueimonde, de los Reyes-Gavilan, & Ruas-Madiedo, 2016).

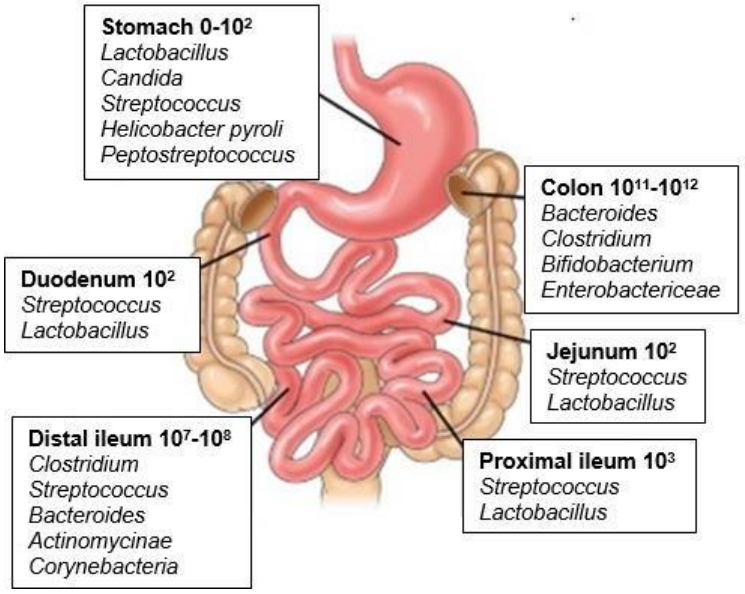

Figure 1.9: Distribution and abundance of bacteria in human GIT, adapted from (Sartor, 2008).

The beneficial association between the gut bacteria and human host was probably first suggested in 1892 by Döderlein, who suggested that bacteria found in the vagina produces lactic acid during fermentation of sugars and that this lactic acid they produce prevents or inhibit the growth of pathogenic bacteria. In 1908, Metchnikoff related the long life of white persons to be related to their high consumption of

fermented milk products, which contained substantial amounts of beneficial bacteria (Holzapfel *et al*., 2001). Originally, the beneficial bacteria were termed as probiotics, used to describe microorganisms promoting the growth of other microorganisms, but according to the present-day interpretation, the term probiotic is used to describe live microorganisms which when administered in adequate amounts confer benefit to the host.

1.1.4.2 Probiotics

The term probiotics, derived from a Greek word meaning “for life”, was first introduced by Vergin (1954), to refer to microbial substances that are favourable to the gut microflora as opposed to antibiotics. After which the term was used by Lilly & Stillwell (1965) to describe microorganisms that promotes the growth of other microorganisms. Afterwards, the term was redefined by Fuller (1989) as non-pathogenic microorganisms that exert a positive influence on host’s health or physiology when ingested. According to the present-day interpretation, probiotics are defined as live microorganisms which when administered in adequate amounts confer a health benefit on the host (WHO, 2006). Many probiotics are members of the genus *Lactobacillus* (Ahrne *et al*., 1998).

Probiotic bacteria, either singly or in combination with other probiotic strains have been added to foods, particularly dairy products to prepare a normal diet that contain biologically active ingredients, which benefits the consumer by enhancing health or reducing risk of diseases, and these prepared foods are termed as functional foods. The term functional food is used to refer to processed foods containing components that aid specific bodily functions in addition to being nutritious, it was first introduced in the mid-1980s, in Japan. Milk products are naturally highly nutritious, as such, developing functionality in them simply means modification with probiotic bacteria to generate a range of products that fit the current consumer demand for functional food. Functional foods made from milk products form the major part and are one of the most successful (Hasler, 1998; Mussatto & Mancilha, 2007; Swinbanks & O'Brien, 1993).

Many health benefits have been claimed for probiotics including prevention of pathogenic bacterial growth, reduction of inflammatory bowel disease, colorectal cancer, breast cancer, and urinary tract infection amongst others. The human body,

particularly the GIT, is a habitat to a large number of probiotic bacteria and the type of food we eat greatly influence the composition of our microbiota. Some food selectively stimulates the growth and activity of probiotic bacteria present in the GIT and are termed as prebiotics.

1.1.4.3 Prebiotics

In the 1950s, researchers described a component in human milk that improved the growth of probiotic bacteria in infants, which was later identified as oligosaccharides and glycans. In the 1980s, oligosaccharides were also found to be present in bovine milk and milk products, but at that time, their physiological role was unclear. It was later in 1995, that Glenn Gibson and Marcel Roberfroid first introduced the concept of prebiotics. They defined prebiotics as “non-digestible food ingredients that beneficially affects the host by selectively stimulating the growth and/or activity of one or a limited number of bacteria in the colon, and thus improves host health”. Since the introduction of the prebiotic concept, the definition of prebiotics has been revised multiple times, but not much has changed from the initial definition (Hutkins *et al*., 2016)

The definition of prebiotics encompasses different kinds of food ingredients, among which much emphasis is given on dietary fibre that are composed of oligosaccharides. Fructo-oligosaccharides (FOS) and galacto-oligosaccharides (GOS), are among the best documented and most commonly used prebiotics on the European and Japanese markets (Grootaert *et al*., 2007). Foods containing prebiotics are believed to stimulate the growth of probiotic bacteria in the colon, thereby improving the host’s health and also bring about reduction in the risk of infection (Gibson & Roberfroid, 1995; Roberfroid *et al*., 2010). Owing to their chemical structures, prebiotics are indigestible in the small intestine and are anaerobically fermented by bacteria in the colon. This fermentation of prebiotics give rise to the production of short chain fatty acids, (SCFAs—acetate, proprionate, butyrate) amongst other metabolites and gases, which have been reported to exert significant positive impacts on intestinal epithelial cell function, including maintenance of metabolism in liver, muscle, heart, kidneys and brain, and promotion of a low pH in the gut environment, thereby favouring the survival of probiotic bacteria with a massive reduction in the growth of pathogenic bacteria, which brings about balance in the gut (Hardy, Harris, Lyon, Beal, & Foey, 2013).

Owing to their individual health benefits, frequently one or more probiotics are combined with a prebiotic to form a “synbiotic”. The function of a synbiotic can either be a function of a probiotic and a prebiotic independently or a function of both as a synergy; whereby a prebiotic is chosen to support the activity of a probiotic. Synbiotics are used in the treatment of gastrointestinal diseases and conditions (Patel & DuPont, 2015).

Probiotic bacteria secrete long-chain polysaccharides with various chemical composition into their surroundings during growth, these polysaccharides they produce are involved in several biological processes ranging from preventing infections, enhancing the immune system as well as providing increased nutritional value to food, to selectively stimulating probiotic bacteria within the gut microbiota. In summary, several benefits have been attributed to polysaccharides produced by probiotic bacteria including pre- and probiotic properties, these polysaccharides are the focus of this research.

1.1.5 EPS biosynthesis pathways

Bacteria use four different pathways in synthesising exopolysaccharides: extracellular synthesis by use of a single glycosyltransferace (GT) enzyme (sucrase), the Wzx/Wzy-dependent pathway, the ATP-binding ABC transporter pathway (sequential) and the synthase-dependent pathway (sequential). Two or more of these pathways can be utilised by one bacterial species in producing its own exopolysaccharides. Two out of the four pathways should be considered as universal pathways for the biosynthesis of exopolysaccharides by LAB and have been well described in the literature. The two pathways are the Wzx/Wzy-dependent pathway and the extracellular synthesis by use of a single glycosyltranferance (sucrase) enzyme (Zeidan *et al*., 2017).

1.1.5.1 Extracellular synthesis pathway

EPSs can either be a chain of a single type of sugar i.e. homo-polysaccharides or a chain of several types of sugars termed as hetero-polysaccharides (Harutoshi, 2013). LAB normally utilise the extracellular synthesis pathway to synthesize homo-

polysaccharides, this pathway has been described in the genera *Weissella*, *Leuconostoc*, *Lactobacillus* and *Pediococcus* (Zeidan *et al*., 2017). Homo-polysaccharides are generally synthesised in the extracellular matrix by an extracellular glycosyltranferase (GT) and are composed of D-glucose (α or β glucans) or D-fructose (α or β fructans) (van Hijum, Kralj, Ozimek, Dijkhuizen, & van Geel-Schutten, 2006). This pathway involves a specific GT and an extracellular sugar donor, the specific GT involved can either be glucansucrase or fructansucrase depending on the homo-polysaccharide that is being synthesised. The extracellular sugar donor can also be either sucrose (for the biosynthesis of glucans) or other fructose containing oligosaccharides such as raffinose (for the biosynthesis of fructans). The type of GT encoded in the LAB genomes is responsible for the type of glycosidic bond, branching, size and molecular weight of the homo-polysaccharide (Galle & Arendt, 2014; Patten & Laws, 2015; van Hijum *et al*., 2006).

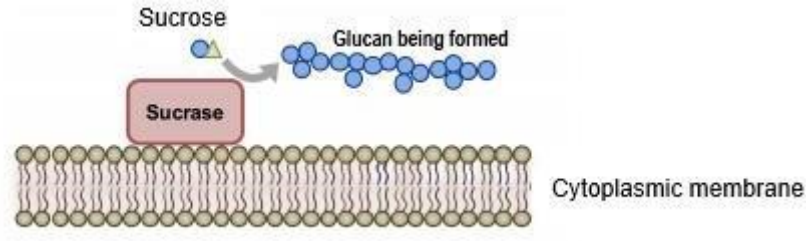

Figure 1.10: Extracellular synthesis of a glucan by the use of a single GT (glucansucrase) protein. Blue circle, glucose; green triangle, fructose, adapted from (Zeidan *et al*., 2017).

The main process involved in the synthesis of a glucan is highlighted in Fig. 1.10 via the extracellular synthesis pathway. The main process of polymerisation is assisted by glucansucrase enzyme in promoting the glucose in sucrose to be transferred to the growing polysaccharide chain, after which the polymerised homo-polysaccharide will be directly released to the extracellular environment. This pathway is a relatively simple biochemical route, the processes involved are not coupled with the central metabolic processes, as such, they are not energetically demanding for the cell and are also not prone to complex regulatory mechanisms, therefore, cellular energy expenditure is restricted to the synthesis and export of the GT. In fact, the energy that is released during the cleavage of the glycosidic bond of sucrose is used for the synthesis of the new glycosidic bonds in the polymerisation of the homo-polysaccharide (glucan).

Table 1.1: Homopolysaccharides synthesised by Lactic acid bacteria, adopted from (Ruas-Madiedo, Hugenholtz, & Zoon, 2002)

Homopolysaccharide	Predominant linkage ≥ 50 %	Species
α-Glucan		
Dextran	α-D-Glucopyranose (1→6)	*Lactobacillus reuteri* *Lactobacillus sakei* *Lactobacillus fermentum* *Lactobacillus parabuchneri* *Leunonostoc mesenteroides* *Streptococcus mutans* *Streptococcus sobrinus* *Streptococcus salivarius* *Streptococcus gordonii*
Mutan	α-D-Glucopyranose (1→3)	*Lactobacillus reuteri* *Streptococcus mutans* *Streptococcus downie* *Streptococcus sobrinus*
Alternan	α-D-Glucopyranose (1→6)/ α-D-Glucopyranose (1→3)	*Leunonostoc mesenteroides*
Reuteran	α-D-Glucopyranose (1→4)	*Lactobacillus reuteri*
Others	α-D-Glucopyranose (1→2) Unknown	*Leunonostoc mesenteroides* B-1355 *Lactococcus lactis* 1.8
β-Glucan	β-D-Glucopyranose (1→3)	*Lactobacillus diolivorans* G77 *Pediococcus damnosus* 2.6/ *Pediococcus parvulus* 2.6
	Unknown	*Oenococcus oeni* *Pediococcus parvulus* *Propionibacterium freudenreichii*
Fructan **Levan**	β-D-Fructopyranose (2→6)	*Lactobacillus reuteri* *Lactobacillus sanfranciscensis* *Streptococcus sobrinus* *Streptococcus salivarius*
Inulin-like	β-D-Fructopyranose (2→1)	*Lactobacillus reuteri* *Lactobacillus citreum* *Streptococcus mutans*
Others	Unknown	*Lactobacillus frumenti* *Lactobacillus panis* *Lactobacillus pontis* *Weisella confusa*
Polygalactan	α-D-Galactopyranose/ β-D-Galactopyranose	*Lactobacillus lactis* subsp. *lactis* H414

1.1.5.2 The Wzx/Wzy-dependent pathway

The Wxz/Wzy-dependent pathway is the pathway utilised by most LAB strains including the genera *Lactococcus, Lactobacillus and Streptococcus* to synthesise hetero-polysaccharides (Ryan, Ross, Fitzgerald, Caplice, & Stanton, 2015; Torino, Font de Valdez, & Mozzi, 2015). The biosynthesis of polysaccharides in the Wxz/Wzy-dependent pathway is a complex intracellular process that is more complicated than the extracellular synthesis of homo-polysaccharides. In Wxz/Wzy-dependent pathway, more enzymes and interacting sites are involved, as such polysaccharides that are synthesised via this pathway have larger variability in structure than homo-polysaccharides produced via the extracellular synthesis pathway. Four distinct steps are involved in this process with the help of four different groups of enzymes (Zhou, Cui, & Qu, 2018).

All the steps involved in the synthesis of hetero-polysaccharide via the Wxz/Wzy-dependent pathway takes place intracellularly, except for the final step that involves polymerisation of repeating units and release of the long chain, which happens extracellularly. (Mishra & Jha, 2013; Schmid, Sieber, & Rehm, 2015; Zeidan *et al*., 2017).

1.1.5.2.1 Monosaccharides and disaccharides transportation and phosphorylation

The first step of the Wxz/Wzy-dependent pathway involves uptake of the carbon source. Bacteria have various forms of transport systems which allow larger molecules (≥ 100 Da) through the cytoplasmic membrane, these transport systems include: active transport, diffusion, or group translocation. Depending on the environmental situation, bacteria utilise these systems alternatively. Monosaccharides and disaccharides such as glucose, galactose and lactose are imported into the cytoplasmic membrane via active transport or group translocation systems (Roseman, 1972; Todar, 2006). Sugar uptake can be achieved using either of two transport systems: (i) the phosphoenolpyruvate transport system (PTS); in this system, transportation and phosphorylation of the incoming sugar is achieved in a single step

via group translocation. A phosphate group that is released as the result of the conversion of phosphoenolpyruvate to pyruvate, catalysed by pyruvate kinase, is transferred to incoming sugar and transported into the cytoplasmic membrane or (ii) by a membrane assisted protein i.e. permease-assisted which transports the incoming sugar into the cytoplasmic membrane via active transport but cannot phosphorylate it. In this case, phosphorylation is achieved by the help of a specific intracellular enzyme (kinase), which phosphorylates the incoming sugar. The former system is adopted by many LAB as it is more energetically favoured (Boels, van Kranenburg, Hugenholtz, Kleerebezem, & De Vos, 2001; Todar, 2006; Zeidan *et al*., 2017; Zhou *et al*., 2018).

Irrespective of the mode of transport, the final result is that monosaccharides enter into the cytoplasm as either free sugars or in phosphorylated form, in any case, sugars such as glucose and galactose are transported into the cytoplasm and phosphorylated into glucose-6-phosphate (Glc-6-P) and galactose-1-phosphate (Gal-1-P) respectively whereas disaccharides e.g. lactose is either hydrolysed by β-glucosidase into glucose and galactose, which are also transported and phosphorylated into Glc-6-P and Gal-1-P respectively via active transport or transported into the cytoplasm as lactose phosphate via PTS, which is hydrolysed by phospho-β-glucosidase into glucose and Gal-6-P. Glucose in then phosphorylated by glucokinase into Glc-6-P and the Gal-6-P is either secreted into the medium, or metabolised via tagatose-6-P pathway (Boels *et al*., 2001; Salminen & Von Wright, 2004).

1.1.5.2.2 Activation of monosaccharides

The second step involves the activation of the phosphorylated sugar. Sugars formed by phosphorylation in the first step are converted into a central metabolite; glucose-1-phosphate (Glc-1-P) by the action of phosphoglucomutase. The Glc-1-P formed then reacts with uridine triphosphate (UTP) to form uridine diphosphate glucose (UDP-glucose) with the assistance of an enzyme; UDP-glucose pyrophosphorylase (Zhou *et al*., 2018).

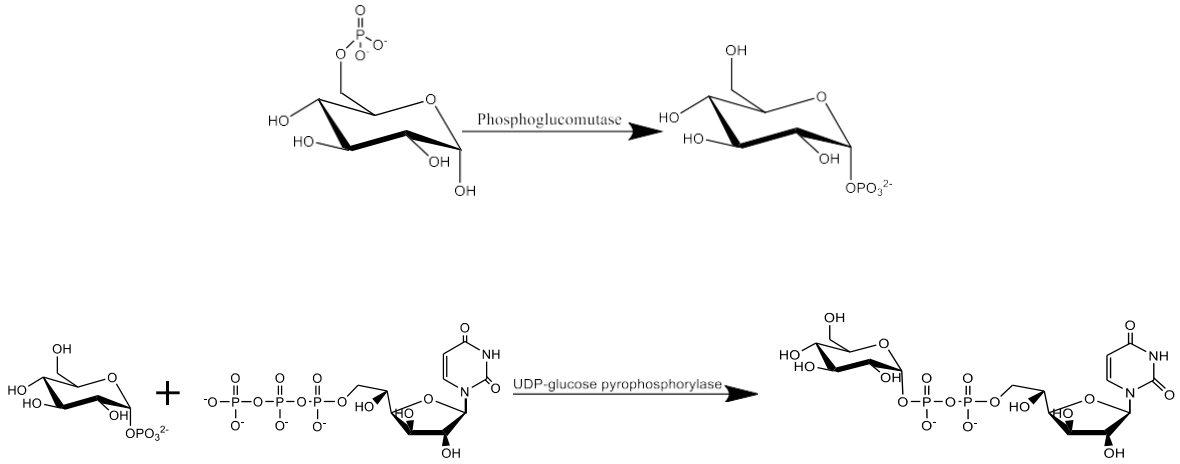

The UDP-glucose formed can be subsequently converted into a range of activated sugars including UDP-galactose or UDP-glucuronic acid by the action of UDP-galactose epimerase and UDP-glucose dehydrogenase respectively (Boels *et al*., 2001).

1.1.5.2.3 Synthesis and translocation of repeating units

The third step involves synthesis and translocation of repeating units. In this step, the first residue from the phosphorylated monosaccharide e.g. UDP-glucose formed in the second step is transferred to an undecaprenyl pyrophosphate anchor (present in the plasma membrane that allows the transfer of monomers synthesised inside the bacterial cell to translocate to the extracellular surface) the reaction is catalysed via a priming GT, after which the repeating units consisting of different sugars are then built up on the UDP-sugar attached to the undecaprenyl pyrophosphate anchor. The repeating unit is then assembled by a group of glycosyltransferases acting in succession. The assembled repeating units are then translocated from the intracellular surface to the extracellular surface with the help of a hydrophobic enzyme, flippase (Wzx) (Zhou *et al*., 2018).

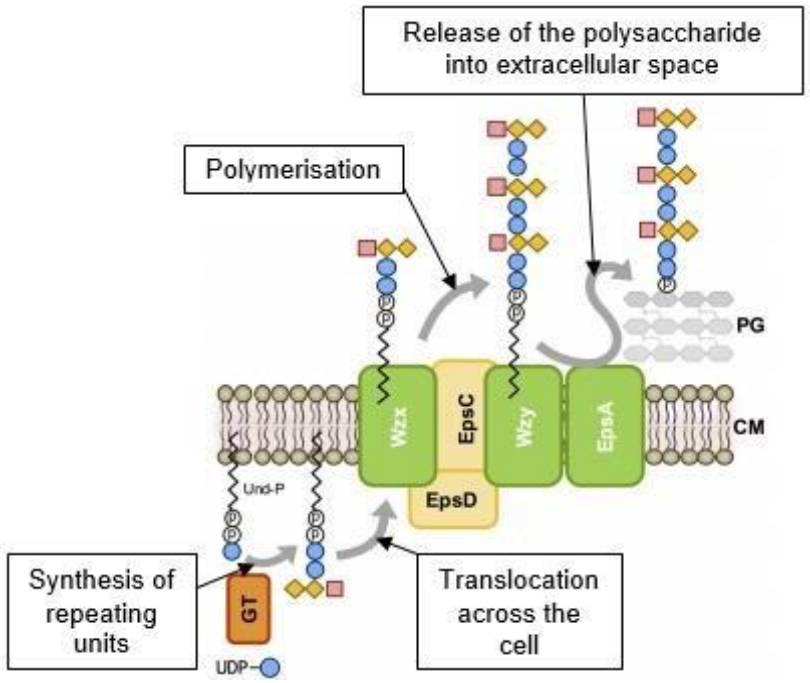

Figure 1.11: The Wxz/Wzy-dependent pathway for EPS synthesis. Blue circle, glucose; yellow diamond, galactose; pink square, rhamnose. PG, peptidoglycan; GT, glycosyltransferase; Und-P, undecaprenylphosphate; P, phosphate; EpsA, gene responsible for polysaccharide assembly ;EpsD and EPSC, genes responsible for phosphoregulatory system that controls polysaccharide assembly, adapted from Zeidan *et al*., (2017).

1.1.5.2.4 Polymerisation of repeating units and release of the long chain

The fourth and final step involves the polymerisation of repeating units and the release of the polysaccharide. The polysaccharide is formed by joining the reducing terminals of the repeating units via generation of new glycosidic bonds, catalysed by an outer membrane polymerisation protein (Wzy). In *Gram positive* bacteria, the length of the EPS chain is regulated by chain-length regulation protein (Wzz) and finally the EPS is released in the extracellular space. The EPSs produced by LAB via the Wzy-dependent pathway are found to consist of repeating units of two or more (usually 3-8) different types of sugars. Glucose, rhamnose and galactose are found to be the most frequently occurring monosaccharides, and to a lesser extent, *N*-acetylglucosamine and *N*-acetylgalactosamine are often present. Other monosaccharides (uronic acids, fucose, fructose, xylose, arabinose, and mannose) and acetylated derivatives (*N*-acetylmannosamine) have occasionally been found, some as contaminants from the growth medium, or cell lysis (L De Vuyst & De Vin, 2007; Liu, Cole, & Reeves, 1996; Margaritis, Pace, Blanch, Drewand, & Wang, 1985; Robijn *et al*., 1996; Ruas-Madiedo, Salazar, & Clar, 2009; Zeidan *et al*., 2017; Zhou *et al*., 2018).

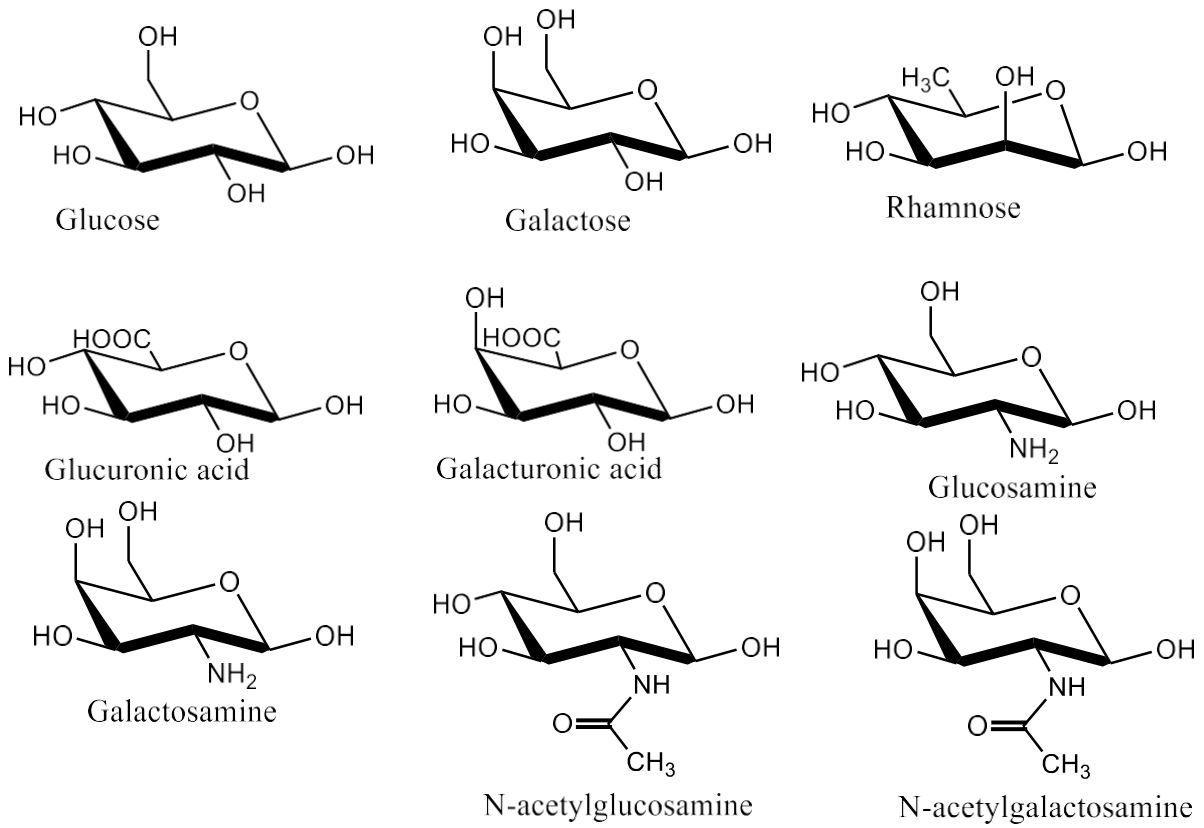

Figure 1.12: Structures of some neutral, acidic and amino sugars.

The structures of heteropolysaccharides synthesised by LAB are diverse. The structural diversity is due to the variations in type of sugar residues, linkage patterns, substitution and branching present in the repeating units and even the molecular masses of the EPSs. Table 1.2 (below) contains a limited number of structures previously published on heteropolysaccharides synthesised by LAB showing the structural diversity in LAB-EPSs.

Table 1.2: Some published structures of heteropolysaccharides synthesised by LAB.

Strain	Repeating unit	Reference
Lactobacillus delbrueckii ssp. *bulgaricus* OLL1073R-1	→2)-α-D-Glc*p*-(1→3)-β-D-Glc*p*-(1→3)-β-D-Gal*p*-(1→4)-α-D-Gal*p*-(1→	(Van Calsteren, Gagnon, Nishimura, & Makino, 2015)
Lactobacillus paracasei DG	→3)-[β-D-Gal*p*-(1→2)]-α-L-Rha*p*-(1→3)-α-L-Rha*p*-(1→3)-β-D-Gal*p*NAc-(1→2)-α-L-Rha*p*-(1→2)-α-L-Rha*p*-(1→	(Balzaretti *et al*., 2017)
Lactobacillus casei LOCK 0919 *Lactobacillus rhamnosus* GG	→3)-β-D-Gal*f*-(1→3)-β- D-Gal*p*-(1→4)-[β-D-Gal*f*-(1→6)]-α-D-Glc*p*NAc-(1→3)-α-L-Rha*p*-(1→3)-α-D-Gal*p*-(1→	(Górska *et al*., 2016; Landersjö, Yang, Huttunen, & Widmalm, 2002)
Lactobacillus rhamnosus KL37B	→4)-α-D-Gal*p*-(1→6)-α-D-Gal*p*-(1→6)-β-D-Gal*p*(1→6)-[α-D-Glc*p*-(1→2)-β-D-Glc*p*-(1→3)]-β-D-Gal*f*-(1→3)-β-D-Glc*p*-(1→6)-β-D-Gal*f*-(1→6)-β-D-Gal*f*-(1→	(Górska-Frączek *et al*., 2011)
Streptococcus thermophilus EU20	→6)-β- D-Gal*p*-(1→6)-α-DGlc*p*-(1→3)-[α-L-Rha*p*-(1→2)]-β-L-Rha*p*-(1→4)-β-D-Glc*p*-(1→6)-α-D-Gal*f*-(1→6)-β-D-Glc*p*-(1→	(V. M. Marshall *et al*., 2001)

Different types of structural forms of EPSs are produced by numerous LAB strains, these bacteria and the structures of EPSs they produce have not been identified as having any harmful effects and as such have been awarded the status generally regarded as safe (GRAS) microorganisms (Luc De Vuyst *et al*., 2001; Jolly, Vincent, Duboc, & Neeser, 2002; Yadav, Prappulla, Jha, & Poonia, 2011). As a result of LAB having GRAS status and the non-toxic nature of LAB-derived EPSs, these have made LAB and the EPS they produce a first-line choice in food industries for developing products with low levels of additives for which they can recently claim health benefits when consumed.

1.1.6 LAB and EPSs in foods

More recently, the use of foods that benefits health and reduces the risk of infection have become popular as people are becoming more and more health conscious. EPSs produced by LAB are being applied in a number of foods including bakery products.

As a result of the recent interest and high demand in gluten free foods, most especially for people with autoimmune diseases such as Celiac disease (inflammation due to the presence of gluten in the small intestine), in-situ production and physiochemical properties displayed by LAB-EPS, has shown the potential of EPS to enhance the quality of gluten free foods where the EPS helps in maintaining water binding and gas retention during fermentation while increasing the loaf volume and moisture content, thereby providing a more softer product (Lynch, Zannini, Coffey, & Arendt, 2018).

Since before the exploration of LAB EPS being used in bakeries, EPS producing LAB have been traditionally used in the dairy industry due to their ability to confer the desired rheological and textural properties. They have been used as texturizers, thickeners, viscosifers, emulsifiers and syneresis-lowering agents due to their water binding capacity, all without changing the flavour or bringing about an unwanted feel of the product (Han *et al*., 2016; Nikolic *et al*., 2012). In addition, LAB EPSs can also increase fat retention of cheese thereby increasing cheese yield and providing a much softer and creamier product (Xu *et al*., 2019)

EPSs produced by LAB have been generally considered to play a vital role in meat spoilage, however, its potential application in processed meat has been reported by Dertli *et al*., (2016), who found out that the textural properties of processed meat products e.g. sausages could be enhanced by LAB EPS, providing harder and less adhesive products. The potential beneficial application of LAB EPS in processed meat is still not widely explored (Prechtl, Wefers, Jakob, & Vogel, 2018; Xu *et al*., 2019). In ice cream, EPS produced by *Streptococcus thermophilus* strains brought about high viscosity without the need for any additives (Dertli, Mayer, Colquhoun, & Narbad, 2016; Dertli, Toker, *et al*., 2016; Xu *et al*., 2019).

1.1.6.1 Possible health effects of LAB and their EPSs and the mechanisms by which they exert health benefits

As stated earlier, LAB and the EPSs they produce have more recently received renewed interest due to the claims of their ability, once consumed, to provide health benefits. As a result, they have been administered through functional foods such as dairy products to improve host health (Bajpai *et al*., 2015). *Lactobacilli* and *bifidobacteria* are currently the most marketed probiotic bacteria worldwide, they have

been attributed to enhancing the host defence system against pathogens when consumed.

The first line of defence against pathogen attack is the GI barrier composed of a layer of epithelial cells coated in mucin, this GI barrier separates the intestinal gut microflora from the blood system and organs of the body. In an ideal situation, the presence of highly viscous mucin and a tightly packed layer of epithelial cells prevents penetration of pathogens and toxic substances through to the blood and organs of the body. *Lactobacilli* and *bifidobacteria* enhances the host defence system by promoting mucin production, thereby preventing penetration of pathogens via reduction in intestinal permeability (Ewaschuk *et al*., 2008; Johnson-Henry *et al*., 2008). These probiotic bacteria also inhibit the growth of many pathogenic bacteria via the production of SCFAs as end products of their fermentation, which create an acidic environment that is inhibitory to pathogens. The production of these SCFAs can also be enhanced by prebiotics, which are non-digestible in the stomach and are used by Lactobacilli and bifidobacteria for metabolism in the intestine (Saulnier, Spinler, Gibson, & Versalovic, 2009; Spinler *et al*., 2008). Amongst the SCFAs produced by LAB, butyrate has attracted much attention as a product of prebiotic fermentation that inhibits the growth of colonic cancer cells *in vitro* (Pool-Zobel & Sauer, 2007).

Cholesterol lowering and antidiabetic activities of LAB-EPSs have also been reported (Dilna *et al*., 2015; Sasikumar, Vaikkath, Devendra, & Nampoothiri, 2017). EPS drastically inhibited the activity of α-glucosidase activity to prevent digestion of starch and other α-glucans into glucose, thereby decreasing blood sugar levels (Ganeshpurkar *et al*., 2013; Bajpai *et al*., 2016). The concentration of blood and liver cholesterol was decreased by the addition of EPS (Maeda *et al*., 2004; Sasikumar *et al*., 2017).

1.1.6.1.1 Immunomodulatory activity of LAB-EPS

It has been reported that LAB and the EPS they produce can either stimulate the immune response by influencing the production of pro-inflammatory mediators (TNF-α, IL-6, IL-β, IL-12, nitric oxide) or supresses the immune response by influencing the release of anti-inflammatory mediators (IL-4, IL-10). The expression of PRRs such as

TLR2 and TLR4 that triggers endothelial cells to secrete pro-inflammatory mediators such as TNF-α was modulated by *L. crispatus* in the colonic mucosa of mice, which prevents damage that can occur as a result of over secretion of pro-inflammatory mediators e.g. as occurs in autoimmune diseases (Voltan *et al*., 2007; Waldan, 2014). The immunosuppressive effects on pro-inflammatory mediators of EPS producing *L. casei* was evaluated by analysing wild and mutant type strains. The mutant strains were found not be able to exert the immunosuppressive effects as opposed to the wild type strains (Yasuda, Serata and Sako, 2008). Balzaretti *et al*., (2017) also reported that, the immune response triggered by other bacterial antigens can be modulated by certain LAB EPSs. In addition, the ability of EPS to supress excessive immune response has also been demonstrated (Schiavi *et al*., 2016; Gotoh *et al*., 2017; Dinic *et al*, 2018). Work already published from this research has shown that the EPS from *L. fermentum* LF2 can induce immunomodulation (Vitlic *et al*., 2019).

1.1.6.1.2 Importance of EPS for bacterial adhesion and its beneficial effects through protection

The gut microbiome is a natural environment harbouring a diverse collection of microbes, it is therefore all about the survival of the fittest and the elimination of the unfit. This competition between individual species determines the homeostatic composition of the gut microbiota. The key to existence of individual species is space for growth, binding receptor sites and access to nutritional resources within the GIT. EPSs are involved in the protection of the EPS-producing bacteria against harsh conditions in the gut and they also assist in colonising the human GIT (Ruas-Madiedo *et al*., 2009; Gänzle & Schwab, 2009). Bile acids are one of the major components of the biological fluid in the gut and are responsible for its antimicrobial properties (Sánchez *et al*., 2008). The presence of an EPS layer has been attributed to the enhanced survival of LAB in the human GIT through bile tolerance. Various direct and indirect experiments showed that, a long term resistance of LAB towards the action of bile salts and acids was provided by the presence of EPS (Alp and Aslim, 2010; Fanning *et al.,* 2012; Sánchez *et al.,* 2014; Wickramasinghe *et al.,* 2015). In contrast, the presence of EPS in *S. thermophilus* CRL 1190, *L. casei* CRL 87, *P. parvalus* and

L. lactis did not confer advantage for bacterial cells survival at low pH in the human digestive tract (Mozzi *et al*., 2009; Fernandez de Palencia *et al*., 2009; Looijesteijn *et al*., 2001). The difference observed in the roles that the presence of EPS played might be as a result of the diverse structural composition of the EPS produced by LAB, which raises the need for better understanding of the relationship between levels of structural diversity of EPS and how this is related to bioactivity, and this research will attempt to address this issue.

Adhesion of LAB to the intestinal mucosa is an important feature for long persistence, which is needed by them for survival and for them to be able exert their health promoting effects. Although the role of EPS in bacterial adhesion and its involvement in probiotic functionality is still controversial, many studies have shown that the adhesion of LAB to the intestinal epithelium promotes exclusion of pathogens, protects the epithelial cells and enhances healing of damaged intestinal mucosa. This adhesion to the intestinal epithelial cells is considered the first step in the persistent colonisation of the host by *Lactobacillus* strains which frequently involves forming biofilms. The populations of microorganisms that are formed and attached to a surface in response to a variety of environmental signals from the host immune system that hinders or have antagonistic effect on their survival are termed as biofilms (Saadat *et al*., 2019).

LAB requires biofilm formation for their survival in the GIT and EPS from LAB plays a vital role in biofilm formation and surface adhesion of LAB to different environments (Dertli *et al*., 2015; Zannini *et al*., 2016). Studies have shown that EPS produced by *P. parvulus* increased its adhesion thereby enabling biofilm formation (Fernandez de Palencia *et al*., 2009; Garai-Ibabe *et al*., 2010; Garcia-Ruiz *et al*., 2014). The adhesion of LAB to the intestinal epithelium is also determined by its interplay with other molecules of different nature within biofilms, including proteins, lipids and carbohydrates. Some strain specific interplay of EPSs with lectins, adhesion molecules and lipoproteins assisted the binding of LAB to the GIT mucosa (Gleinser *et al.,* 2012; Guglielmetti *et al.,* 2008; Kavanaugh *et al.,* 2013; Roger *et al.,* 2010; Wang *et al.,* 2017). Zhang *et al.,* (2011) reported that; EPS producing *L. Salivarius* REN also binds to the intestinal mucus and epithelial cells with high affinity, thereby enhancing their survival in the colon. This is especially true for *L. mucosae*, a strain studied in this research.

However, biofilm formation by pathogenic bacteria causes difficulty in the treatment of chronic and re-current infections, as well as food safety problems. Kim *et al*., (2009) reported that EPS produced by probiotic bacteria inhibited the formation of biofilm by pathogenic bacteria. Li *et al*., (2014) also reported that EPS produced by *L. helveticus* MB2-1 supressed the formation of biofilm by three pathogenic bacteria. The formation of biofilm on medical devices was limited by the action of EPS produced by *L. fermentum* LB-69 (Sarikaya *et al*., 2017). The activity of antibiofilm formation was also demonstrated by EPS from *L. casei* (Merghni *et al*., 2017).

In contrast, Ruas-Madiedo *et al*., (2006) analysed the role of biofilm formation in the adhesion of probiotic bacteria to a human intestinal epithelium model and their ability to exclude pathogens. The results obtained suggested that the probiotic bacteria adhere more to the human intestinal epithelium model in the absence of EPS, without differences in the pathogens' adhesion. The adhesion of probiotic bacteria might also be hindered due to the presence of EPS, the hindrance might be from the shielding effect of EPS on specific adhesion factors present on the bacterial cell surface and/or interference of the EPS with electrostatic binding of these adhesion factors to the receptors on mucosal surface, thereby interfering with the recognition mechanisms needed for stable adhesion (Dertli *et al*., 2015; Remus *et al*., 2012; Lebeer *et al*., 2009; Denou *et al*., 2008). Dertli *et al*., (2015) knocked out the genes involved in EPS synthesis of *L. johnsonii* FI9785 and observed that; a reduction in EPS production increased its adhesion to an *in vitro* chicken gut, with a reduction in the ability of the bacteria to survive stress. The increase in adhesion came with a compromise, the reduction in EPS production might have exposed the adhesion factors on the bacterial cell surface, thereby enhancing the bacterial attachment, but has also de-shielded the bacterial cell to other inhibitory factors such as stress. In this regard, it can be said that, the uncertain effect of EPS produced by LAB might depend on their structural composition (Fernandez de Palencia *et al*., 2009).

The potential application of LAB EPSs in the food industry and the health benefits associated with them are influenced by their molecular mass, type of linkages and monosaccharides that make up the polymer. Glucans are the most naturally abundant polysaccharides found in nature. Amongst the glucans, β-Glucans are the most significant polysaccharides of fungal origins and the bacterial EPS β-Glucan has been reported to be associated with many health-promoting and prebiotic properties.

1.1.6.1.3 β-Glucans

In a more general discussion about the structures of microbial EPSs and how structure is related to biological activity, attention would be given to a particular class of homopolysaccharides, the β-Glucans. β-Glucans is the common name given to a long- or short- chain polymers of high molecular weight, produced by bacteria, algae, fungi and plants, that are of (1→3)-β-linked glucose moieties. These glucans may be linear or branched and have been shown to promote healthy cholesterol and blood sugar levels, as well as prevent autoimmune diseases by enhancing the immune system functions. The first bacterial β-(1→3)-glucan to be identified was curdlan; which is a colourless, odourless and tasteless, linear and unbrached β-(1→3)-D-glucan, first identified in *Agrobacterium* biovar 1 and is the simplest form of glucan (Barsanti, Passarelli, Evangelista, Frassanito, & Gualtieri, 2011; Mcintosh, Stone, & Stanisich, 2005).

Curdlan is indigestible in the upper alimentary canal due to the lack of digestive enzymes able to catabolise it and as such has been used as a fat substitute. It has been assessed for safety *in vitro* as well as in animal studies and is registered in the United States as a food additive. It has also been approved in Korea, Japan and Taiwan as an inert dietary fibre. Curdlan and other β-(1→3)-glucans belong to a class of compounds that are known as biological response modifiers; these class of compounds are known to enhance immune defences and/or restore normal immune functions. The effectiveness of the biological response modifiers depends on their chemical structure, molecular mass and conformation (Mcintosh, Stone, & Stanisich, 2005).

1.1.6.1.3.1 Difference in molecular mass of β-Glucans and how this is related to bioactivity

The difference in molecular mass of EPSs in general has been attributed to specific positive effects they exert on hosts. When streamlined down to β-glucans, Low molecular mass β-glucans have been shown to decrease the levels of low-density lipoproteins; these lipoproteins make up most of the body's cholesterol and in high

levels raise the risk of cardiovascular disease. The mechanism by which β-glucans lower the levels of the low-density lipoproteins is regarded to be mediated by the ability of the β-glucan to bind to bile acids (Barsanti, Passarelli, Evangelista, Frassanito, & Gualtieri, 2011). Kim and White (2009) showed that decrease in molecular mass of β-glucans from 6.87×10^5 $gmol^{-1}$ to 1.56×10^5 $gmol^{-1}$ decreases the viscosity of the solution, thereby increasing the *in vitro* bile-acid binding. And the low molecular mass β-glucan produced more short-chain fatty acids compared to high molecular mass β-glucans which was attributed to greater water solubility of the low molecular mass β-glucans. As β-glucans are non-digestible in the small intestine but are fermented by the bacteria in the colon, the fermentation results in cholesterol-lowering via the formation of the major short-chain fatty acids (acetate, propionate and butyrate). Amongst the major short-chain fatty acids, propionate was produced more which in turn reduces cholesterol by suppressing cholesterol synthesis in the liver (Kim and White, 2009).

On the other hand, in previous studies, it has been shown that high molecular mass is required to enhance multiple immunological activities. It has been reported that hydrolysed β-glucans with a degree of polymerisation that is less than 50 are not effective anti-tumour agents (Sasaki, Abiko, Sugino, & Nitta, 1978), and that high molecular weight β-glucans are the most effective in inducing the release of TNF-α, whereas debranching of β-glucans also induces the release of TNF-α (Okazaki, Adachi, Ohno, & Yadomae, 1995).

It is well known that not all LAB-EPSs have the ability to either promote health benefits or to improve the technological properties of fermented foods (Amrouche, Boutin, Prioult, & Fliss, 2006; Hassan, 2008). Therefore, the structural properties of the EPS must be the key parameter in further understanding the biological and functional properties of the EPS. This research focuses mainly on characterising EPS from LAB and how its structure is related to biological activity. Various depolymerisation and debranching methods were employed in this research in order to further understand the structure-activity relationship of the high molecular mass (HMw) β-glucan.

1.2 Strain Selection

1.2.1 *Lactobacillus fermentum* LF2

Lactic acid bacteria (LAB) are valuable for commercial food fermentations and have also been recognised as health-promoting micro-organisms. LAB have been known to synthesise exopolysaccharides (EPS). Unfortunately, dairy LAB are very low EPS producers compared to other microorganisms, their EPS yields are in the range of milligrams per litre of fermentation medium rather than grams. *Lactobacillus fermentum* LF2 (*L. fermentum* LF2), is a probiotic bacteria that was isolated as a non-starter culture in Cremoso cheese and produces a high crude EPS level (~ 2 g/L) in optimised conditions (Semi-Defined Medium (SDM) broth, pH 6.0, 30 ^{0}C, 72 h) *(Ale et al.*, 2019). The EPS has been applied as a dairy food additive to improve water holding capacity and increase hardness. The EPS from *L. fermentum* LF2 has shown the potential to be used as a functional natural ingredient, as it provides protection against *Salmonella* infection in a murine model according to previous studies (Ale et al., 2016). Despite these investigations, the structure of the EPS produced by *L. fermentum* LF2 has not been characterised. It is therefore important to elucidate the structure of the EPS in order to understand the relation between the structure and its biological activity.

Some works have previously been performed on EPS produced by *L. fermentum* strains. Leo *et al*., (2007) have reported the strain *L. fermentum* TDS030603 to produce a viscous EPS composed of a tetra-saccharide repeating unit with galactose and glucose in the molar ratio of 2:5. Gerwig *et al*., (2013) further studied the linkage pattern of the polysaccharide produced by *L. fermentum* TDS030603, they proposed the structure of the polysaccharide to consist of terminal D-Glc*p*, 3-substituted D-Glc*p*, 2,3-disubstituted D-Glc*p*, and 6-substituted D-Gal*p* in an average molar ratio of 1.3:1.0:1.1:1.1, with a trace of terminal D-Gal*p* (0.1). After mild acid hydrolysis, an oligosaccharide consisting of a branched tetrasaccharide repeating unit was isolated. The tetrasaccharide repeating unit was proposed to have the following structure:

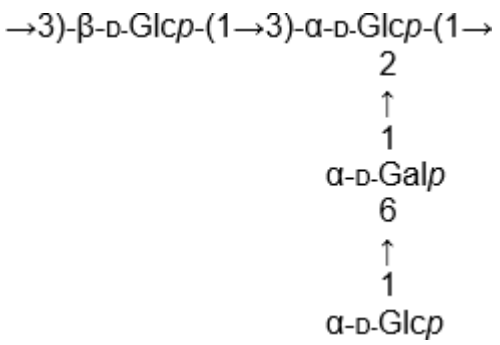

Figure 1.13: Proposed structure of the oligosaccharide isolated after mild acid hydrolysis of EPS produced by *L. fermentum* TDS030603 showing the branched tetrasaccharide repeating unit.

Zhang *et al*., (2011) studied another *L. fermentum* strain F6, isolated from a traditional dairy product in Inner Mongolia. Although the EPS structure produced by the strain has not been fully characterised, they found that the viscous EPS consists of galactose and glucose, with a molar ratio of 4:3 respectively. The structure of EPS produced by *L. fermentum* V10 and its potential in enhancing the rheological characteristic and sensory attributes of a low-fat yoghurt like product was studied by Behare *et al*., (2013). The EPS structure has also not been fully characterised, but monomer analysis performed on the isolated EPS showed that, the EPS was composed of glucose, galactose and rhamnose in a ratio of 1:1.5:13 respectively.

1.2.2 *Lactobacillus mucosae* VG1

The species *L. mucosae* was first identified by Roos *et al*., (2000), who isolated a gene encoding a cell-surface protein with mucus-binding activity from pig intestine isolate *L. reuteri* strain 1063. In order to further understand the relationship between the possession of this gene and the ability of the bacteria to adhere to pig mucus, the small intestine of a pig was screened for other bacteria that possess the gene responsible for the good adherence to mucosal material. Interestingly, a number of strains that displayed good binding ability to mucus material were isolated and further examined. Further examination revealed that these new isolates indeed share a similarity with *L. reuteri* strain 1063 in its mucus binding ability, but the new isolates are not *L. reuteri* strain 1063. The examination was based on 16S rRNA sequence

analysis which revealed that the strains are closely related to *L. reuteri* (95.1 %), *L. fermentum* (94.4 %) and *L. pontis* (94.6 %). DNA-DNA hybridization performed on the total DNA from the new strains with their closest relatives (*L. reuteri*, *L. fermentum* and *L. pontis*) clearly showed that the new isolates are different as their overall sequence homology ranged from 40.5 to 52.2 %. The name *Lactobacillus mucosae* (*L. mucosae*) was proposed for the new isolates and it was found out that three out of the twenty Lactobacillus strains previously isolated from pig small intestine by Axelsson & Lindgren (1987) belonged to the new strain.

Since its first identification in the year 2000, several other potentially probiotic *L. mucosae* strains have been isolated from other mucosal niches, such as the human cervix and the vagina, which were linked based on 16S rDNA sequence. The genome of *L. mucosae* LM1 that was isolated from faeces of a healthy piglet by Lee *et al*., (2012) was fully sequenced (Valeriano *et al*. 2017). As a result of the complete genome sequencing performed on *L. mucosae* LM1, two gene clusters responsible for EPS production were identified. However, whether LM1 produces EPS or not, is yet to be determined.

Previously, Tieking *et al*., (2005) isolated an EPS producing *L. mucosae* strain, that was said to be a fructan-forming strain, but no characterisation studies have been performed on the structure of the EPS. London *et al*., (2014) also isolated an EPS producing *L. mucosae* DPC 6426 and the EPS was found to be composed of mannose, galactose and glucose. Recent work by Ryan *et al*., (2019) demonstrated that *L. mucosae* DPC6426 has both cardio-protective and anti-inflammatory properties and that the anti-inflammatory activity of the *L. mucosae* strain DPC6426 is associated with the production of EPS.

L. mucosae are interesting potential candidates for use as probiotics as they are acid and bile tolerant, they have the capacity to adhere to the host's intestinal epithelial cells and possess the ability to inhibit pathogens, which would facilitate their survival in the GIT. The biological activity of *L. mucosae* could be attributed to their EPS production, but unfortunately, very little is known about their EPS. This thesis reports the isolation and structure determination of a novel EPS that is secreted by *L. mucosae* VG1, a novel strain isolated from a faecal sample of an individual who had adhered to a strict vegetarian diet for nine years.

1.2.3 *Lactobacillus salivarius* 702343

Lactobacillus salivarius (*L. salivarius*) are inhabitants of the gastrointestinal tract (GIT) and oral cavity of humans and hamsters. *L. salivarius* got its name from the 'salivary' properties of the oral cavity where they were first isolated from (Rogosa, Wiseman, Mitchell, Disraely, & Beaman, 1953). More recently, the species have been isolated from infant faeces and breast milk (Arroyo *et al*., 2010; Martín et al., 2006), intestinal tracts of swine (Casey *et al*., 2004) and chickens (Hilmi, Surakka, Apajalahti, & Saris, 2007). They have been reported to have complex nutritional requirements and are normally found in diverse, carbon-rich environment (Tannock, 2005). Strains of *L. salivarius* have gained attention in recent years as potential or promising probiotics and as vaccine carriers (Neville & O'Toole, 2010; Raftis, Salvetti, Torriani, Felis, & O'Toole, 2011).

The ability of *L. salivarius* to inhibit pathogens and tolerate host antimicrobial defences demonstrates the adaptation of this species to the gastrointestinal niche (Ahrne *et al*., 1998; Neville & O'Toole, 2010; Sarkar & Mandal, 2016). EPS production is believed to be one of these adaptations. Furthermore, the EPS produced by LAB remains stable in the gastrointestinal tract of their host, thus enhancing the colonisation of beneficial bacteria

Previously, researchers have demonstrated that the species *L. salivarius* is capable of producing EPS. Much of the work with these strains has been to study the genes used for EPS synthesis. Mercan *et al.,* (2015) detected genes responsible for homopolymeric EPS production in three different *L. salivarius* strains and a gene responsible for production of a heteropolymeric EPS in one *L. salivarius* strain. A single gene is required for the production of a homopolymeric type of EPS, whereas for a heteropolymeric type of EPS production, an entire EPS gene cluster is required (Horn *et al*., 2013).

This research will provide more insight regarding EPS production by *L. salivarius* by focusing on growing different strains of *L. salivarius*, isolating and attempting to characterise their EPSs.

1.3 Production and Isolation of EPS

1.3.1 Development of culture media

When isolating and characterising EPS, it is important to ensure that the media used is suitable for growth of the bacteria and the components present in the media do not interfere with the characterisation studies. Several Lactobacilli media have been developed over the years, tomato juice medium was first developed by Briggs (1953) and then modified by Cox & Briggs (1954) and has been widely used. The need for a non-selective medium, a medium that would support good growth of lactobacilli in general arose when it was discovered that some strains of lactobacilli, belonging to several species couldn't grow on the tomato juice media. Two different media were developed in response: Hirsch & Grinstead (1954) developed Reinforced Clostridial Media (RCM) for the cultivation and enumeration of *Clostridia*. The agar version of the media has also been used to enumerate *Clostridia* in food (Barnes, Despaul, & Ingram, 1963; Barnes & Ingram, 1956). Since its initial introduction, RCM has been used to grow various anaerobic and facultative bacteria when incubated anaerobically (McFaddin, 1985). At the same time, de Man, Rogosa & Sharpe (1960) developed a medium that supports the growth of all lactobacilli from different origins without the requirement of tomato juice. The bacteria were from a variety of origins including: from the oral cavity (De Man, Rogosa, & Sharpe, 1960), from dairy products (R. T. Marshall, 1992), from foods, faeces and other sources (MacFaddin & Wilkins, 1985).

Since the development of MRS and RCM media, a wide range of culture media have been developed primarily aimed at supporting the growth of lactic acid bacteria. Most of the media have been able to support excellent growth of lactic acid bacteria cultures, but the presence of yeast and beef extracts which contain high molecular weight polysaccharides interferes with EPS characterisation and quantification. This interference was first noticed in 1992 when Cerning *et al*., reported that the presence of mannans in yeast extract interferes with EPS characterisation and quantification. This is often overlooked and may account for many discrepancies in the literature. Kimmel & Roberts, (1998) showed that, the combination of yeast extract, beef extract and proteose-peptone used in preparing MRS broth (See table 1.3 for content of MRS)

to grow an EPS producing LAB accounted for 94% of the total background polysaccharide. They developed a low polysaccharide containing medium; semi-defined medium (SDM), based on MRS, by replacing the three ingredients that accounted for the 94% of the total background with yeast nitrogen base and bacto casitone. The SDM they developed supported the growth of the *Lactobacilli* just as good as MRS, but this time with minimal interference to EPS analysis.

Alhudhud, Humphreys, & Laws, (2014) developed a media (HBM), which provides a polysaccharide free broth-based culture media, that simplifies EPS isolation, purification and limits interferences with the analytical techniques used for structural analysis of EPSs. The media is prepared by either treating essential cell growth components to remove polysaccharide materials or replacing them with polysaccharide free materials, before the addition of other ingredients that do not interfere with quantification and characterisation (Alhudhud, Humphreys, & Laws, 2014). Table 1.3 (below) compares the content of HBM to that of RCM and MRS.

Table 1.3: Comparison between the ingredients involved in the formulations of RCM, MRS, SDM and HBM media.

Formulation	RCM (g/ L)	MRS (g/ L)	SDM (g/ L)	Formulation	HBM (g/ L)
Starch	1.0	-	-	**-**	-
Mixed peptones	10.0	10.0	-	**-**	-
Yeast extract	3.0	5.0	-	**Yeast nitrogen base**	3.0
Beef extract	10.0	10.0	-	**Treated beef extract**	10.0
Glucose	10.0	20.0	20.0	**Glucose**	10.0
Dipotassium phosphate	-	2.0	2.0	**-**	-
Sodium acetate	3.0	5.0	5.0	**Sodium acetate**	3.0
Triammonium citrate	-	2.0	2.0	**-**	
Magnesium sulphate	-	0.2	0.2	**-**	
Manganese sulphate	-	0.05	0.05	**-**	
Tween 80	-	1.08	1.08	**-**	
Sodium chloride	5.0	-	-	**Sodium chloride**	5.0
Yeast nitrogen base	-	-	**5**	**Treated casein acid hydrolysate**	10.0
Bacto casitone	-	-	**10**	**L-cysteine-HCl**	0.5

The next step after fermentation is isolation and purification of the EPS produced. The complexity of the method to be used for isolation and purification will depend on the composition of the culture medium used in the fermentation.

1.3.2 Method development for EPS Isolation

The Isolation of a purified EPS is required for their characterisation, it is therefore very important to make sure that the procedures involved should not alter the chemical and physical properties of the EPS. Moreover, the isolation method to be employed can also play an important role in the amount of EPS produced at the end. The simplest procedure for EPS isolation involves cell removal by centrifugation followed by dialysis of the supernatant against distilled water, after which the dialysate is freeze-dried. This technique was used by Marshall *et al*., (1995) and Kranenburg *et al*., (1997) to isolate EPS from certain LAB strains grown in a chemically defined medium (CDM). This same isolation procedure has been employed with the addition ethanol precipitation after cell removal by centrifugation in order to concentrate the EPS before dialysis (Jutta Cerning, Bouillanne, Desmazeaud, & Landon, 1986; Van Geel-Schutten et al., 1999). Less frequently, EPS concentration by precipitation has been performed using acetone instead of ethanol, or using a combination of both (Faber, Zoon, Kamerling, & Vliegenthart, 1998; Stingele, Neeser, & Mollet, 1996).

In a situation whereby a fermentation media has a high protein content such as when skim milk is used, it has become necessary to add more purification steps in order to reduce the protein content and other components in the final EPS precipitation. For protein removal, three approaches are commonly used before dialysis and freeze-drying: precipitation of proteins with trichloroacetic acid (TCA) (Garcia-Garibay & Marshall, 1991), protein digestion using proteinase (Jutta Cerning et al., 1986) or a combination of both (Gancel & Novel, 1994). The most common procedure employed in isolation from complex media involves precipitation of proteins with TCA which are then removed by centrifugation, followed by ethanol precipitation of the supernatant for EPS concentration and then dialysis and freeze-drying (Ruas-Madiedo & De Los Reyes-Gavilán, 2005).

This research will employ the use of a less complex growth media that has been shown to be free from polysaccharide components and which has minimal amounts of high molecular weight proteins (HBM) for fermentations.

1.3.3 EPS Purification by size exclusion chromatography and anion exchange chromatography

Once the crude EPS has been isolated, it is frequently necessary to purify the material. This is routinely performed using an initial step involving exhaustive dialysis against distilled water in order to remove carryover of small sugars used in the carbon feed and to remove any remaining salts and small proteins as described earlier, which is followed by freeze-drying. Further purification processes are also available when highly pure samples are required. Techniques such as microfiltration and preparative size-exclusion chromatography (SEC) can be employed (Gruter, Leeflang, Kuiper, Kamerling, & Vliegenthart, 1992). Filtration via synthetic membranes allows separation of high molecular weight EPS from low molecular weight components present in fermentation media. Differences between filtration procedures are mainly based on the molecular weight cut off of the membrane through their pore sizes (Ruas-Madiedo & De Los Reyes-Gavilán, 2005).

The dialysed EPS samples can be fractionated using preparative SEC with direct detection using a refractive index detector or by anion exchange chromatography (AEC) if charged EPSs are expected. Frequently, the fractions eluting from SEC and AEC-columns are then tested for the presence of simple sugars and polysaccharides using colorimetric methods. The phenol-sulphuric acid (Dubois) method is widely employed in the determination of simple sugars. The phenol-sulphuric acid method was first reported by Dubois *et al.,* (1956), the analysis depends on the formation of furfural derivatives that yields a stable orange –yellow colour when reducing sugars are treated with phenol and concentrated sulphuric acid under the condition of heat, this gives a maximum absorbance at 490 nm and can be measured using UV-Vis spectrophotometry.

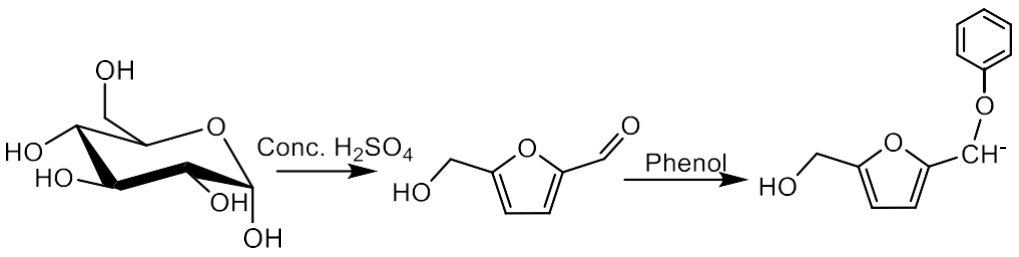

Figure 1.14: Dehydration of carbohydrates without a chromophore to a furan derivative with a strong absorbing UV chromophore at 490 nm, using glucose as an example (Zhou & Zhang, 2016).

Since the introduction of the Dubois method, several modifications have been reported in an attempt to optimise the procedure, from varying the phenol concentrations (Buysse & Merckx, 1993), the incubation time (Cuesta, Suarez, Bessio, Ferreira, & Massaldi, 2003), to sample requirement. In its original form, the method required 50-450 nmol of sugars or equivalent for analysis, which does not favour precious samples, Lee, McKelvy and Lang (1969) developed a method that required 10-80 nmol of sugars and more recently Masuko *et al.,* (2005) reported a method requiring only 1-50 nmol with excellent sensitivity.

1.3.4 Molecular mass determination of exopolysaccharides

Molecular characterisation of EPSs requires knowledge of molecular mass, and this knowledge of molecular mass determination has been recognised as one of the contributing factors in EPS functionality (Luc De Vuyst & Degeest, 1999). The ability of EPSs synthesised by probiotic bacteria to stimulate immune responses has been attributed to the molecular mass of EPSs (Hidalgo-Cantabrana *et al*., 2012) . It is therefore essential to accurately determine the molecular mass of an EPS in order to further understand the relation between molecular size and biological activity. Different methodologies have been previously used in molecular mass determination; these involve determination of molecular mass of various polysaccharide molecules using Gel Permeation Chromatography (GPC) or Gel Filtration Chromatography (GFC) based on comparison of their hydrodynamic volume with controlled standards of a particular molecular mass. The idea that gels might be used for separation based on molecular size was first proposed by Synge & Tiselius (1950) and was confirmed experimentally by Mould & Synge (1954). Starch particles were then used as filtration gels and later replaced by cross-linked synthetic gels such as dextran gels in order to address the limitations of starch's instability, poorly defined composition and the high resistance to flow of the starch columns (Calmon & Kressman, 1957). The GPC method required a large quantity of sample and relied on comparison with controlled standards of a particular molecular mass. This limitation was addressed in 1974 by Ouano and Kaye who used low angle laser light scattering (LALS) to measure polymer molecular mass distributions without conventional SEC column calibration methods (SEC-LALS). SEC-LALS was then regarded as the most accurate method in molecular weight determination, as it measures molecular weight directly after initial

calibration. The relation between the intensity of light scattering and the mass of a molecule is linked by the Rayleigh equation:

$$\frac{KC}{R_0} = \frac{1}{M_w} + 2A_2C$$

Where R_0 is the Rayleigh Ratio at zero scattering angle,

M_w is the weight-average molecular mass,

C is the concentration of the solution,

A_2 is the 2nd virial coefficient,

K is an optical constant that includes the refractive index increment of the solution (dn/dc)

For solutions of low concentration, the concentration-dependent term is usually ignored, thereby rearranging the equation into a simpler and direct form:

$$R_0 = KCM_W$$

This equation relates scattered light intensity directly to molecular weights, and in SEC-LALS, the scattered light is measured at a single angle, i.e. a low angle close to zero. The use of SEC-LALS attached in a series with a concentration detector; the refractive index and/or UV-Vis detector, whose peak area is proportional to the analyte concentration addressed a number of limitations that came with SEC-LALS (Jordan, 1980). Polysaccharides have a range of molecular weights; as such, they are polydispersed molecules. Polydispersity $= \frac{\mathrm{Mw}}{\mathrm{Mn}}$, i.e. it is a ratio of weight average molecular weight (M_w) to the number-average molecular mass (M_n). In the determination of molecular mass of EPSs, the polydispersity value is very important as it describes the size homogeneity within a polysaccharide population. An increase in polydispersity value is synonymous to a larger difference between the sizes of the largest and smallest molecules. However, the problem encountered when analysing EPS on SEC is that, EPS samples have large molecular masses ranging from 2.5×10^4 to $9.0 \times 10^6\ gmol^{-1}$, as such they can be too large to enter the pores of a SEC column, thereby having access to only the void volume and are eluted closer to the exclusion limits of the available stationary phases as a single peak at the beginning of the chromatography (J Cerning, Bouillanne, Landon, & Desmazeaud, 1990; Nichols

et al., 2005; Ruas-Madiedo & De Los Reyes-Gavilán, 2005). The advent of High-Performance Size Exclusion Chromatography (HPSEC) addressed this issue, a combination of certain HPLC columns was of particular significance in developing the application of SEC-LALLS for the determination of molecular masses, the averages and the distributions of masses in polymers. The columns which are connected in series have different fractionation range, some have large pore sizes which the high molecular mass polysaccharides are able to enter and are successfully separated, and therefore not eluted as a single peak at the beginning of the chromatography.

The advent of light scattering photometers that could measure the angular variations of the scattered light intensity at 15 different scattering angles simultaneously prompted Wyatt *et al.,* (1993) to introduce a novel approach to use differential (multiangle) light scattering measurements in combination with HPSEC (HP-SEC-MALLS) for molecular weight determination of macromolecules. MALLS measures the scattered light at two or more angles, and the data is extrapolated back to the zero angle for more accurate molecular mass determination. MALLS permitted other important deductions from the light scattering theory, these includes: determination of molecular conformation, structure, branching ratios, mean square radius and its various averages.

The numerical value of dn/dc is a key requirement for the determination of molecular masses of EPS. The concentration of EPS can be determined by differential refractive index detector through the equation that relates the rate of change of the refractive index with the concentration of a solution $(\frac{dn}{dc})$, the refractive index of the pure solvent (n_s) and the refractive index of the solution (n_r).

$$\Delta c = \frac{(n_s - n_r)}{(dn/dc)}$$

Since the measurement of EPS concentration is critically dependent on the measurement of dn/dc value, it is important to note that the dn/dc value is affected by temperature and laser wavelength. For polysaccharides in an aqueous buffer at room temperature (25 °C), the dn/dc value ranges from 0.14 to 0.18. The value can be adopted from literature references and from prior datasets taken under similar conditions since it's intuitively related to the density/specific volume of molecules. A dn/dc value of 0.147 mL/g that was published for a pullulan standard, a neutral

homopolysaccharide of known molecular mass (1.10 x 10^5 Da), will be adopted from and used in all the average molecular mass measurements in this research (Bahary, Hogan, Jilani, & Aronson, 1995).

1.4 Characterisation of Exopolysaccharides

EPS characterisation is essential in understanding the relationship between the EPSs structure and its biological activity. In order to fully characterise an EPS, further information is needed apart from its molecular mass, this includes: information on the different sugar residues that form the repeating unit of the EPS, the pattern and order in which the sugar residues occur in the repeating unit i.e. the way in which the monosaccharide units are bonded to one another through glycosidic bonds to form the repeating unit structure, the anomeric configuration (i.e. α or β) of the glycosidic linkages, the absolute configuration of the sugar residues that form the repeating unit (i.e. D- or L- configuration) and their ring size (i.e. furanose or pyranose) .

1.4.1 Application of monomer analysis for the characterisation of polysaccharides

Monomer analysis provides information on which sugar residues that are present in the repeating unit of the EPS synthesised by the probiotic bacteria. Monomer analysis has historically been performed using GC-MS by employing a two-stage process that involves acid hydrolysis and derivatisation of the hydrolysed EPS into volatile compounds detectable by GC-MS. The derivatisation involves reduction of monomers obtained after hydrolysis into sugar alditols, followed by acetylation (i.e. conversion of the sugar alditols into alditol acetates). This two-stage process was developed by Albersheim *et al.,* (1967) and Blake *et al.,* (1970) and is required because of the non-volatile nature of carbohydrates which require derivatisation for detection by GC-MS. The process is time-consuming, and a simpler and less time-consuming procedure was introduced by Knapp (1979). In 1983, Rocklin & Pohl developed an alternative one-stage process, the process involves only acid hydrolysis, and the hydrolysed EPS sample is directly analysed for its monosaccharide composition by high-pressure

anion exchange chromatography in combination with pulsed amperometric detection (HPAEC-PAD) using sodium hydroxide as eluent. The technique works on the principle that carbohydrates are weak acids having high pKa values ranging from 12-14. At high pH, carbohydrates are transformed into oxyanions which can readily be separated using highly effective anion-exchange columns (Corradini, Cavazza, & Bignardi, 2012). Using these anion-exchange columns, monosaccharides are readily separated under alkaline conditions where they are eluted in order of their decreasing pKa values (Corradini, Lantano, & Cavazza, 2013).

In monomer analysis using either GC-MS or HPAEC, the cleavage of the glycosidic linkages of the polysaccharides is firstly achieved by hydrolysis using an acid catalyst, forming sugar monomers. The most commonly used acid catalysts are: hydrochloric acid (HCl), sulphuric acid (H_2SO_4) and trifluoroacetic acid (TFA). TFA is the simplest to use as it has an advantage of being easily removed because of its volatility (Neeser & Schweizer, 1984). This research will employ TFA in both GC-MS and HPAEC-PAD methods of monomer analysis. Reduction using $NaBD_4$ will also be employed as it distinguishes the primary alcohols on the first and last carbon atoms of alditols derived from hexoses.

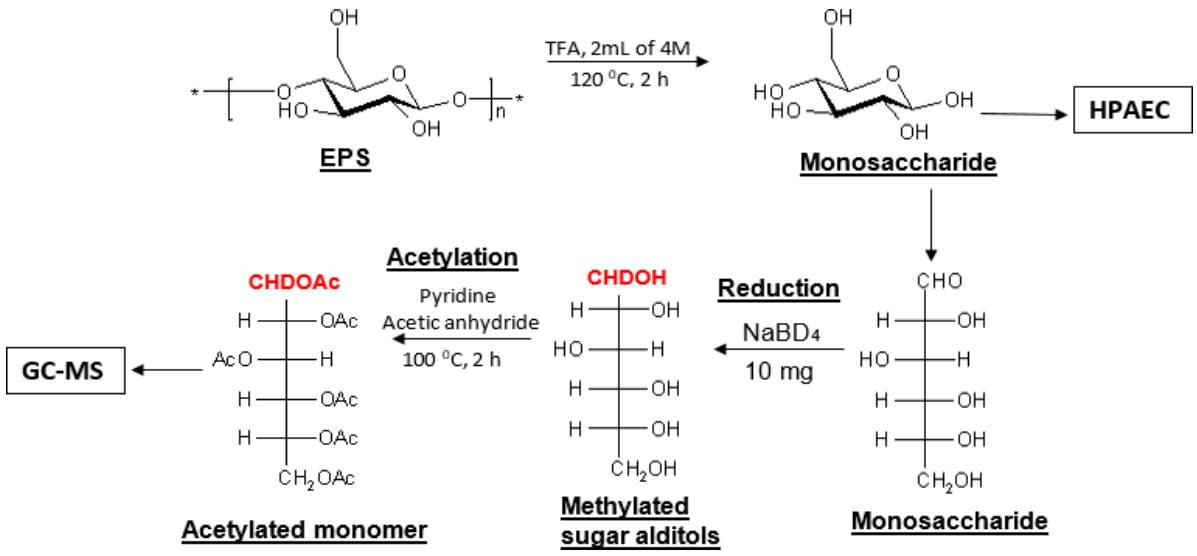

Scheme 1: An outline of the hydrolysis, reduction and acetylation reactions on an EPS to give monomers (starch as an example).

1.4.2 Linkage Analysis

Linkage analysis is used to determine how the different sugar residues are bonded to one another in the repeating unit that are present. The method is very similar to the basic procedure applied in monomer analysis using GC-MS, however, in linkage analysis, there is an addition of a methylation step prior to hydrolysing the polysaccharide (i.e. methylation, hydrolysis, reduction and acetylation). The primary aim of methylation is to achieve etherification of all the free –OH groups in the polysaccharide, so that after the last step of acetylation, the carbon atoms carrying the –OMe groups are known not be involved in any linkage. The methylation step was first performed by repeated treatment with silver oxide in boiling methyl iodide in 1903 by Purdie *et al.,* and since then, the methylation step has undergone several optimisations. In 1913, Denham and woodhouse further developed the methylation step by employing a mixture of dimethyl sulphate and NaOH, which was also used by Haworth in 1915. Since then, both methods developed by Purdie *et al.,* (1903), Denham & Woodhouse, (1913) and Haworth, (1915) have been routinely used for the methylation step in linkage analysis with little modifications until 1964, when Hakamori developed a new method which involved addition of sodium methylsuphinyl carbanion solution (dimsyl ion) and methyl iodide to carbohydrates dissolved in dimethylsulphoxide (DMSO), which provided a better quality of methylation compared to the ‘Purdie’ and ‘Howarth’ methods.

The ‘Hakamori’ method had some setbacks because of the hazardous nature of the dimsyl ion and the under methylation of carbohydrates among others, which called for alternative methods to be developed. Ciucanu & Kerek, (1984) developed a method that involved the dissolution of carbohydrates in dimethylsulphoxide and treatment with powdered sodium hydroxide and methyl iodide, which was found to produce high yields of fully methylated carbohydrates (Scheme 1.1).

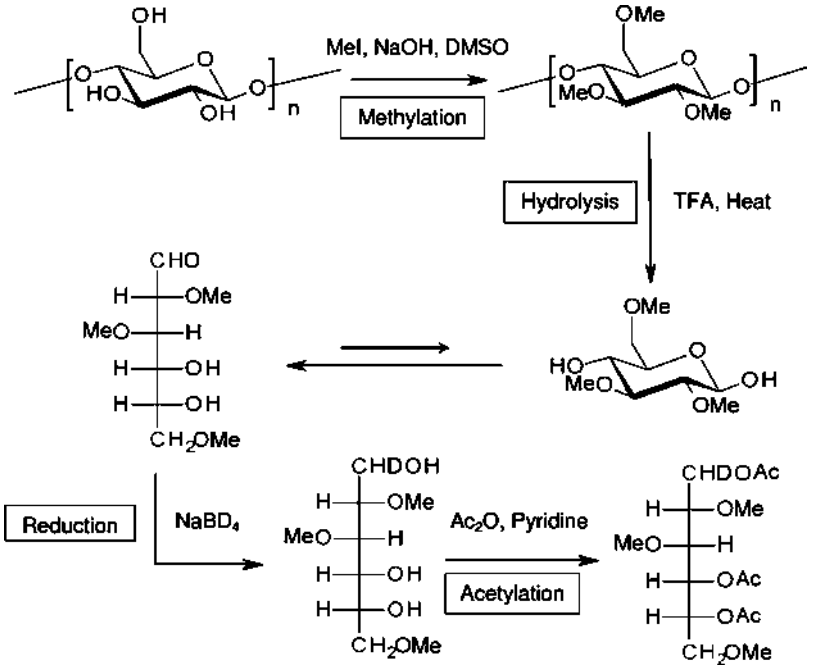

Scheme 1.1: An outline of methylation, hydrolysis, reduction and acetylation reactions on an EPS to give monomers (starch as an example).

In this work reported here, the Ciucanu & Kerek methylation procedure will be adopted.

1.4.3 Absolute Configuration Analysis

In order to determine the absolute configuration of the sugar residues that make up the repeating unit present in the polysaccharide synthesised by the probiotic bacteria, the polysaccharide has to be hydrolysed, and each residue can be determined for its absolute configuration. The location or rather position of the –OH group around the chiral carbon most distant from carbon 1 in monosaccharides determines whether the monosaccharide is assigned as D- or L- configuration. If the –OH group on the chiral carbon most distant from carbon 1 is on the right, it is designated as D-, and if the hydroxyl group on the chiral carbon farthest from carbon 1 is on the left, it is designated as L- (Biermann & McGinnis, 1988).

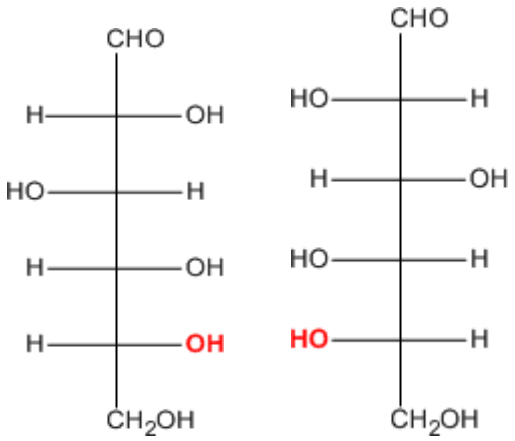

D-glucose L-glucose

Figure 1.15: Fischer projection of D- and L-glucose

Many monosaccharides, pentoses and hexoses, occur naturally in both D and L configurations; these include glucose, galactose, arabinose and rhamnose. None of the three methods discussed so far (Monomer analysis by GC-MS, HPAEC and Linkage analysis by GC-MS) is capable of determining the absolute configuration of monosaccharides. For instance, in linkage analysis, where acetylated methyl glycosides are formed, methyl glycosides being enantiomers have identical boiling points, and therefore conventional GC-MS used in separating monosaccharides fail to separate them, and as such, they are eluted as a single peak. In order to obtain the absolute configuration of monosaccharides using GC-MS, samples are converted into diastereomers, which have different boiling points and as such are separable by GC. In order to obtain the absolute configuration of a monomer or to resolve the enantiomeric mixture of a particular monomer, the monomers are converted to diastero-isomers using a chiral secondary alcohol such as *(S)*-(+)-2-butanol or *(S)*-(+)-2-octanol. This secondary alcohol is linked via the chiral centre to the glycosidic oxygen of the monosaccharide forming diastereomers which are readily separated by GC-MS (Gerwig, Kamerling, & Vliegenthart, 1978).

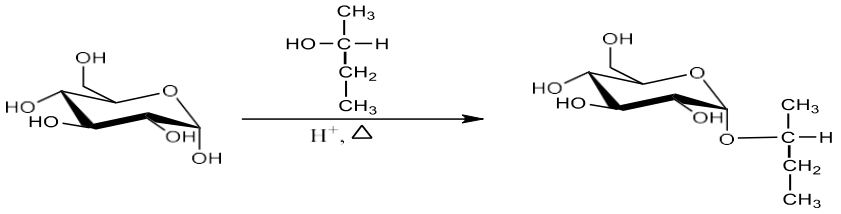

Figure 1.16: Scheme of absolute sugar analysis of glucose using a chiral secondary alcohol separated by GC-MS adapted from (https://glycopedia.eu/e-chapters/gas-chromatography-mass/Acetylated-Octyl-Glycosides).

1.4.4 Use of 1D and 2D-Nuclear Magnetic Resonance (NMR) to characterise EPS

NMR is a powerful analytical tool for characterising bacterial EPSs; it is a non-destructive technique that can be applied to solid and/or liquid samples, and provide information about the monosaccharide composition, the linkage patterns as well as the conformation of an EPS (Freitas *et al*., 2009). Doco *et al*., (1990) were one of the first to employ NMR spectroscopy in the determination of the structure of an EPS produced by *Streptococcus thermophilus* CNCMI 733.

1.4.4.1 ^{1}H-NMR spectra for carbohydrates

The ^{1}H-NMR spectra of a polysaccharide is split into two regions which are dependent on the chemical environment of the ^{1}H; the first is the anomeric region (situated downfield due to the electron withdrawing effects of the neighbouring ring oxygen atoms, 4.4 to 5.6 ppm) and the second is the bulk region (where the remaining ring protons are situated, 3.2 to 4.4 ppm) (See Fig. 1.17). A good starting point for structural characterisation of an EPS is the anomeric region, where identification of number of signals and determination of integral ratios in the region identifies the number of monosaccharides present in the repeating oligosaccharide unit, as such, particular attention is given to the region (4.4-5.6 ppm) (Abeygunawardana, Williams, Sumner, & Hennessey Jr, 2000; Hatzakis, 2019).

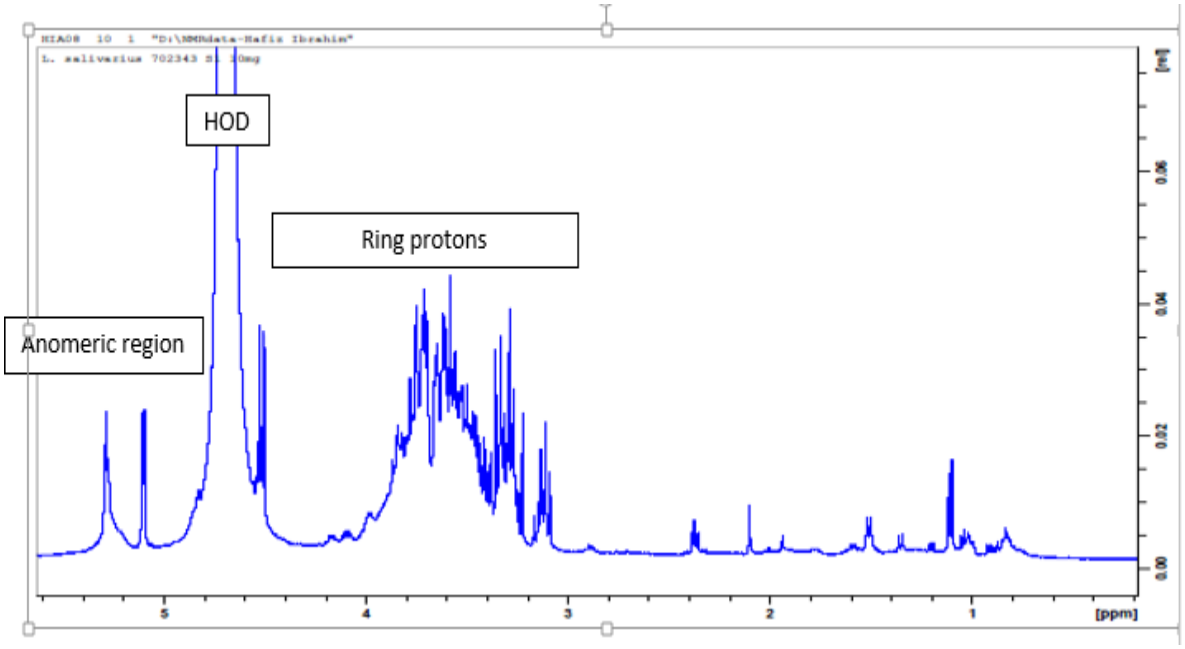

Figure 1.17: A representative ^{1}H-NMR spectra showing the anomeric region, the water signal and the ring protons.

The signal splitting in the anomeric region can be used to derive information about the anomeric configuration of the sugar as a result of the interactions between neighbouring protons facilitated through the bonding electrons, measured by coupling constants (*J*). The coupling constants magnitude depends on the distance and the dihedral angle between nuclei, which is of importance for structural characterisation. As described by Tafazzoli & Ghiasi, (2007), the Karplus curve, which shows the relationship between dihedral angle and the $^{3}J_{1,2}$ coupling constants, can be used to determine the configuration of the anomeric proton from ^{1}H-NMR spectra using a combination of the $^{3}J_{1,2H\text{-}H}$ and $^{1}J_{C\text{-}H}$ coupling constants (Fig. 1.18).

A hexose normally has an α-anomeric configuration when the $^{3}J_{1,2}$ coupling constant is less than 4Hz and that the hydrogen attached to C_1 is in an equatorial position and that attached to C_2 is in axial position, as such the dihedral bond angle will be 60^{0}. For an α-anomeric configuration, the peaks in the anomeric region of the ^{1}H-NMR spectra are normally observed as broad singlets (less than 600 MHz).

β-anomeric configuration normally give rise to $^{3}J_{1,2}$ coupling constant greater than 7.5Hz with both hydrogens attached to C_1 and C_2 being axial, so the dihedral bond

angle is larger and greater than 120^0. For a β-anomeric configuration, the peaks in the anomeric region of the ^{1}H-NMR spectra are observed as doublets.

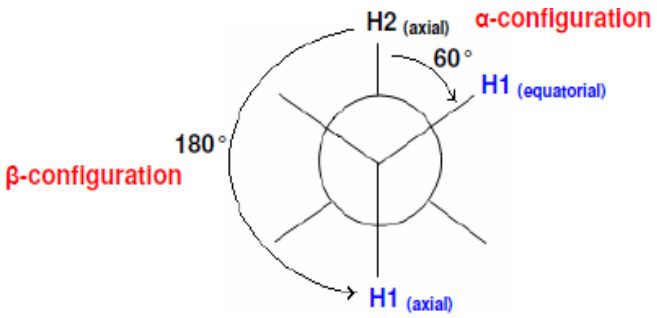

Figure 1.18: Newman projection showing the Dihedral angles in D-glucose.

The resonance positions for protons and carbons of most monosaccharides can be found in the literature. The literature sources are valuable reference materials which can be frequently employed to differentiate between two similar hexoses, for example, in ^{1}H-NMR, for glucose, $\delta_{H\text{-}4}$ is located in the range of 3.40-3.80 ppm whereas, $\delta_{H\text{-}4}$ is located in the range of 3.90-4.35 ppm for galactose (Harding *et al*., 2005)

1.4.4.2 ^{13}C-NMR spectra for carbohydrates

Unfortunately, ^{13}C-NMR spectra can be challenging to obtain as they require significant amounts of sample as a result of the low abundance of ^{13}C in nature. The number of anomeric carbon resonances present in a 1D ^{13}C NMR spectrum further confirms the number of different monosaccharides present in the repeating oligosaccharide unit as indicated in 1D ^{1}H NMR. In a manner similar to ^{1}H NMR, ^{13}C chemical shift can also be used to inform the anomeric configuration of sugars, but most importantly heteronuclear coupling constants in pyranoses are used to determine the anomeric configuration clearly. A $^1J_{C1\text{-}H1}$ ~170 Hz indicates an α-anomer whereas a $^1J_{C1\text{-}H1}$ ~160 Hz indicates a β-anomer of D-sugars, the reverse is the case for L-sugars.

A DEPT 135 ^{13}C-NMR spectrum shows all carbons present that are attached to a hydrogen (–CH, $–CH_2$ and $–CH_3$) in the sample. Methine (-CH) and methyl ($-CH_3$) carbons are shown as positive peaks, whereas methylene carbons ($-CH_2$) e.g. C_6 are

shown as negative peaks. Being next to the ring oxygen atom, the anomeric carbons (C_1) are located downfield (98-110 ppm). The signals for C_6 (-CH_2OH) are observed as negative peaks are generally located in the range of 60-70 ppm, C_6 involved in glycosidic linkages typically occur at 65 ppm while unlinked C_6 occur at 60 ppm. Carbon atoms bearing secondary hydroxyl groups (-CHROH) gives signals between 65-85 ppm. Signals of alkoxylated carbon atoms including C_5 in pentopyranoses (e.g. 67.2 ppm in α-D-arabinopyranose and C_4 in furanoses e.g. 71.5 ppm in β-D-galactofuranose are shifted 5 – 10 ppm to a lower field) when compared to the corresponding hydroxyl-substituted carbon atoms, C_1 (97.6, 101.8 ppm), C_2 (72.9, 82.2 ppm), C_3 (73.5, 76.6 ppm) C_4 (69.6, 82.8 ppm), C_6 (-, 63.6 ppm) respectively (Bock & Pedersen, 1983).

A change in ring size is also accompanied by a change in chemical shifts, as such, furanosese and other five membered rings e.g. β-D-glucofuranose (C_1, 103.8 ppm) have chemical shifts downfield from those of the configurationally related six membered rings e.g. β-D-glucopyranose (C_1. 96.7 ppm). Any –CH_3 groups, from either rhamnoses, fucoses, *N*-acetyl-amino sugars or such, are observed at a lower chemical shift (20.0 ppm), which can be quickly used to identify them.

1.4.4.3 Multidimensional NMR experiments

The primary aim of multidimensional NMR experiments is to provide information about the neighbouring nuclei (Hatzakis, 2019). In a multidimensional experiment (for example 2D), better resolution is obtained in comparison to 1D NMR as 2D experiments comprises of a series of 1D experiments that provides two frequency dimensions which shows cross peaks or correlation peaks indicating a correlation (coupling) between two different nuclei. These two different nuclei can either be of the same type (homonuclear) or of different types (heteronuclear). Common 2D experiments used in the structural characterisation of EPSs include COSY, TOCSY, HSQC, ROESY and HMBC, although more advanced techniques such as HSQC-TOSCY, DOSY and other sophisticated approaches are also being used. In this research reported here, the main spectra recorded are:

- COSY is a correlation spectroscopy spectrum which shows the scalar coupling of neighbouring protons
- HSQC is a heteronuclear single quantum coherence spectrum that shows the scalar coupling of carbon and hydrogen through one bond;
- ROESY is a rotating frame enhancement spectrum that shows the interaction of protons through space;
- TOCSY is a Total Correlation Spectroscopy spectrum that divides the proton signals into groups or coupling networks, especially when there is similarity in chemical shifts;
- HMBC is a Heteronuclear Multiple Bond Correlation spectrum that shows the scalar coupling of carbon and hydrogen through more than one bond.
- DOSY is a Diffusion Ordered Spectroscopy used to analyse mixtures of small molecules.

1.4.5 The use of Smith degradation and mild acid hydrolysis in the characterisation of polysaccharides

Oxidation using periodic acid, have been widely applied in carbohydrate chemistry for structural characterisation (Jackson, 1944). Various researches conducted have shown that this oxidation cleaves bonds between two adjacent carbon atoms carrying hydroxyl groups, irrespective of whether the two hydroxyl groups are of the *cis* or *trans* type, although the former is attacked at a greater rate (Klosterman & Smith, 1952). Reitz, Smith & Plumlee (1960) reported the application of a new procedure involving periodate oxidation in the structural determination of a type of dextran produced by *Leuconostoc mesenteriodes* NRRL-B-152. This procedure requires oxidation of the polysaccharide with sodium periodate followed by reduction of the periodate-oxidized polysaccharide with hydrogen and Raney nickel catalyst or with sodium borohydride in aqueous solution, and lastly, hydrolysis of the corresponding new polyalcohols with boiling dilute mineral acid.

Smith degradation works on the principle that, when monosaccharide residues that are linked together, such that the OH groups that occupy the C_2 and C_3 positions are free, are subjected to periodate oxidation, followed by reduction, and then hydrolysis, they give rise to erythritol and glycolic aldehyde. Similar chemistries apply to 4- and 4, 6- substituted residues. Using glucose as an example, for residues with free OH groups at their C_3 and C_4 positions as in terminal, 2-, 6- or 1, 2, and 6- substituted glucose residues will yield glycerol instead of erythritol. However, for glucose residues that have no pair of adjacent OH groups present, they will not be affected by periodate oxidation and as such will appear as free glucose or un-oxidized linked glucoses after the final mild acid hydrolysis step. For a terminal, a, 2-, 4- and 6- substituted glucose residues, the following products are obtained respectively:

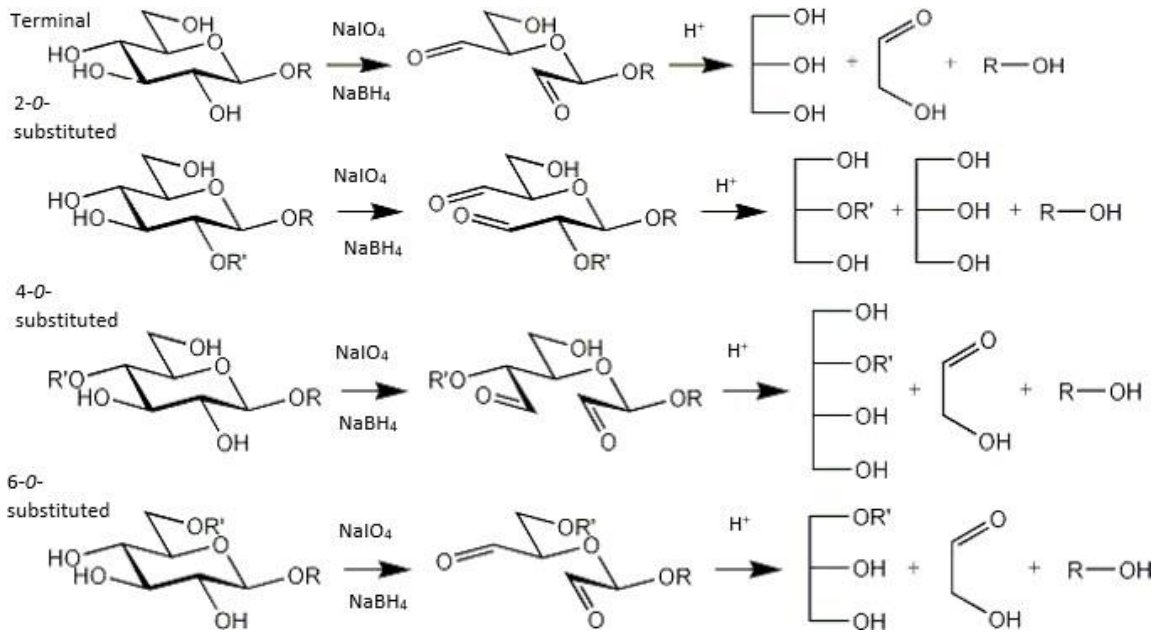

Figure 1.19: Smith degradation on a terminal, a 2-, a 4- and 6- substituted glucose residues respectively, adopted from http://www.stenutz.eu/sop/sop101.html

A 3-substitited glucose lacks hydroxyl groups next to each other and therefore cannot be oxidized, this is illustrated in a Smith degradation of a model polysaccharide containing 3-, 4- and 6- substituted glucose moieties.

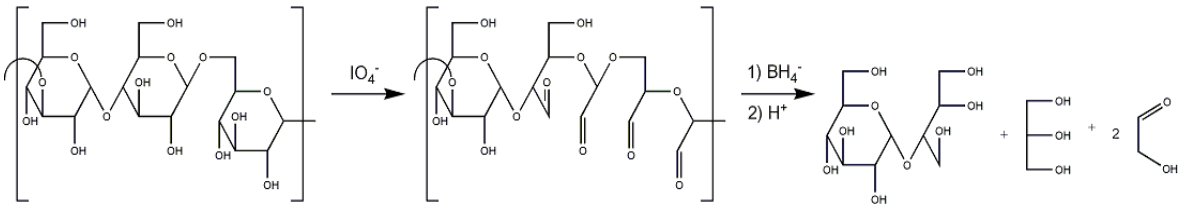

Figure 1.20: Smith degradation products of a model polysaccharide containing 3-, 4- and 6- substituted glucose moieties, clearly showing the un-oxidised 1, 3 linked glucose as a non-reducing terminal glucose, adopted from http://www.stenutz.eu/sop/sop101.html

The final step in Smith degradation involves mild acid hydrolysis. Mild acid hydrolysis alone has been employed in structural characterisation of polysaccharides. Lemoine et al., (1997) employed mild acid hydrolysis to investigate the structures of EPSs synthesised by *Streptococcus thermophilus* SFi39 and SFi12.

Aims

When grown on a fermentation medium supplemented with sucrose, the bacterial strain *L. fermentum* LF2 synthesis a mixture of polysaccharides of up to 2 g/L. In previous studies, it has been reported that the polysaccharide mixture has the potential to be utilised as a techno-functional natural ingredient, as it has also been shown to provide protection against *Salmonella* infection in a murine model. Despite this investigation, the structures of the polysaccharides produced by *L. fermentum* LF2 have not been characterised. The first aim of this research was to separate and purify the polysaccharide mixture synthesised by *L. fermentum* LF2 and to elucidate the structure of each EPS in order to understand the relation between their structures and their chemical, physical and biological activities.

A novel strain of *L. mucosae* (*L. mucosae* VG1) was isolated at University of Huddersfield from a faecal sample of a vegetarian who had been on a strict vegetarian diet for nine years. The strain was found to have a ropy phenotype amongst others, which is considered as a characteristic signifying EPS production. The second aim of this research was to grow, isolate and characterise the EPS synthesised by *L. mucosae* VG1 with a view to assessing its biological activity.

L. salivarius are natives of the GIT and have been found to inhibit the growth of pathogens and are increasingly being employed as probiotics, with the EPS potentially contributing to the health benefits. Previous research performed on the species has focused mainly on the genes responsible for EPS synthesis. The third aim of this research was to isolate, purify and characterise the EPSs synthesised by the strain *L. salivarius* 702343.

The fourth aim of this research was to determine the optimal growth conditions for the growth of the strains *L. fermentum* LF2 and *L. salivarius* 702343 for maximum EPS recovery.

The fifth aim was to reduce the molecular mass of a high molecular mass β-glucan and relate its different sizes to its biological activity.

2 Materials and Methods

2.1 General reagents

All general reagents used for the purpose of this research were bought from either Sigma-Aldrich Co. Ltd (Gillingham, Dorset, UK) or Fisher Scientific (Loughborough, United Kingdom), unless otherwise stated.

2.2 Fermentation of bacterial cultures

This section will cover the procedures involved in the production and isolation of exopolysaccharides from *L. fermentum* LF2, *L. mucosae* S32 and *L. salivarius* 702343.

2.2.1 Bacterial cultures

The bacterial culture *L. fermentum* LF2, a cheese isolate, was a kind gift from Facultad de Ingenieria Quimica (UNL), Instituto de Lactologia Industrial (UNL-CONICET), Santiago del Estero, Santa Fe, Argentina. *L. mucosae* VG1 is a human isolate that was isolated from faecal sample from a vegetarian (a vegetarian for 9 years) at the University of Huddersfield by Omololu Fagunwa, a PhD researcher working with Prof Paul Humphreys, *L. salivarius* 702343 was purchased from the National Collection of Industrial, Marine and food Bacteria (NCIMB), Aberdeen, UK. The cultures were revived by breaking the ampoule containing the bacteria and adding Huddersfield broth media (HBM, 0.5 mL) into the ampoule and the contents mixed. The numbered filter paper was then transferred on the tip of a Pasteur pipette on to a solid nutrient culture medium, MRSc agar plate, after which the remaining liquid was added to a separate MRSc agar plate for isolation of the best colony. Details of the conditions used for bacterial culture growth on the MRSc agar plates is stated in section **2.2.4**. The best colonies were stored in a cryoprotectant (10 % glycerol) on plastic beads in -80 ^{o}C freezer until required.

2.2.2 Preparation of MRSc Agar plates

In this work, MRS-c agar media was selected. To prepare MRS-c agar media (1.0 L), MRS powder (70.0 g) was dissolved in ultrapure water (1.0 L) and L-cysteine-HCl (0.05 %) was added as a reducing agent to enhance the growth of the Lactobacillus under anaerobic conditions. The media was stirred, autoclaved at 121 ^{o}C for 15 min and placed in a water bath at 37 ^{o}C to cool down. The resulting solution was then poured on to the Petri dishes. The MRS agar powder was purchased from Neogen LabM, Heywood, United Kingdom, and is made up of the components listed in table 2.1.

Table 2.1: MRS agar powder components

Media component	**Percentage (%)**
Glucose	2.0
Beef extract	1.0
Peptone	1.0
Agar	1.0
Sodium acetate trihydrate	0.5
Yeast extract	0.4
Triammonium citrate	0.2
Dipotassium hydrogen phosphate	0.2
Polysorbate 80	0.1
Magnesium sulfate heptahydrate	0.02
Magnesium sulfate tetrahydrate	0.005

2.2.3 Preparation of Huddersfield Broth Media (HBM)

In order to precipitate the polysaccharide equivalent (EPS-E), the beef extract and casein hydrolysate (acid) were treated before being added as media components. This was performed by dissolving beef extract (10.0 g) and casein hydrolysate (10.0 g) in a 1.0 L Schott bottle containing ultrapure water (200.0 mL). The resulting solution was stirred for 10 min and then autoclaved at 121 ^{o}C for 10-15 min. After 15 min, the solution was cooled down to room temperature. Absolute ethanol (2.5 volumes) was added to the cooled solution and the resulting suspension was left for 48 h at 4 °C.

After 48 h, the mixture was centrifuged (25000g for 30 min at 4 °C) (Avanti J-26S XPI-Beckman Coulter, Inc., USA) so as to remove the EPS-E from the solution. The

clear supernatant, obtained after centrifugation, containing ethanol used for the precipitation was distilled, thereby removing ethanol from the supernatant. After distillation, another centrifugation under the same conditions was performed on the supernatant to further remove any remaining EPS-E before the addition of the rest of the media components, which are listed in table 2.2 (below):

Table 2.2: Huddersfield Broth Media (HBM) components

FORMULATION	**HBM (g/L)**
Yeast Nitrogen Base	3.0
Treated Beef Extract	10.0
Glucose	10.0
Sodium acetate	3.0
Sodium chloride	5.0
Treated Casein Acid Hydrolysate	10.0
L-Cysteine-HCl	0.5

The solution containing all the ingredients was topped up to 1 L with ultrapure water, which was then autoclaved at 121 °C for between 10 to 15 min. The sterilized HBM was then kept in the cold room until required.

In a similar manner, another HBM broth was prepared by supplementing the media with different carbon sources i.e. by replacing glucose with either galactose or galacto-oligosaccharide (GOS). This was to check if the bacteria produces more when using a different carbon feed.

2.2.4 Fermentation

The bacterial strains were collected from the -80 °C freezer where they were stored on beads. The beads were spread on the surface of the already prepared MRS-c Agar plates; this was performed in a sterile class II cabinet. The MRS-c Agar plates containing the bacteria were then placed in an anaerobic chamber (80 % nitrogen, 10 % carbon dioxide, 10 % hydrogen, 37 ^{o}C) for a period of 36 to 48 h.

After 48 h, the best colony was selected by visual examination for further incubation; the selection was based on their phenotypic characteristics i.e. surface, shape, size, colour, elevation and edge. The selected colony was transferred into the prepared HBM (20.0 mL) and kept in the anaerobic chamber under the same conditions for 24 h. After 24 h, 5 % (v/v) from the 20.0 mL HBM containing the bacterial strain was transferred into another 20.0 mL bottle containing fresh HBM medium. This was also left in the anaerobic chamber under the same conditions for 24 h. A portion, i.e. 20 % (v/v) from the second 20 mL medium was then transferred into a HBM broth (500 mL) and fermented for a period of 72 h. An outline of the fermentation processes carried out in the anaerobic chamber as explained.

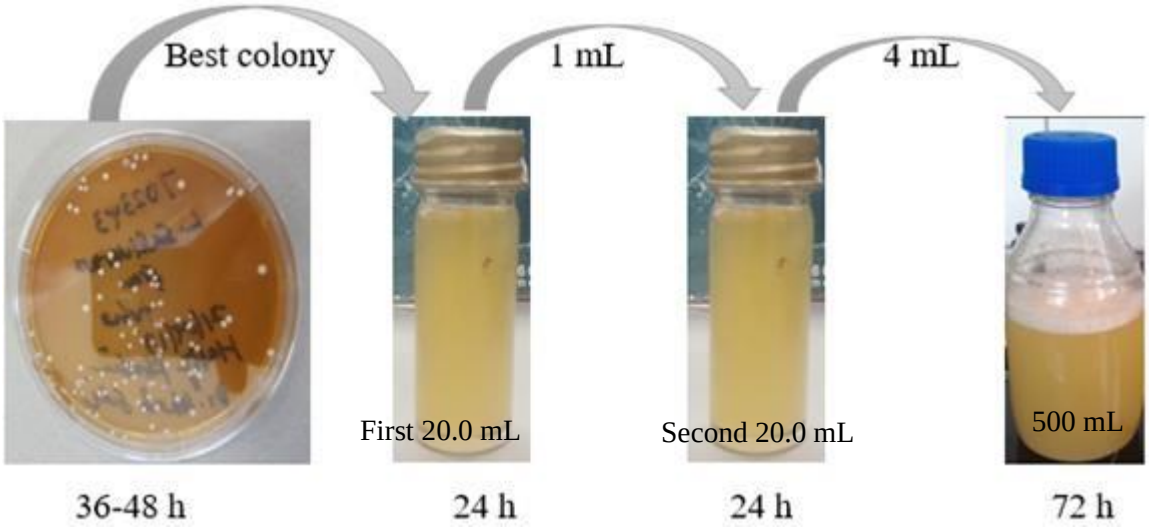

Figure 2.1*:* Fermentation process from plates to 500 mL HBM broth.

2.2.5 Bacterial Growth Measurements

2.2.5.1 Bacterial cell growth-optical density measurement

Bacterial cells multiply as they grow, the cell multiplication can be monitored when cultures are grown in a liquid medium. The more cells that are present, the more turbid the media will be. As such, cell growth can be monitored by measuring the turbidity of the broth media at time intervals. A graph of absorbance against time gave an overview of the time period when the bacteria grew exponentially and the graph was also used to identify the stationary and death phases of the bacterial cell growth.

The cell growth was monitored at two hourly intervals by measuring the turbidity-optical density spectrophotometrically. After every 2 h during the 72 h period of the fermentation, 2 mL was taken out from the fermentation media (500 mL) and the turbidity was measured using a Biochrom WPA Biowave II UV/Visible spectrophotometer, (Biochrom Ltd., Cambridge, UK) at 600 nm, using disposable polystyrene 3 mL, 10 × 4 × 45 mm cuvettes.

2.2.5.2 pH measurements

Although the type of carbon source and pH at which bacteria produces optimum amount of EPS are strain dependent, it has been proposed that bacteria converts sugar to EPS more efficiently at pH 5.8. It has also been reported that the optimal pH for optimum EPS synthesis by a number of LAB strains is within the range of 5.8 to 6.5. The idea was to monitor the pH of the fermentation broth for the duration of the fermentation (0-72 h), if it drops below 5.8, the pH of the fermentation will then have to be systematically controlled by adding NaOH to keep the pH within the range throughout the duration of the fermentation. The pH of the fermentation media was monitored at two hourly intervals. After every 2 h, 2 mL was taken out from the fermentation media (500 mL) and the pH was measured using a pre-calibrated Jenway 3510 pH meter.

2.2.6 Isolation of capsular and exo-polysaccharides from the growth media

After 72 h inoculation, the growth media (500 mL) was centrifuged (10,000g for 12 min at 4 °C) to separate the loosely bounded EPS (collected in the supernatant) and the tightly bound CPS, collected as pellets, adhering to the cell biomass.

2.2.6.1 Isolation of loosely bound exopolysaccharides

To the supernatant (500 mL) obtained after centrifugation (section 2.2.6, above), a volume of chilled absolute ethanol (500 mL) was added and the resulting mixture was kept in the cold room at 4 °C for 48 h, after which time the mixture was centrifuged (25,000g for 32 min at 4 °C). The solid content (S_1) obtained after centrifugation was re-dissolved in deionised water (10.0 mL) and the solution stirred overnight. To the supernatant, a second volume of chilled absolute ethanol (500 mL) was added and

the resulting solution was kept in the cold room at 4 °C for 72 h, after which time the solution was centrifuged (25,000g for 32 min at 4 °C). After centrifugation, the supernatant was discarded, whereas, the solid content (S_2) was also dissolved in deionised water (10.0 mL) and stirred overnight. The resulting solutions obtained after overnight stirring (S_1 and S_2) were separately dialysed against tap water for 3 days with 3 water changes per day, after which the dialysate was freeze-dried for 48-72 h (Edwards Freeze Dryer - Inc. vacuum pump-Modulyo EF4). The freeze-dried solids were weighed and kept in sample vials for further analysis. In situations where S_1 were not precipitated, two volumes of chilled absolute ethanol (1.0 L) were added to the supernatant immediately after the first centrifugation (section 2.2.6) and the steps in extracting S_1 were skipped. A schematic representation of the extraction protocol involved in isolating S_1 and S_2, (S_1 isolation steps highlighted in blue) is shown in scheme 2.

EPS Isolation Protocol

The culture after 72 h

Centrifuge

10,000g for 11min at 4 °C

Supernatant

Pellet Cells

Add 1 volume of ethanol

48 h

Centrifuge

25,000g for 30min at 4 °C

Supernatant

Solid

Re-dissolved in ultra-pure water

Add 2nd volume of ethanol

Dialysis

Three water changes per day for 3 days

48 h

Centrifuge

Freeze drying content in the dialysis bag

25,000g for 30min at 4 °C

S_1 – solid

Supernatant - Discard

Solid

Re-dissolved in ultra-pure water

Dialysis

Three water changes per day for 3 days

Freeze drying content in the dialysis bag

S_2 – solid

Scheme 2: Schematic representation of the extraction protocol involved in isolating S_1 and S_2, (S_1 isolation steps highlighted in blue)

2.2.6.2 Isolation of tightly bound capsular polysaccharides from the growth media

The cells obtained after centrifugation (section **2.2.6**) were treated with NaOH (200 mL, 1M) and left to stir overnight. The treated cells were then centrifuged (10,000g for 12 min at 4 °C) and the recovered solid was discarded. To the supernatant, one volume of chilled absolute ethanol (500 mL) was added and the resulting mixture was kept in the cold room at 4 °C for 48 h. After 48 h, the precipitate was recovered as a solid (C_1) by centrifugation (25,000g for 32 min at 4 °C), which was then dissolved in deionised water (10.0 mL) and left to stir overnight. To the supernatant, a second volume of chilled absolute ethanol (500 mL) was added and the resulting solution was kept in the cold room at 4 °C for 72 h, after which time it was centrifuged (25,000g for 32 min at 4 °C) and the supernatant discarded. The solid obtained (C_2) was dissolved in deionised water (10.0 mL) and left to stir overnight. The resulting solutions obtained after stirring overnight (C_1 and C_2) were separately dialysed against tap water for 3 days with 3 water changes per day, after which the dialysate was freeze-dried for 48-72 h. The freeze dried solids were weighed and kept in sample vials for further analysis. A schematic representation of the extraction protocol involved in isolating C_1 and C_2 is included in scheme 2.1

CPS Isolation Protocol

The culture after 72 h

Centrifuge

10,000g for 11 min at 4 ^{0}C

Supernatant

Pellet Cells

Add 200mL of 1M NaOH

Stir overnight at 4 ^{0}C

Centrifuge

10,000g for 11 min at 4 ^{0}C

Supernatant

Pellets - Discard

Add 1volume of ethanol

48 h

Centrifuge

25,000g for 30 min at 4 ^{0}C

Supernatant

Add 2nd volume of ethanol

48 h

Centrifuge

25,000g for 30 min at 4 ^{0}C

Supernatant - Discard

Solid

Re-dissolved in ultra-pure water

Dialysis

Three water changes per day for 3 days

Freeze drying content in the dialysis bag

C_2 – solid

Solid

Re-dissolved in ultra-pure water

Dialysis

Three water changes per day for 3 days

Freeze drying content in the dialysis bag

C_1 – solid

Scheme 2.1: Schematic representation of the extraction protocol involved in isolating C_1 and C_2

2.2.6.3 Preparation of Dialysis tubes

The dialysis tubes, composed of regenerated cellulose, were stored in glycerol by the manufacturers to keep them moist. The glycerol used as a humectant was removed by washing the tubing under running water for 3-4 h, after which time the residual sulphate salts formed during the manufacturing process were also removed by heating the tubing at 80 °C for 1 minute with 0.3 % (w/v) of sodium sulphide. The tubing was then washed with hot water at 60 °C for 2 min, followed by acidification with a 0.2 % (v/v) solution of sulphuric acid. The tubing was then rinsed with hot water (60 °C) to remove the acid. The tubing was further rinsed with ultrapure water to ensure that no acid was left, after which the tubing was stored in ultrapure water at 4 °C. The tubing will retain most materials with molecular weight of greater than or equals to 12,000 Da.

2.2.6.4 Purification of EPS

Prior to EPS characterisation, it is important to improve purity and solubility of the polysaccharide so as to avoid any potential broadening of signals in the NMR and to also ensure that it is free from all other components that may interfere with its characterisation. Specific enzymes and chemicals responsible for removal of non-carbohydrate moieties have been reported in the literature. In this part, several methods of deproteinization and de-acetylation were employed in an attempt to find the most efficient and suitable method to purify the EPS prior to its characterisation.

2.2.6.4.1 Deproteinization using proteinase K

To remove protein residues, the crude EPS (5.0 mg) was dissolved in a phosphate buffered saline solution (pH 7.4, 10.0 mL) and was treated with proteinase K (50.0 mL, 20.0 µg / mL). The resulting solution was then incubated for 2-3 h at 37 ^{o}C. After 3 h, proteinase K was inactivated by heating the solution at 80 °C for 30 min, which was then removed by centrifugation (25,000g for 30 min at 4 °C). The EPS was precipitated from the supernatant by adding two volumes of chilled absolute ethanol (60.0 mL), followed by dialysis and freeze-drying as described in 2.2.2.6. The freeze-dried EPS was analysed for purity using Size Exclusion Chromatography coupled with Multi-

Angle Laser Light Scattering (SEC-MALLS-Wyatt technology, Santa Barbara, CA, USA). The SEC-MALLS was equipped with an in-line UV detector (Shimadzu, Milton Keynes, UK) that was utilised for the detection of proteins and nucleic acids. Details of the sample preparation and analysis using SEC-MALLS is described in section **2.2.7.1**.

2.2.6.4.2 Deproteinization by Savage method

The Savage method was employed to remove protein residues. EPS samples (EPS, 5.0 mg) was dissolved in ultrapure water (10.0 mL). The resulting solution was then transferred into a separating funnel and three volumes of Savage's reagent ($CHCl_3$ and n-BuOH in a ratio of 4:1) was added and the mixture was shook vigorously for 5 min. The mixture was left to equilibrate for 15 min and the lower organic layer containing the protein residues was discarded. This was repeated three times and the resulting aqueous layer was treated with two volumes of chilled ethanol and the solution was left for 48 h at 4 °C so as to precipitate the EPS. The EPS was collected by centrifugation (25,000g for 30 min at 4 °C) and was washed with absolute ethanol (50.0 mL) and diethylether (50.0 mL) respectively. The washed EPS was dissolved in ultrapure water (25.0 mL), dialysed against deionised water for three days (with three water changes per day), and then freeze-dried for 48-72 h. The freeze-dried EPS (3.0 mg) was dissolved in D_2O (0.65 mL) and analysed by 1D (^1H) NMR as described in section **2.2.8.5**.

2.2.6.4.3 Deproteinization by Anion exchange column chromatograpy

As proteins are built up of many different ionisable groups, a DEAEC-Sephacel anion exchange column (GE Healthcare, Fisher Scientific, UK) based on beaded cellulose was used to separate proteins from the EPS. The column was filled with diethylaminoethyl anion-exchange resin and had an exclusion limit of approximately 1 x 10^6 Da. The column was connected to an AKTA PRIME system (AKTA PRIME - Amersham Pharmacia, Biotech, GE Healthcare Life Sciences, Buckinghamshire, UK). A solution of the EPS (100.0 mg) was prepared in ultrapure water (5.0 mL) and stirred overnight to ensure that the EPS was completely dissolved. The dissolved sample

(5.0 mL) was injected into the AKTA PRIME system and eluted at a flow rate of 0.5 mL/min, using sodium chloride (600 mM) as the mobile phase.

In total, sixty 5 mL fractions were collected and the sample elution was monitored at a wavelength of 254 nm for UV detection. The location of proteins was identified by inspecting the UV peak for each fraction, whereas the location of polysaccharides in every fraction was identified by determining the total carbohydrate content of each fraction using the Dubois method (section 2.2.7.3). Fractions containing the EPS were pooled and freeze-dried for 48-72 h. The freeze-dried EPS (15.0 mg) was dissolved in D_2O (0.65 mL) and analysed by 1D (^1H) NMR as described in section **2.2.8.5**.

2.2.6.4.4 De-acetylation using aqueous ammonium hydroxide

The EPS (1 mg/mL) was *O*-deacetylated by treatment with aq ammonia (12.5 %) at 37 °C for 16 h. The *O*-deacetylated EPS was recovered by drying under a constant stream of nitrogen after which time it was re-constituted with water (5.0 mL). The reconstituted *O*-deacetylated EPS was dialysed against deionised water for three days, with three water changes per day and the dialysate was freeze-dried for 48-72 h. The freeze-dried EPS (6.0 mg) was dissolved in D_2O (0.65 mL) and analysed by 1D (^1H) NMR as described in section **2.2.8.5**.

2.2.6.4.5 De-acetylation using sodium hydroxide

A crude EPS sample (15.0 mg) was dissolved in ultrapure water (20.0 mL) and left to stir overnight. Deuterated sodium hydroxide (NaOD) was added to make the solution up to 0.1M and was left for 24 h. After 24 h, the solution was dialysed against deionised water for three days with three water changes per day and the dialysate was freeze-dried for 48-72 h. The freeze-dried EPS (10.0 mg) was dissolved in D_2O (0.65 mL) and analysed by 1D (^1H) NMR as described in section 2.2.8.5.

2.2.6.4.6 Removal of nucleic acid using DNase

To a test tube containing EPS (20.0 mg), phosphate buffered saline solution (pH 7.2, 5.0 mL) was added and sonicated for 20-30 min. After 30 min, DNase I (20 U/mL, 20 µL) and DNase buffer (20 U/mL, 20 µL) were added into the test tube and the tube incubated for 16-20 h at 37 °C. The solution was then heated at 75 °C for 10 min to

inactivate the enzyme, after which it was dialysed for 3 days (with three water changes per day) and the dialysate freeze-dried for 48-72 h. The freeze-dried EPS was analysed for purity using Size Exclusion Chromatography coupled with Multi-Angle Laser Light Scattering (SEC-MALLS-Wyatt technology, Santa Barbara, CA, USA) equipped with an in-line UV detector (Shimadzu, Milton Keynes, UK) was used for the detection of proteins and nucleic acids as described in section 2.2.7.1.

2.2.7 Characterisation of the isolated exopolysaccharides

2.2.7.1 Determination of the purity and weight average molecular mass of the isolated exopolysaccharides

Size Exclusion Chromatography coupled with Multi-Angle Laser Light Scattering (SEC-MALLS-Wyatt technology, Santa Barbara, CA, USA) was used to determine the purity and composition of the EPS. EPS samples (1 mg/mL) were prepared in aq. $NaNO_3$ (0.1 M) and stirred for 16 h to ensure the EPS was completely dissolved. Samples (100 µL) were injected, in triplicate, into a SEC-MALLS system (three columns connected in series: PL Aquagel-OH 40, 50 and 60 (8 µm, 30 cm × 7.5 mm, Agilent, Cheadle, UK) with a flow rate of 0.7 mL min^{-1}. A differential refractometer (Optilab rEX, Wyatt technology, Santa Barbara, CA, USA) was used to determine the concentration of the polysaccharide and a Dawn-EOS MALLS detector (laser operating at 690 nm) was used to determine the weight average molecular mass of the polysaccharide. An in-line UV detector (Shimadzu, Milton Keynes, UK) was used for the detection of proteins and nucleic acids. ASTRA version 6.0.1 software (Wyatt technology, Santa Barbara, CA, USA) was used for the data analysis.

2.2.7.2 Preparative chromatography

EPS samples (100.0 mg) were prepared in ultrapure water (5.0 mL) and stirred overnight to ensure that the EPS was completely dissolved. The dissolved samples (5.0 mL) were injected into an AKTA PRIME system (AKTA PRIME-Amersham Pharmacia, Biotech, GE Healthcare Life Sciences, Buckinghamshire, UK), connected to a preparative column (depending on the fractionation range) and fractions were collected (see section below).

2.2.7.2.1 Sephacryl S 500 HR column

The first column used was a prepacked HiPrep Sephacryl S500 HR column (XK26/60-GE Healthcare, Fisher Scientific, UK) with an internal diameter of 26.0 mm, a bed height of 60.0 cm and a bed volume of approximately 320.0 mL, filled with a cross linked copolymer matrix of *N*, *N'*-methylene bisacrylamide and allyl dextran, and has a fractionation range of 4.0×10^4 to 2.0×10^7 Da. Ultra-pure water was used as the mobile phase with a flow rate of 5.0 mL/min (unless otherwise stated) and sample elution was monitored at a wavelength of 254 nm for UV detection. At the end of the run, sixty 10 mL fractions were collected and each fraction was analysed for its total carbohydrate content using the Dubois method (section **2.2.7.3**). Fractions were combined based on the Dubois results and freeze-dried for 48-72 h. The freeze-dried fractions were weighed, dissolved in D_2O (0.65 mL) and analysed by 1D (^1H) NMR as described in section **2.2.8.5**.

2.2.7.2.2 Sephacryl S 200 HR column

The second column used was a prepacked HiPrep XK16/60 Sephacryl S200 HR column (with an internal diameter of 16.0 mm, a bed height of 60.0 cm and a bed volume of approximately 120.0 mL), also filled with a cross-linked copolymer of allyl dextran and *N*, *N*-methylene bisacrylamide. However, for the Sephacryl S200 HR column, the fractionation range is 1.0×10^3 to 8.0×10^4 Da. Ultra-pure water was also used as the mobile phase at a flow rate of 2 mL/min (unless otherwise stated) and the UV detector was set at a wavelength of 254 nm. In total, sixty 5 mL fractions were collected and the location of polysaccharides was determined by analysing each fraction for its total carbohydrate content using the Dubois method (section 2.2.7.3). Fractions were combined based on the Dubois results and freeze-dried for 48-72 h. The freeze-dried fractions were weighed, dissolved in D_2O (0.65 mL) and analysed by 1D (^1H) NMR as described in section **2.2.8.5**.

2.2.7.3 Dubois Method

The colorimetric phenol-sulphuric acid (Dubois) method of determining total carbohydrate content was employed in estimating the amount of carbohydrates

present in each of the fractions collected, using glucose as a reference standard. Five glucose standards with concentrations ranging between 0 and 100 ppm were prepared. Phenol solution (5%, 0.5 mL) was added to the prepared standards and the fractions collected from the preparative column (0.5 mL) in a high temperature resistant thick glass tubes, this was then followed by the addition of concentrated sulphuric acid (2.5 mL) with caution, after which a yellowish colour started to appear. The mixture was shaken with caution and kept in a water bath at 70 °C for 20 min, to ensure that the reaction was complete. After 20 min, the solution was cooled in a water bath at 10 °C for 20 min, after which time the samples were individually transferred into disposable polystyrene (3 mL, 10 × 4 × 45 mm) cuvettes and the absorbance for each of the standards and fractions were recorded spectrophotometrically using a Biochrom WPA Biowave II UV/Visible spectrophotometer, (Biochrom Ltd., Cambridge, UK) at a wavelength of 490 nm. The total carbohydrate content of each fraction was determined by generating a calibration curve of the absorbance of the five glucose standards measured against their known concentrations: ranging between 0 and 100 ppm.

2.2.8 Structural characterisation of EPS

2.2.8.1 Monosaccharide Analysis with HPAEC-PAD

Trifluoroacetic acid (TFA, 2 mL of 2M) was added to a pressure tube containing the EPS sample (3.0 mg) and the tube was sealed. The sealed pressure tube was then subjected to heating at 120 °C for 2 h. After 2 h, the sample was cooled to room temperature and the solution was evaporated to dryness under a constant stream of nitrogen at 60 °C to give monomers as dry solid residues. The dried residues were dissolved in ultra-pure water (3.0 mL) and half (1.5 mL) was analysed by HPAEC-PAD.

2.2.8.1.1 HPAEC-PAD analysis

All HPAEC-PAD experiments in this research were performed using either a Dionex ICS-3000 or a Dionex ICS-5000 ion chromatography system (Dionex Corporation, CA, USA). Both instruments were equipped with a Dionex AS (Auto Sampler), EO (Eluent

Organiser), DC (Detector Chromatography), DP–Dual Pump System, EG–RFIC, (EG-Eluent Generator, RFIC-Reagent-Free Ion Chromatography) and Chromeleon® Xpress software was used for the processing of the data.

The column used in both systems was a CarboPac PA20 analytical column (3x150 mm, 6.0 µm particle size) attached to a guard column (CarboPac PA20, 3x30 mm) and an injection volume of 25.0 µL. The system was ran isocratically with NaOH (10 mM) as the mobile phase for 30 min and was regenerated in between the runs with NaOH (200mM). Flow rates of 0.3 mL/min and 0.5 mL/min were used on the ICS-3000 and ICS-5000 systems respectively. Monomer standards were used for each run to identify the retention time of the different sugars.

2.2.8.2 Monosaccharide Analysis with GC-MS:

2.2.8.2.1 Reduction to alditols

In order to reduce the sugar monomers to their alditols, sodium borodeuteride ($NaBD_4$, 10.0 mg) was added to the other half (1.5 mL) of the reconstituted hydrolysed EPS (2.2.8.1; above). The tube was sealed and heated at 40 °C for 2 h and after the 2 h period had elapsed; the solution was dried under a constant stream of nitrogen at 60 °C. To the dried residue, glacial acetic acid (1.0 mL) was added and evaporated to dryness under a stream of nitrogen after which methanol (3 x 1.0 mL) was then added and subsequently evaporated in order to remove the borate complexes to give the sugar alditols as dried residues.

2.2.8.2.2 Acetylation of alditols

The dried residues (sugar alditols) obtained after the reduction process were dissolved in pyridine (2.0 mL) and acetic anhydride (2.0 mL) in a pressure tube and heated at 100 °C for 2 h in order to acetylate the sugar alditols. After 2 h, the solution was evaporated at 40 ^{o}C to dryness under a constant stream of nitrogen. The dried residue (acetylated alditols) was then suspended in ultra-pure water (5.0 mL) and extracted with chloroform (3 x 10.0 mL). The total organic layer was then washed with ultra-pure water (2.0 mL). The organic layer was dried with anhydrous sodium sulphate for 30 min. The solution was then filtered and the liquid evaporated to dryness under

a constant stream of nitrogen at 40 °C. The resulting residue was then dissolved in acetone (2.0 mL) and analysed by GCMS.

2.2.8.2.3 Monomer analysis using GC-MS

The GC-MS used in this research was an Agilent 7890A GC system with an Agilent 7683B injector and Agilent 5975B inert XL EI/CI MSD (Agilent Technologies, Eidinburgh, UK). The Agilent GC-MS and the Agilent MSD configuration was used in data processing. The column used was an Agilent 19091S-433 with the dimensions 30 m x 250 µm x 0.25 µm. A split mode injection (10:1) was used with helium as the carrier gas at a flow rate of 1.0 mL/min and an injection volume of 10 µl. All these conditions were same for both monomer and linkage analysis, however, the two operate with different temperature programs.

For monomer analysis, the starting temperature was 180 °C, held for 1 min., which was increased by 1 °C /min until 220 °C was reached, this was then held for 5 min.

2.2.8.3 Absolute configuration

To a pressure tube containing the EPS sample (0.5 mg), TFA (0.5 mL, 2M) was added and the resulting solution was heated at 120 °C for 30 min. After 30 min, the solution was evaporated to dryness with a stream of nitrogen and methanol (0.5 mL) was added and evaporated, this was repeated once. The dry residue was reconstituted with (+)-2-butanol (0.2 mL) and acetyl chloride (15.0 µL) and nitrogen was bubbled through the solution for 30 sec. The sample was 'Butanolysed' for 8 h at 80 °C after which time the solution was evaporated to dryness with a stream of air and methanol (0.5 mL) was added, then evaporated. The addition of methanol and evaporation was repeated once. Subsequently, the sample was acetylated with acetic anhydride (0.2 mL) and pyridine (0.1 mL) at 120 °C for 30 min. The solution was then evaporated and toluene (0.5 mL) was added and evaporated to dryness. The addition of toluene was repeated once. The dry residue was partitioned between H_2O (0.5 mL) and EtOAc (0.5 mL). The upper (EtOAc) phase was transferred to a new tube. The extraction was repeated twice with EtOAc, the combined EtOAc phases were concentrated to dryness, and the dry residue was then dissolved in EtOAc (0.2 mL), transferred to a new sample tube, and concentrated to 25-50 µL, which was then

analysed by GC-MS. The chromatographic conditions for absolute sugar analysis on GC-MS were same as that of monomer analysis stated in section 2.2.8.3.2 (above).

2.2.8.4 Linkage analysis

2.2.8.4.1 Methylation

EPS (3.0 mg) was added in a pressure tube along with anhydrous dimethylsulphoxide (0.7 mL) and stirred at room temperature until the formation of a slurry was observed. Dried and crushed sodium hydroxide (70.0 mg) was added with stirring along with methyl iodide (60.0 µL). After 20 min, the resulting solution (methylated polysaccharide) was then separated and extracted with ultrapure water (1.0 mL) and dichloromethane (1.0 mL). The dichloromethane phase was then washed with ultrapure water (5.0 mL) three times. The resulting liquid was then evaporated to dryness under a constant stream of nitrogen at 40 °C, to give the methylated polysaccharide as a solid, which was used directly in the next steps: hydrolysis as described in section **2.2.8.1**, reduction as described in section **2.2.8.2.1** and acetylation as described in section **2.2.8.2.2**.

2.2.8.4.2 Linkage analysis using GC-MS

As stated earlier, all conditions listed in section **2.2.8.2.3** were same for both monomer and linkage analysis, however, the two operate with different temperature programs. For linkage analysis, the starting temperature was 140°C, which was held for 1 min, then increased by 2.5 °C /min until 220 °C was reached, this was then held for 13 min.

2.2.8.5 NMR analysis

All NMR experiments in this research were either performed using a Bruker Avance (AVIII) 400 MHz, a Bruker Avance (AVI) 500 MHz or a Bruker Neo 600 MHz spectrometer (equipped with a cold prodigy probe) by Dr. Neil McLay. For NMR analysis, the freeze-dried EPS samples (15.0 mg) (unless otherwise stated) were dissolved in D_2O (0.65 mL). The chemical shifts were recorded in part per million

referenced to acetone. Both 1D (^{1}H, ^{13}C, ^{13}C DEPT 135) and 2D (COSY, HSQC, ROESY, TOCSY, HSQC-TOCSY and HMBC) were recorded.

The EPS samples were also analysed at an elevated temperature (70 °C), this elevated temperature increases solubility thereby increasing resolution due to reduction in sample viscosity and most importantly, it shifts the HOD signal from D_2O into a clear region of the spectrum so it no longer interferes with any carbohydrate signals. Some samples were analysed at room temperature and the chemical shifts were adjusted with respect to HOD signal before recording (HOD adjusted from 4.79 to 4.29). In instances where a poor spectra is obtained in a particular 2D experiment, the number of scans were increased (doubled or quadrupled) for improved signal to noise (S/N).

2.2.8.6 Smith degradation

EPS (37 mg) was dissolved in sodium acetate buffer (pH 3.9, 25 mL, 0.1 M). The resulting solution was treated with sodium metaperiodate (8.5 mL, 0.2 M) and was left in the dark at 4 °C for 120 h. The excess periodate was destroyed by the addition of ethylene glycol (2 mL) and the solution was dialysed against distilled water for 3 days with 3 water changes per day. Sodium borohydride (200.0 mg) was added to the dialysate and left for 4 h. The excess borohydride was destroyed by the addition of 50 % acetic acid. The solution was adjusted to pH 4.5 using the same acetic acid solution and was then dialysed against distilled water for 3 days with 3 water changes per day. The dialysate was then freeze-dried for 48-72 h. After 72 h, TFA (0.5 M, 5.0 mL) was added to the freeze-dried sample and was left for 24 h at room temperature. The resulting solution was dried under a constant stream of nitrogen.

2.2.8.7 Ultrasonic disruption of exopolysaccharides

EPS (10.0 mg) was dissolved in ultrapure water (10.0 mL) and the resulting solution (10.0 mL, 1000 ppm) was transferred into a falcon tube (50.0 mL). The falcon tube was placed in an ice-bath, after which the tip of the ultrasonic probe (3 mm, VCX130, Sonics and Materials Inc, Connecticut, USA) was lowered into the centre of the falcon tube leaving a distance of approximately 2 mm between the bottom of the falcon tube and the tip of the ultrasonic probe. The solution was sonicated with 30 sec of

sonication, followed by a 30 sec cooling mode every minute for an hour, a power of 25% (Max 130 watts) was applied, and aliquots (0.5 mL) were removed after every 10 min and injected into the HP-SEC-MALLS for analysis using the chromatographic conditions described in section 2.2.7.1. The change in average molecular weight of the EPS per 10 min sonication time was determined.

2.2.8.8 Microwave assisted depolymerisation

EPS (4.0 mg) was dissolved in ultrapure water (4.0 mL) and the resulting solution (4 mL, 1000 ppm) was transferred into a teflon insert (max volume 4.0 mL). The teflon insert was placed on a sample holder and inserted into a HTC protection shield cylinder with teflon cover on the top. The cylinder was tightened in the tightening vessel and was placed into the MicroSYNTH – Advanced Microwave Synthesis Lab Station and a temperature probe added into the small hole provided on top of the cylinder. The sample was set to be heated at 120 °C for 5 min using the easyCONTROL-640; it takes approximately 10 min for the microwave to attain the desired temperature and another 10 min to cool off, which takes the analysis time to 25 min, this was repeated 5 times. After every 25 min, aliquots (0.5 mL) were removed and injected into the HP-SEC-MALLS for analysis using the chromatographic conditions described in section 2.2.7.1. The change in average molecular weight of the EPS per 5 min microwave heating time was determined.

2.2.8.9 Debranching using Mild acid hydrolysis

TFA (0.05 M, 0.65 mL) was added to the EPS (15 mg); the resulting solution was heated at 100 °C for several hours, taking the sample for NMR at hourly intervals.

2.2.9.0 Enzyme hydrolysis using β-Glucanase and β-Glucosidase:

EPS (1.0 mg) was dissolved in ultra-pure water (3 mL). The solution was left to fully dissolve overnight. Once fully dissolved the enzyme (1 mg) was added to the solution and the solution heated for 1 h at 37 °C in a heating block. The solution was then analysed by HPAEC-PAD.

Results and Discussion Sections

3. Structural characterisation, optimisation of production and evaluation of immunomodulatory activity of a high molecular mass EPS produced by *Lactobacillus fermentum* LF2

4. Structural characterisation of two novel medium molecular mass EPSs produced by *Lactobacillus fermentum* LF2

5. Production and structural characterisation of a novel EPS produced by *Lactobacillus mucosae* VG1

6. Production and isolation of polysaccharides from *Lactobacillus salivarius* 702343

3 Structural characterisation, optimisation of production and evaluation of the immunomodulatory activity of a high molecular weight EPS produced by *L*actobacillus *fermentum* LF2

3.1 Introduction

This chapter contains a discussion of the characterisation of the high molecular weight polysaccharide synthesised by *L. fermentum* LF2. As far as the author of this report is aware, this is the first ever report on the characterisation of the EPSs synthesised by *L. fermentum* LF2. The synthesis of more than one polysaccharides of different molecular weight by a given strain is somewhat frequent in LAB (Ruas-Madiedo, Salazar, & Clara, 2009). In this research, various purification methods were applied to obtain a pure polysaccharide for structural characterisation. The EPSs were separated, then the purity and quantity of the EPSs were analysed.

The crude EPS produced by *L. fermentum* LF2 was a gift from Facultad de Ingenieria Quimica (UNL), Instituto de Lactologia Industrial (UNL-CONICET), Santiago del Estero, Santa Fe, Argentina. In earlier work by Ale *et al*., (2016), the EPS has been applied as a dairy food additive to reduce syneresis, improve water holding capacity and increase hardness of dairy products. Ale *et al*., (2016) have shown the potential of the strain and its EPSs to be used as a functional natural ingredient, as it has been demonstrated that it provides protection against *Salmonella* infection in a murine model. Despite these investigations, the structure of the polysaccharides produced by *L. fermentum* LF2 have not been characterised. It is important to elucidate the structure of the EPS in order to understand the relation between its structure and its chemical, physical and biological activity.

3.2 Structural investigation of the crude EPS produced by *Lactobacillus fermentum* LF2

Initially, the crude EPS produced by *L. fermentum* LF2 sent by the collaborating institution in Argentina was analysed using both ^{1}H-NMR spectroscopy and SEC-MALLS. NMR spectra were run as described in the experimental section **2.2.8.5**. The ^{1}H-NMR spectra recorded on the crude EPS produced by *L. fermentum* LF2 showed an anomeric region with four large signals and five small signals. The signals were of different integral ratios, as displayed in Fig. 3.1 (0.5:2.1:0.5:0.5:1.8:0.5:1.0:2.0:0.9) and these ratios varied for different batches of material generated in different fermentation.

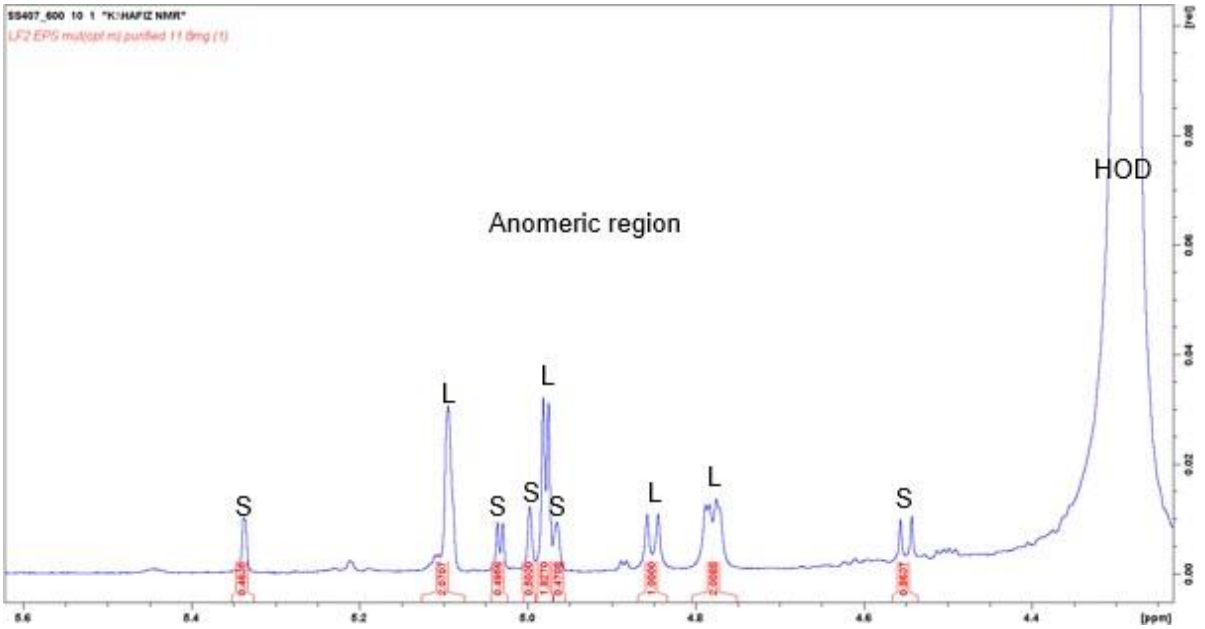

Figure 3.1: ^{1}H-NMR spectra recorded at 70 ^{o}C on the crude EPS produced by *L. fermentum* LF2.

The results from the ^{1}H-NMR suggest that the crude EPS might be composed of more than one polysaccharide, as such, the crude EPS was further analysed by SEC-MALLS to determine the molecular weight profile of the EPS mixture. The weight average molecular mass of the EPS mixture was determined by SEC-MALLS as described in the experimental section **2.2.7.1**, the instrument was assessed for its ability and accuracy to determine the actual molecular weight of macromolecules using a pullulan standard, a neutral homopolysaccharide of known molecular weight (1.10 x 10^{5} $gmol^{-1}$), employing a dn/dc = 0.147 mL/g as described in the literature (Bahary et

al., 1995). A 1000 ppm solution of a pullulan standard was ran on the SEC-MALLS using the procedure described in section **2.2.7.1**. A single peak of 1.19 x 10^5 $gmol^{-1}$ eluted at a RT = 33 min (Fig 3.2) and the measured polydispersity (M_w/M_n) was 1.07. The pullulan was run as a control and confirms the accuracy and the capability of the instrument to determine the precise molecular weights of neutral polysaccharides.

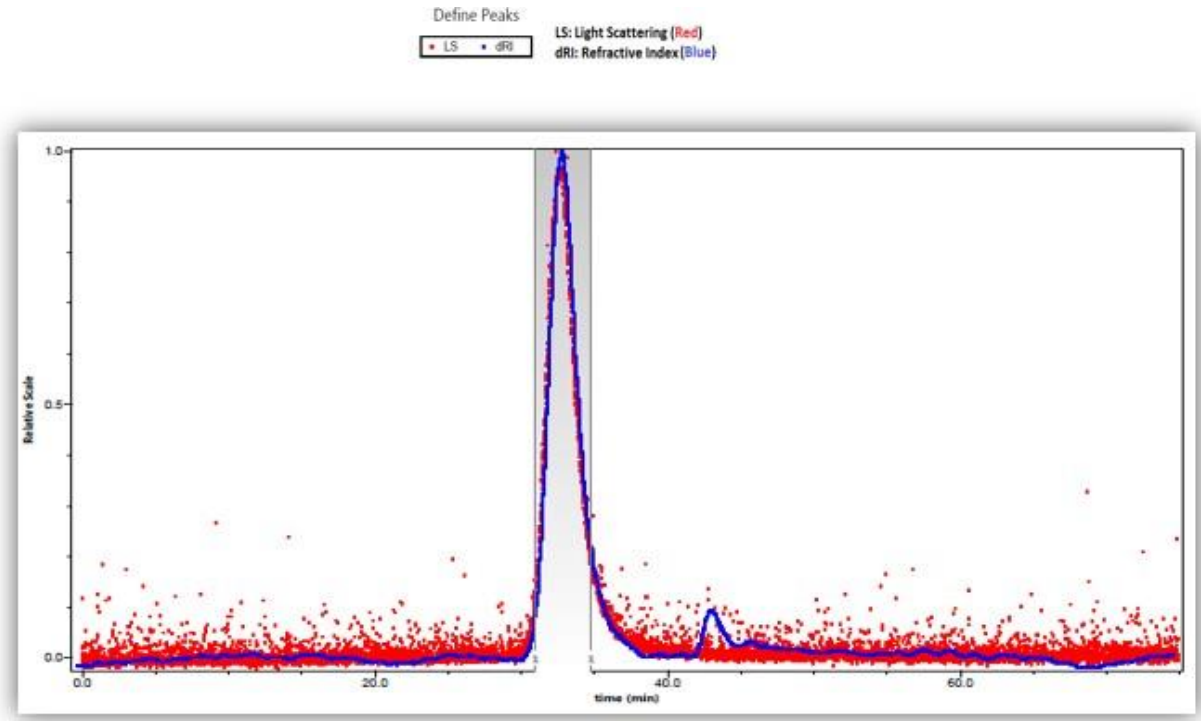

Figure 3.2: SEC-MALLS chromatogram of Pullulan standard (1.10 x 10^5 $gmol^{-1}$).

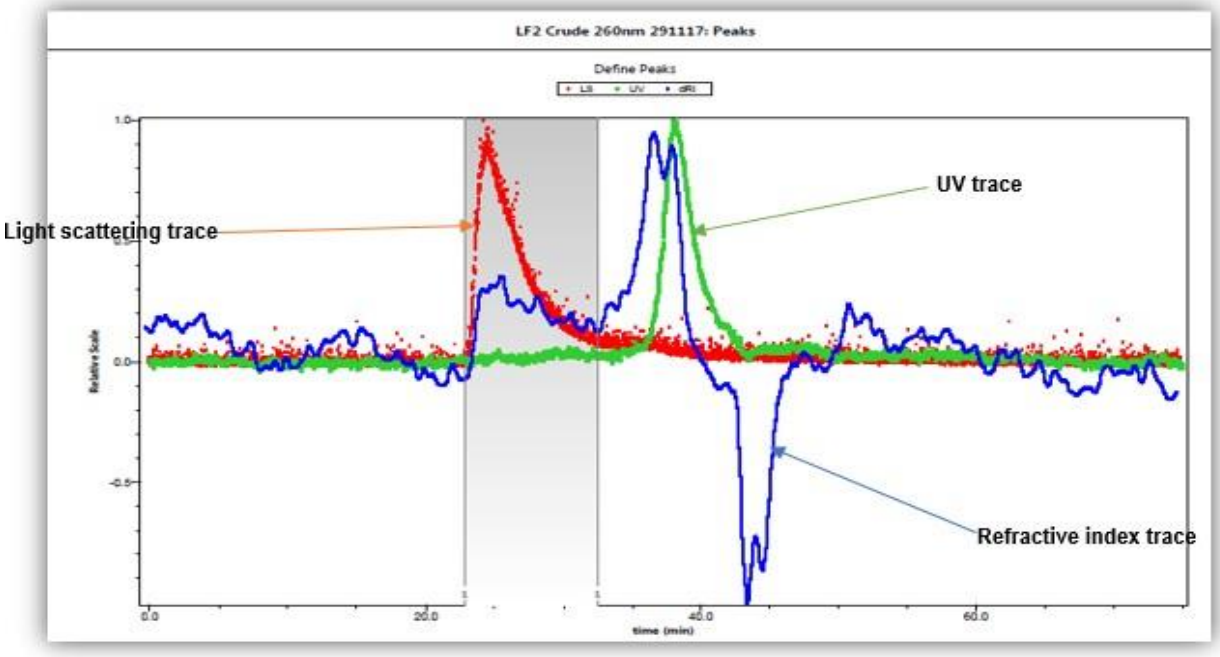

Figure 3.3: SEC-MALLS chromatogram of the crude LF2.

The crude EPS was ran on SEC-MALLS on the chromatogram trace (Fig. 3.3), two light scattering peaks were observed (one large and one very small with RT 26 mins and 38 mins respectively) indicating the presence of potentially two populations of polysaccharides of different molecular masses, a high molecular mass (HMw) of about 1.23 x 10^6 $gmol^{-1}$ and a medium molecular mass (MMw) of about 8.80 x 10^4 $gmol^{-1}$. The refractive index peaks (blue trace) that accompanied the two peaks suggested that the MMw is more concentrated than the HMw, and the UV peak (green trace) suggested that a UV absorbing species was co-eluting with the MMw material, the HMw is free from UV absorbing impurities. The UV absorbing material could be proteins or DNA. An attempt was made to separate the different polysaccharides using a preparative size exclusion chromatography (S-500 HR) whose fractionation range is between 4.0 x 10^4 to 2.0 x 10^7 $gmol^{-1}$ (https://www.scientificlabs.co.uk).

3.2.1 Purification and separation of the high and medium molecular weight polysaccharides produced by *L. fermentum* LF2

Fractionation by size exclusion chromatography was performed on the crude EPS using a Sephacryl S-500 HR column, with polysaccharides being eluted with ultrapure water, using the procedure described in section **2.2.7.2.1**.

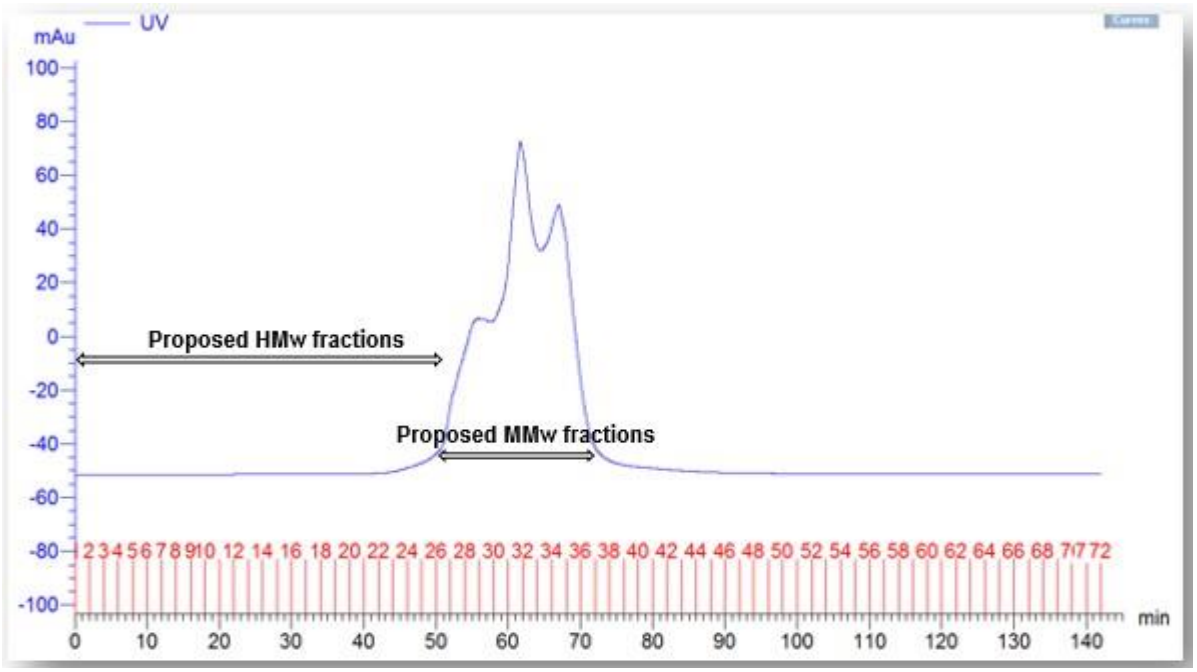

Figure 3.4: UV trace of the Sephacryl S-500 column ran on the crude EPS.

Analysis of the UV trace obtained from the UV detector connected to the AKTA PRIME instrument suggested that, UV absorbing material that eluted after the light scattering peaks passed through the column between fractions 26-36.

3.2.2 Quantification and determination of carbohydrate content of fractions eluting from the Sephacryl S-500HR column

To determine the location of the polysaccharides, the total carbohydrate content of each fraction was estimated by the Dubois method (phenol/sulfuric acid method) as described in section **2.2.7.3**. A calibration curve for glucose standard ranging from 20 to 100 ppm was plotted and the absorbance of the fractions were compared to that of the standards.

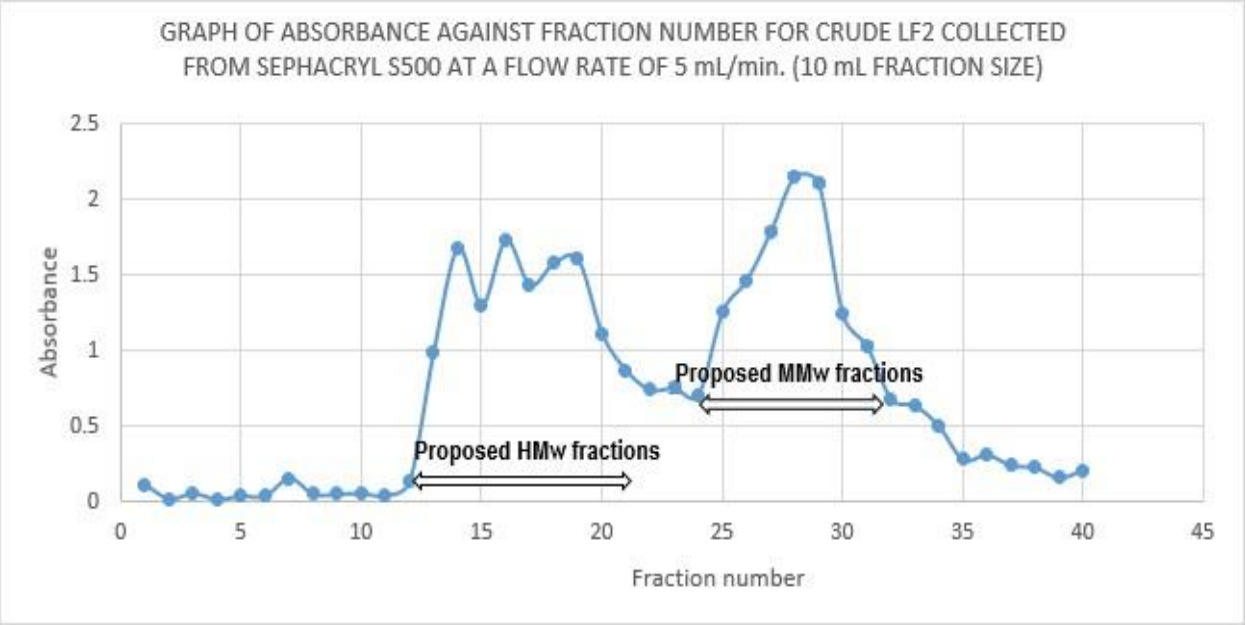

Figure 3.5: Carbohydrate concentration of fractions 1-40 collected from Sephacryl S-500 HR column.

Based on comparison between the UV trace obtained from AKTA PRIME instrument connected to the Sephacryl S 500 HR column and the Dubois results, fractions 1-9, 10-14, 15-19, 20-24, 25-30, 31-34 and 35-40 were combined respectively, with the expectation that the earlier fractions would contain the HMw polysaccharide and the later fractions would contain the MMw polysaccharide that elutes close to the UV peak. The combined fractions were concentrated, solid products

recovered by freeze-drying and ^{1}H-NMR spectra were recorded for each of the combined fractions.

Table 3.1: Quantity in (mg) of EPS recovered from Sephacryl S-500 HR column after lyophilising the fractions.

S/N	Fractions	Amount (mg)
1	1-9	0.0
2	10-14	5.8
3	15-19	5.0
4	20-24	3.8
5	25-30	22.4
6	31-34	17.5
7	35-40	0.8

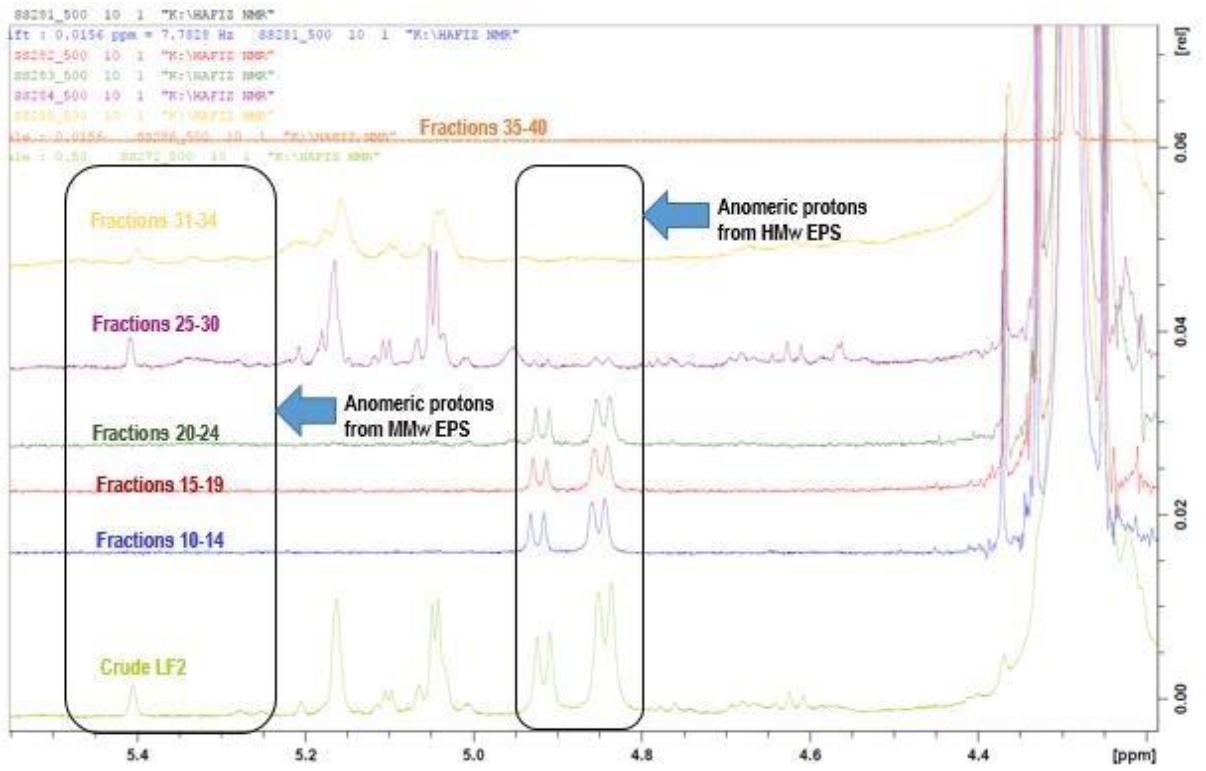

Figure 3.6: ^{1}H-NMR spectra recorded at 70 ^{o}C on the combined fractions collected from Sephacryl S 500 HR column eluted with ultrapure water, at a flow rate of 5 mLmin^{-1}, collecting 10 mL per fraction.

Analysis of the anomeric region of the combined fractions suggest that, the early eluting fractions (fractions 10-24) contained the HMw polysaccharide, whereas the MMw polysaccharide eluted in the later fractions (25-34). The amount (mg) of the combined fractions validated the SEC-MALLS results that the MMw polysaccharide

(22.4 mg) is more abundant than the HMw polysaccharide (14.6 mg). The combined HMw fractions were injected into SEC-MALLS using the procedure described in section **2.2.7.1**.

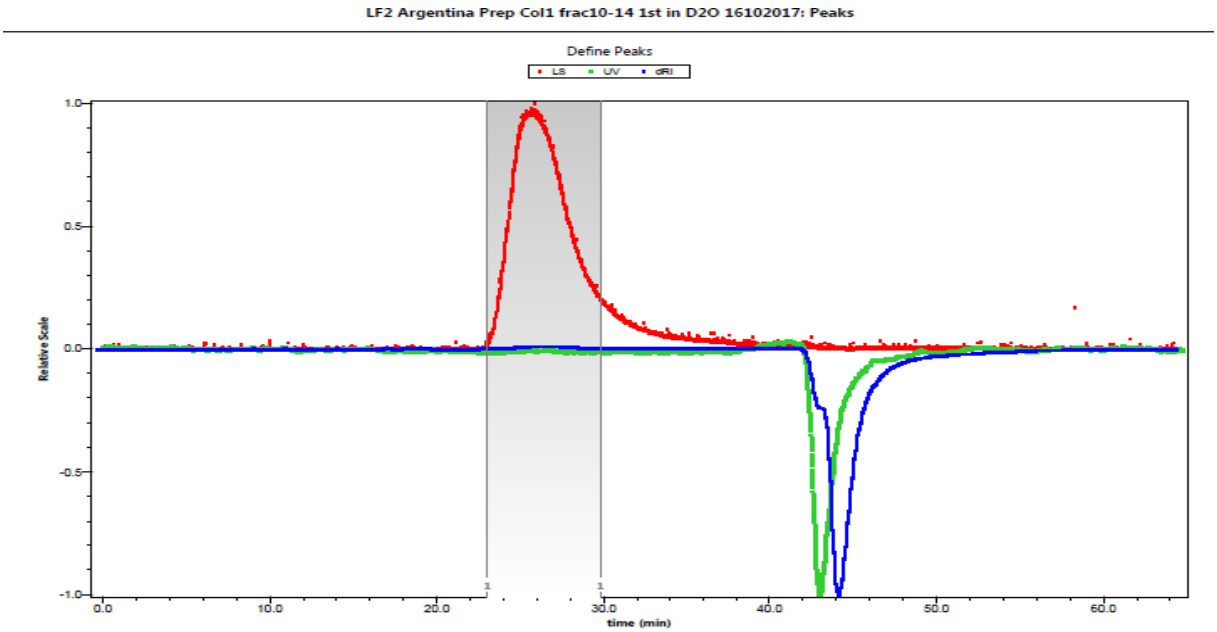

Figure 3.7: SEC-MALLS chromatogram of the combined fractions 10-14.

The SEC-MALLS trace for the combined HMw fractions (Fig 3.7) shows only one light scattering peak (RT = 26) with no UV trace. The HMw polysaccharide was determined to have a weight average molecular mass of 1.232 x 10^6 $gmol^{-1}$ and a polydispersity value of 1.104.

3.3 Structural characterisation of a HMw EPS produced by *L. fermentum* LF2

The fractions collected for the HMw material using the Sephacryl S500-HR column were freeze dried and used in characterising the structures.

3.3.1 Monomer analysis of the HMw polysaccharide by GC-MS

Monomer analysis of the HMw EPS by GC-MS was conducted after converting the EPS into its alditol acetates using the procedure described in section **2.2.8.2**. The acetylated monomers were then ran on the GC-MS. The retention time of the peak

obtained (RT=12.827 min) was compared with the alditol acetate standards of neutral sugars prepared for the purpose of this research and a mixture purchased from Sigma Aldrich, UK, containing inositol, mannitol, glucitol and galactitol.

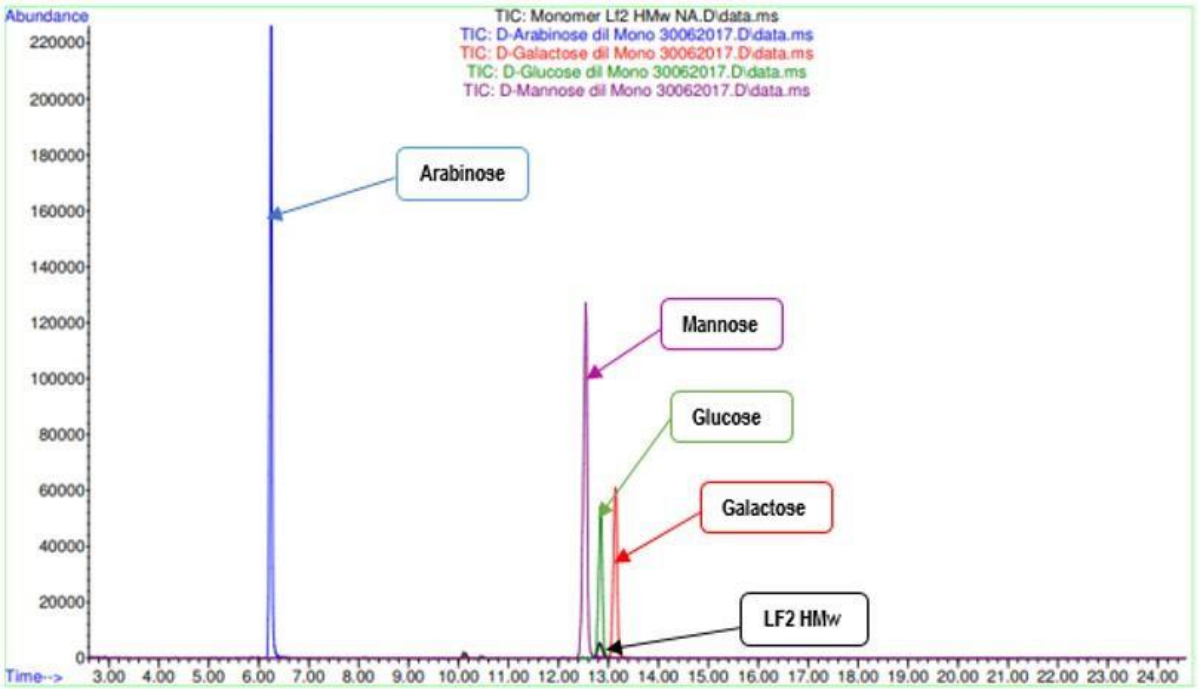

Figure 3.8: Overlaid GC trace of monomer analysis performed on the hydrolysed alditol acetate HMw EPS and that of alditol acetates of arabinose, galactose, glucose and mannose standards.

Comparison of the retention times of the standard sugar alditol acetates obtained: arabinose, 6.26; mannose, 14.49; glucose, 12.85 and galactose, 13.14 min, and that of the hydrolysed alditol acetate HMw EPS (12.83 min) suggests that the HMw EPS is a glucan (Fig 3.8).

3.3.2 Monomer analysis of the HMw polysaccharide by HPAEC-PAD

Monomer analysis of the HMw EPS was also performed by HPAEC-PAD using the procedure described in section **2.2.8.1**. Standards: fucose, rhamnose, galactose, glucose, xylose, mannose and fructose were run and their retention times were recorded. In order to obtain information on the presence of the respective monomer present in the sample, the retention time of the single peak produced by the hydrolysed HMw EPS (RT= 6.67 min) was compared to those generated by the standards. The retention time of the single peak corresponded to that which was generated by the

glucose standard as shown in the overlaid chromatogram in Fig 3.10. This validates the earlier result obtained from the monomer analysis performed by GC-MS, that the HMw EPS is a glucan.

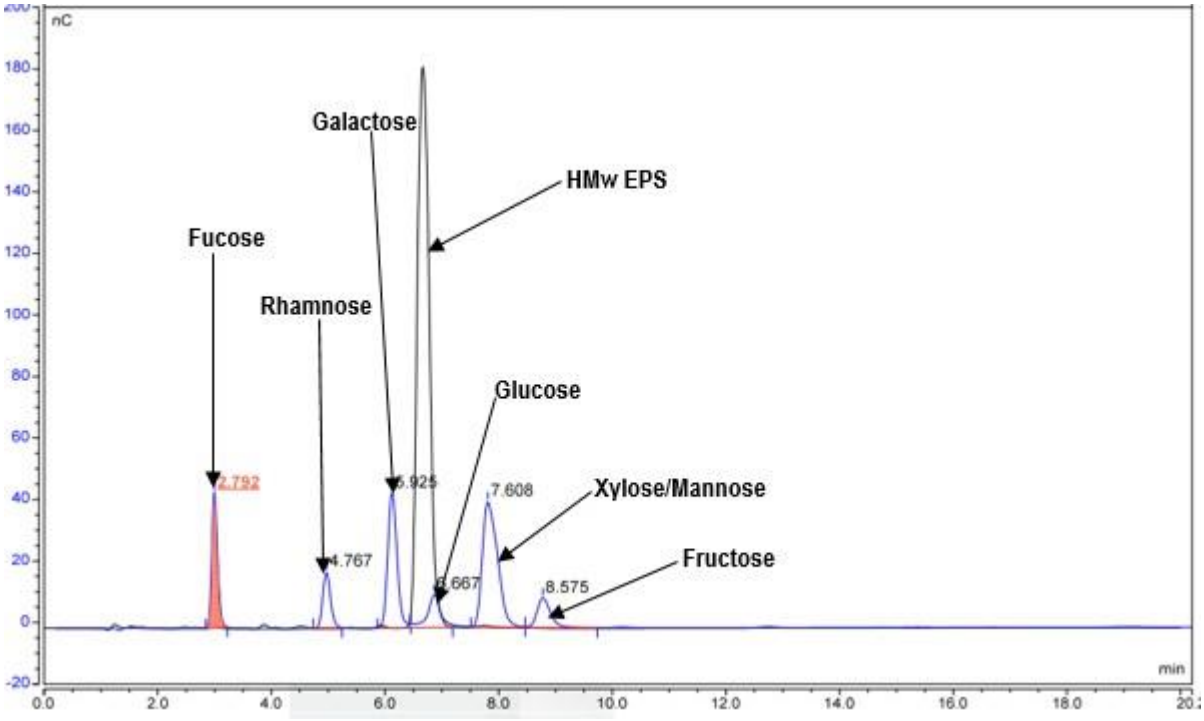

Figure 3.9: Overlaid HPAEC-PAD chromatogram of the monosaccharide standards (fucose, rhamnose, galactose, glucose, xylose, mannose and fructose) with the HMw EPS.

The HMw sample was further spiked with a glucose standard (50 ppm) and analysed again by HPAEC-PAD, the spiked sample eluted as a single glucose peak at (RT= 6.64 min) with a quantitative increase in the response factor (120 to 150) and an increase in peak area (21.44 to 32.91) which validates the earlier results.

3.3.3 Linkage analysis of the HMw glucan by GC-MS.

Methylation of the free hydroxyl groups of the HMw glucan and hydrolysis of the glycosidic linkages was performed. This was followed by reduction and acetylation as described in section **2.2.8.4**. Analysis of the partially methylated alditol acetates performed by GC-MS revealed the presence of three distinct peaks at 12.06, 15.05 and 17.96 min. respectively.

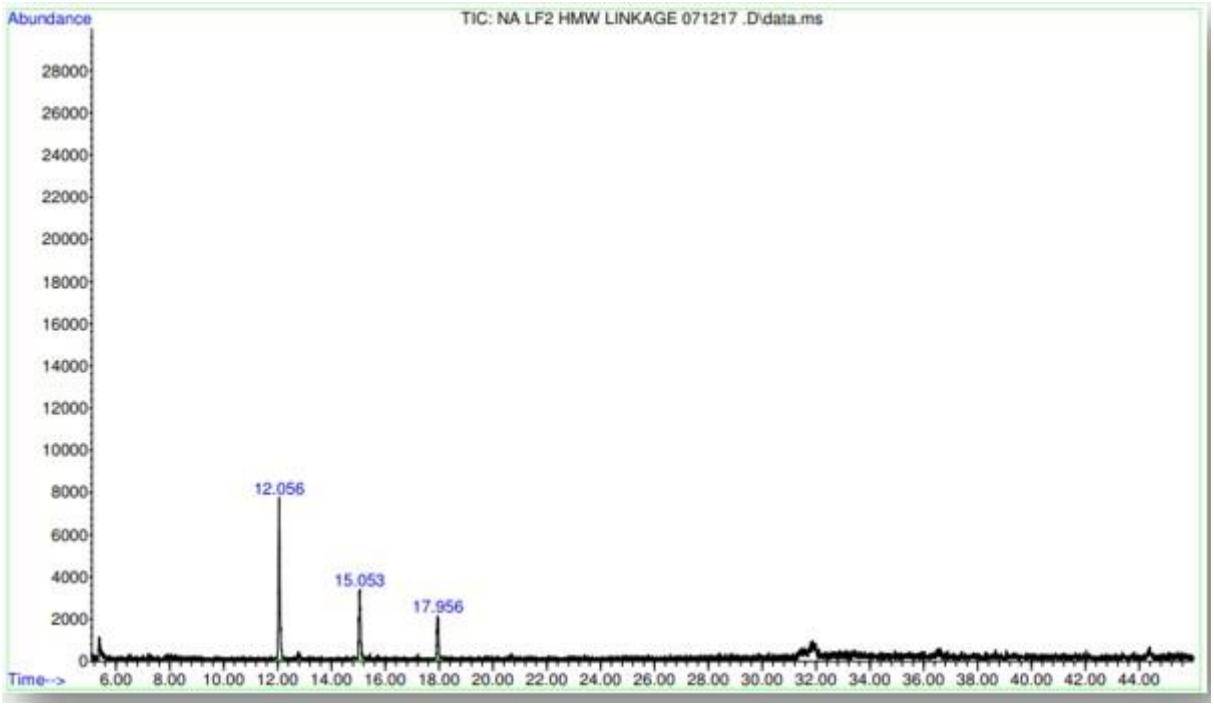

Figure 3.10: GC trace of linkage analysis on the HMw glucan.

The first peak on the chromatograph has a MS spectra corresponding to that of a non-reducing terminal hexose derivative. The methylated alditol acetate has a neighbouring methoxy groups on carbons 2, 3 and 4 which favours the cleavage between them and as such results in the formation of fragments with m/z 118, 161, 162 and 205 with relatively high abundances, (highlighted in red Fig 3.11a). The secondary cleavage of the fragment m/z 205 results in the formation of a fragment m/z 145 due to loss of acetic acid (Mw = 60). In a similar manner, fragments m/z 161 and 162 also resulted in the formation of a fragments m/z 101 and 102 respectively all due to loss of acetic acid. In addition, the secondary cleavage of fragments m/z 161 and 162 resulted in the formation of m/z 129 and 130 respectively due to loss of methanol (Mw = 32).

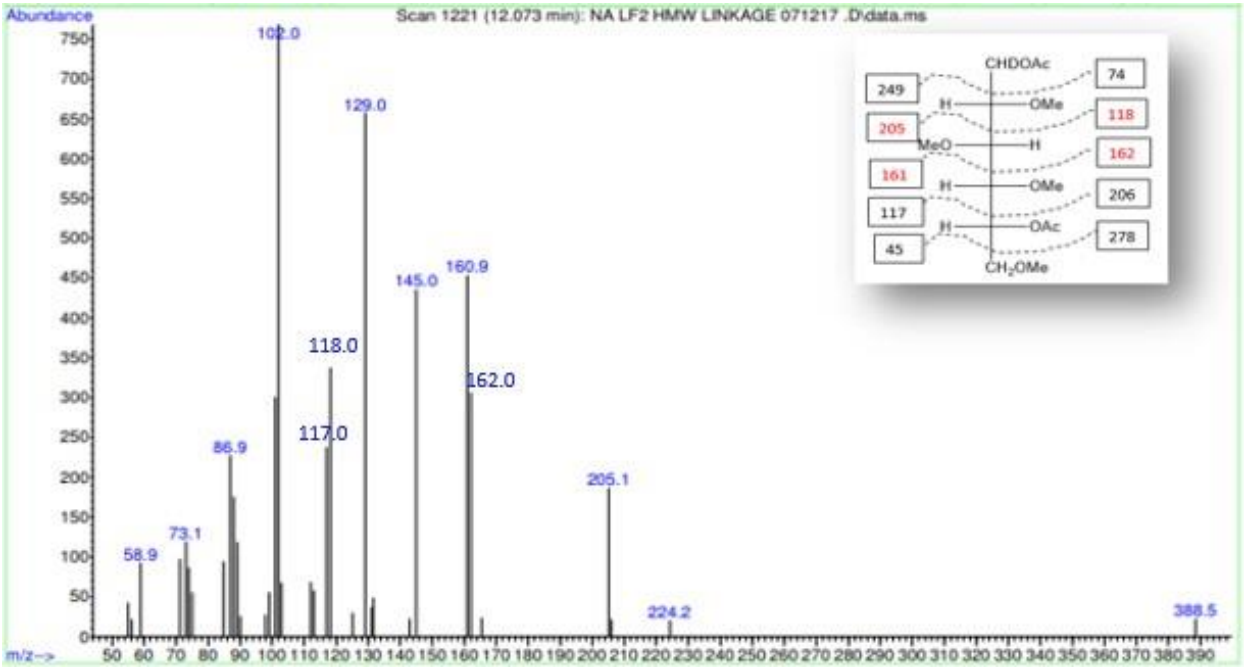

Figure 3.10a: MS fragmentation pattern of 12.06 min peak.

The MS fragmentation pattern generated was also analysed and compared with that which has been reported in the literature (McGinnis & Biermann, 1989). The MS of the 12.06 min peak is consistent with the presence of 1,5-di-*O*-acetyl-(1-deuterio)-2,3,4,6-tetra-*O*-methylglucitol derived from a non-reducing terminal glucose.

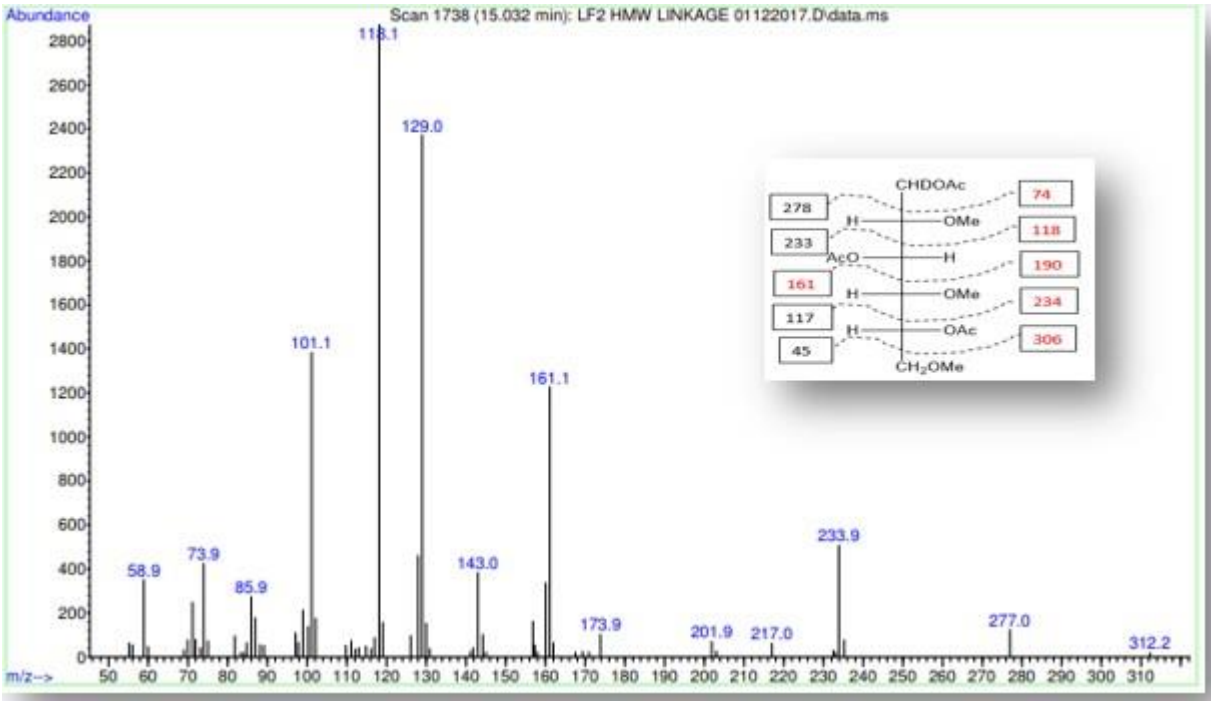

Figure 3.10b: MS fragmentation pattern of 15.04 min peak.

The second peak at 15.04 min peak is consistent with the presence of 1,3,5-tri-*O*-acetyl-(1-deuterio)-2,4,6-tri-*O*-methylglucitol derived from a 1,3-linked glucopyranose derivative in the main chain. The MS spectra of a 1,3-linked hexopyranose derivative reported in the literature was compared with that which was derived from the 15.038 min peak and both revealed the presence of primary fragments with m/z of 101, 118, 129, 161, 234 and 277 (McGinnis & Biermann, 1989). Uniquely for a 1,3-linked hexopyranose sugar, the acetyl group on carbon 3 and the methoxy groups on carbons 2 and 4, give rise to the formation of the primary fragments with m/z of 118 and 161 with relatively high intensities. This confirmed that the 15.038 min peak is derived from a 1,3-linked glucopyranose.

The third peak at 17.956 min peak revealed the presence of 1,2,3,5-tetra-*O*-acetyl-(1-deuterio)-4,6-di-*O*-methylglucitol derived from a 1,2,3-brached glucopyranose in the main chain bearing the side chain. Uniquely, for a 1,2,3-linked hexopyranose sugar, the acetyl group on carbons 2 and 3 and the methoxy group on carbon 4, give rise to the formation of the primary fragment with m/z of 262. This further confirmed that the 17.956 min peak is from a 1,2,3-linked glucopyranose.

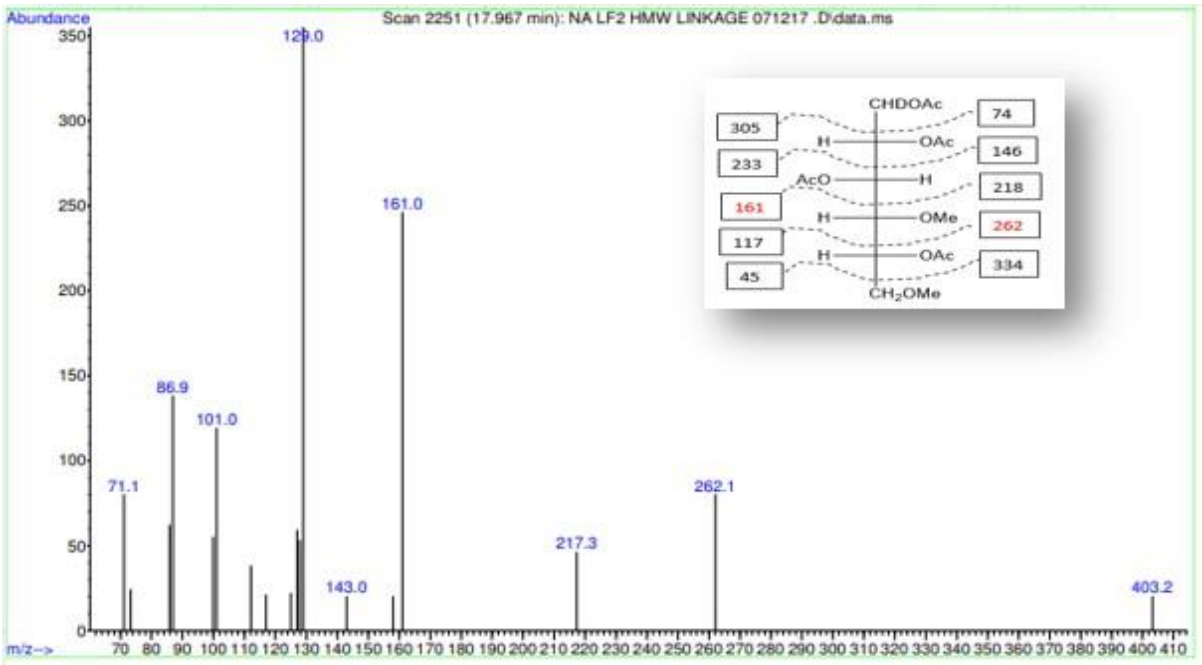

Figure 3.10c: MS fragmentation pattern of 17.96 min peak.

Table 3.2: Linkage types deduced for the HMw EPS produced by *Lactobacillus fermentum* LF2.

Peak	Retention time	Linkage type
1	12.06	Non-reducing-terminal glucopyranose
2	15.04	1,3-linked glucopyranose
3	17.96	1,2,3-linked glucopyranose

3.3.4 Determination of absolute configuration of the HMw glucan by GC-MS.

The analysis by GC-MS of the acetylated (+)-2-butyl glycosides derivatives produced from the HMw glucan was performed using the procedure described in section **2.2.8.3**. The analysis of the peaks generated by GC-MS on the HMw glucan was performed by the comparison of the retention times with peaks generated using D- and L-glucose standards. Two peaks were generated for each of the acetylated (+)-2-butyl glycosides standards (D- and L- glucose), as well as the hydrolysed acetylated (+)-2-butyl glycosides from the HMw glucan. The retention time of the peaks generated by the hydrolysed acetylated (+)-2-butyl glycosides from the HMw glucan were compared with those of the standards (D- and L-glucose) and the comparison showed that the glucose that makes up the HMw EPS has the D-configuration, as indicated in table 3.3 below.

Table 3.3: Retention times of D- and L-glucose standards, and that of the HMw by GC-MS.

Sample	Retention time of the 1st peak (min.)	Retention time of the 2nd peak (min.)
D-Glucose	**11.75**	**12.55**
L-Glucose	11.92	12.29
LF2 HMW	**11.74**	**12.55**

3.3.5 1D-NMR

The number of monosaccharides present in the repeating unit of the glucan was determined by inspecting the anomeric region of the ^{1}H NMR spectrum recorded for

the HMw EPS produced by *L fermentum* LF2 using the procedure described in section **2.2.8.5**. The ^{1}H-NMR spectra recorded showed an anomeric region with two distinct peaks at δ 4.93 ppm and δ 4.86 ppm in a ratio of 1:2 respectively, which suggests that the HMw glucan contains a trisaccharide repeating unit. The monosaccharide anomeric protons were labelled (A, B and C). Integral ratios of the ring protons with respect to the single anomeric gave values of 4:1:4:1:6:1:1 which sums up to 18 and accounting for all of the remaining protons.

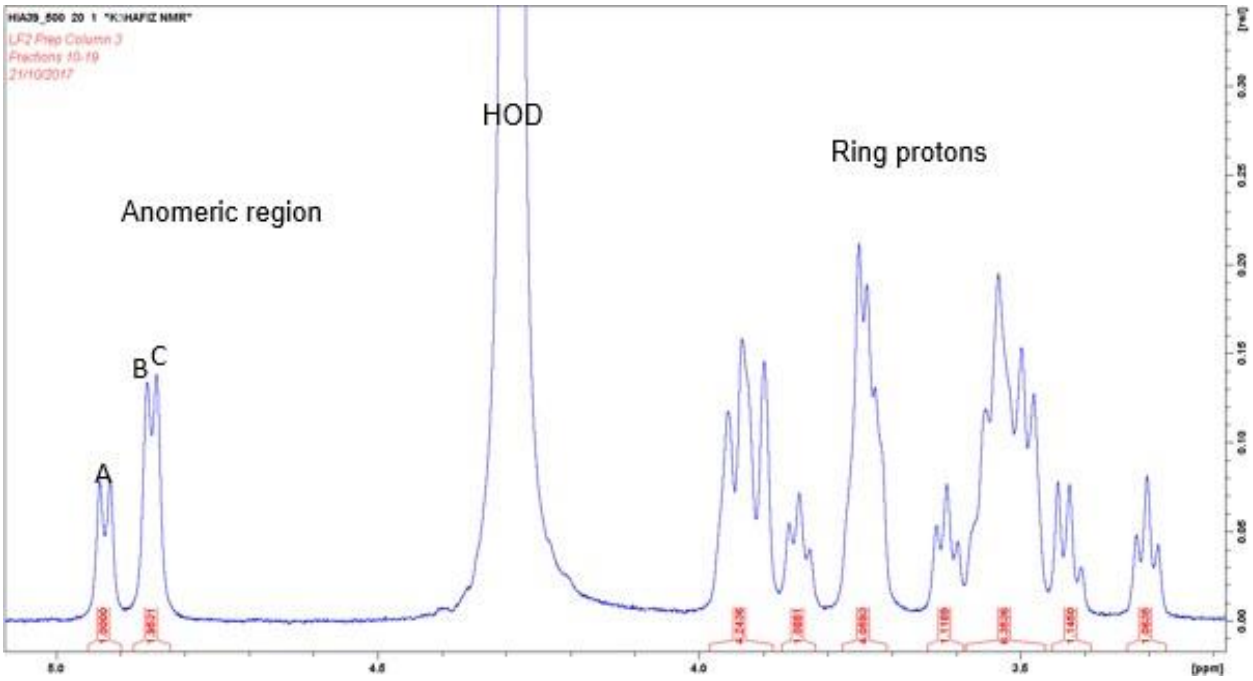

Figure 3.11: ^{1}H-NMR spectra of the HMw glucan recorded at 70 °C.

The appearance of the anomeric protons of A, B and C, all at high field at δ 4.89, 4.82 and 4.82 ppm with $^{3}J_{1,2}$ coupling constants of 7.90, 7.50 and 7.50 Hz respectively, coupled with the visual observation of their peaks as doublets is an indication that the D-glucopyranoses are in their β-anomeric configuration. It can then be said that, the trisaccharide repeating unit is composed of β-D-glucopyranose moieties.

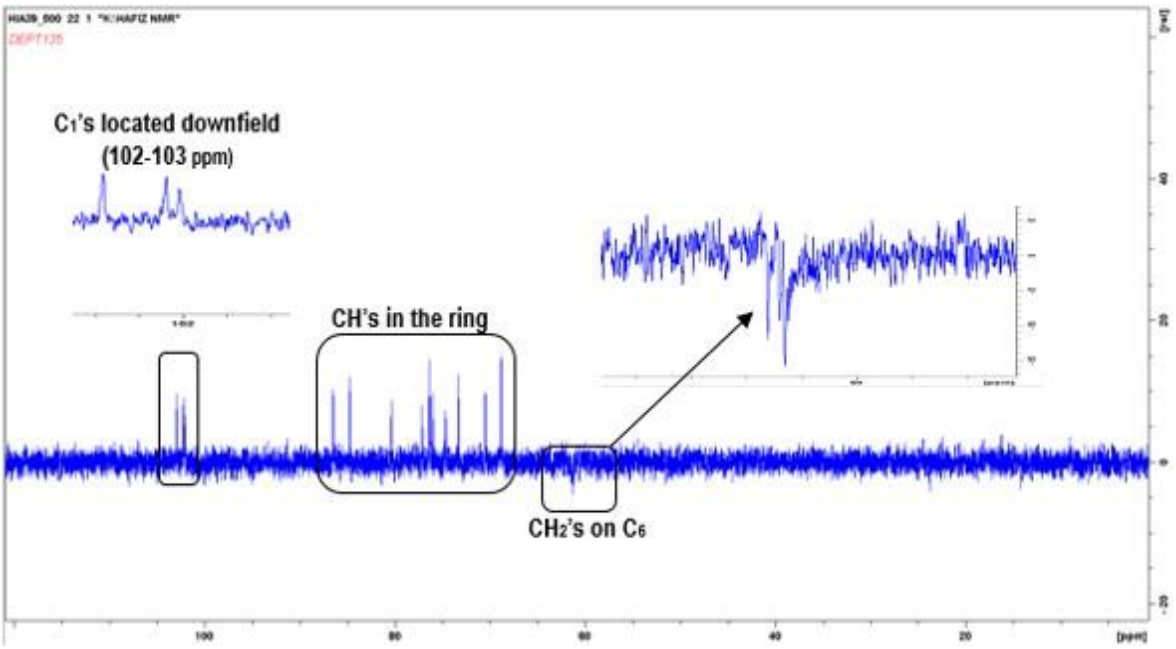

Figure 3.12: DEPT 135 ^{13}C-NMR spectra of the HMw β-D-glucan.

A DEPT 135 ^{13}C-NMR spectrum performed on the purified HMw glucan showed all the carbons present that are attached to a hydrogen (–CH and –CH_2) in the sample. On the DEPT spectrum, CH are shown as positive peaks (70-85 ppm), whereas the CH_{2s} on C_6 are shown as negative peaks (60-63 ppm) and are characteristic of those expected for monosaccharides that are not engaged in glycosidic linkages via the C-6 position. Being next to the ring oxygen atom, the C_{1s} are located downfield between 102 to 103 ppm. The three signals observed downfield are consistent with the ^{1}H-NMR spectrum recorded on the HMw glucan which showed an anomeric region with two distinct peaks at δ 4.93 ppm and δ 4.86 ppm with the latter peak suspected to be from two overlapping doublets, which further confirms that the HMw β-D-glucan contains a trisaccharide repeating unit.

3.3.6 2D- NMR

Several 2D-NMRs were generated and used in obtaining the chemical shifts of individual protons and carbons that forms the repeating unit of the HMw β-D-glucan. Inspection of a ^{1}H-^{1}H-COSY spectrum enabled identification of H1-H2 cross peaks and identification of the H2 protons via scalar coupling. Starting from the anomeric

proton, the scalar coupling could be tracked to H2. Each H2 contour of A, B and C appeared in a clear part of the spectrum, the contours were distinct and each has a unique chemical shift, these were labelled as $A_{H\text{-}2}$ (3.273 ppm), $B_{H\text{-}2}$ (3.813 ppm) and $C_{H\text{-}2}$ (3.585 ppm).

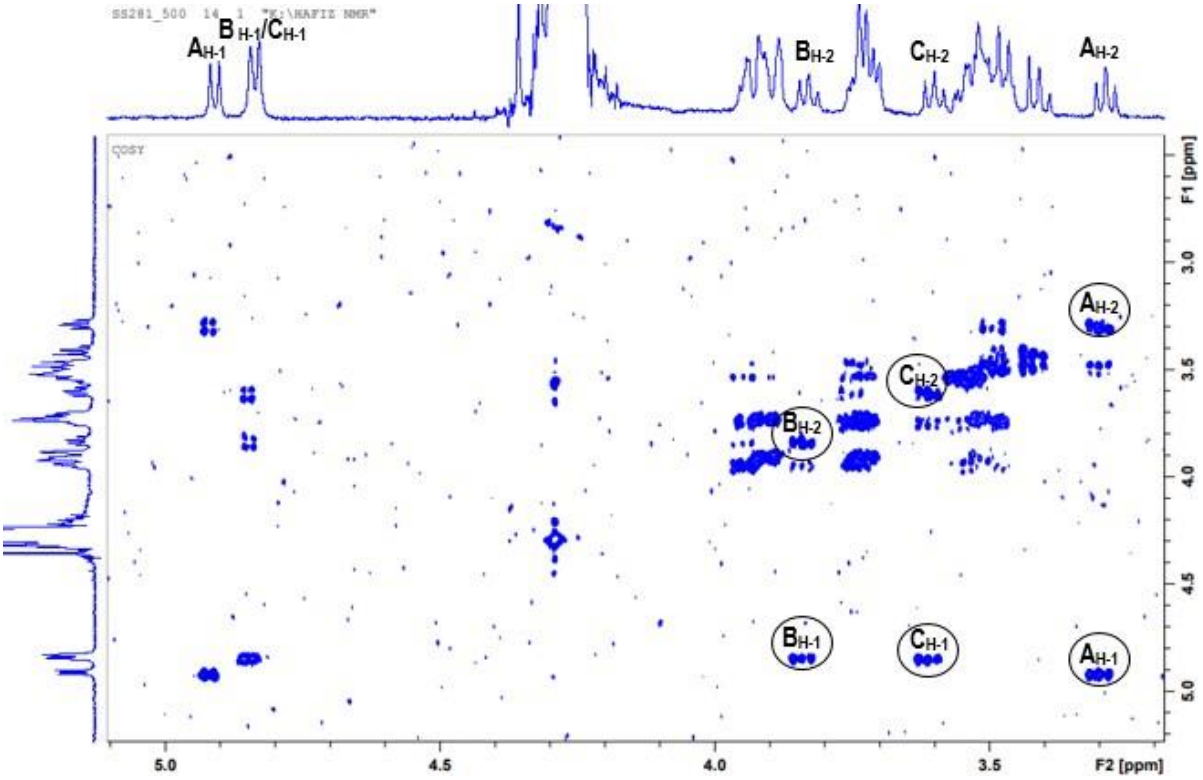

Figure 3.13: ^{1}H-^{1}H-COSY spectrum for the HMw β-D-glucan recorded at 70 °C on a Bruker 500 MHz spectrometer**.**

The chemical shifts of the remaining ring protons were determined and assigned by following the transmission of scalar coupling (H2 to H6) on the ^{1}H-^{1}H-TOCSY spectrum, which enables the detection of protons within a common spin system that are interacting through bonds (three bonds, attached to adjacent carbons). As such, by using a combination of ^{1}H-^{1}H-COSY (blue contours in Fig 3.14) and ^{1}H-^{1}H- TOCSY spectrum (black contours in Fig 3.15), the scalar coupling of each of the protons in A, B and C were tracked from the anomeric protons to the remaining ring protons.

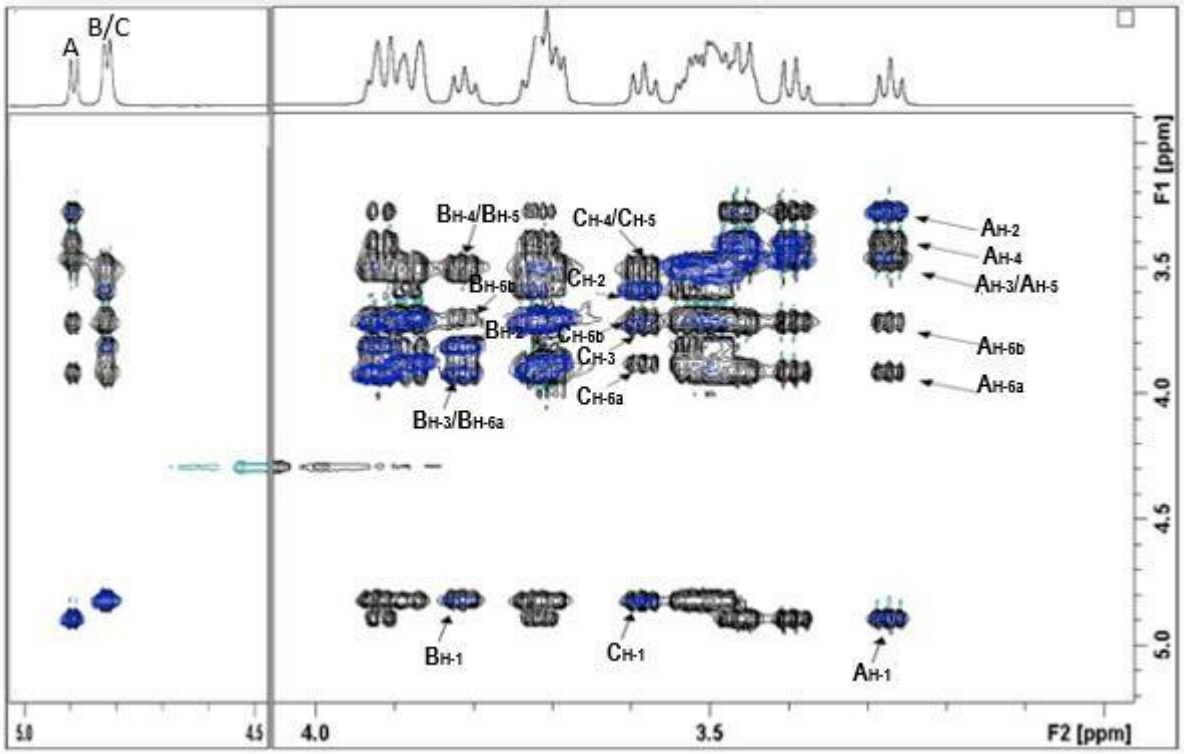

Figure 3.14: Overlaid ^{1}H-^{1}H-COSY (blue contours) and ^{1}H-^{1}H-TOCSY (black contours) spectra for the HMw-β-D-glucan recorded at 70 °C a Bruker 500 MHz spectrometer.

From the combination of ^{1}H-^{1}H-COSY and ^{1}H-^{1}H- TOCSY spectra, (Fig 3.14), itcan be deduced that the H-4s of A (3.39 ppm), B (3.51 ppm) and C (3.51 ppm) were located in the range of 3.40-3.80 ppm, which are characteristic of those expected for H-4s of a glucan (Harding et al., 2005).

A ^{1}H-^{13}C-HSQC-TOCSY spectrum (Fig 3.15) was used to identify the location of the carbon resonances present in A, B and C. Being next to the ring oxygen atom, the anomeric carbons (C-1s) were located downfield 102.85, 102.14 and 101.97 ppm for A, B and C respectively. The carbon atoms carrying primary hydroxyl groups at the sixth position were located at 61.55, 61.33 and 61.22 ppm for A, B and C which are characteristic of those expected for C-6s not involved in glycosidic linkages. The chemical shifts for the ^{1}H and ^{13}C resonances for A, B and C assigned from the ^{1}H-^{13}C-HSQC-TOCSY spectrum (Fig 3.15) are shown in table 3.4.

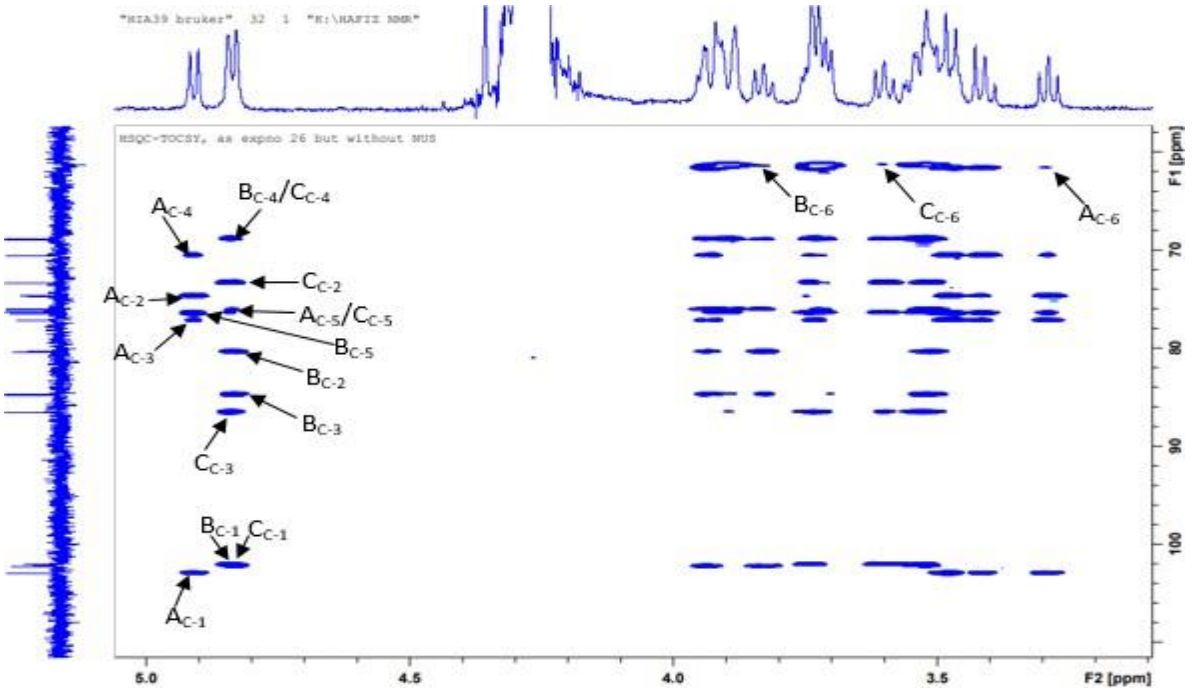

Figure 3.15: ^{1}H-^{13}C-HSQC-TOCSY spectrum recorded at 70 °C on a Bruker 400 MHz spectrometer.

Table 3.4: ^{1}H and ^{13}C NMR chemical shifts (δ, ppm) for the HMw polysaccharide

	H-1 **C-1**	**H-2** **C-2**	**H-3** **C-3**	**H-4** **C-4**	**H-5** **C-5**	**H-6a** **C-6**	**H-6b** **C-6**
A	4.93 102.7	3.31 74.7	3.50 77.0	3.40 70.4	3.50 76.3	3.96 61.6	3.75 61.6
B	4.85 102.2	3.84 **80.1**	3.95 **84.2**	3.55 68.8	3.45 75.8	3.94 61.6	3.74 61.6
C	4.85 101.9	3.62 73.2	3.75 **86.6**	3.51 68.8	3.47 76.3	3.90 61.2	3.73 61.2

Table 3.5: ^{1}H and ^{13}C NMR chemical shifts (δ, ppm) for a methyl-β-D-glucopyranoside (Bock & Pedersen, 1983); (www.organ.su.se/gw/doku.php/id=sop:a703)

	H-1 **C-1**	**H-2** **C-2**	**H-3** **C-3**	**H-4** **C-4**	**H-5** **C-5**	**H-6a** **C-6**	**H-6b** **C-6**
β-Glc	4.37 104.0	3.28 74.1	3.50 76.8	3.40 70.6	3.46 76.8	3.74 61.8	3.92 61.8

The points of linkages of the sugars A, B and C in the HMw β-D-glucan were identified by comparing the carbon chemical shifts to those of an unsubstituted methyl-β-D-glucopyranoside published in the literature (Bock & Pedersen, 1983). The high chemical shifts of C-2 (80.1 ppm) and C-3 (84.2 ppm) observed in B relative to the C-2 (74.1 ppm) and C-3 (76.8 ppm) in methyl-β-D-glucopyranoside (table 3.06) identifies

C as being a 2,3-liked β-D-glucopyranose. The chemical shift of C-3 in C, shifted to 86.6 ppm from the normal C-3 of a methyl-β-D-glucopyranoside identifies it as a 3-liked β-D-glucopyranose. The resonance positions of C-1 to C-6 for A are similar to that which is observed for a methyl-β-D-glucopyranoside, and as such was identified as a terminal β-D-glucopyranoside. This validates the linkage analysis which suggested the presence of a non-reducing terminal, a 1,3-linked and a 1,2,3-linked glucopyranose.

The sequence in which the monosaccharides occur in the repeating unit was determined by interpretation of a ROESY spectrum. In the ROESY spectrum, inter-residue coupling of protons through space (less than 5Å) can be determined. On the ROESY spectrum performed on the HMw β-D-glucan, inter-residue NOEs that show interactions between different protons based on linkages were observed between the anomeric proton on A (A_{H-1}, 4.93 ppm) and B_{H-2} (3.84 ppm), which confirms the linkage between the anomeric position on A to the 2-position of B. Another inter-residue NOE showed a strong interaction correlating the anomeric proton of C (C_{H-1}, 4.85 ppm) to the H-3 proton on B (B_{H-3}, 3.95 ppm) and that of the anomeric proton of B (B_{H-1}, 4.85 ppm) to the H-3 proton on C (C_{H-3}, 3.75 ppm).

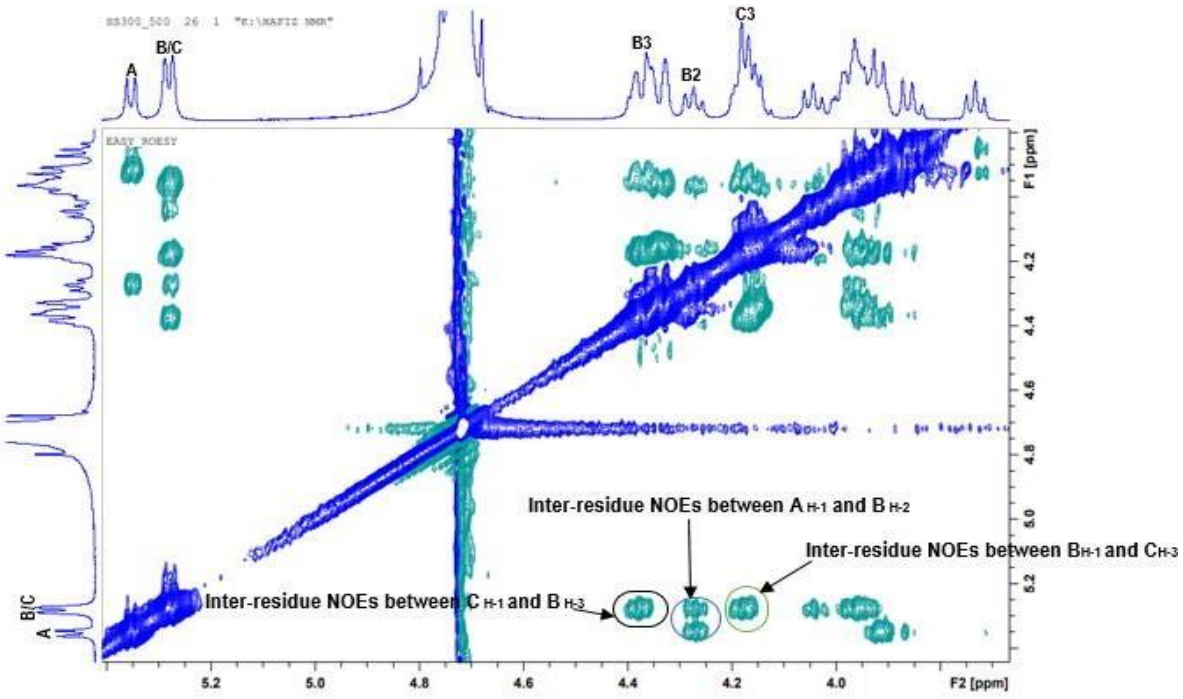

Figure 3.16: ROESY spectrum of the HMw glucan showing the cross peaks derived from two protons based on inter-residue coupling through space: black, C_{H-1} to B_{H-3}; blue, A_{H-1} to B_{H-2}; green, B_{H-1} to C_{H-3}

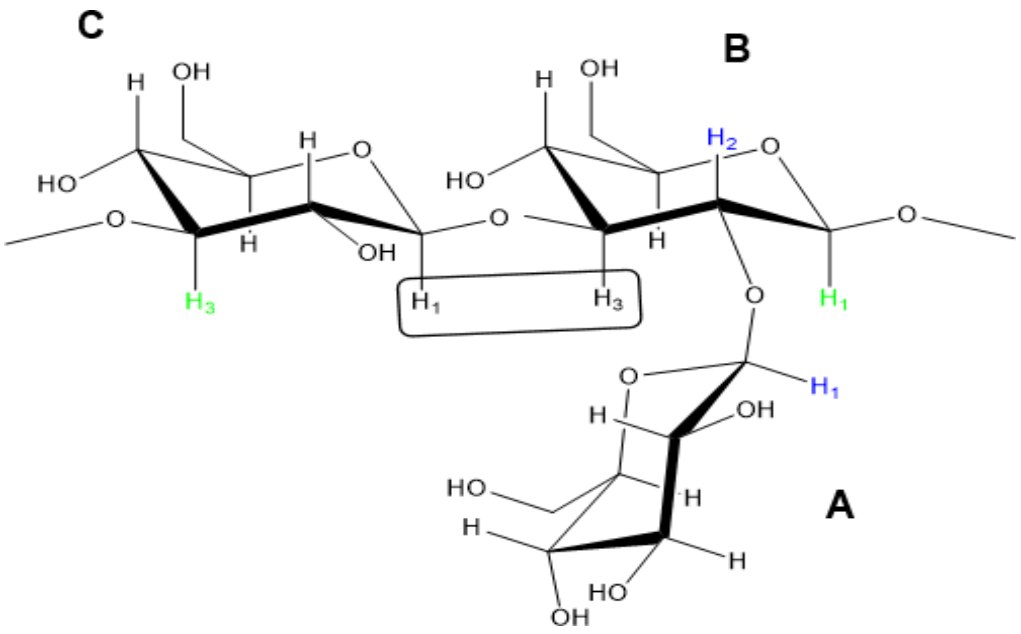

Figure 3.17: Arrangement of the trisaccharide repeating unit in the HMw polysaccharide showing the interactions between protons based on inter-residue coupling through space: black, C_{H-1} to B_{H-3}; blue, A_{H-1} to B_{H-2}; green, B_{H-1} to C_{H-3}.

The sequence of which the monosaccharides occur in the repeating sugar units was confirmed by the examination of a HMBC spectrum. In a HMBC spectrum, the scalar coupling of carbon and hydrogen through more than one bond can be determined. On the HMBC spectrum performed on the HMw β-D-glucan, examination of the cross peaks that shows interactions between a proton and a carbon either side of glycosidic bond were observed between the anomeric proton on A ($A_{H-1,}$ 4.93 ppm) and carbon 2 on B_{C-2} (80.1 ppm), which confirms the linkage between the anomeric position on A to the 2-position of B. Another two sets of cross peaks showed strong interactions correlating the anomeric proton of C ($C_{H-1,}$ 4.85 ppm) to the third carbon on B ($B_{C-3,}$ 84.2 ppm) and that of the anomeric proton of B ($B_{H-1,}$ 4.85 ppm) to the third carbon on C ($C_{C-3,}$ 86.6 ppm).

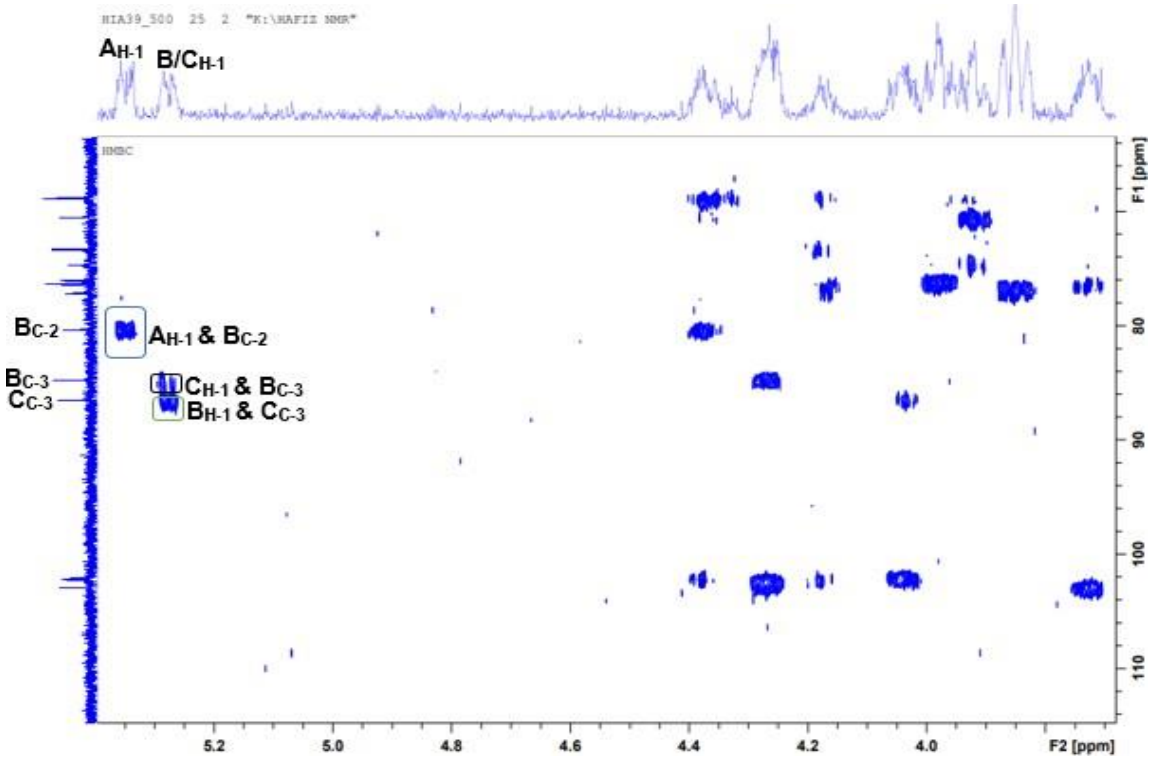

Figure 3.18: HMBC spectrum of the HMw glucan showing the cross peaks derived from a proton and a carbon based on inter-residue coupling via glycosidic bond: C_{H-1} to B_{C-3}; black, A_{H-1} to B_{C-2}; blue, B_{H-1} to C_{C-3}; green.

In summary, the bacterial strain *L. fermentum* LF2 synthesized two EPSs fractions during growth, these two fractions were separated by preparative size exclusion chromatography using a Sephacryl S 500 HR column to give a HMw (1.23×10^6 $gmol^{-1}$) and MMw (8.8×10^4 $gmol^{-1}$) polysaccharides. Analysis of the HMw polysaccharide on SEC-MALLS revealed that it is free from proteins and other contaminants. Monomer analysis performed on the hydrolysed HMw polysaccharide using HPAEC-PAD and GC-MS revealed that the HMw EPS is a glucan. Determination of absolute configuration by GC-MS showed that the glucan had the D-configuration. ^{1}H-NMR indicated that it contained a trisaccharide-repeating unit and each had a β-anomeric configuration. Linkage analysis by GC-MS showed the presence of a terminal, a 1,3-linked and a 1,2,3-linked glucopyranose. A combination of COSY, TOSCY and HSQC NMR experiments identified the individual protons and carbons present in the repeating unit. The linkages were assigned to the glucose moieties present in the repeating unit by examining the change in carbon resonances revealed on the HSQC-TOCSY spectrum. ROESY and HMBC experiments confirmed the sequence of the repeating sugar units based on interactions through space and via the glycosidic bond

respectively. As such, the HMw polysaccharide has been shown to possess a trisaccharide-repeating unit having the following structure:

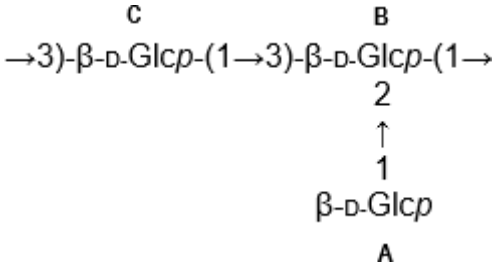

As mentioned in the introduction, β-glucans are generated by a number of microorganisms, including fungi and bacteria. β-Glucans have been associated with numerous health-promoting benefits, in the prevention and control of obesity, cardiovascular diseases, diabetes and cancer, as well as prebiotic properties (Maheshwari, Sowrirajan, Joseph, & Fibre, 2019; Stack, Kearney, Stanton, Fitzgerald, & Ross, 2010) . Stack et al., (2010) discovered that the β-glucan produced by *Lactobacillus paracasei* NFBC 338 was associated with significant increase in protection of the strain when subjected to: heat stress (60-fold increase), acid stress (20-fold), stimulated gastric juice stress (15-fold) and a 5.5-fold increase when subjected to bile stress in comparison to the control strain. The addition of a 2-substituent to -(1,3)-β-D-glucan has been shown to augment stress tolerance, enhance growth and increase the probiotic potential of three lactobacilli strains (Russo *et al*., 2012). Most of these β-glucans generated have main chains composed of β-(1,3)-linked glucoses, but only a small number include 1,2-linked branches. The structure of the HMw EPS produced by *L. fermentum* LF2 was found to be the same as that which was produced by three other strains of bacteria including: *Pediococcus damnosus* 2.6, *Lactobacillus spp*. G-77 and *Oenococcus oeni* I4.

Our collaborators from Argentina have previously reported the biological activity of the crude EPS from *L. fermentum* LF2, they reported that the EPS mixture protected mice against *Salmonella* infection and have shown some moderate immunomodulatory activity. With this in mind, work was undertaken to study the biological activity of the HMw EPS. The biological activity of the purified HMw EPS was investigated by Dr Ana Vitlic at the University of Huddersfield. A quick summary

of the results is provided below. The purified HMw material from the characterisation studies reported above was used in the biological activity assay.

3.4 Evaluation of immunomodulatory activity of the HMw EPS

In order to examine immunomodulatory effect of the purified HMw EPS; peripheral blood mononuclear cells (PBMC) were used. These cells, although different in composition and activation status than immune cells of gastrointestinal tract (GIT) share some of the characteristics with them, such as pattern recognition receptors as well as cytokine production in response to various stimuli (Abbas *et al*., 2014). This, in combination with them being easily isolated from the whole blood, make PBMC a useful tool for better understanding of effect of different compounds on mucosal immunity of the GIT.

Evaluation of immunomodulatory activity of the HMw β-glucan performed on PBMC for 24 h led to an increase in cell viability, as well as an increase in the production of TNF-α in comparison with controls. On the other hand, exposure of PBMC to the HMw β-glucan for 24 h and subsequent removal of the EPS, followed by exposure of the PBMC to LPS revealed significant reduction in TNF-α production. This result indicates that the HMw β-glucan imparts immunotolerance in PBMC and the EPS could play a vital role during the release of proinflammatory cytokines by preventing an excessive inflammatory response. Given the fact that TNF-α has a central role in causing inflammatory bowel diseases such as Crohn's disease and ulcerative colitis, this is a very promising result.

The structure and size of EPS produced by different LAB strains are responsible for the EPS's ability to stimulate immune responses (Hidalgo-Cantabrana *et al*., 2012). Hidalgo-Cantabrana *et al*., (2012) proposed that, low molecular weight EPS and/or EPS having a negative charge are able to act as mild stimulators of immune cells, whereas high molecular weight EPS with no charge, present a suppressive profile. Indeed, the proposal seemed to have worked well, as the HMw EPS synthesised by *L. casei* Shirota acted by reducing excessive production of pro-inflammatory cytokines such as TNF-α, IL-12, IL-10 and IL-6 by immune cells against its own stimulating

components and also against endotoxins such as LPS that normally would induce an immune response (Yasuda, Serata, & Sako, 2008). Similarly, a HMw EPS producing *L. rhamnosus* RW-9595M induced low levels of TNFα and IL-6. Immune suppression within peripheral blood mononuclear cells (PBMC) was also induced by a HMw EPS producing *Lactobacillus paraplantarum* BGCG11 (Hidalgo-Cantabrana *et al*., 2012). Fanning *et al*., (2012) reported similar behavioural patterns of the immune cells when EPS produced by *Bifidobacterium breve* UCC2003 was used as stimulant on spleen cells, thereby significantly lowering the levels of pro-inflammatory cytokines including TNF-α and IL-12, although the EPS has not been fully characterised, the EPS was said to be of HMw.

On the other hand, as earlier stated in the introduction, structure has an impact on the water solubility of polysaccharides; solubility increases with decrease in molecular weight and solubility is assumed to be an important parameter in the biological recognition and effects of glucans. Reduction in molecular weight of β-glucans from 6.87×10^5 to 1.56×10^5 has previously been shown to decrease the viscosity of the solution, thereby increasing the *in vitro* bile-acid binding. Low molecular weight β-glucans produce more short-chain fatty acids compared to high molecular weight β-glucans which was attributed to greater water solubility of the low molecular weight β-glucans (Kim & White, 2009).

The HMw β-glucan produced by *L. fermentum* LF2 has already shown a role in reducing inflammation produced by LPS. Various depolymerisation methods were employed in this research in an attempt to reduce the size of the β-glucan in order to further understand its structure-activity relationship. This was performed in collaboration with an undergraduate project student, Rhys Carr.

3.5 Depolymerisation of the HMw β-glucan

Since biological activity of an EPS has previously been related to the size of the EPS, experiments were undertaken in this research to see if it was possible to reduce the molecular mass of the HMw β-glucan. At the time of performing this work, it was not possible to get access to SEC-MALLS, as such, an alternative method was needed

for determining the molecular mass of the sample. A slightly more detailed method was employed in which the elution volume of the samples were compared with that of known standards having similar structures and defined molecular masses.

Depolymerisation of the β-glucan was monitored by plotting a graph of the log of the known average molecular mass of standards against their elution volumes, the resultant equation obtained from the graph was used in calculating the average molecular mass of the de-polymerised samples (Table 3.6 below).

Table 3.6: Average molecular mass of the standards, their log average molecular weight and their elution volumes.

Standard	Molecular mass ($gmol^{-1}$)	Log molecular mass	Elution volume (min)
Pullulan	800000	5.90	18.87
Pullulan	110000	5.04	22.69
Dextran	50000	4.70	24.39
Dextran	25000	4.40	25.14
Dextran	12000	4.08	26.20
Dextran	5000	3.70	27.26

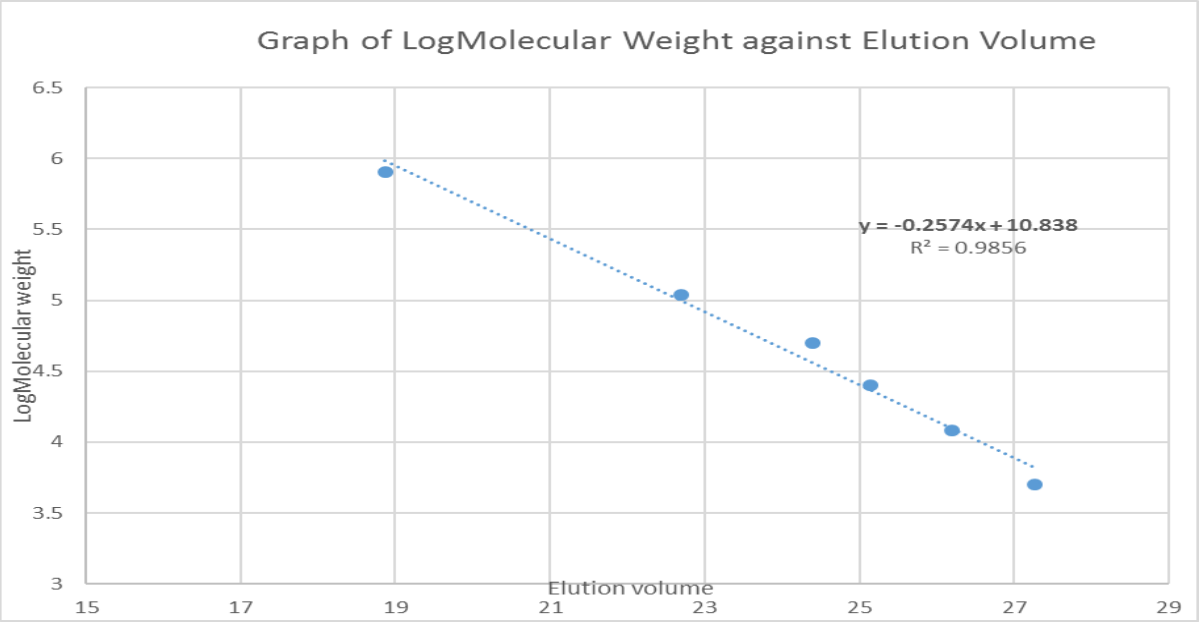

Figure 3.19: Graph of Log molecular mass of the standards against their elution volumes.

3.5.1 Microwave assisted depolymerisation of the HMw β-glucan

The first procedure that was employed to depolymerise the samples was microwave heating. The β-glucan (1000 ppm, 4 mL) was placed in a microwave and heated for 5 min at 120 °C using the procedure described in section **2.2.8.8**. After every 5 min, aliquots (0.5 mL) were removed and injected into the analytical SEC for analysis using the chromatographic conditions described in section **2.2.7.1**. The change in average molecular weight of the β-glucan per 5 min microwave heating time was determined. The heating was repeated 5 times and the average molecular mass of the samples was obtained by comparison of their elution volumes with the calibration curve of molecular weight standards (Fig 3.19).

Table 3.7: Average molecular mass of the β-glucan before and after heating at 120 °C for 5 min, repeated 5 times.

Run number	Average molecular mass ($gmol^{-1}$)	Percentage of initial molecular mass (%)
0	1109716	100.0
1	351444	31.7
2	194292	17.5
3	115330	10.4
4	92072	8.3
5	77994	7.0

A graph of the average molecular mass of the samples was plotted against their run number, Fig 3.20 (below):

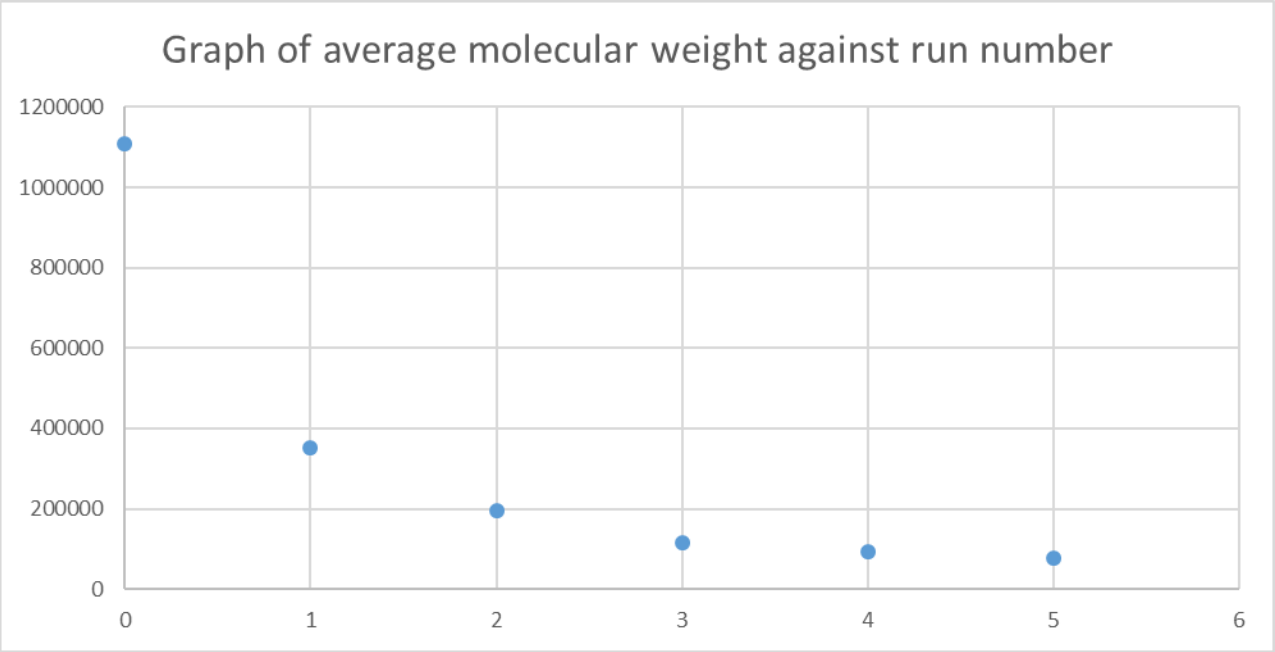

Figure 3.20: Graph of average molecular mass of the β-glucan before and after heating every 5 min for 25 min against the run times.

From the results obtained, it can be deduced that microwave assisted depolymerisation significantly decreased the molecular mass of the β-glucan to 31.7 % of the original Mw after the first 5 min of microwave heating, after which time the percentage reduction in molecular mass reduces with each subsequent five minute heating period suggesting that more energy was needed to break small chains of polysaccharides. This implies that shear and physical forces are responsible for breaking the chains. The total reduction in Mw was from 1.1×10^6 to 7.8×10^4 corresponding to a 93 % reduction in size. In future work, the biological activity of the small Mw products will be examined.

3.5.2 Ultrasonic Disruption of the HMw β-glucan

The second approach used to produce small Mw EPS was ultrasonic disruption. The β-glucan (10.0 mL, 1000 ppm) solution prepared in ultrapure water was sonicated with a power of 25% (Max 130 watts) using the procedure described in section **2.2.8.7** and aliquots (0.5 mL) were removed after every 10 min and injected into the HP-SEC-MALLS for analysis using the chromatographic conditions described in section **2.2.7.1**. The change in average molecular mass of the β-glucan per 10 min sonication time was determined.

Table 3.8: Average molecular mass of the β-glucan before and after sonication with a power of 32.5 watts after every 10 min for 50 min.

Ultrasonic cell disruptor 25% amplitude		
Run time (min)	Molecular mass ($gmol^{-1}$)	Percentage of initial molecular mass (%)
0	1546521	100
10	347303	22.6
20	264426	17.1
30	211102	13.7
40	174632	11.3
50	164583	10.4

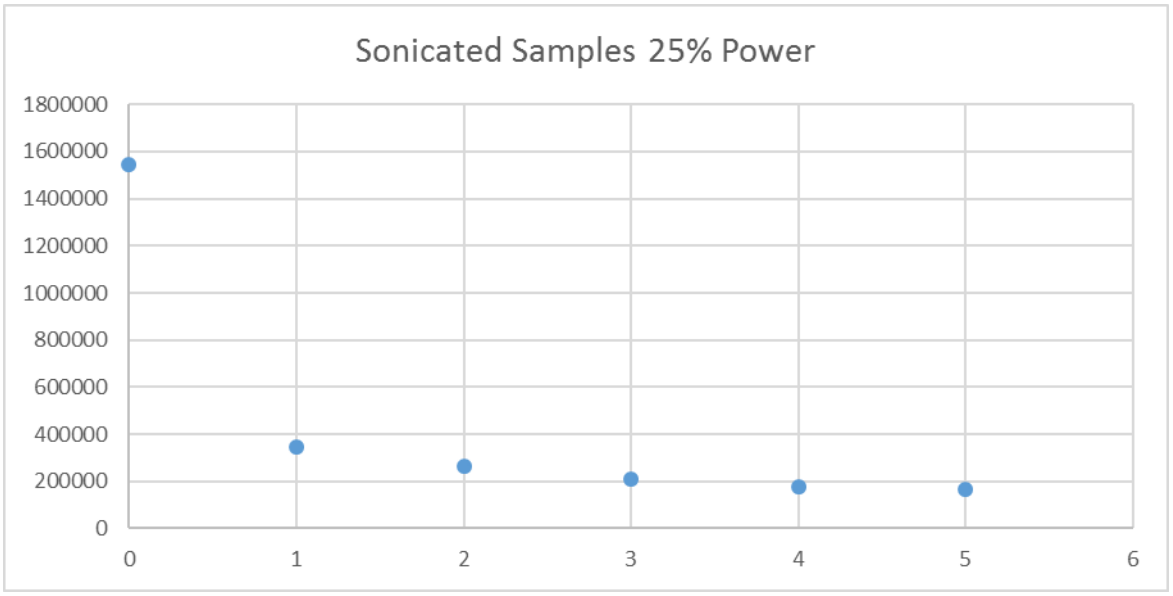

Figure 3.21: Graph of average molecular mass of the β-glucan before and after sonication with a power of 32.5 watts after every 10 min for 50 min against the run times.

From the results obtained, it can be deduced that ultrasonic disruption of the HMw β-glucan using a power of 32.5 watts resulted in 22.6 % decrease in molecular mass after the first 10 min of sonication, after subsequent sonication, the decrease in molecular mass was much smaller until a more or less constant weight was observed. The result suggest that small chains need more energy to break the glycosidic bonds which is consistent with the bond fission being driven by mechanical forces induced by application of shear forces.

As it was not possible to reduce the molecular mass further using 25 % power, the amount of power applied within the ultrasonic probe was increased to 100 %. The power was increased to 100% and the β-glucan was sonicated for 1 h, after which time the sonicated sample was injected into the HP-SEC-MALLS for analysis using the same chromatographic conditions described in section **2.2.7.1**. The change in average molecular mass of the β-glucan per sonication time was determined.

Table 3.8a: Average molecular mass of the β-glucan after sonication with a power of 130 watts for 1 h.

Ultrasonic cell disruptor 100% amplitude		
Run time (min)	Molecular mass ($gmol^{-1}$)	Percentage of initial molecular mass (%)
60	88331	5.7

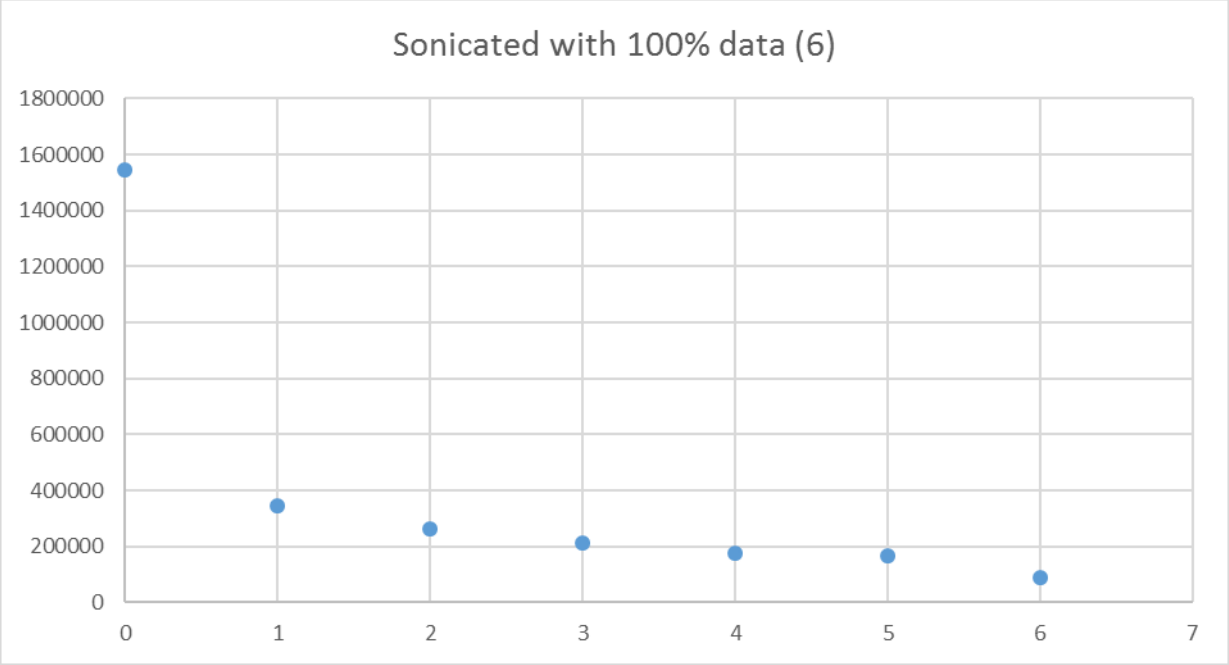

Figure 3.22: Graph of average molecular mass of the β-glucan before and after sonication with a power of 130 watts after 1 h against the run time (data point 6).

An increase in sonication power from 25 % to 100 % for 1 h resulted in the decrease in molecular weight of the β-glucan to 5.7 % of its initial molecular mass. Despite this large reduction in molecular weight, ^{1}H-NMR performed on the sonicated sample before and after 100 % power sonication revealed that the β-glucan retained its structure. As such, it can be said that, ultrasonic disruption decreases the molecular weight of the β-glucan without any debranching or changing the structure of the EPS.

3.6 Optimisation of EPS production by *L. fermentum* LF2 strain

In this research, a different media (HBM) was used for the growth of *L. fermentum* LF2 to study the effect of the media on the yield of EPS produced in comparison with that which is produced by the bacterial strain in SDM by our collaborators in Argentina. Different carbon sources were also used in an attempt to improve the yield of the HMw β-glucan. In an attempt to favour production of one polysaccharide in preference to the other, changes were made to the fermentation conditions.

3.6.1 Growth of *L. fermentum* LF2 in HBM and SDM without pH control

The bacterial strain was supplied by our collaborators in Argentina and was revived according to the procedure outlined in section **2.2.1**. The bacteria was grown on MRSc plates and transferred into the broth media using the procedure described in section **2.2.4** and the yields of EPS recovered were recorded (Table 3.9)

Table 3.9: EPS yield of *L. fermentum* LF2 grown in HBM and SDM for 72 h at 37 °C.

Media	Volume (mL)	Carbon source	Temperature (°C)	Fermentation time (h)	EPS yield (mg)
HBM	1000	Glucose	37	72	465.2
HBM	500	Glucose	37	72	77.0
SDM	1000	Glucose	37	72	~85.0
SDM	500	Glucose	37	72	35.2

The 2-fold increase observed by comparing the EPS yields produced in 500 mL SDM (35.2 mg/L) and HBM (77.0 mg/L) suggest that, the HBM is a more appropriate choice of media in the growth of *L. fermentum* LF2. This was further investigated when the volume of HBM was increased to 1000 mL so as to compare the EPS yield with amount published for production in 1000 mL SDM by *L. fermentum* LF2, highlighted in yellow in table 3.9 (Ale *et al*. 2016). Using the same culture conditions, a crude EPS yield of 465.2 mg/L was achieved when the bacterial strain was grown in 1000 mL HBM as compared to ~85.0 mg/L recovered by Ale *et al*., (2016). The unexpected 6-fold (77.0 mg/500 mL to 465.2 mg/L) increase in EPS produced in HBM may indicate the possibility that a large reaction volume facilitate EPS production.

3.6.2 Influence of carbon source on the yield and composition of EPS produced by *L. fermentum* LF2

The influence of carbon source on the EPS yield and composition was studied. *L. fermentum* LF2 was grown in HBM supplemented with either glucose, *N*-acetyl glucosamine, lactose or GOS using the procedure described in section **2.2.4**.

Table 3.10: EPS yield of *L fermentum* LF2 grown in HBM supplemented with glucose, N-acetyl glucosamine, GOS and lactose for 72 h at 37 °C.

Media	Volume (mL)	Carbon source	Temperature (°C)	Fermentation time (h)	EPS yield (mg)
HBM	500	Glucose	37	72	77.0
HBM	20	*N*-acetyl glucosamine	37	72	-
HBM	500	GOS	37	72	71.4
HBM	500	Lactose	37	72	112.3
HBM	500	Glucose/ *N*-acetyl glucosamine	37	72	44.0

When *L. fermentum* LF2 was grown in HBM supplemented with *N*-acetyl glucosamine, no cell growth was observed. A significant decrease and a small

decrease in EPS yield (71.4 mg and 44.0 mg) were observed when *L. fermentum* LF2 was grown in HBM supplemented with GOS and a mixture of Glucose/ *N*-acetyl glucosamine (50:50) respectively, as compared to the amount (77.0 mg) produced when the bacterial strain was grown in HBM supplemented with glucose. On the other hand, an increase in EPS yield (112.3 mg) was observed when the strain was grown in HBM supplemented with lactose. This suggest that, the HBM supplemented with lactose is a more appropriate choice of carbon source for the growth of *L. fermentum* LF2 for optimum EPS production.

EPS yield in LAB is dependent on the composition of the growth medium and the conditions of growth (J Cerning et al., 1990). Raftis *et al*., (2011) reported that the highest EPS yield in *L. salivarius* CCUG4481 was observed when the strain was grown in sucrose supplemented medium, as compared to glucose and galactose supplemented media (Raftis *et al*., 2011). The bacterial strain *L. casei* CG11 synthesises EPS in growth media supplemented with various carbon sources (glucose, galactose, lactose, sucrose, maltose and melibiose); however, the highest EPS production was observed in glucose supplemented medium (JCMC Cerning et al., 1994).

The composition and ratio of the two polysaccharides produced by *L. fermentum* LF2 when grown in HBM supplemented with glucose, *N*-acetyl glucosamine/ glucose (50:50), lactose and GOS was checked by ^{1}H NMR. Analysis of the ratios of the unique resonances from the HMw and MMw polysaccharides contained in the anomeric region of the ^{1}H NMR spectra revealed that, the integral ratio of a single representative resonance belonging to the MMw polysaccharide (5.35 ppm) to that belonging to the HMw polysaccharide (4.85 ppm) was 1:9.6, 1:15.3 and 1:21.7 for EPS produced by *L. fermentum* LF2 in glucose, lactose and GOS supplemented media respectively. The integral ratios of the two protons were all in favour of the HMw polysaccharide, but it can be noted that EPS produced by *L. fermentum* LF2 in GOS supplemented media favoured more of the HMw (1:21.68) as compared to lactose (1:15.3) and glucose (1:9.6) supplemented media respectively.

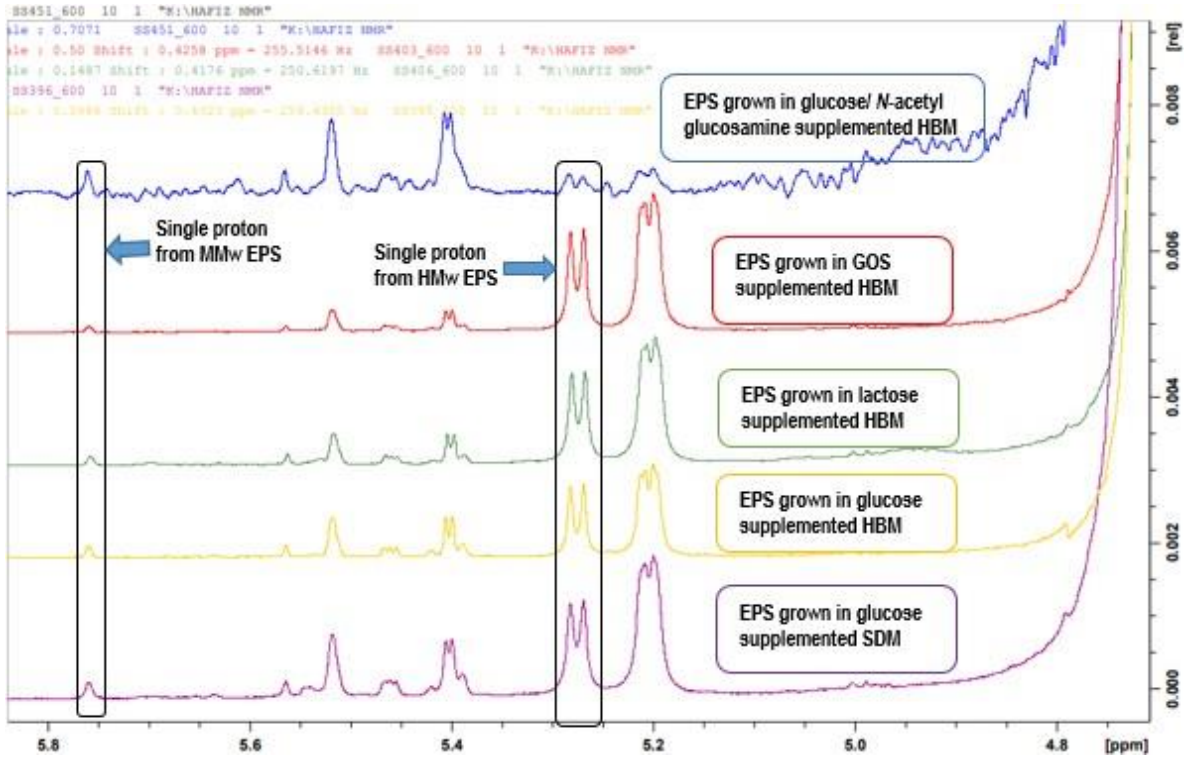

Figure 3.23: ^{1}H-NMR spectra of EPS produced by *L. fermentum* LF2 in SDM supplemented with glucose in Argentina and that which was grown in HBM supplemented with glucose, lactose and GOS.

L. fermentum LF2 produces a mixture of HMw and MMw polysaccharide in both SDM and HBM and that growth of the bacterial strain in HBM favours more of the HMw polysaccharide being synthesised. The type of carbon source used in the fermentation media significantly influences the yield as well as composition of EPSs synthesised by probiotic bacteria (Yilmaz, Celik, Aslim, & Onbasili, 2012). Gobben *et al*., (1996) suggested that, in the bacterial strain *L bulgaricus* NCFB 2772, the regulation of EPS biosynthesis pathway could be attributed to the type of carbon source used in the growth media (Grobben, Smith, Sikkema, & De Bont, 1996).

On the other hand, the peaks in the anomeric region generated by the two polysaccharides synthesised by *L. fermentum* LF2 when grown in HBM supplemented *N*-acetyl glucosamine/ glucose (50:50) remained the same. However, analysis of the ratios of the unique resonances from the HMw and MMw polysaccharides contained in the anomeric region of the ^{1}H NMR spectra revealed that, the integral ratio of a single representative resonance belonging to the MMw (5.35 ppm) polysaccharide to that belonging to the HMw polysaccharide (4.85 ppm) was 1.0:3.2. Although the integral ratio was still in favour of the HMw polysaccharide, the drastic decrease in the synthesis of the HMw EPS was notable. It is therefore possible that, the bacterial

strain *L. fermentum* LF2 does not accept *N*-acetyl glucosamine as a carbon source, but when a mixture of glucose and *N*-acetyl glucosamine was added to the growth medium, an inhibitory effect was invoked on the production of the HMw EPS.

3.6.3 Timed experiment

The final set of experiments was performed with the help of an undergraduate project student, Rhys Morgan, to track the synthesis of EPS by the bacterial strain *L. fermentum* LF2 using the procedure described in section **2.2.5**. After 36 h of growth on MRS-c agar plates in the anaerobic chamber, the best colonies were chosen based on their morphological parameters and were transferred into the broth. The synthesis of EPS by the strain in the broth was monitored at twelve hourly intervals by isolating and purifying the EPS in the broth media and employing the procedure described in section **2.2.6**. After which time ^{1}H-NMR spectroscopy was used to determine the composition of the purified EPSs at 12 h intervals.

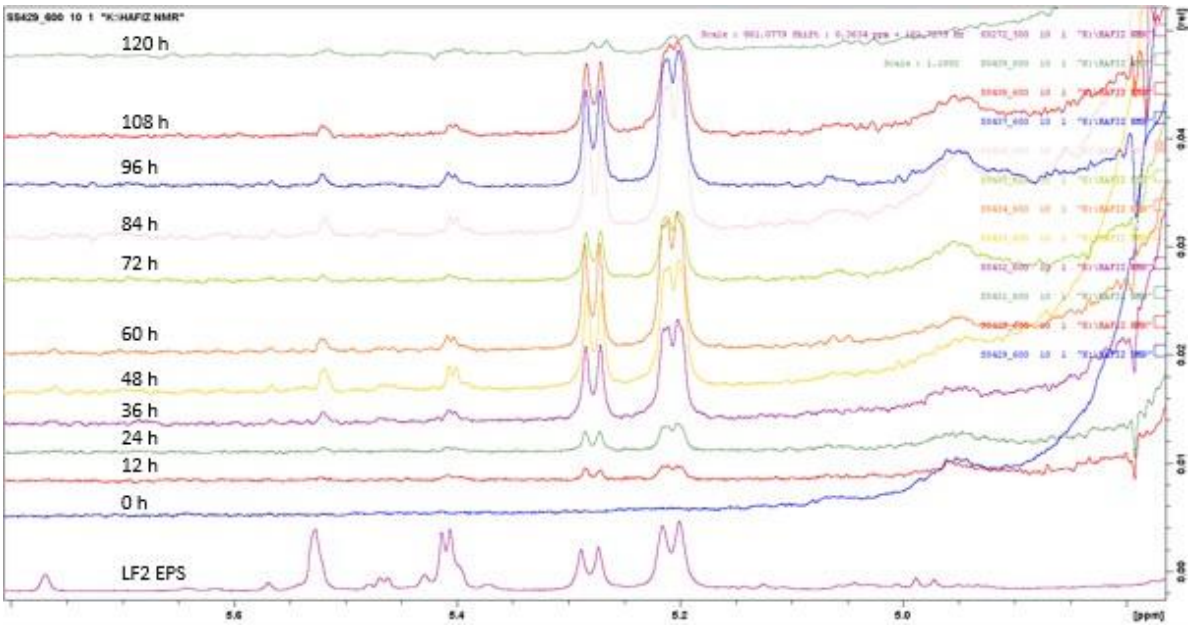

Figure 3.24: Overlaid ^{1}H-NMR spectra of monitored EPS production by *L. fermentum* LF2 in HBM from 0-120 h.

Inspection of the overlaid ^{1}H-NMR spectra recorded on EPS produced by *L. fermentum* LF2 at 12 h interval showed an anomeric region dominated by peaks from the HMw EPS. It is possible that the HMw EPS is released into the fermentation

medium during growth, whereas, the MMw EPS is attached to the cell wall of the EPS and is only released after cell lysis.

3.7 Conclusion

In summary, ^{1}H-NMR and SEC-MALLS performed on the crude EPS produced by *L. fermentum* LF2 indicated the presence of more than one polysaccharides with two populations of molecular masses: a HMw of 1.23 x 10^{6} $gmol^{-1}$and a MMw of 8.80 x 10^{4} $gmol^{-1}$. Fractionation by preparative SEC performed of the crude EPS using a Sephacryl S-500 HR column separated the two populations of polysaccharides. The fractions were combined and lyophilised. SEC-MALLS results performed on the combined fractions showed that the HMw polysaccharide is pure and free from nucleic acids, proteins and other UV absorbing contaminants. ^{1}H-NMR performed on the combined fractions containing the HMw EPS showed that it contained a trisaccharide-repeating unit each with all sugars having a β-anomeric configuration. Monomer analysis by GC-MS and HPAEC confirmed that the trisaccharide-repeating unit contained only glucose and therefore the HMw EPS is a glucan. Determination of the absolute configuration by GC-MS showed that the glucose had D-configuration. Linkage analysis by GC-MS showed the presence of terminal glucose, a 1,3-linked glucose in the main chain and a 1,2,3-linked glucose in the main chain bearing the side chain. COSY, TOSCY, HSQC, HSQC-TOCSY and DEPT 135 ^{13}C NMR experiments identified the individual protons and carbons present in the repeating unit. The sequence of the glucose units in the repeating sugar units was determined by interpretation of ROESY and HMBC spectra, which confirmed the HMw polysaccharide to possess a trisaccharide-repeating unit having the following structure:

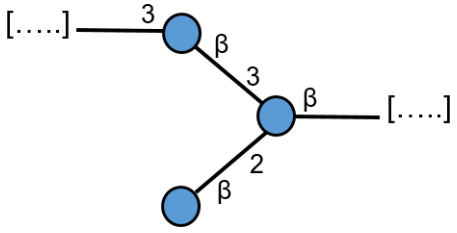

Evaluation of immunomodulatory activity of the HMw β-glucan performed on PBMC for 24 h led to an increase in cell viability, as well as increase in the production of TNF-α in comparison with controls. On the other hand, exposure of PBMC to the HMw β-glucan for 24 h and subsequent removal of the EPS, followed by exposure of the PBMC to LPS revealed significant reduction in TNF-α production. This result indicates that the HMw β-glucan imparts immunotolerance in PBMC and could play a vital role during the release of proinflammatory cytokines by preventing an excessive inflammatory response. Given the fact that TNF-α has a central role in causing inflammatory bowel diseases such as Crohn's disease and ulcerative colitis, this is a very promising result. Microwave assisted depolymerisation and ultrasonic disruption effectively decreases the molecular weight of the β-glucan in a controlled manner. Inspection of the ^{1}H-NMR of the depolymerised samples revealed that, the decreases in molecular weight of the β-glucan does not alter its structure.

HBM was used in the growth of *L. fermentum* LF2 to study the yield of EPS produced in comparison with that which is produced by the bacterial strain in SDM. A 2-fold increase in the EPS yields was observed which suggests that, HBM is the appropriate choice of media for the growth of *L. fermentum* LF2. Different carbon sources were used to study their effect on growth of the bacterial strain and on the yield of the HMw β-glucan. A decrease in EPS yield was observed when *L. fermentum* LF2 was grown in HBM supplemented with GOS as compared to when the bacterial strain was grown in HBM supplemented with glucose. On the other hand, an increase in EPS yield was observed when *L. fermentum* LF2 was grown in HBM supplemented with lactose, which suggest that, HBM supplemented with lactose is a more appropriate choice of carbon source for the growth of *L. fermentum* LF2 for optimum EPS production. When compared with the EPS grown in SDM by the collaborating institute in Argentina, it was noted that *L. fermentum* LF2 produces a mixture of HMw and MMw polysaccharide in both SDM and HBM and that growth of the bacterial strain in HBM favours more of the HMw polysaccharide being synthesised.

4 Purification and characterisation of the medium molecular mass polysaccharides synthesised by *L. fermentum* LF2

4.1 Introduction

In chapter 3, it has been reported that the bacterial strain *L. fermentum* LF2 synthesises two populations of polysaccharides and that they have different molecular masses, a high molecular mass (HMw) fraction (1.23 x 10^6 $gmol^{-1}$) and a medium molecular mass (MMw) fraction (8.80 x 10^4 $gmol^{-1}$). The two populations of polysaccharides were successfully separated using preparative size exclusion chromatography and the HMw polysaccharide has been fully characterised. In this chapter, the purification and characterisation of the MMw polysaccharides synthesised by *L. fermentum* LF2 will be discussed.

4.2 Determination of weight average molecular mass of the MMw polysaccharide

Separation of the crude EPS by preparative size exclusion chromatography using a Sephacryl S500-HR column eluted a second polysaccharide population (subsequently referred to as MMw) between fractions 25-30, which was confirmed by determining the total carbohydrate content in the fractions using the procedure described in section **2.2.7.3**. The weight average molecular mass of the MMw polysaccharide was determined using SEC-MALLS and employing the procedure described in chapter **2.2.7.1**.

Inspection of the SEC-MALLS chromatogram (Fig 4.1) obtained from analysing the combined fractions containing the MMw polysaccharide revealed the presence of two light scattering detector peaks (red trace), the first peak that eluted at about RT = 25.8 min was determined to be from a small amount of the HMw polysaccharide (1.23 x 10^6

gmol^{-1}). The low quantity present is highlighted by the very small response from the refractive index trace (blue trace). The second peak in the light scattering trace at RT = 36.4 min was accompanied by a large RI peak and a large UV peak, suggesting that the polysaccharide present in this fraction, whose weight average molecular mass was determined to be 8.80 x 10^4 gmol^{-1}, is more concentrated and is contaminated with UV absorbing impurities, that could be proteins or DNA. A small late eluting peak was also observed on the RI trace which is also associated with a UV response at RT = 43.7 min suggested the potential presence of another polysaccharide/protein.

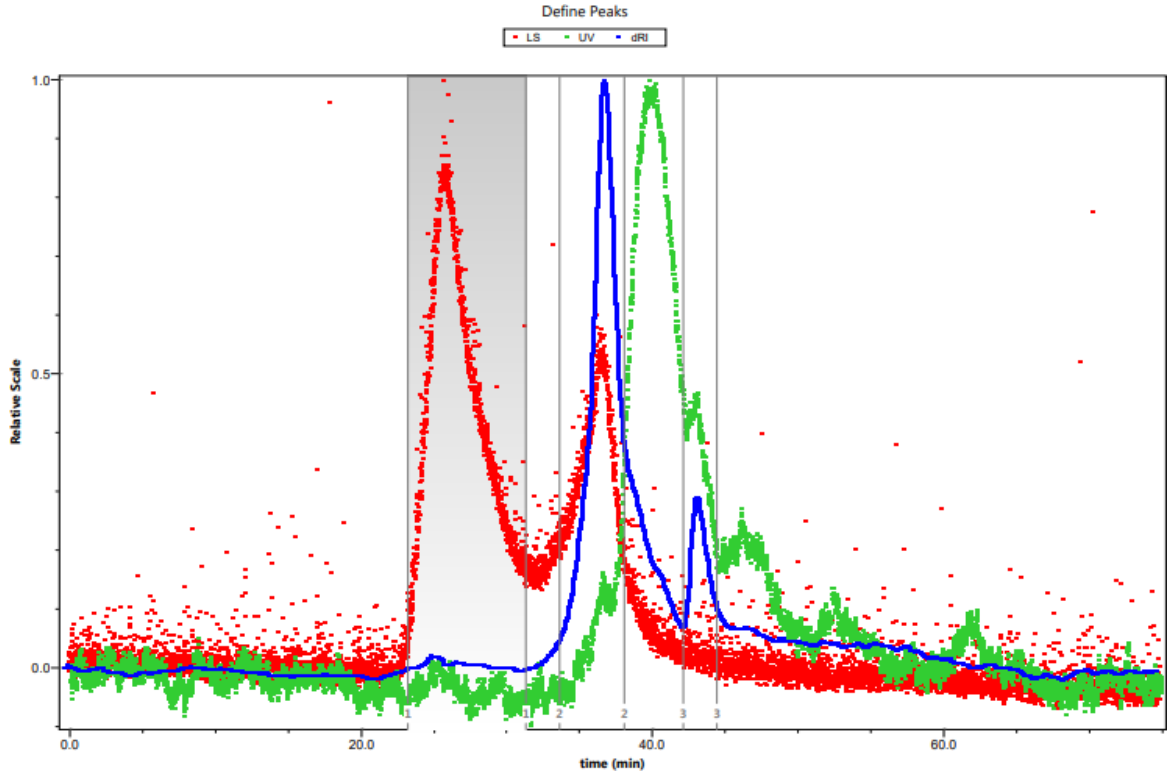

Figure 4.1: SEC-MALLS chromatogram of the MMw polysaccharide mixture.

4.3 ^{1}H-NMR spectra of the combined fractions 25-30

The MMw polysaccharides were analysed by ^{1}H-NMR spectroscopy using the procedure described in section **2.2.8.5**. Inspection of the anomeric region revealed the presence of one large pair of signals with integral ratio of 1 and a set of smaller signals (Fig 4.2).

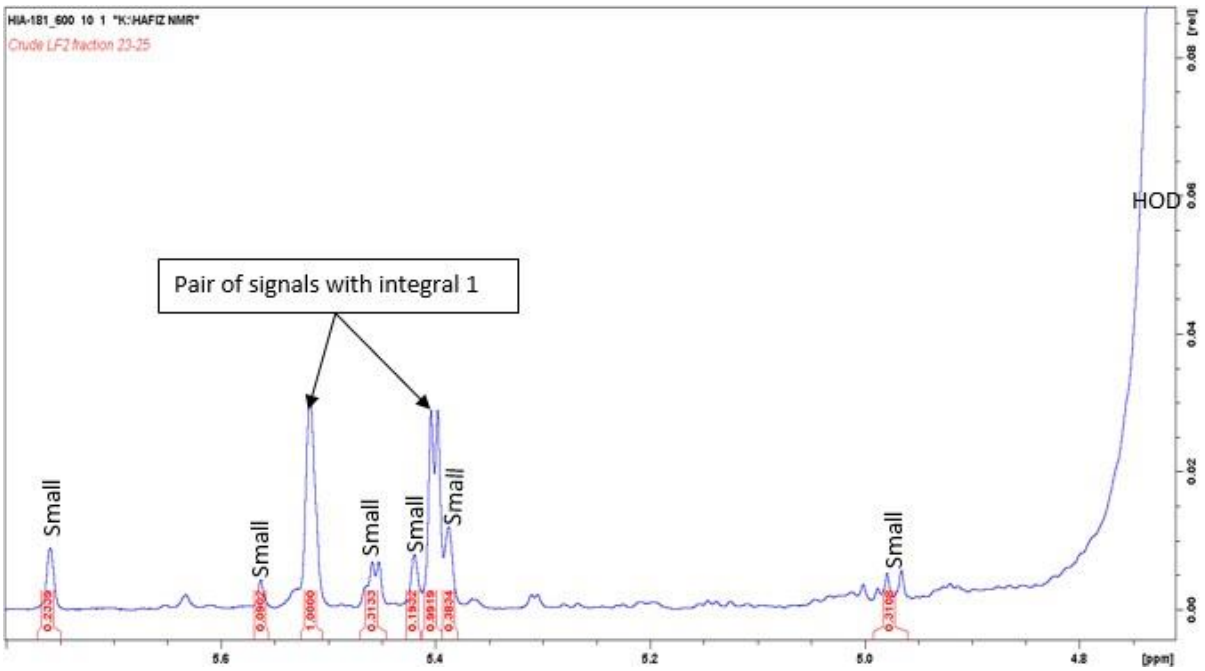

Figure 4.2: ^{1}H-NMR spectrum recorded at room temperature of the MMw polysaccharide mixture.

The varying integral ratios observed in the anomeric region of the ^{1}H-NMR spectra (Fig 4.2) are consistent with the SEC-MALLS result which suggested the presence of more than one polysaccharide.

4.4 Purification and separation of polysaccharides present in the combined fractions 25-30.

In an attempt to recover highly pure MMw polysaccharides, a sample of the crude EPS was again passed through a Sephacryl S500-HR column using the same conditions described in section **2.2.7.2**. Instead of combining fractions, each fraction was lyophilised and analysed separately by NMR.

Table 4.1: Quantity in (mg) of EPS recovered from Sephacryl S-500 HR column after lyophilising the fractions.

S/N	Fraction number	Amount (mg)
1	25	0.3
2	26	10.5
3	27	8.7
4	28	9.6
5	29	8.2
6	30	0.7

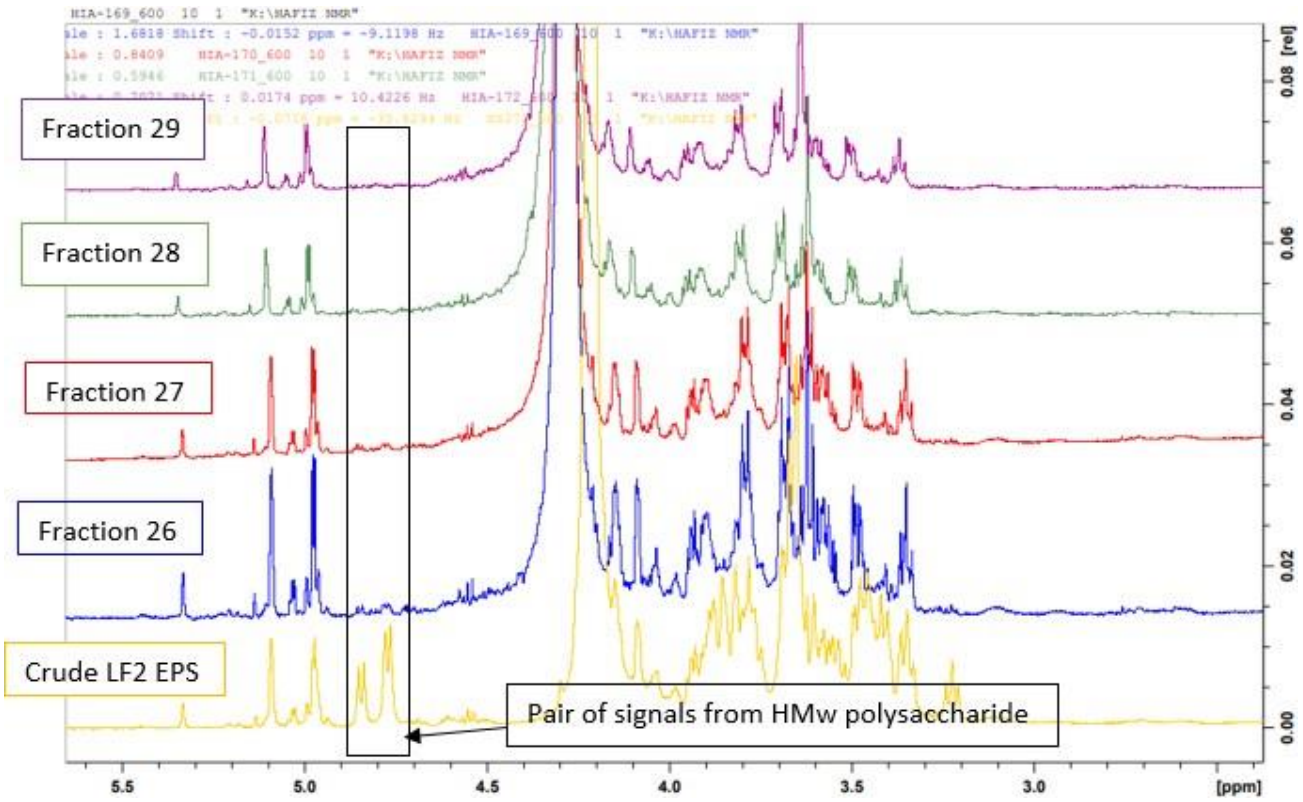

Figure 4.3: Overlaid ^{1}H-NMR spectra of the crude LF2 EPS and individual fractions 26, 27, 28 and 29 containing the proposed MMw polysaccharides.

Inspection of the anomeric region in the overlaid spectra for each of the fractions containing the MMw polysaccharide(s) (Fig 4.3) revealed that, although lyophilising the fractions individually separated the MMw polysaccharides from the HMw

polysaccharide as the fraction number increases, separation by preparative size exclusion chromatography using Sephacryl S500 HR-column couldn't separate the different MMw polysaccharides. The anomeric region of each fraction contained the same pattern of signals with similar integral ratios. Because there was no visible change in the anomeric region of all the fractions, another size exclusion chromatography using a smaller pore size packing material with a much reduced fractionation range was employed in an attempt to separate the two MMw polysaccharides.

4.4.1 Separation of the two MMw polysaccharides

The purified fractions containing the MMw polysaccharides were combined, dissolved in ultra-pure water and injected into the smaller pore size column (Sephacryl S200 HR).

4.4.1.1 Separation using Sephacryl S200 HR column

A prepacked HiPrep XK16/60 Sephacryl S200 HR column with a fractionation range of 1.0×10^3 to 8.0×10^4 $gmol^{-1}$ for purifying medium size proteins was employed (https://www.scientificlabs.co.uk). Two different flow rates were employed (2mL/min and 0.5 mL/min) in an attempt to separate the MMw polysaccharides. In total, sixty 5 mL fractions were collected using the procedure described in section **2.2.7.2.1**. Location of the polysaccharides was determined by analysing each fraction for its total carbohydrate content using the Dubois method described in section **2.2.7.3**. Fractions containing carbohydrates were lyophilised individually. The freeze-dried fractions were weighed, dissolved in D_2O (0.65 mL) and analysed by ^1H NMR as described in section **2.2.8.5**.

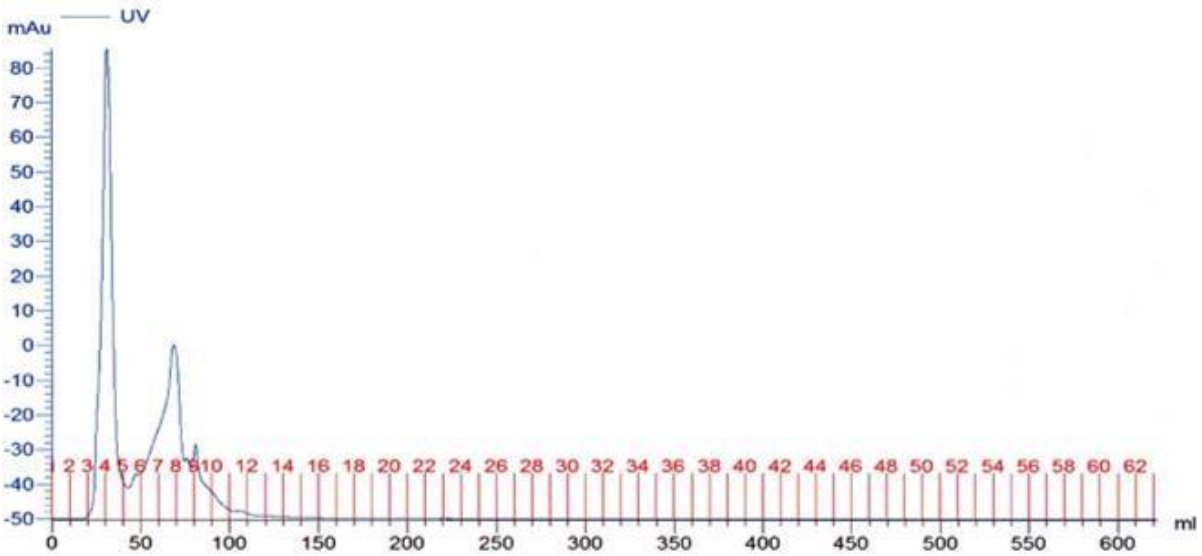

Figure 4.4: UV trace of the Sephacryl S-200 HR column ran on the MMw polysaccharide mixture at a flow rate of 2 mLmin^{-1}

The UV detector connected to the AKTA PRIME system that was ran at a flowrate of 2 mL/min generated two peaks, the first peak appeared within fractions 4-5 and the second peak appeared between fractions 7-9, suggesting that the MMw polysaccharides have eluted in the void volume and the material is too big to enter the pores of the stationary phase. Each fraction was also analysed for its total carbohydrate content using the Dubois method.

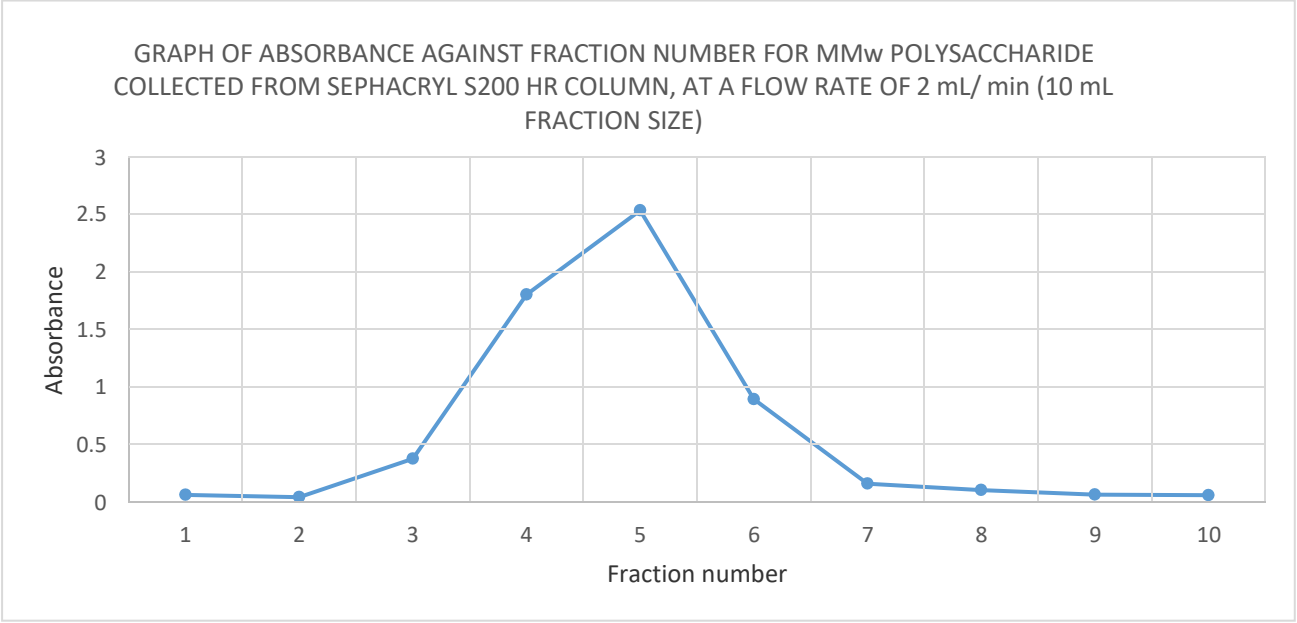

Figure 4.5: Carbohydrate concentration of fractions 1-10 from the Sephacryl S-200 HR column, at a flow rate of 2 mLmin^{-1}

The graph of absorbance against fraction number was plotted for the total carbohydrate (Fig 4.5) which also suggested that the MMw polysaccharides eluted within fractions 2-8. Each fraction was lyophilised individually and weighed (table 4.2). No material was present in fractions 1,2,8,9 and 10, as such only the fractions containing substantial amount of the sample were analysed by ^{1}H-NMR.

Table 4.2: Quantity in (mg) of EPS recovered from Sephacryl S-200 HR column with 2 mL/min flowrate.

S/N	Fraction number	Amount (mg)
1	1	-
2	2	-
3	3	0.85
4	4	7.08
5	5	6.54
6	6	2.61
7	7	3.38
8-10	8-10	-

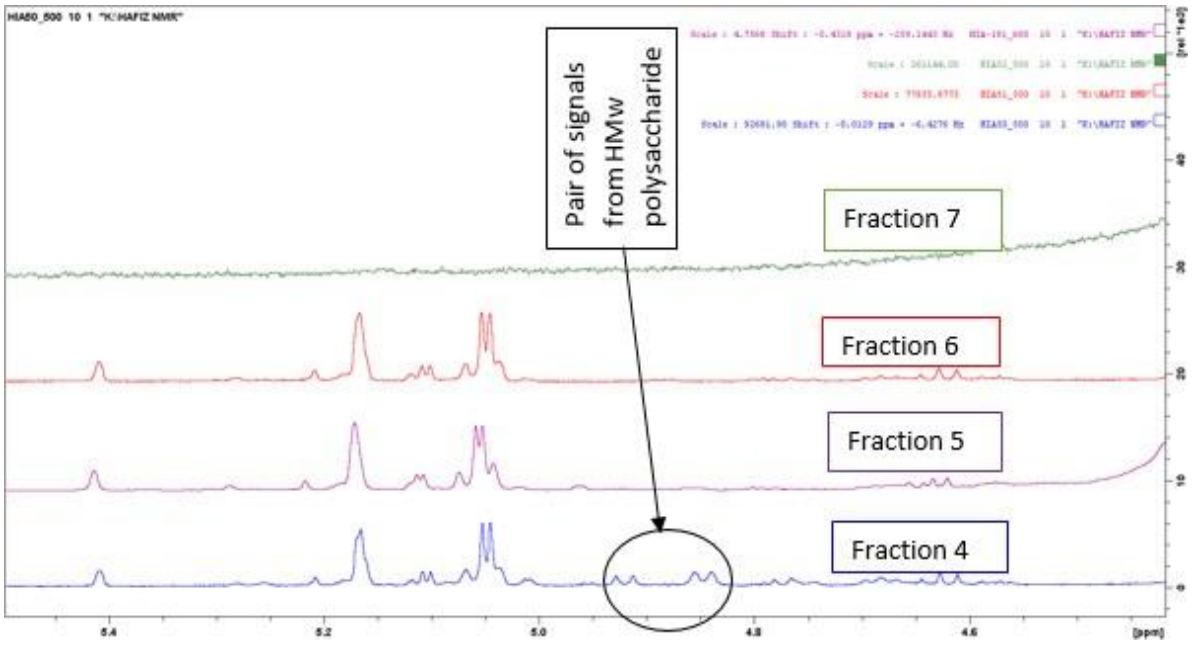

Figure 4.6: Overlaid 1H-NMR spectra of fractions 4-7 collected from the Sephacryl S-200 HR column, at a flow rate of 2 mLmin^{-1}.

Analysis of the overlaid ^{1}H-NMR spectra recorded for each fraction (Fig 4.6) showed that fraction 4 contained the MMw and small traces of the HMw polysaccharide. Fractions 5 and 6 contained the MMw polysaccharides, whereas Fraction 7 had nothing in the anomeric region. ^{1}H-NMR spectra of fractions 4, 5 and 6 that contained the MMw polysaccharides showed that the two polysaccharides that were potentially present had not been separated. Since using a flow rate of 2 mL/ min eluted the MMw polysaccharide within the first 10 fractions, a lower flow rate was employed to give the sample a longer time to equilibrate within the column.

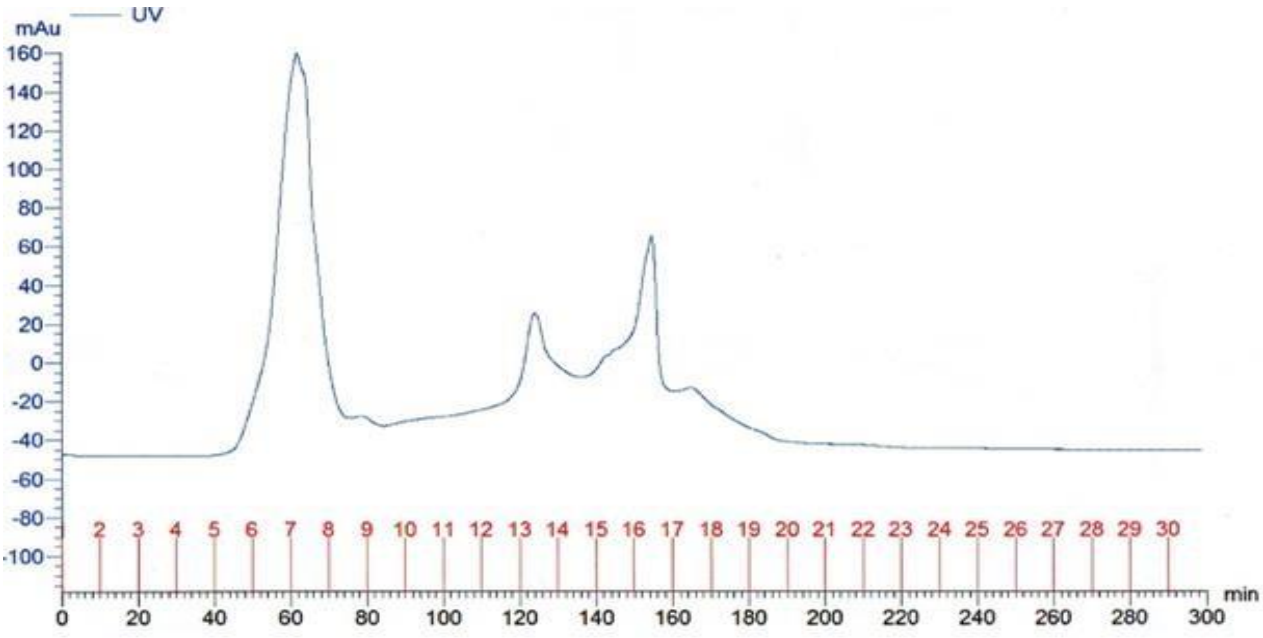

Figure 4.7: UV trace of the Sephacryl S-200 HR column ran on the MMw polysaccharide at a flow rate of 0.5 mL/ min.

Analysis of the UV trace generated by the AKTA PRIME system using the flow rate of 0.5 mL/ min (Fig 4.7) revealed that the UV peaks were spread out over fractions 5-20, again suggesting that the MMw polysaccharides have eluted in the void volume and the material is too big to enter the pores of the stationary phase. Each fraction (1-30) was freeze-dried, but only fractions 6-12 had significant amount of material in them. The fractions with samples present were analysed by ^{1}H-NMR.

Table 4.3: Quantity in (mg) of EPS recovered from Sephacryl S-200 HR column with 0.5 mL/min flowrate.

S/N	Fraction number	Amount (mg)
1	1,2,3,4 and 5	No sample
2	6	2.30
3	7	5.00
4	8	4.00
5	9	2.00
6	10	1.30
7	11	0.10
8	12	0.10

^{1}H-NMR analysis (Fig 4.8) revealed that the MMw polysaccharides started to elute at fraction 6. Fractions 7, 8, 9, 10 and 11 also had the same pattern of peaks in their anomeric regions as fraction 6 in similar integral ratios within error. Fraction 12 had almost nothing in its anomeric region, which suggest that the polysaccharide had all eluted. Visualising the anomeric regions of the fractions that had the MMw polysaccharides showed that, the proposed two MMw polysaccharides could not be separated by size exclusion chromatography using both the Sephacryl S-500 HR and the Sephacryl S-200 HR columns as all the fractions contained the same pattern of peaks.

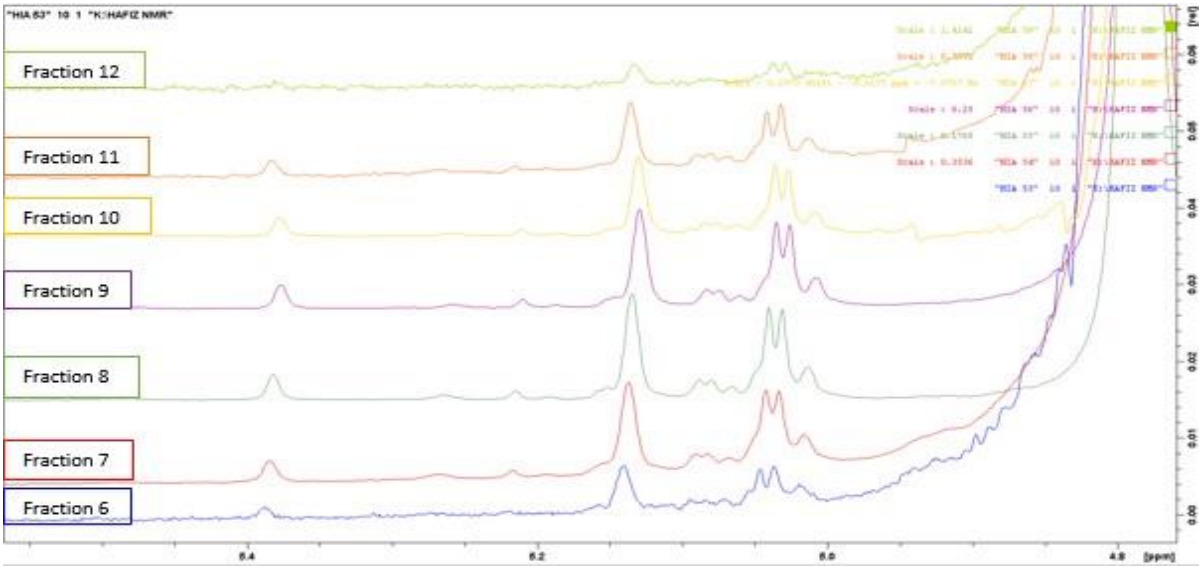

Figure 4.8: Overlaid ^{1}H-NMR spectra of the fractions recovered from Sephacryl S-200 HR column, using a flow rate of 0.5 mL/ min.

4.4.1.2 Use of mild acid hydrolysis to separate the MMw polysaccharides

Although the ^{1}H-NMR spectra was still crowded with impurities, a ^{1}H-^{13}C-HSQC NMR experiment was performed on the MMw polysaccharide mixture (Fig 4.9). The presence of ^{13}C anomeric resonances at unusually low field (δ 106.7, 107.0, 108.4 and 108.5 ppm) suggests that the resonances are from C-1 derived from furanose sugars (Bock & Pedersen, 1983).

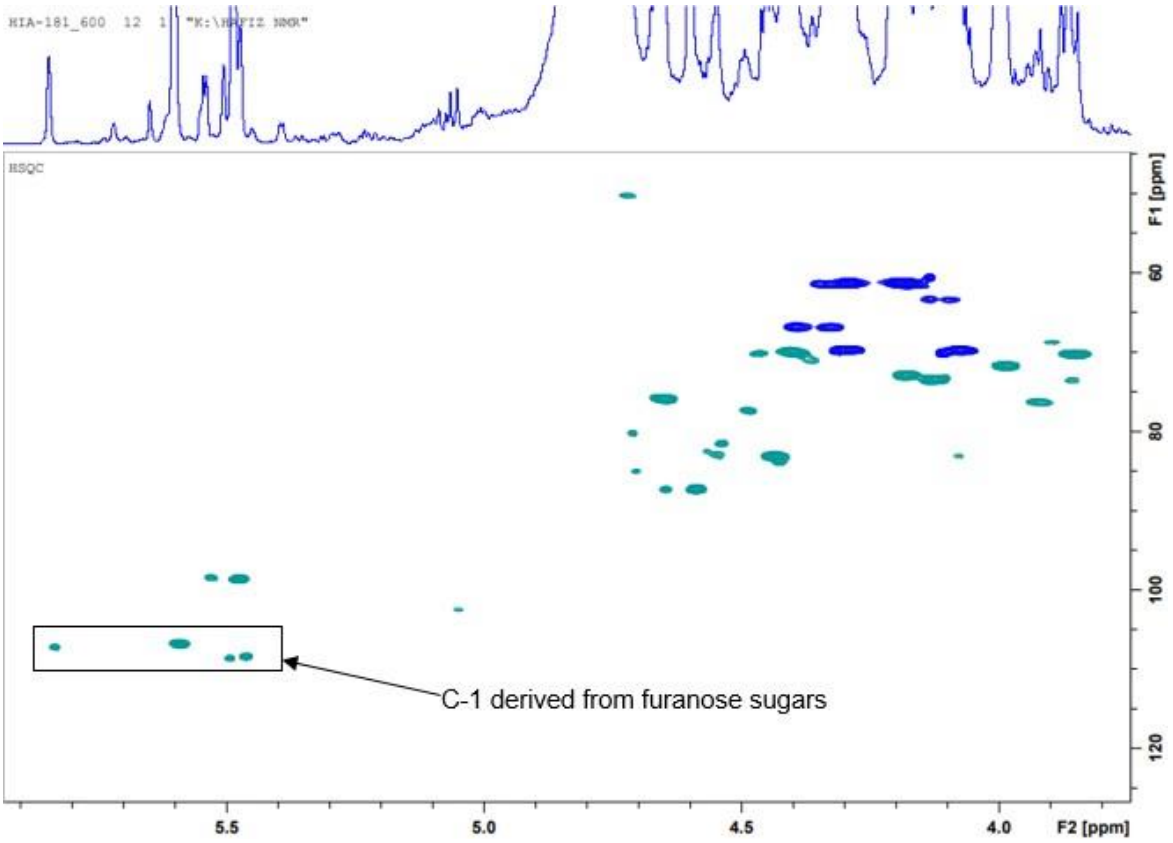

Figure 4.9: ^{1}H-^{13}C-HSQC spectrum recorded on the MMw polysaccharide mixture.

With the view that glycosidic bonds to furanoses are often acid labile and easily cleaved when subjected to mild acid hydrolysis, the MMw polysaccharide mixture was subjected to mild acid hydrolysis and employing different concentrations of the acid at different temperatures using the procedure described in section **2.2.8.9**. The idea was that if one of the MMw polysaccharides contained all the furanose sugars, mild acid

hydrolysis will cleave the one containing the furanose sugars and potentially leave the other MMw polysaccharide available for isolation.

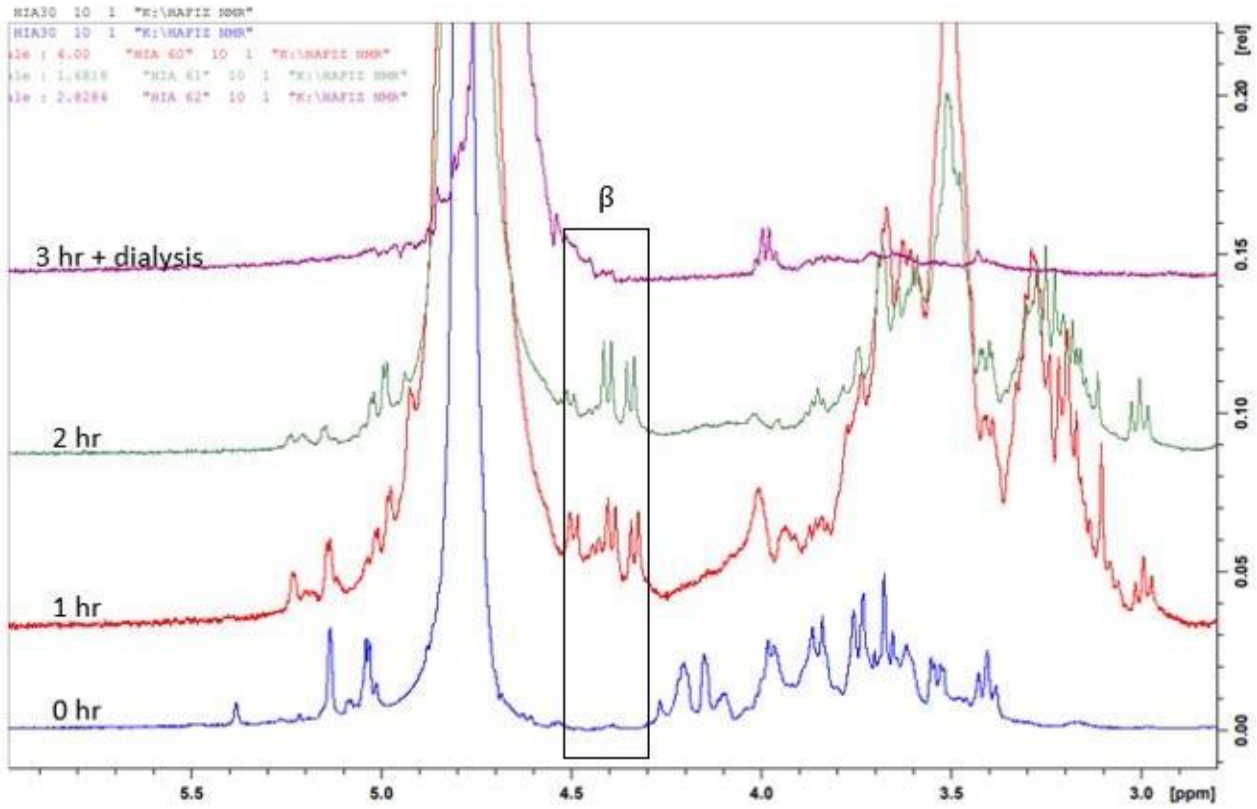

Figure 4.10: Overlaid ^{1}H-NMR spectra of the MMw polysaccharide mixture subjected to 0.5M TFA acid hydrolysis for 0, 1, 2 and 3 h respectively after which the sample was dialysed.

The MMw polysaccharide mixture was subjected to mild acid hydrolysis (0.5M, TFA, 100 °C) for 0, 1, 2 and 3 h, during which time ^{1}H-NMR was recorded before and after the heating process, after which time the sample was dialysed. The peaks corresponding to β-configurations of newly formed chain ends of oligosaccharides were seen immediately after the first hour of heating as highlighted in Fig 4.10. The sample was dialysed after 3 h of heating and ^{1}H-NMR spectra recorded on the dialysis bag content which revealed the absence of peak(s) in the anomeric region, suggesting that the MMw polysaccharides have been completely hydrolysed under this condition. As such, a lower concentration (0.05 M) of the acid was used.

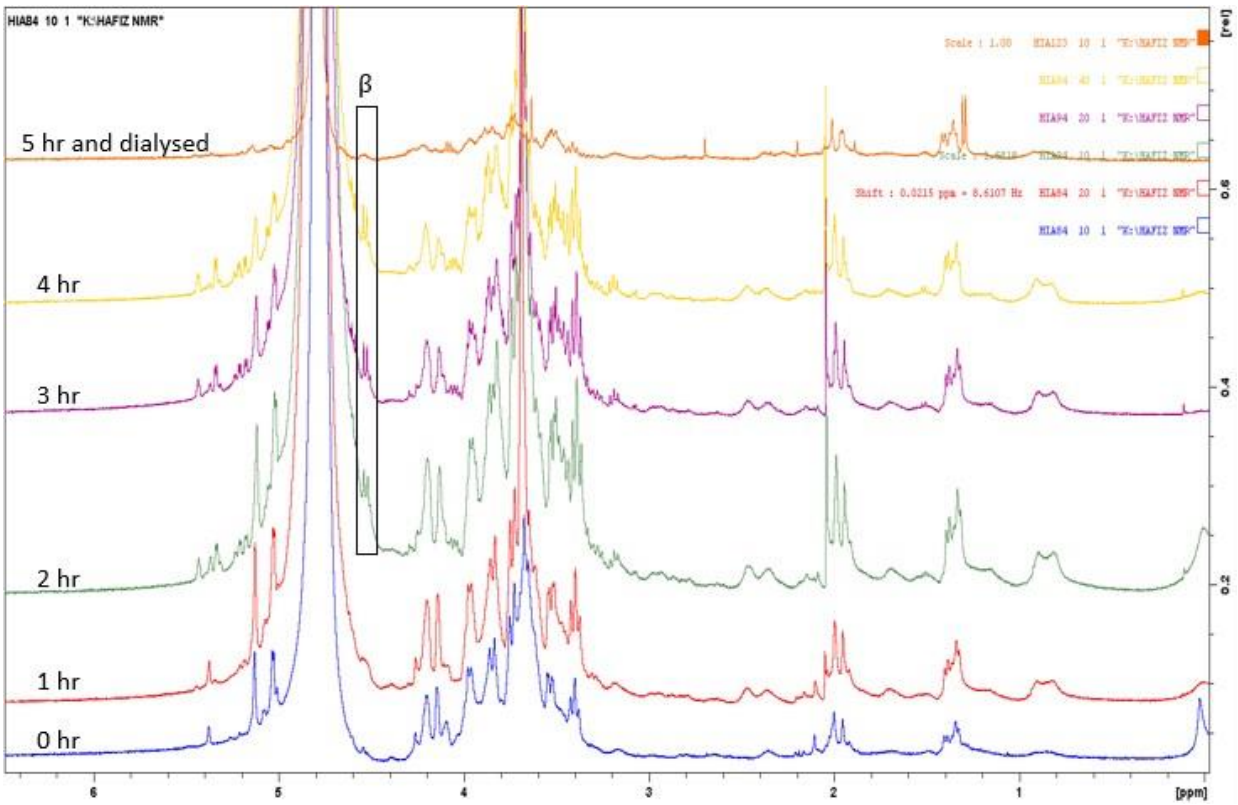

Figure 4.11: Overlaid ^{1}H-NMR spectra of the MMw polysaccharide mixture subjected to 0.05M TFA acid hydrolysis for 0, 1, 2, 3, 4 and 5 h respectively after which the sample was dialysed.

On the ^{1}H-NMR spectra generated by the MMw polysaccharide mixture after treatment with a much lower concentration of the acid (0.05 M) (Fig 4.11), it can be seen that after the second hour of heating, the peaks corresponding to the β-configurations of chain ends of oligosaccharides could be noticed. Unfortunately, after 5 h of heating and dialysis, no sample was left in the dialysis bag, which is an indication of complete hydrolysis of the MMw polysaccharides. This result would be expected if both of the MMw polysaccharides contained acid labile glycosidic bonds.

In summary, mild acid hydrolysis also could not separate the two polysaccharides and could also not provide a clearer spectrum.

4.4.1.3 Treatment with proteinase K and DNase

Based on the SEC-MALLS results obtained for the population containing the MMw polysaccharide mixture (Fig 4.1), both polysaccharides were contaminated with materials which was able to absorb UV light at 260 nm, as such, an attempt was made

to remove the UV absorbing impurities that absorb UV light at 260 nm (proteins) using Proteinase K as described in section **2.2.6.4.1**.

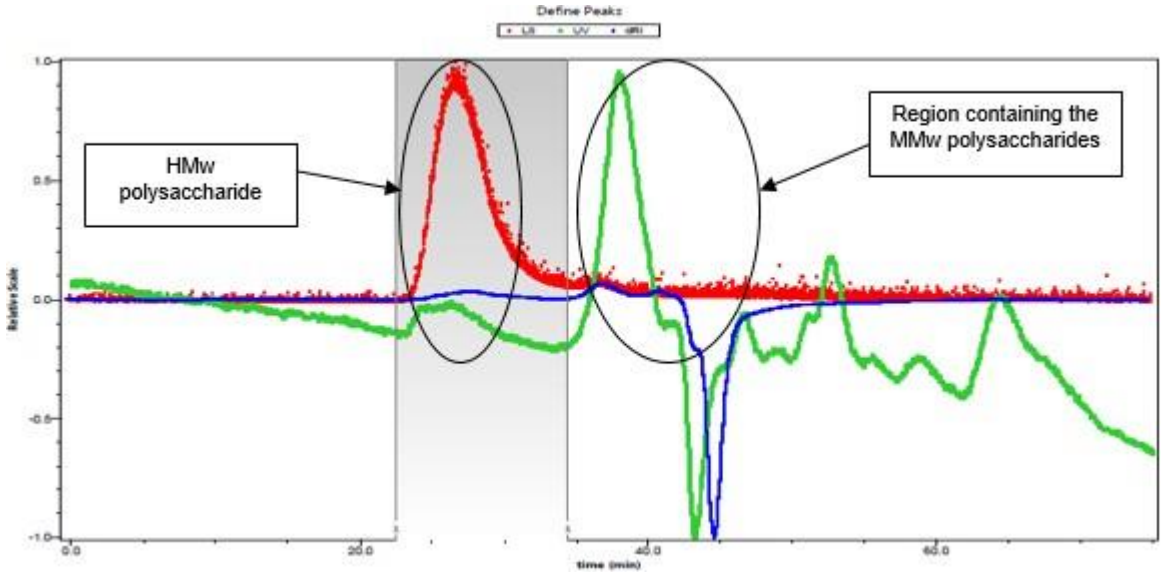

Figure 4.12: SEC-MALLS chromatogram of the crude LF2 after treatment with proteinase K.

It can be seen that, treatment with proteinase K could not remove the UV peak that accompanied the MMw polysaccharides. Further analysis of the treated sample using ^{1}H-NMR revealed that, the peaks that appeared within 1 and 2.5 ppm (region for lactates, acetates, methyls, amines and other impurites) were still present. This implies that, proteinase K could not remove the UV absorbing contaminants.

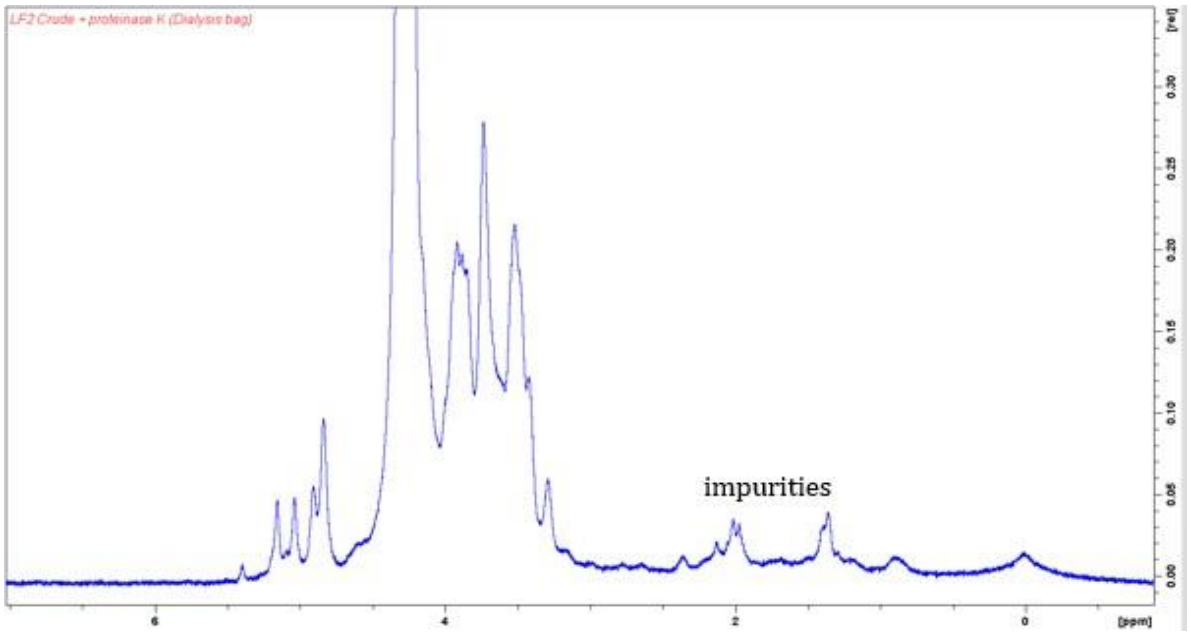

Figure 4.13: ^{1}H-NMR spectra of the crude LF2 after treatment with proteinase K.

Giving the fact that, proteinase K could not remove the UV peak, the crude material was analysed on SEC-MALLS at 280 nm where nucleic acids absorb UV light. SEC-MALLS results showed that the sample absorbs UV at 280 nm and therefore the impurities are more likely to be nucleic acid based materials such as DNA and RNA. The sample was then treated with DNase to remove the UV peak.

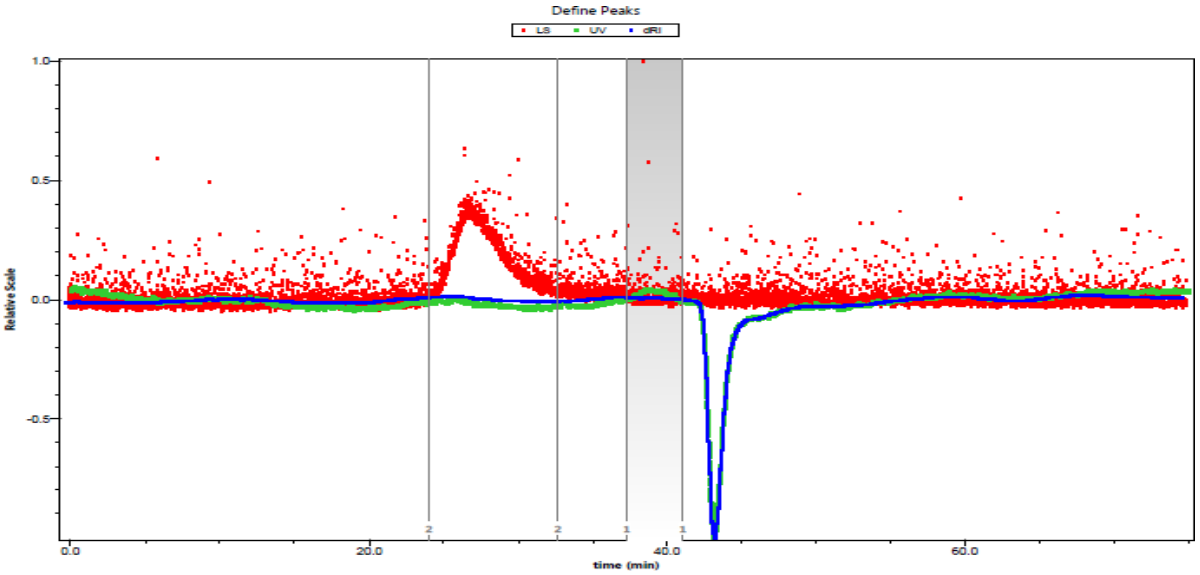

Figure 4.14: SEC-MALLS chromatogram of the crude LF2 after treatment with DNase.

Treatment of the sample with DNase removed the UV peak that accompanied the MMw polysaccharides. The treated sample was further analysed using ^{1}H-NMR.

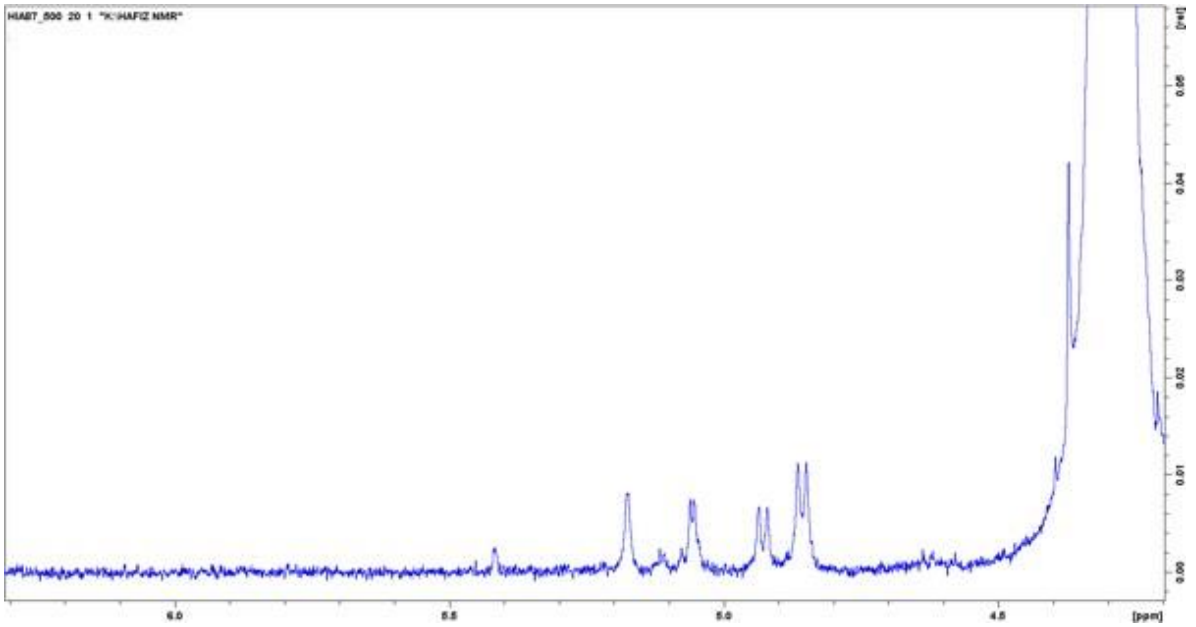

Figure 4.15: ^{1}H-NMR spectra of the crude LF2 after treatment with DNase.

Although treatment of the crude LF2 removed the UV peak that came with the MMw polysaccharide, ^{1}H-NMR spectra (Fig 4.15) showed that the same mixture of anomeric peaks were present. Unfortunately, all attempts to purify and separate the two MMw polysaccharides using a smaller pore-size column, an anion exchange column (work performed by an undergraduate student), mild acid hydrolysis, treatment with proteinase and DNase, failed. It was then decided to attempt to directly characterise the two polysaccharides as a mixture.

4.5 Monomer analysis of the medium molecular weight (MMw) polysaccharides

Monomer analysis of the MMw polysaccharide mixture was performed by HPAEC-PAD using the procedure described in section **2.2.8.1**. Standards (fucose, rhamnose, galactose, glucose, xylose, mannose, fructose, *N*-acetyl glucosamine, *N*-acetyl galactosamine, glucosamine, and galactosamine) were ran in triplicates and their average retention times were recorded. The combined fractions containing the MMw polysaccharides was hydrolysed and analysed in triplicate, using fructose as an internal standard. The average retention time of the peaks generated by the MMw polysaccharides were compared with those generated by the standards.

Table 4.4: Average retention time (min) of the standards ran on HPAEC-PAD

Monomer	Average Retention Time (Min)	Standard Deviation
Fucose	2.71	0.088
Galactosamine	4.41	0.009
Rhamnose	4.69	0.022
Glucosamine	5.30	0.005
Galactose	5.87	0.025
Glucose	6.61	0.002
N-Acetyl Glucosamine	6.86	0.005
N-Acetyl Galactosamine	7.05	0.009
Xylose	7.61	0.005
Mannose	7.77	0.005
Fructose	8.58	0.000

Table 4.5: Average retention time (min) of the hydrolysed MMw polysaccharide ran on HPAEC-PAD

LF2 MMw	Average Retention Time (min)	Standard Deviation
Peak 1	4.50	0.098
Peak 2	5.39	0.005
Peak 3	5.95	0.004
Peak 4	6.68	0.002
Peak 5	7.74	0.002
Peak 6 (Fructose) as Internal Standard	8.63	0.000

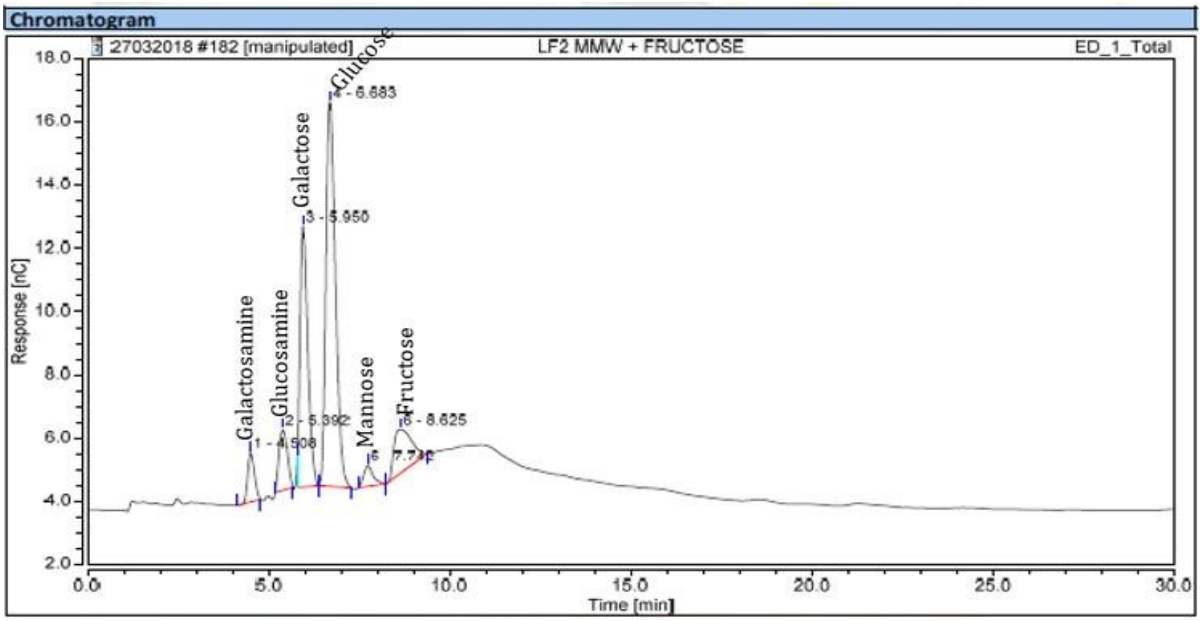

Figure 4.16: A representative HPAEC-PAD chromatogram of the hydrolysed MMw polysaccharides.

The average retention time of the peaks generated by the hydrolysed MMw polysaccharide mixture on HPAEC-PAD corresponded with those which were generated by galactosamine, glucosamine, galactose, glucose and mannose respectively. The presence of the amino sugars (galactosamine and glucosamine) doesn't exclude the possibility that the amino sugars were present in the native polysaccharide in their *N*-acetylated forms, because, *N*-acetyl groups of amino sugars are removed during hydrolysis with acid (Biermann & McGinnis, 1988).

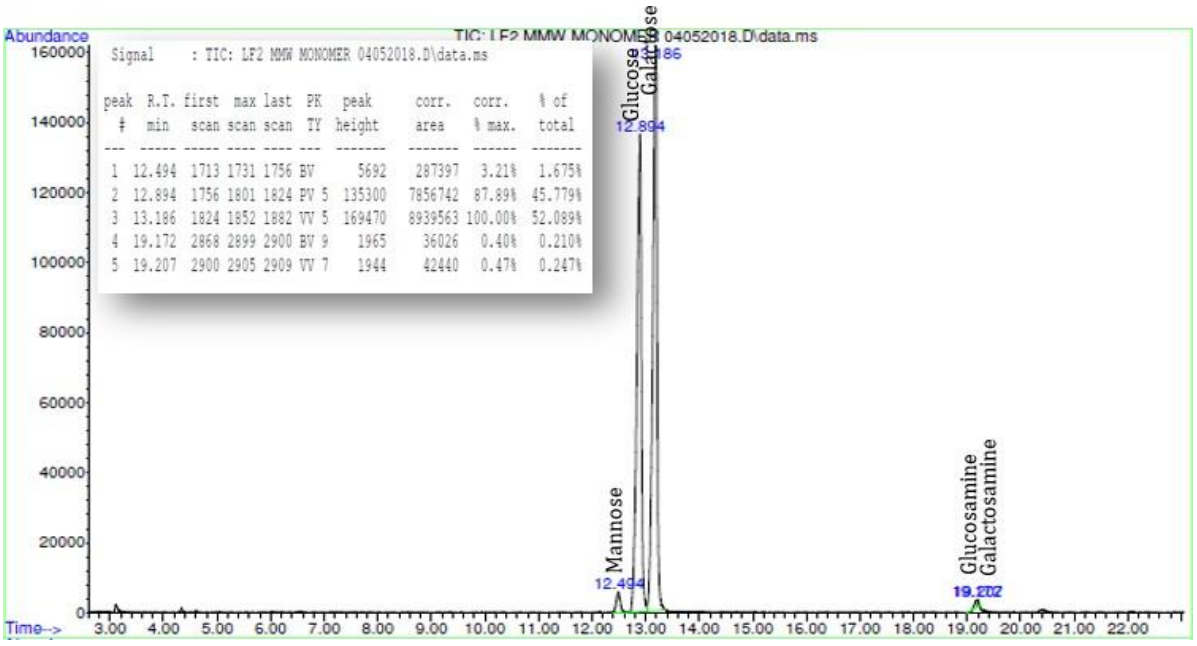

Figure 4.17: GC trace of monomer analysis performed on the combined fractions containing the MMw polysaccharides.

Monomer analysis was also performed on the combined fractions containing the MMw polysaccharides by GC-MS using the procedure described in section **2.2.8.2**. Analysis of the MMw polysaccharide mixture generated five alditol acetate peaks at 12.49, 12.89, 13.19, 19.17 and 19.21 min in a ratio of 0.2:4.6:5.2:0.02:0.03 (detector response) respectively. Comparison of the two main peaks at 12.89 and 13.19 min (ratio 4.6:5.2) with that which was generated by the standards identified the two main peaks as glucose and galactose respectively. The other small peaks at 12.49, 19.17 and 19.21 min, of which their combined peak area was less than 3 % of that of glucose and galactose, were identified as mannose, glucosamine and galactosamine respectively.

Table 4.6: GC retention times of monomer analysis performed on some standards and on the MMw polysaccharides.

Standard	Retention Time	Lf2 Mmw	Retention Time
Mannose	12.55	Peak 1	12.49
Glucose	12.88	Peak 2	12.89
Galactose	13.14	Peak 3	13.19
Glucosamine	19.17	Peak 4	19.17
Galactosamine	19.21	Peak 5	19.21

Monomer analysis by both HPAEC-PAD and GC-MS confirmed that glucose and galactose were the main constituents of the MMw polysaccharides and that the presence of small amounts of mannose, glucosamine and galactosamine are likely to be from small amounts of either cell wall materials or small amounts of polysaccharide carryover from the fermentation medium.

4.6 Absolute configuration analysis of the MMwpolysacchrides

Absolute sugar analysis was performed on the combined fractions containing the MMw polysaccharides using the procedure described in section **2.2.8.3**. The peaks generated by the MMw polysaccharides on GC-MS were compared with those generated from the standards. The retention times of the peaks generated by the MMw polysaccharides corresponded to those generated by D-Glucose and D-Galactose, which confirm that both glucose and galactose are of D-absolute configuration.

Table 4.7: Retention times generated by D- and L- glucose and galactose standards and that which was generated by *L fermentum* LF2 MMw polysaccharides

Sample	Retention time of the 1st peak (min.)	Retention time of the 2nd peak (min.)	Retention time of the 3rd peak (min.)	Retention time of the 4th peak (min.)	Retention time of the 4th peak (min.)
L-Galactose	11.21	11.56	12.10	-	-
D-Galactose	**11.28**	**11.60**	**12.29**	-	-
D-Glucose	**11.75**	**12.55**	-	-	-
L-Glucose	11.92	12.29	-	-	-
LF2 MMw	**11.27**	**11.59**	**11.75**	**12.29**	**12.55**

4.7 Linkage Analysis for the MMw polysacchrides

Linkage analysis using per-methylated alditol acetates was performed on the combined fractions containing the MMw polysaccharides using the procedure described in section **2.2.8.4**. The GC trace generated by the MMw polysaccharides contained two large peaks at 12.05 and 20.19 min, and three small peaks at 15.04, 15.95 and 16.83 min.

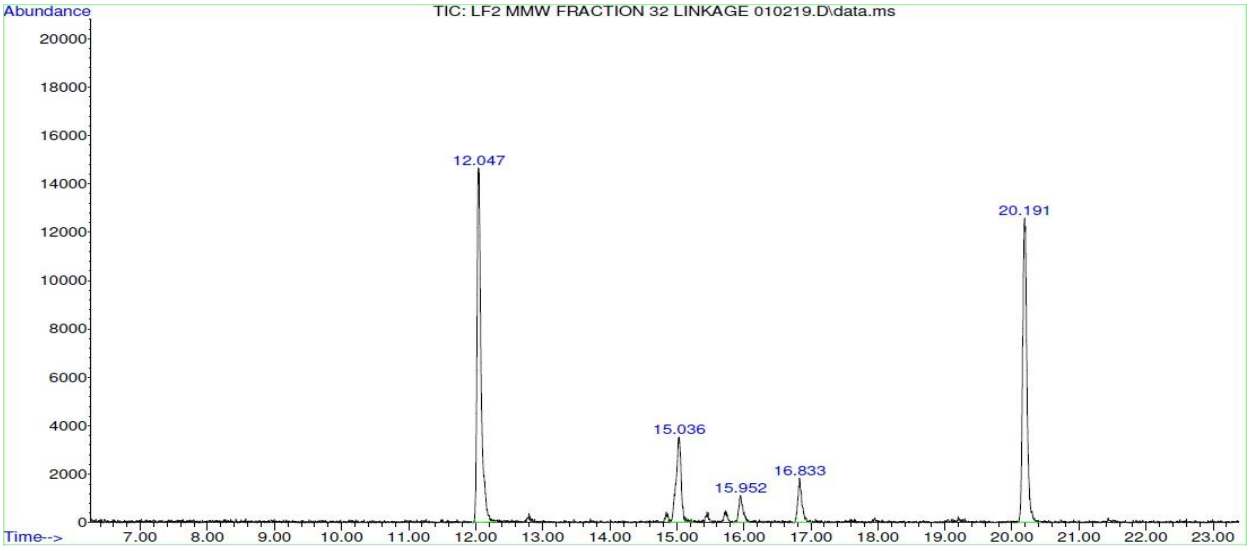

Figure 4.18: GC trace of linkage analysis performed on the combined fractions containing the MMw polysaccharides.

The two large peaks on the chromatogram at 12.05 and 20.19 min generated MS patterns corresponding to a 1,5-di-*O*-acetyl-(1-deuterio)-2,3,4,6-tetra-*O*-methylhexitol (from a non-reducing terminal hexose derivative) and to a 1,2,4,6-tetra-*O*-acetyl-(1-deuterio)-3,5-di-*O*-methylhexitol (from a 1,2,6-linked hexofuranose) respectively (Fig 4.18a and Fig 4.18b).

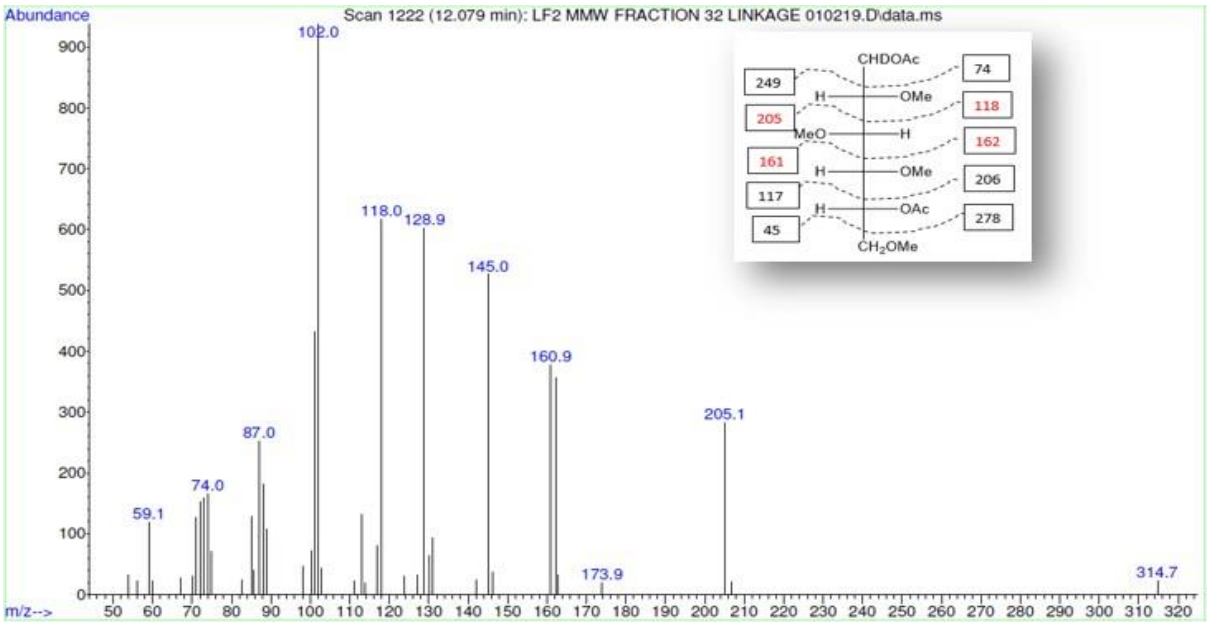

Figure 4.18a: MS fragmentation pattern of 12.05 min peak.

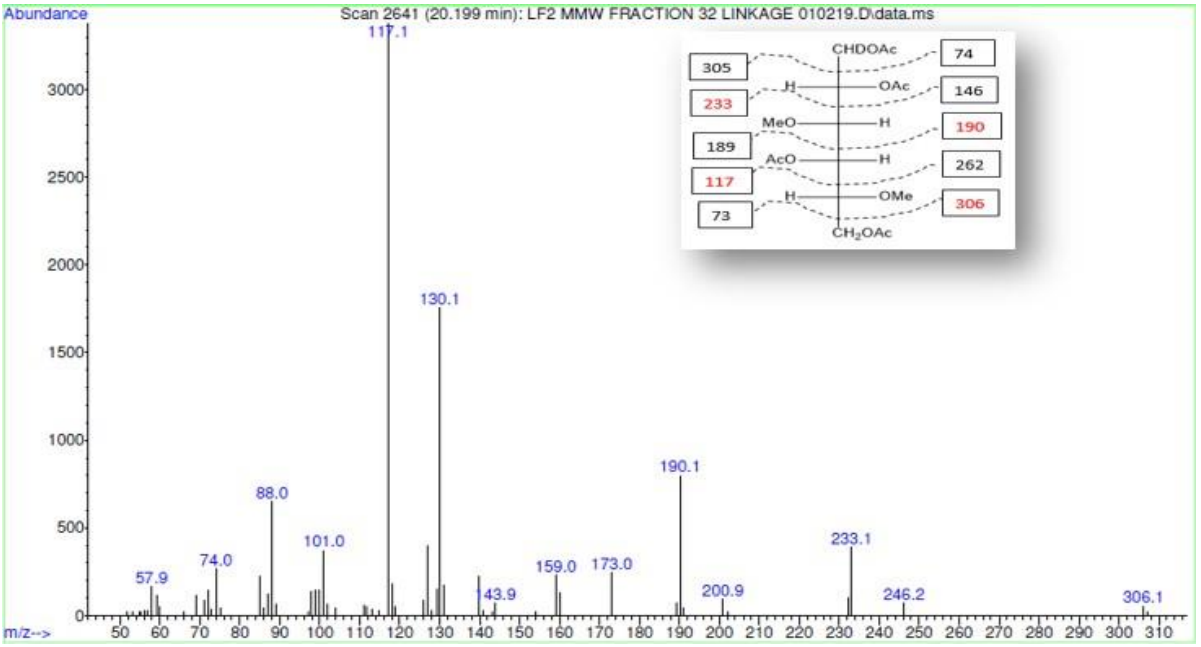

Figure 4.18b: MS fragmentation pattern of 20.19 min peak.

The three remaining small peaks at 15.04, 15.95 and 16.83 min were identified as being a 1,3,5-tri-*O*-acetyl-(1-deuterio)-2,4,6-tri-*O*-methylhexitol (from a 1,3-linked hexopyranose), a 1,4,6-tri-*O*-acetyl-(1-deuterio)-2,3,5-tri-*O*-methylhexitol (from a 1,6-linked hexofuranose) and a 1,3,5-tri-*O*-acetyl-(1-deuterio)-2,5,6-tri-*O*-methylhexitol (from a 1,3-linked hexofuranose) respectively (Fig 4.18c, Fig 4.18d and Fig 4.18e).

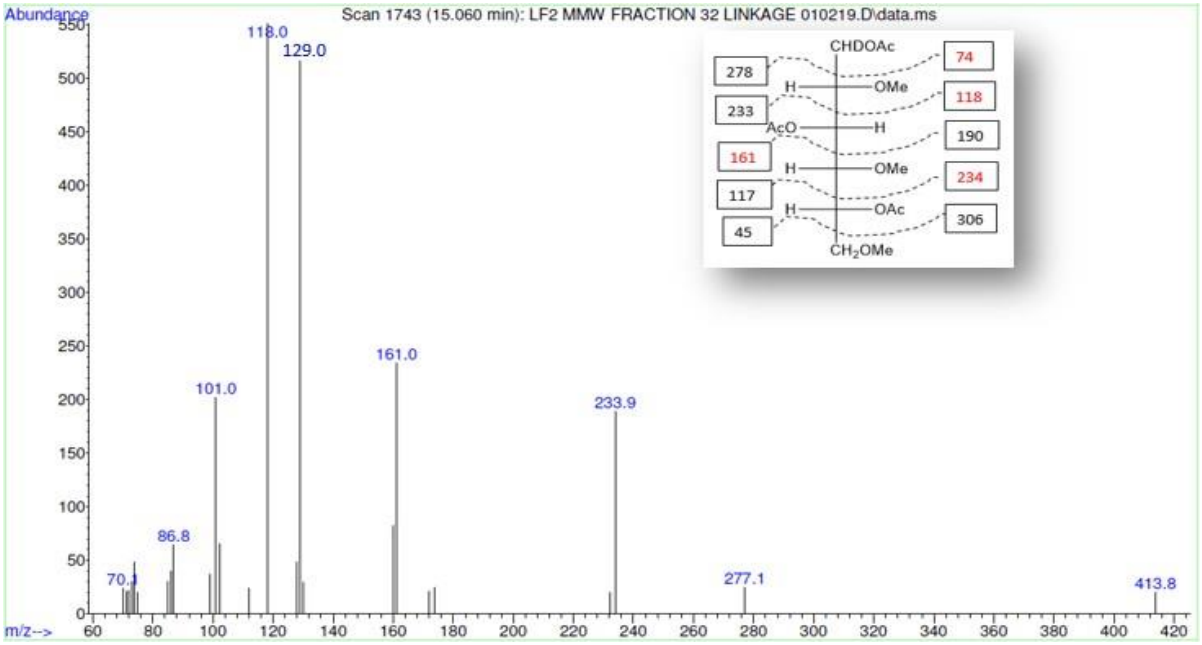

Figure 4.18c: MS fragmentation pattern of 15.04 min peak.

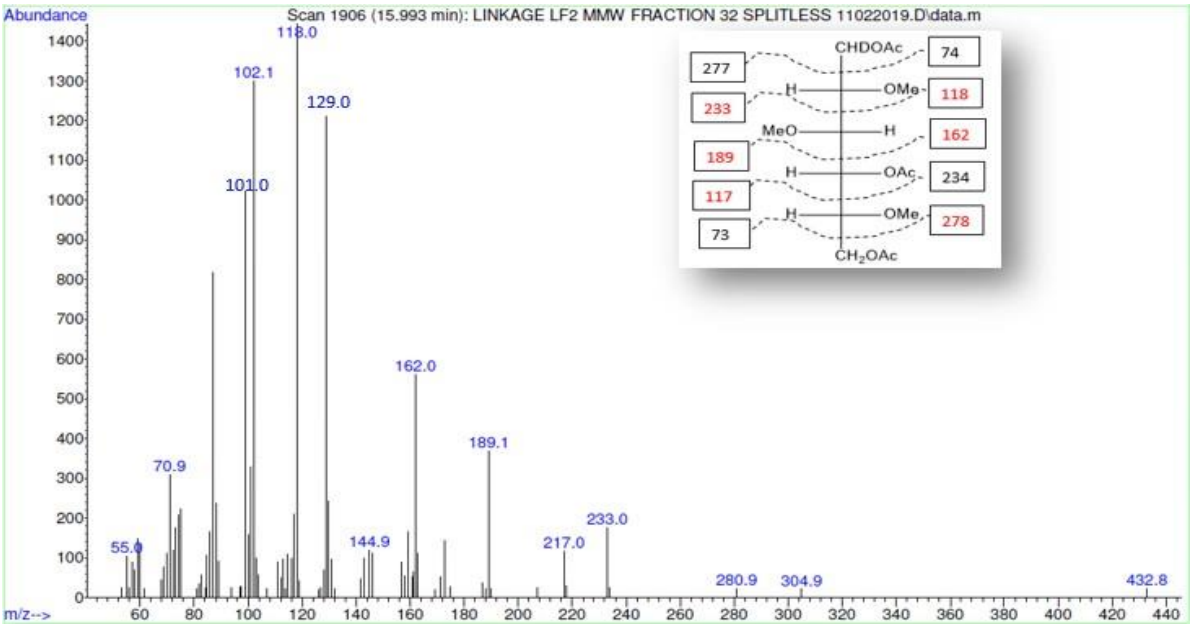

Figure 4.18d: MS fragmentation pattern of 15.95 min peak.

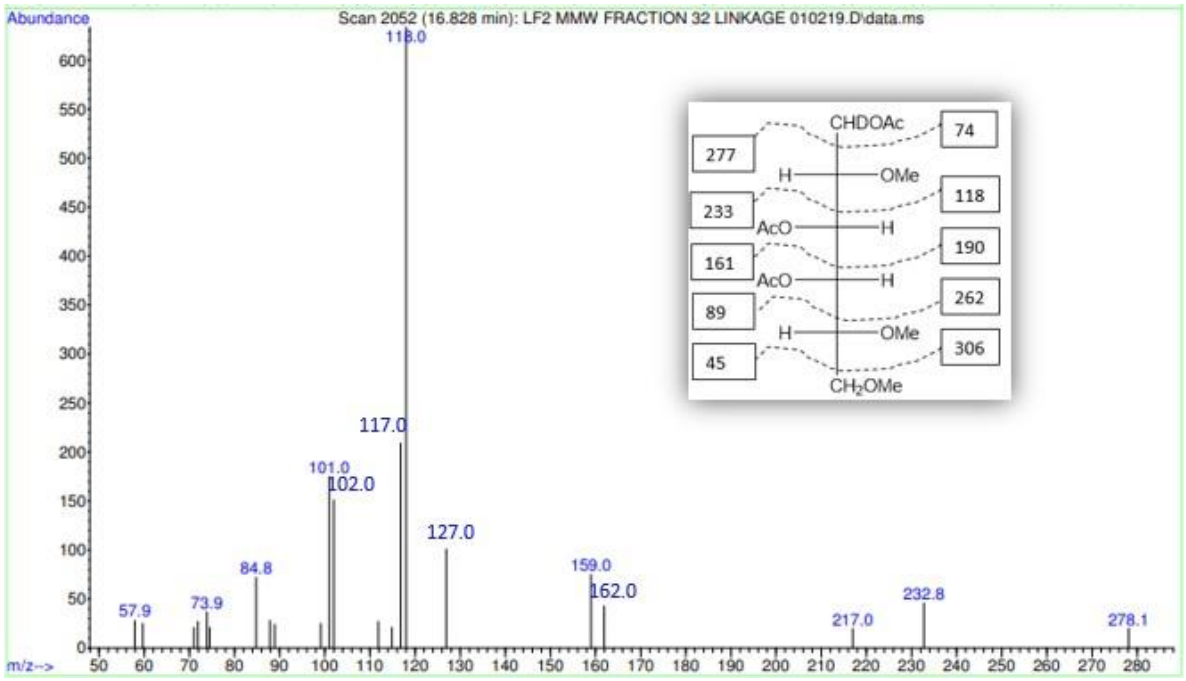

Figure 4.18e: MS fragmentation pattern of 16.83 min peak.

4.8 Smith degradation of the native MMw EPS

Smith degradation was employed to provide more insight about the structure of the MMw polysaccharides synthesised by *L. fermentum* LF2. The native MMw EPS mixture was subjected to Smith degradation using the procedure described in section **2.2.8.6**. This was performed three times and the batches were recorded as batch 1, 2 and 3. If the main backbone of the any of the MMw EPSs is resistant to oxidation, then the oligosaccharide repeating unit would be retained in the dialysis bag. On the other hand, if the main backbone is susceptible to oxidation, then small oligosaccharides/monosaccharides would be generated which would pass through the dialysis bag and thus would not be retained. However, majority of the material was retained in the dialysis bag.

4.8.1 Monomer analysis of the Smith degraded products

Monomer analysis was carried out by GC-MS on the products retained in the dialysis bag after Smith degradation of the native MMw polysaccharides using the procedure

described in section **2.8.2.2**. The GC trace of the alditol acetates generated from the Smith degraded products contained a small early eluting peak at 6.217 min and two other peaks; one small peak at 12.819 and one large peak at 13.122 min. Comparison of the retention times of the peaks generated by the Smith degraded products with that generated by the standards revealed the presence of arabinose obtained from Smith degradation of a 1,3-linked hexofuranose (see later discussion) as the early eluting peak, glucose as the small peak at 12.82 min and galactose as the large peak at 13.12 min.

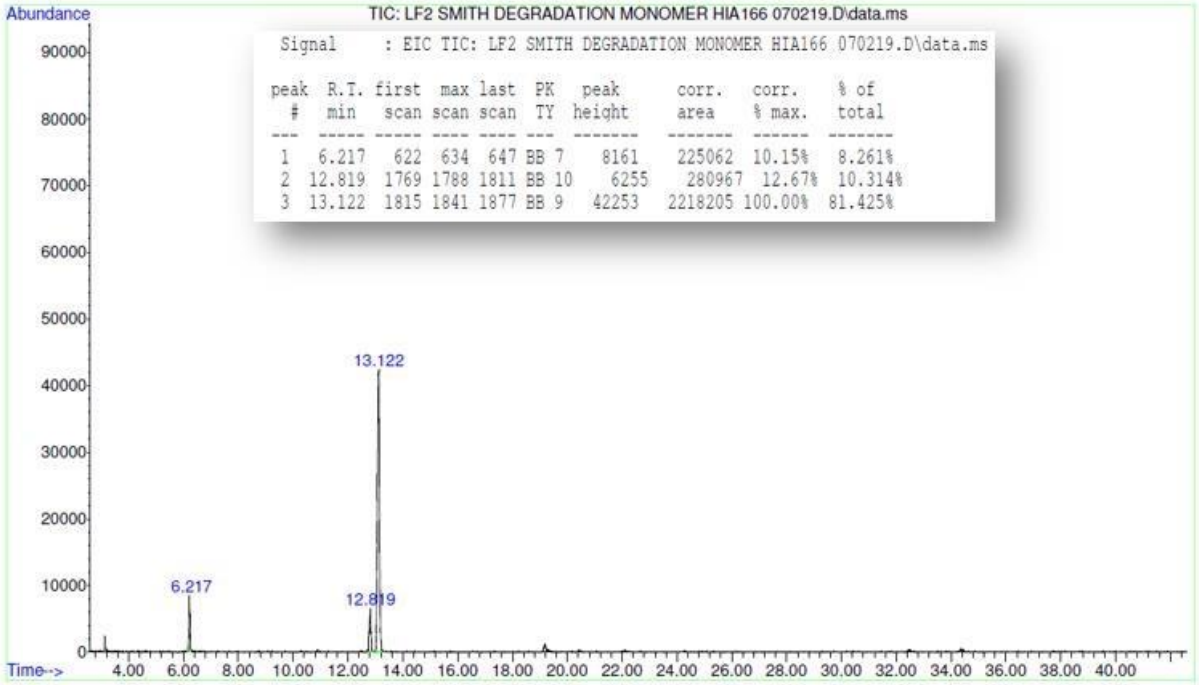

Figure 4.19: GC trace of monomer analysis performed on the Smith degraded MMw polysaccharides.

4.8.2 NMR analysis of the Smith degraded products

The identity of the sugars present in the repeating unit of the Smith degraded MMw polysaccharides was determined by ^{1}H-NMR spectroscopy using the procedure described in section **2.2.8.5**. Inspection of the anomeric region of ^{1}H NMR spectra recorded for the Smith degraded MMw EPS mixture generated three small signals at δ 5.23, 5.00 and 4.53 ppm with an integral ratio of 1.0:1.1:1.3, labelled A, B and D respectively, and a large signal at δ 4.97 ppm, labelled C.

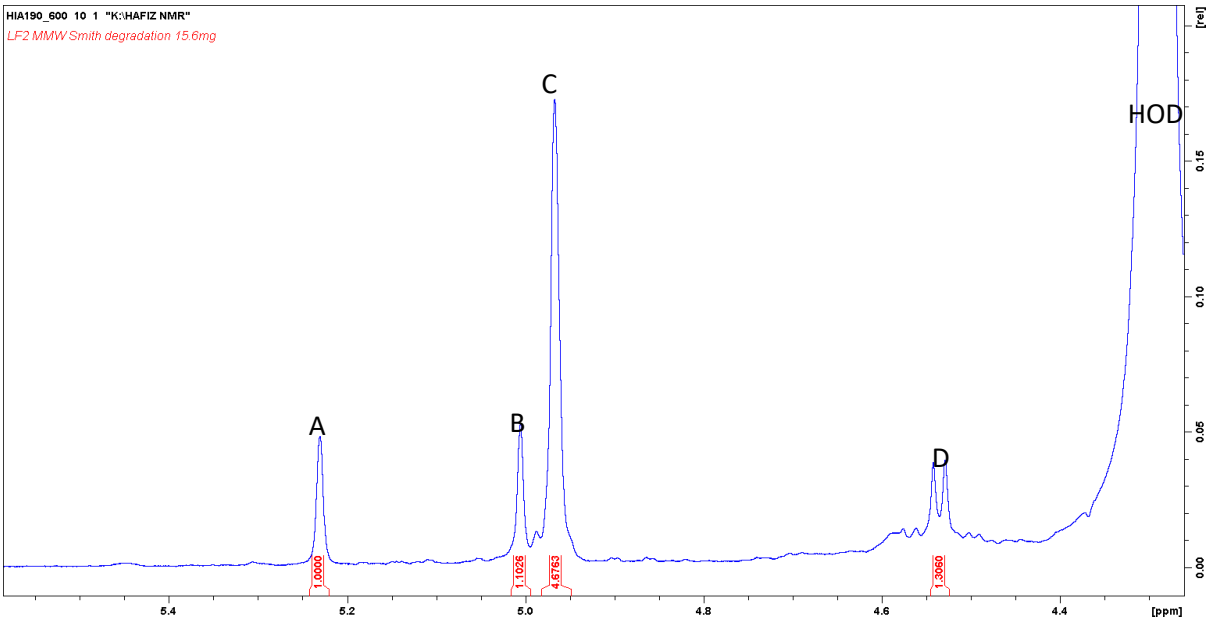

Figure 4.20: Anomeric region of the ^{1}H-NMR spectrum recorded at 70 °C on the Smith degraded MMw polysaccharides.

In all the three batches, within experimental error, the small signals were determined to have the same integral ratios. However, the ratio of the large signal (C) to the first small signal (A) was determined to be 3.97 in batch 1, 3.31 in batch 2 and 4.51 in batch 3. The observation of the same pattern of peaks in the anomeric region for all the three batches with a variable ratio of peak integrals is another indication that two different polysaccharides are present.

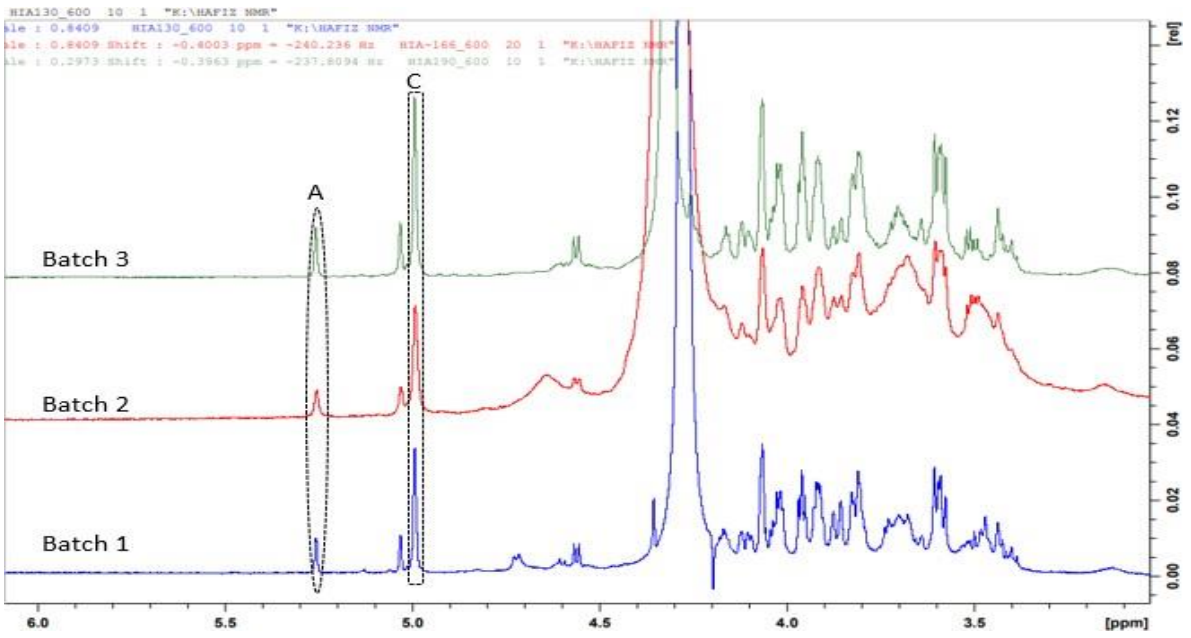

Figure 4.21: ^{1}H-NMR spectrum recorded on the three batches of the Smith degraded MMw polysaccharides at 70 °C.

The chemical shifts for the H1-H4 protons in the monosaccharides contained in the oligosaccharide units after Smith degradation were determined by tracking the scalar coupling, using a combination of a COSY and TOCSY spectrum (Fig 4.22). From the inspection of the chemical shifts obtained from the combination of ^{1}H-^{1}H-COSY and ^{1}H-^{1}H-TOSCY spectra, it can be deduced that the H-4s of three (A, B and C) out of the four monosaccharides present are located in the range of that which is expected for galactose (3.90-4.35 ppm), whereas the H-4 of the remaining monosaccharide (D), was located below 3.50 ppm which suggests that it is the only glucose present (Harding et al., 2005). The appearance of the anomeric proton of D at high field at δ 4.19 ppm with $^{3}J_{1,2}$ coupling constant of 7.97 Hz is indicative that the glucose is in its β-anomeric configuration.

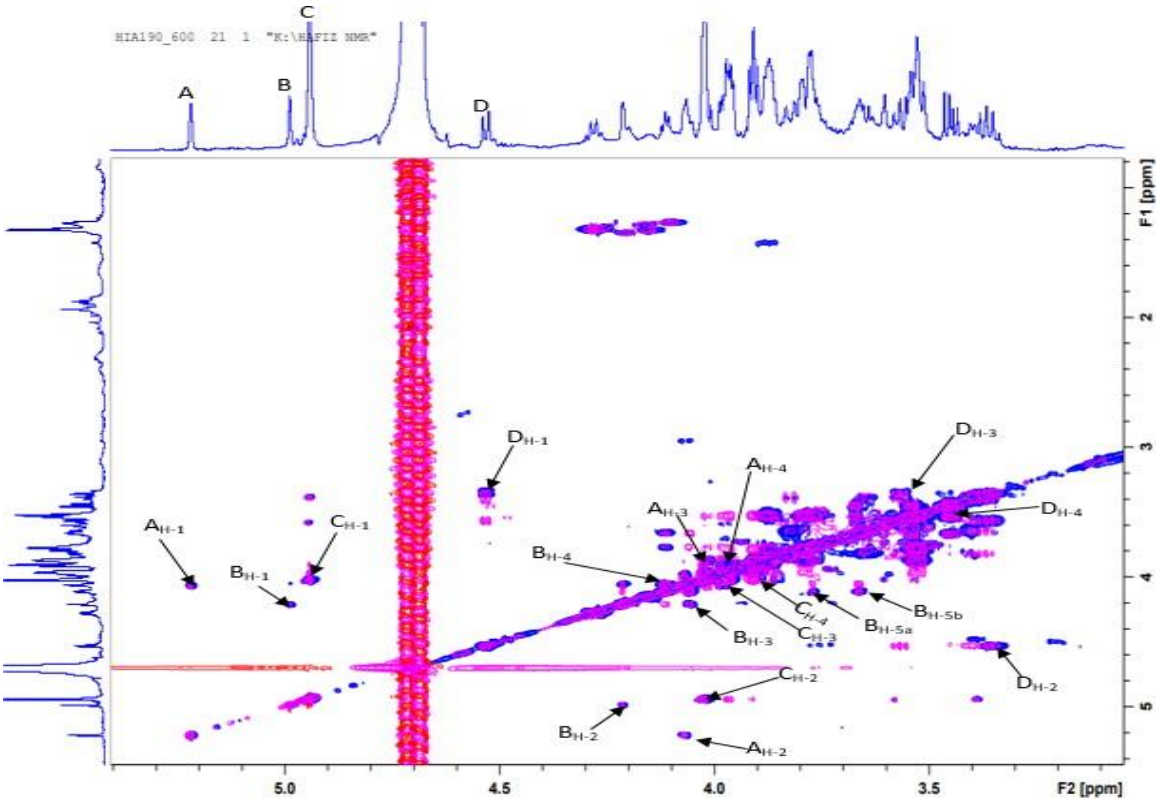

Figure 4.22: Overlaid ^{1}H-^{1}H-COSY (blue contours) and ^{1}H-^{1}H-TOCSY (pink contours) spectra for the Smith degraded MMw polysaccharides recorded at room temperature on a Bruker 600 MHz spectrometer.

The corresponding carbon chemical shifts and the remaining ring protons were determined using a combination of an edited HSQC (Fig 4.24) and a HSQC-TOCSY (Fig 4.23) spectrum, the positions of C1 to C6 are indicated in the edited ^{1}H-^{13}C-HSQC spectrum (Fig 4.24) and the chemical shifts of the individual protons and carbons, in each of the different monosaccharides, are listed in table 4.8.

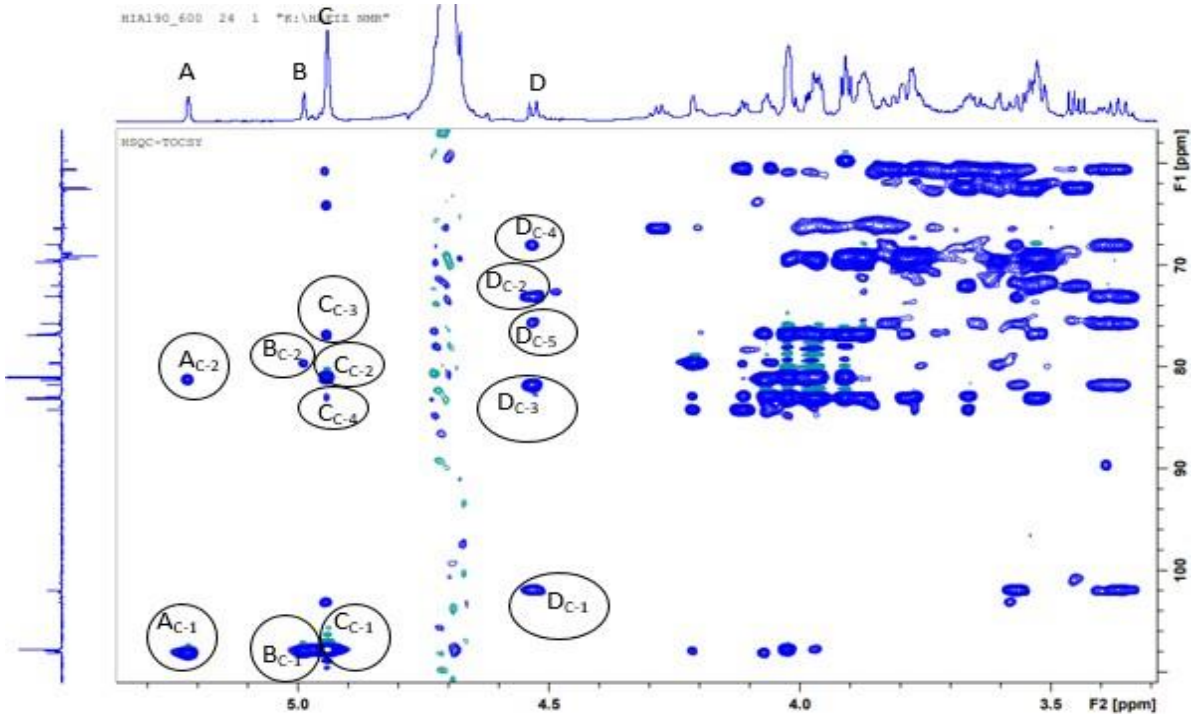

Figure 4.23: HSQC-TOCSY recorded on the Smith degraded MMw polysaccharides at room temperature on a Bruker 600 MHz spectrometer.

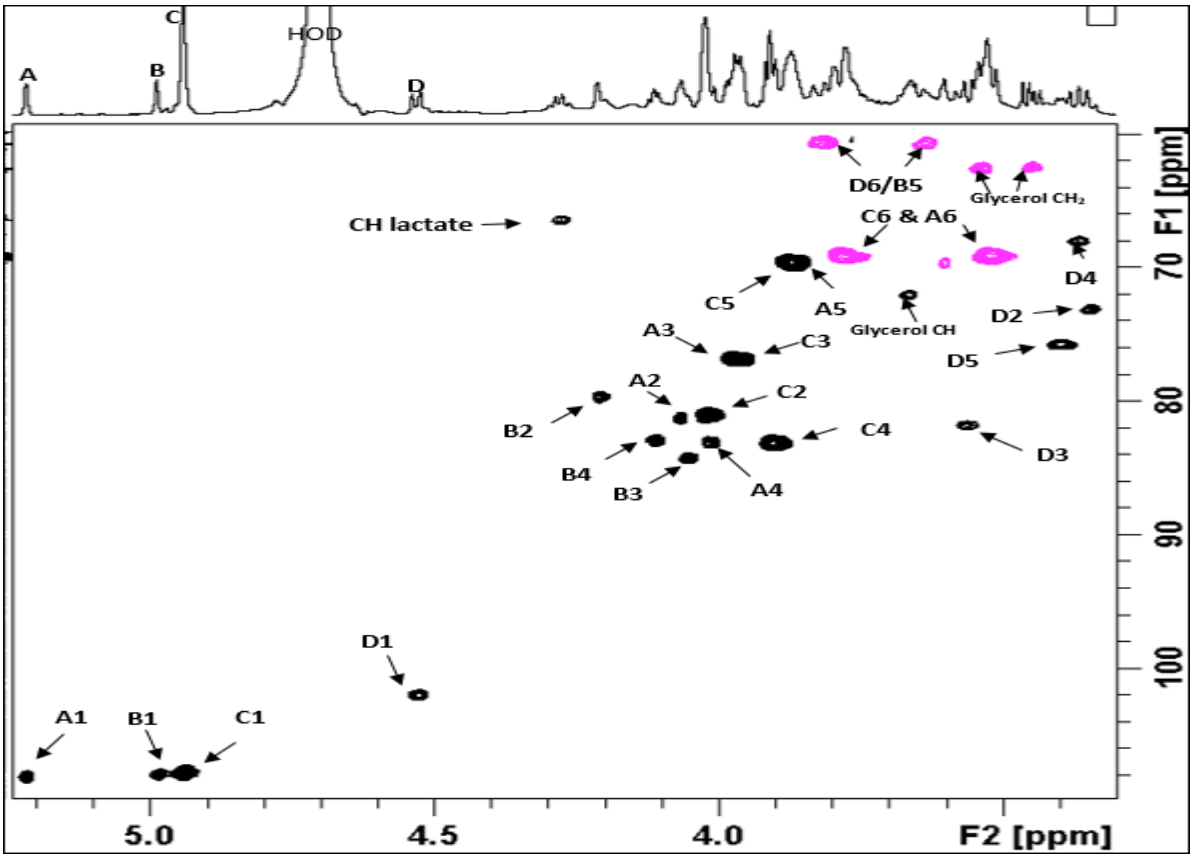

Figure 4.24: Edited ^{1}H-^{13}C-HSQC spectrum (black contours for CH and pink contours for CH_2) and recorded on the Smith degraded MMw polysaccharides at room temperature on a Bruker 600 MHz spectrometer.

Table 4.8: ^{1}H and ^{13}C NMR chemical shifts (δ, ppm) for the Smith degraded MMw polysaccharides.

Residue		C-1	C-2	C-3	C-4	C-5	C5b	C-6
		H-1	*H-2*	*H-3*	*H-4*	*H-5*	*H-5b*	*H-6s*
→6)-β-D-Gal*f*-(1→	**A**	108.08 *5.231*	81.21 *4.096*	76.73 *4.008*	83.06 *4.032*	69.47* *3.902*		69.10 *3.83 & 3.61*
→3)- β-D-Ara*f*-(1→	**B**	107.84 *5.003*	79.61 *4.229*	84.01 *4.073*	82.81 *4.141*	60.56* *3.77*	3.67	NA[#]
→6)-β-D-Gal*f*-(1→	**C**	107.84 *4.965*	80.90 *4.041*	76.83 *3.985*	83.22 *3.931*	69.73* *3.85*		69.28 *3.81 & 3.59*
→3)-β-D-Glc*p*-(1→	**D**	101.94 *4.533*	72.82 *3.367*	82.19 *3.570*	68.03 *3.401*	75.75 *3.417*		60.74 *3.82 & 3.65*

The glycerol observed in Fig 4.24 is an impurity which is from the humectant added to dialysis tubing. The point at which residue D is linked was determined by comparing its carbon resonances with those published in the literature for an unsubstituted methyl-β-D-glucopyranoside (Bock & Pedersen, 1983). Inspection of the carbon resonaces revealed that C-3 in D has shifted to 82.19 ppm from the normal C-3 (76.8 ppm) of methyl-β-D-glucopyranoside which is consistent with D being a 1,3-liked β-D-glucopyranose. In residues A and C, the appearance of their C-1 resonances downfield at 108.08 and 107.84 ppm respectively coupled with the location of their C-2 to C-4 resonances which are similar to those expected for a β-D-Gal*f*OMe. The point at which each of the two residues (A and C) were linked was determined by comparing their chemical shifts with those of an unsubstituted methyl-β-D-galactofuranoside published in the literature (Bock & Pedersen, 1983). The C-6s for both residues A and C appeared downfield at 69.10 ppm and 69.28 ppm respectively from the normal C-6 (63.60 ppm) of an unsubstituted methyl-β-D-galactofuranoside and therefore identifies the two as 1,6-linked-β-D-galactofuranosides which corresponds to the most abundant peak in the linkage analysis performed by GC-MS. Residue B was identified as a five membered ring sugar, corresponding to that which was identified as arabinose in the monomer analysis, resulting from the Smith degradation of the 1,3-linked D-galactofuranose in the native MMw polysaccharide mixture. The location of the C-1 (107.84 ppm) and C-3 (84.01 ppm) resonances of B were similar to those reported in the literature for a β-1,3-linked-L-aribinose in an arabinan oligosaccharide (C-1, 107.87 ppm and C-3, 84.48 ppm) (Wefers, Tyl, & Bunzel, 2014). The formation of 1,3-linked arabinose originating from the oxidation of C-5 and C-6 vicinal -OH in a 1,3-linked

galactofuranose has previously been reported when the native EPS synthesised by *S. thermophilus* SFi39 was subjected to Smith degradation (Lemoine *et al*., 1997).

In order to check if any other small oligosaccharides were produced during the Smith degradation, which might have not be retained during dialysis, the first dialysis water was freeze-dried and a series of NMR spectra was recorded.

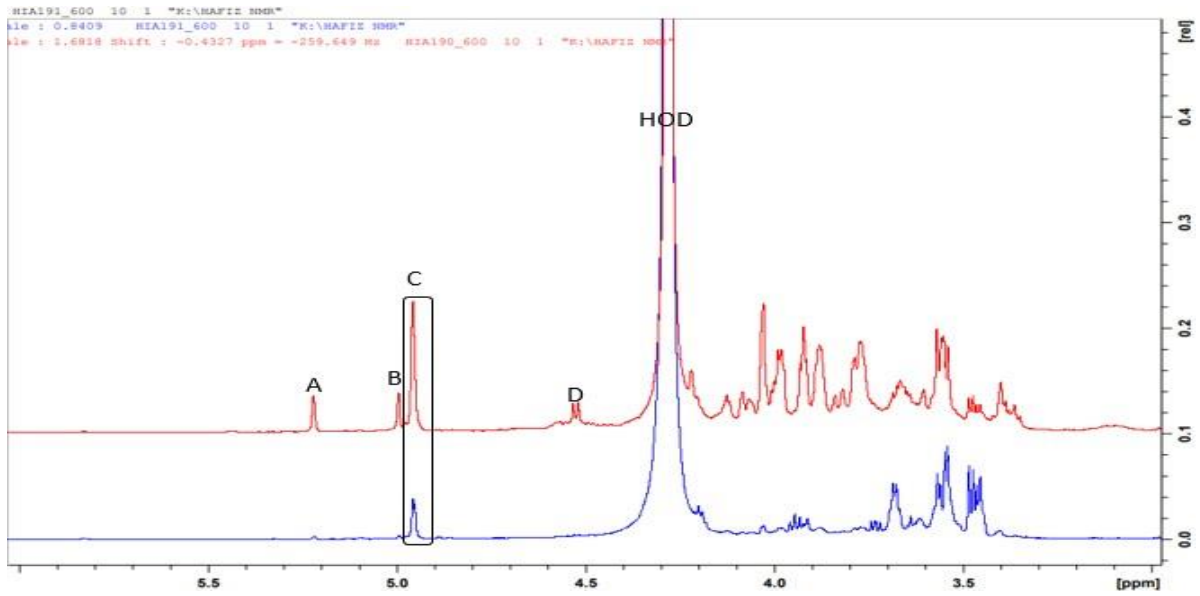

Figure 4.25: Overlaid ^{1}H-NMR recorded at 70 °C of freeze-dried dialysis bag and dialysis water contents of the Smith degraded MMw polysaccharides.

Inspection of the anomeric region of the freeze-dried dialysis water revealed the presence of residue C, earlier identified as a 1,6-linked-β-D-galactofuranoside, suggesting a small amount of lower molecular mass polysaccharide-oligosaccharide is escaping from the dialysis bag. This further suggests the presence of two MMw polysaccharides in the combined fractions, of which one has a backbone containing a 1,6-linked galactofuranose and 1,2,6-linked galactofuranose, which when subjected to Smith degradation would yield a lower Mw polysaccharide-oligosaccharide with 1,6-linked backbone (see scheme 4 on next page). The appearance of C in both the dialysis water and the dialysis bag indicate that C has different molecular masses and this is only possible if the MMw polysaccharide has a main chain containing a 1,2,6-linked galactofuranose and a variable number of 1,6-linked galactofuranoses, which, when subjected to Smith degradation, will form oligosaccharides of different molecular masses depending on where the 1,6-linked galactofuranose occurs; hereafter referred to as MMwb.

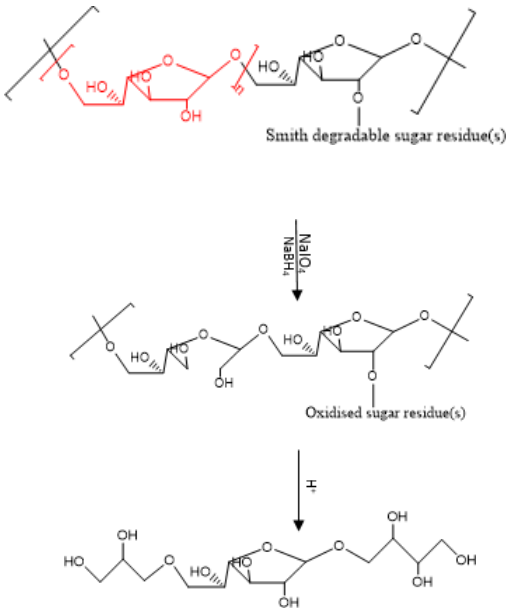

Scheme 4: Smith degradation of MMwb.

The order of the residues in the repeat unit of the second MMw polysaccharide formed during Smith degradation; hereafter referred to as MMwa was, determined by inspecting the inter-residue correlations observed on both HMBC and ROESY spectra between residues A, B and D.

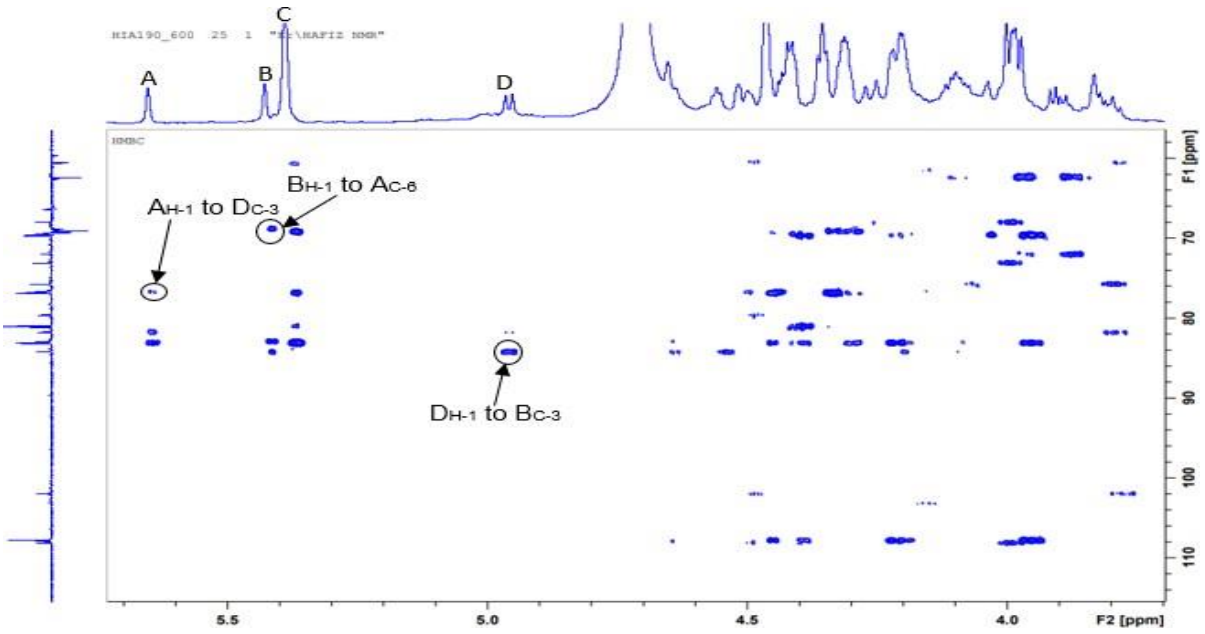

Figure 4.26: HMBC spectrum of the Smith degraded MMw polysaccharides recorded at room temperature showing the cross peaks derived from anomeric protons to carbons in MMwa based inter-residue coupling via glycosidic bond for A, B and D.

On the HMBC spectrum (Fig 4.26), inter-residue correlations were observed between A_{H-1} to D_{C-3}, B_{H-1} to A_{C-6} and D_{H-1} to B_{C-3} identifying a 1,3-linkage between A and D, a 1,6-linkage between B and A and a 1,3-linkage between D and B. These were matched by the presence of inter-residue correlations observed on the ROESY spectrum (Fig 4.27) between A_{H-1} to D_{H-3}, D_{H-1} to B_{H-3} and B_{H-1} to $A_{H-6a/H-6b}$.

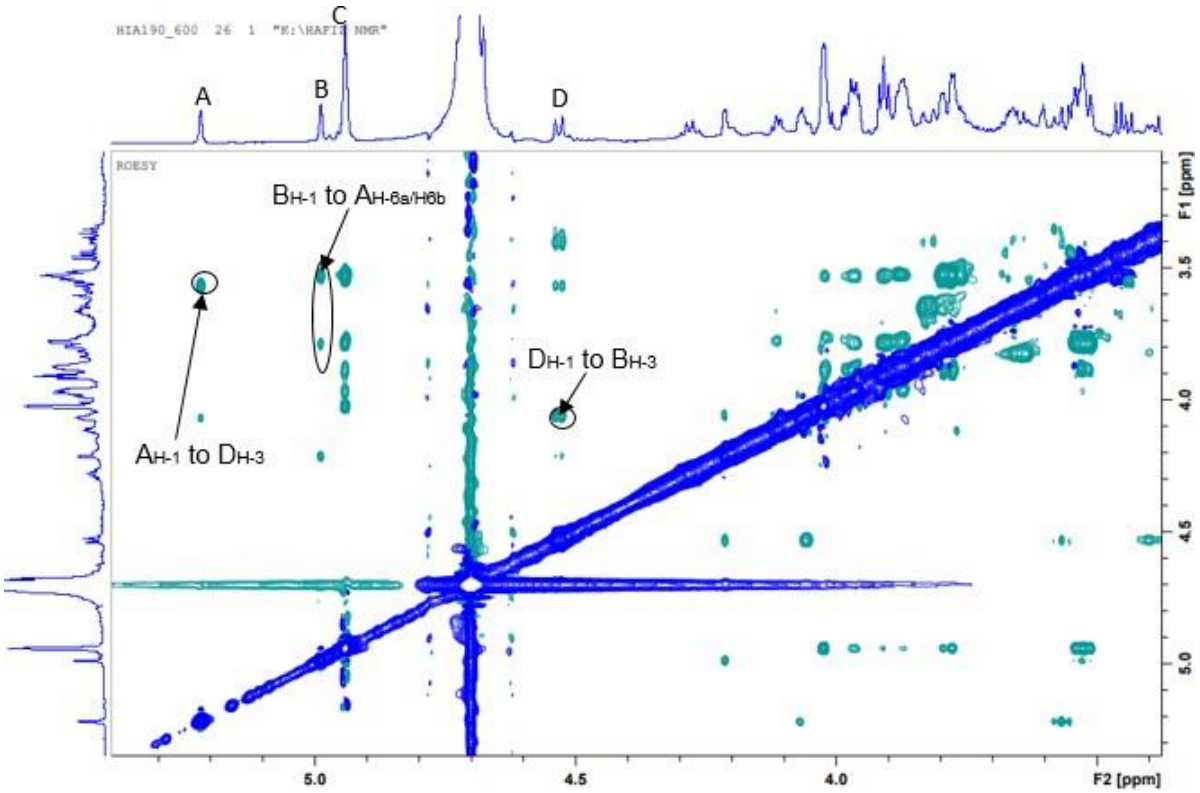

Figure 4.27: ROESY spectrum of the Smith degraded MMw polysaccharides recorded at room temperature showing the cross peaks derived from anomeric protons to the neighbouring protons in MMwa based inter-residue coupling through space for A, B and D.

Given the correlations observed in the HMBC and the ROESY spectra, the structure of the Smith degraded MMwa is most likely to be:

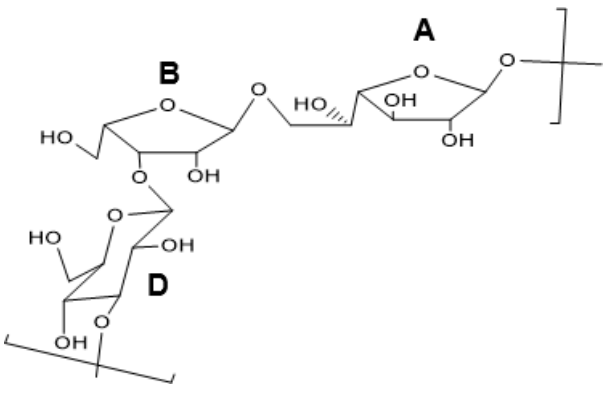

From the proposed structure of the polysaccharide generated after Smith degradation (MMwa), it can be deduced that the β-1,3-linked-D-glucopyranose is derived from the 1,3-linked hexopyranoside earlier identified in the linkage analysis of the native MMw polysaccharides which would be resistant to Smith degradation. The β-1,3-linked-L-aribinose is generated from the Smith degradation of the 1,3-linked D-galactofuranose in the native MMw polysaccharides and the 1,6-linked-β-D-galactofuranoside results from the 1,2,6-linked D-galactofuranose also identified in the linkage analysis of the native MMw polysaccharides. Therefore, the structure of the native MMwa is most likely to be:

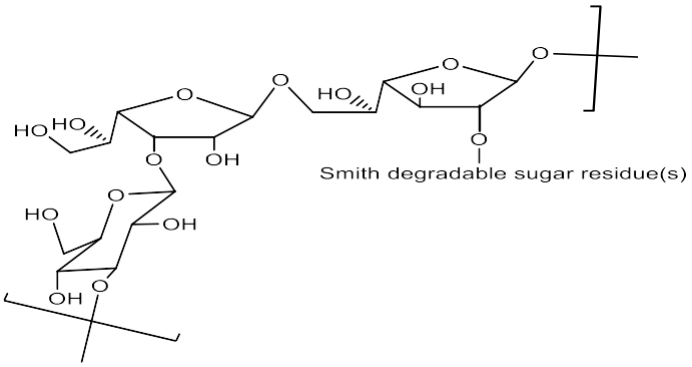

4.9 NMR analysis of the native MMw polysaccharides

In order to characterise the native polysaccharides, the anomeric region of the ^{1}H NMR spectra recorded on the native MMw polysaccharides was inspected. Inspection of the anomeric region revealed the presence of three additional signals which were labelled A', C' and E (Fig 4.34). A and A' have the same integral ratio of 1.0, as does C and C' (3.8) in all batches. E and A also have the same integral ratio of 1.0 in batch 1, but in other batches of the MMw polysaccharides, the integral ratio for E was sometimes lower and on the other occasion was sometimes significantly larger than that of A.

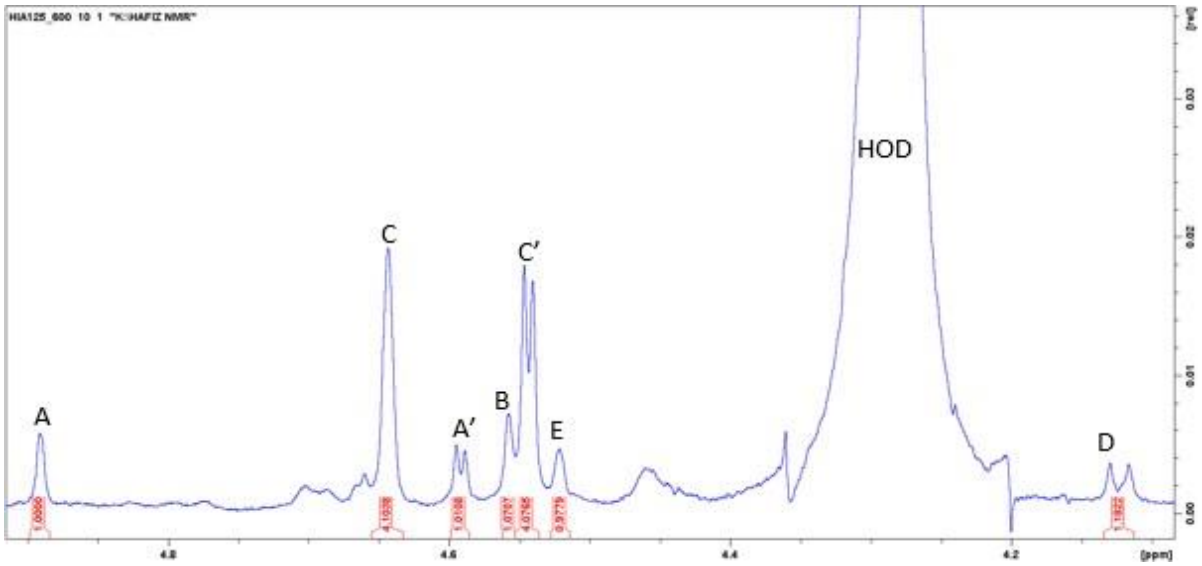

Figure 4.28: ^{1}H-NMR spectrum recorded at 70 °Cof the MMw polysaccharide mixture.

Starting from the anomeric proton, the scalar coupling of the H-2 to H-6 protons for A to D were tracked using a combination of a ^{1}H-^{1}H-COSY and ^{1}H-^{1}H-TOCSY spectra.

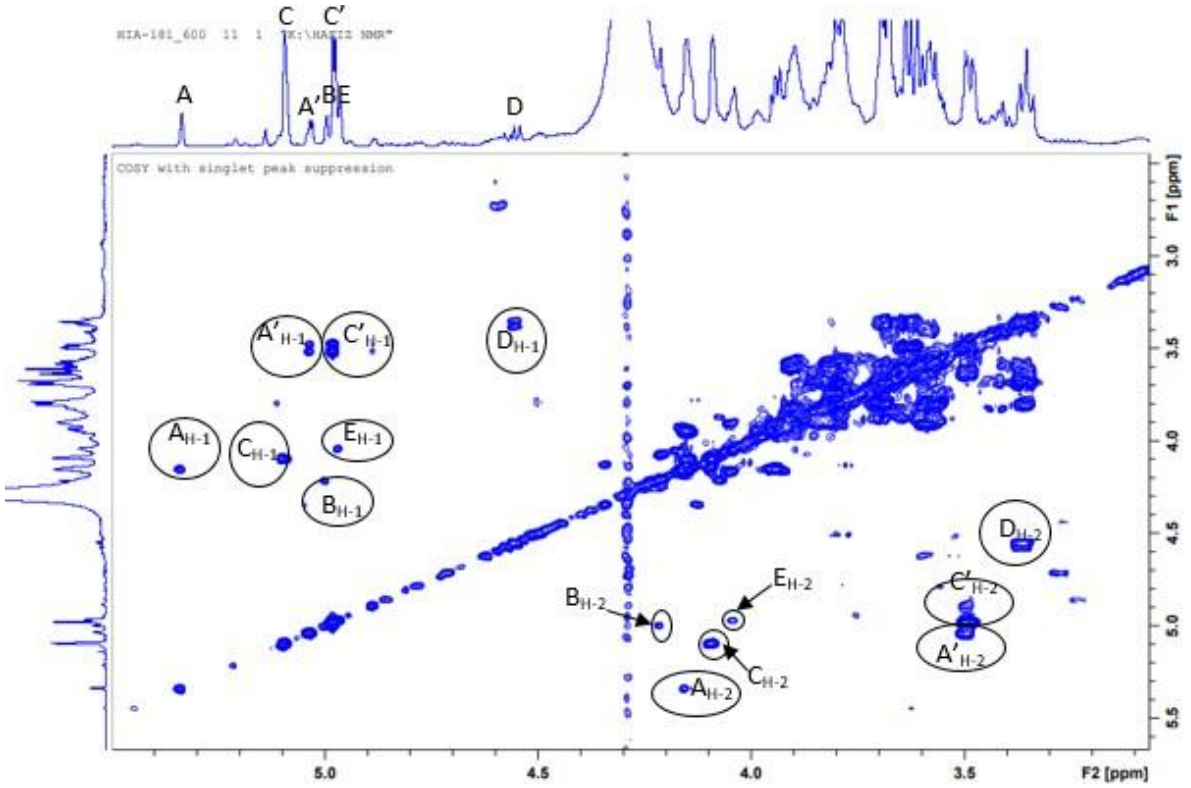

Figure 4.29: ^{1}H-^{1}H-COSY spectrum for the MMw polysaccharide mixture recorded at room temperature on a Bruker 600 MHz spectrometer.

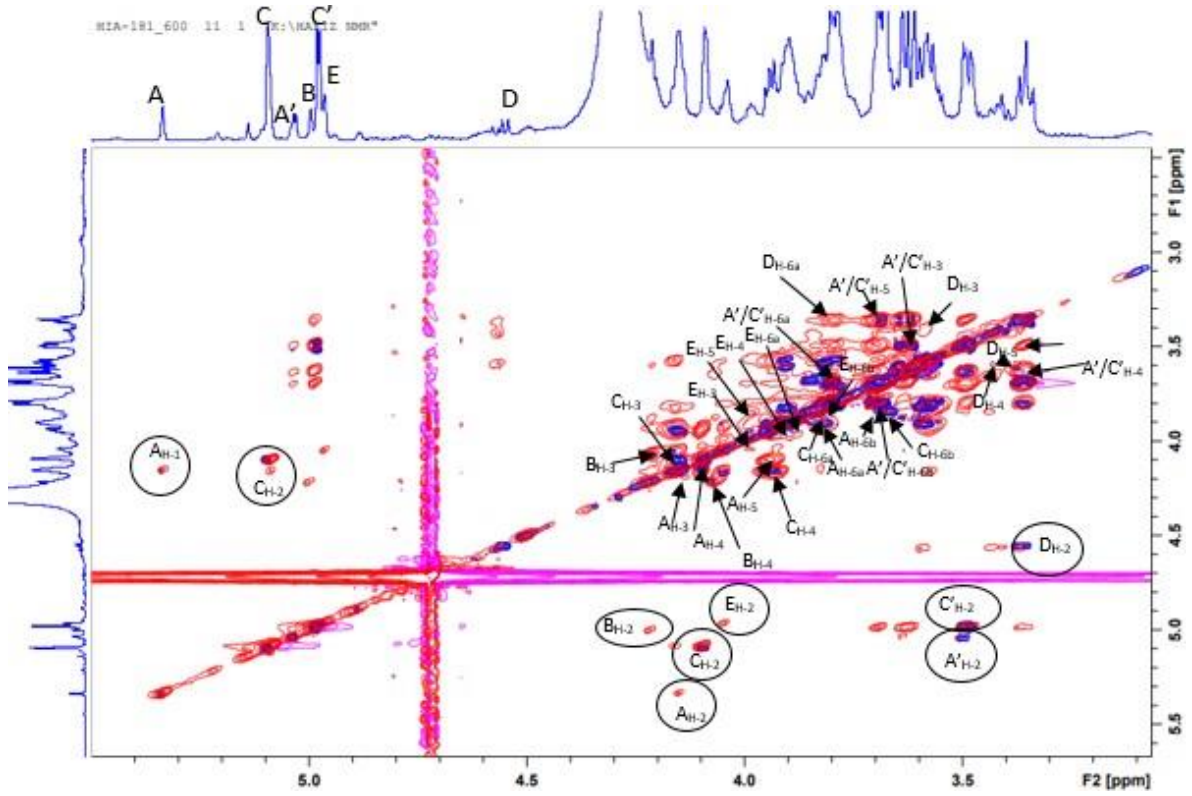

Figure 4.30: Overlaid ^{1}H-^{1}H-COSY (blue contours) and ^{1}H-^{1}H-TOCSY (red contours) spectra for the MMw polysaccharide mixture recorded at room temperature (calibrated) on a Bruker 600 MHz spectrometer.

The location of the carbons C-1 to C-6 was tracked from inspection of a combination of an edited ^{1}H-^{13}C-HSQC spectrum (Fig 4.32) and a ^{1}H-^{13}C-HSQC-TOCSY (Fig 4.31) spectrum, and comparison with those reported in the literature (Bock & Pedersen, 1983). The location of individual carbon and proton resonances are listed in table 4.10 and highlighted on the HSQC spectrum (Fig 4.32).

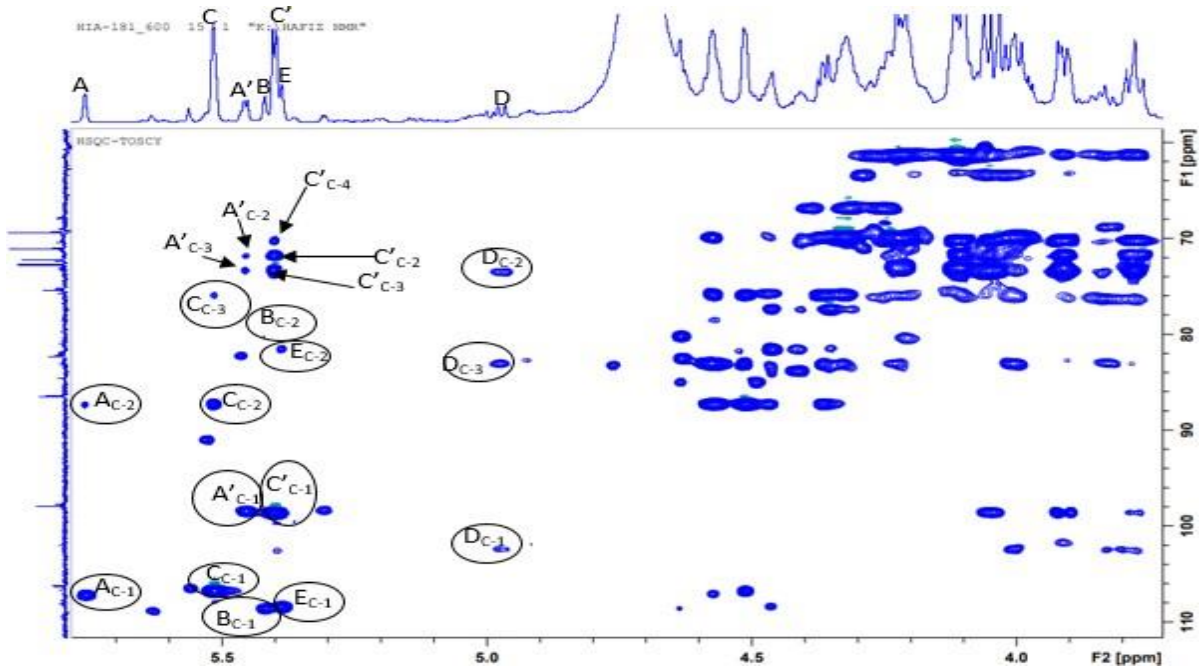

Figure 4.31: HSQC-TOCSY recorded on the MMw polysaccharide mixture at room temperature on a Bruker 600 MHz spectrometer.

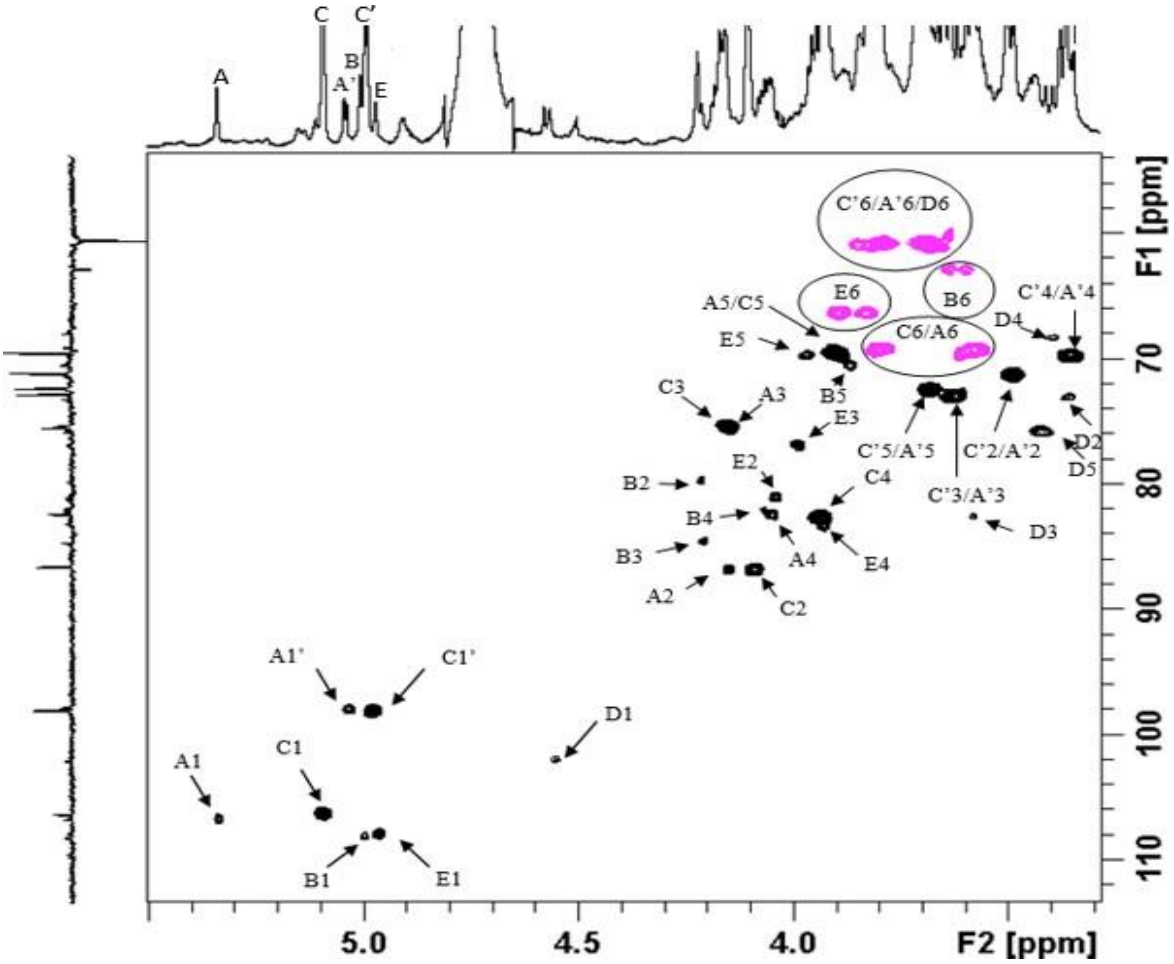

Figure 4.32: Edited ^{1}H-^{13}C-HSQC spectrum recorded at room temperature (black contours for CH and pink contours for CH_2) recorded on the MMw polysaccharides at room temperature on a Bruker 600 MHz spectrometer.

Table 4.9: ^{1}H and ^{13}C NMR chemical shifts (δ, ppm) for the MMw polysaccharides.

Residue		C-1	C-2	C-3	C-4	C-5	C-6
		H-1	*H-2*	*H-3*	*H-4*	*H-5*	*H-6s*
→2,6)-β-D-Gal*f*-(1→	**A**	107.01 *5.338*	87.2 *4.153*	75.8 *4.147*	83.0 *4.051*	69.9* *3.909*	69.7 *3.80 & 3.58*
α-D-Glc*p*-(1→	**A'**	98.3 5.033	71.7# 3.50	73.3# 3.63	70.3# 3.36	72.9# 3.69	61.2# 3.80 & 3.69
→,3)-β-D-Gal*f*-(1→	**B**	108.5 *4.998*	80.1 *4.219*	84.9 *4.210*	82.5 *4.074*	70.8 *3.871*	63.3 *3.64 & 3.60*
→2,6)-β–D-Gal*f*-(1→	**C**	106.7 *5.095*	87.3 *4.095*	75.8 *4.162*	83.1 *3.944*	69.8 *3.910*	69.7 *3.81 & 3.58*
α-D-Glc*p*-(1→	**C'**	98.6 4.979	71.7# 3.50	73.3# 3.63	70.3# 3.36	72.9# 3.69	61.2# 3.80 & 3.69
→3)-β-D-Glc*p*-(1→	**D**	102.5 *4.552*	73.6 *3.362*	83.0 *3.587*	68.7 *3.411*	76.2 *3.418*	61.3 *3.80 & 3.68*
→6)-β-D-Gal*f*-(1→	**E**	108.4 *4.968*	81.4 *4.046*	77.4 *3.990*	83.8 *3.931*	70.0 *3.976*	66.8 3.90 & 3.84

The point of linkage of D was confirmed by comparison with the chemical shifts of an unsubstituted methyl-β-D-glucopyranoside published in the literature (Bock & Pedersen, 1983). Inspection of the chemical shifts revealed that C-3 in D has shifted to 83.0 ppm from the normal C-3 (76.8 ppm) of a methyl-β-D-glucopyranoside which is consistent with D being a 1,3-liked β-D-glucopyranose.

The downfield chemical shift of C-1s of A and C at 107.01 and 106.70 ppm respectively and the location of their C-3 to C-5 resonances are what is expected for a β-D-Gal*f*OMe. Their point of linkages was determined by comparing their chemical shifts with those of an unsubstituted methyl-β-D-galactofuranoside published in the literature (Bock & Pedersen, 1983). The appearance of C-2s/C-6s of A and C downfield identifies the two as the 1,2,6-linked-β-D-galactofuranosides corresponding to the large last peak in the linkage analysis performed by GC-MS on the native MMw polysaccharides.

It was not possible to differentiate between A' and C' as the chemical shifts for their protons (H-2 to H-6) and carbons (C-2 to C-6) were very similar. From the inspection of the location of the H-4 resonances for A' and C', it can be deduced that the H-4s of the two residues are located below 3.5 ppm which falls within the range of that which is expected for a glucose (3.90-4.35 ppm) (Harding et al., 2005). The two residues (A' and C') having $^{3}J_{1,2}$ coupling constants of 3.370 and 3.593 Hz respectively which is an indication that the glucoses are in their α-anomeric configuration. Comparison of the chemical shifts of the carbons in A' and C' with that which has been reported in the literature for a non-reducing terminal α-D-glucopyranose suggests that the two residues are the terminal glucopyranoses observed as the first large peak in the linkage analysis.

The appearance of the C-1 in residue B downfield at 108.50 ppm and the position of its remaining carbon resonances C2- to C-5 identified B as a β-D-Gal*f*OMe. When compared with the chemical shifts of that of an unsubstituted methyl-β-D-galactofuranoside published in the literature Bock & Pedersen, (1983), the chemical shift of C-3 in B appeared downfield at 84.9 ppm as opposed to 78.4 ppm of an unsubstituted methyl-β-D-galactofuranoside. B was identified as 1,3-linked D-galactofuranose seen as a small peak in the linkage analysis of the native MMw

polysaccharide which is oxidised under Smith degradation and changes to a five membered ring sugar, identified as a β-1,3-linked-L-aribinose.

By a process of elimination, the only unaccounted peak remaining in the linkage analysis performed on the native MMw polysaccharide is that of the 1,6-linked galactofuranose which is prone to oxidation and will not appear in the Smith degraded MMw polysaccharides. The remaining residue E has a H-4 proton located at 3.931 ppm which in the range of that which is expected for a galactose (3.90-4.35 ppm) (Harding *et al.*, 2005). The appearance of the C-1 in residue E downfield at 108.40 ppm and the position of its remaining carbon resonances identified E as being a β-D-Gal*f*OMe. When compared with the chemical shifts of that of an unsubstituted methyl-β-D-galactofuranoside published in the literature Bock & Pedersen, (1983), the chemical shift of C-6 in E appeared downfield at 66.8 ppm as opposed to 63.6 ppm for an unsubstituted methyl-β-D-galactofuranoside. E was identified as 1,6-linked D-galactofuranose seen as a small peak in the linkage analysis of the native MMw polysaccharide.

The point of attachment of the two residues (A' and C') to the main chain of the MMw polysaccharides was determined by inspecting the inter residue correlations observed on the ROESY and HMBC spectra. On the ROESY spectrum, strong NOEs were observed between A'_{H-1} and A_{H-2}, and between C'_{H-1} and C_{H-2} which were matched by inter-residue correlations observed on HMBC spectrum between A'_{H-1} and A/C_{C-2}, and between C'_{H-1} and C/A_{C-2}. These therefore suggests that the two residues A' and C' identified as non-reducing terminal α-D-galactopyranosides are linked to the 2-position of A and C respectively. This further suggests the MMwa having the earlier proposed structure, which under Smith degradation will produce the exact same structure as that which has been identified.

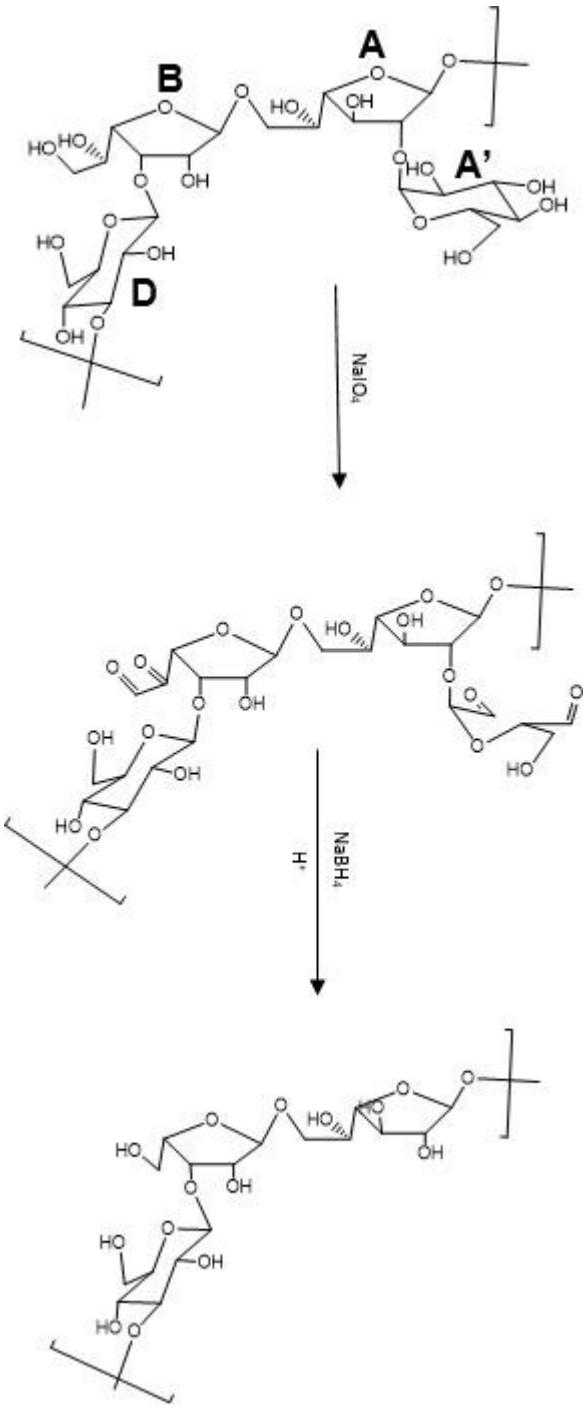

The sequence in which the monosaccharides occur in the repeating sugar units was also confirmed by interpretation of the HMBC and ROESY spectrum. The inter-residue correlations observed between the anomeric proton of each sugar residue to the neighbouring carbon or proton (depending on the spectra) via glycosidic bond and through space were determined and are listed in table 4.11. On the ROESY spectrum,

inter residue NOEs were observed between D_{H-1} and B_{H-3} and between B_{H-1} and $A/C_{H-6a/H-6b}$ which were matched by inter-residue correlations observed on HMBC spectrum between D_{H-1} and B_{C-3} and between B_{H-1} and A_{C-6}.

Table 4.10: H-1 inter-residue correlations to the neighbouring proton via through space coupling obtained from ROESY spectrum and H-1 inter-residue correlations to neighbouring carbons connected via glyosidic bond obtained from HSQC spectrum.

Anomeric proton in sugar residue (δ)	**NOE Correlations to protons in sugar residues (δ)**
A_{H-1} (5.34)	D_{H-3} (3.59)
C_{H-1} (5.10)	A/C_{H-6a} (3.81), A/C_{H-6b} (3.58).
A'_{H-1} (5.03)	A_{H-2} (4.15)
B_{H-1} (5.00)	A/C_{H-6a} (3.81), A/C_{H-6b} (3.58).
C'_{H-1} (4.98)	C'/A'_{H-2} (3.50).
E_{H-1} (4.97)	A/C_{H-6a} (3.81), A/C_{H-6b} (3.58).
D_{H-1} (4.55)	B_{H-3} (4.21)
	HMBC Correlations to carbons in sugar residues (δ)
A_{H-1} (5.34)	A_{C-4} (83.0) or D_{C-3} (83.0).
C_{H-1} (5.10)	C/A_{C-6} (69.7).
A'_{H-1} (5.03)	A_{C-2} (87.2)
B_{H-1} (5.14)	A_{C-6} (69.1).
C'_{H-1} (4.98)	C_{C-2} (87.3).
E_{H-1} (4.97)	A/C_{C-6} (69.7)
D_{H-1} (4.55)	B_{C-3} (84.9)

On the HMBC spectrum, inter residue correlations were observed between E_{H-1} to A/C_{C-6} which were matched by the inter-residue correlations observed between E_{H-1} to $A/C_{H-6a/H-6b}$ on the ROESY spectrum. The integral ratio of E often exceeded that of A, which implies that A is more likely to be linked to C via C-6. This confirms the proposed structure of the MMwb polysaccharide having a main chain of 1,2,6-linked-β-D-galactofuranosides and a variable number of 1,6-linked-β-D-galactofuranosides. The extent to which the 1,6-linked-β-D-galactofuranoside is substituted at the 2-position is very dependent on the fermentation conditions.

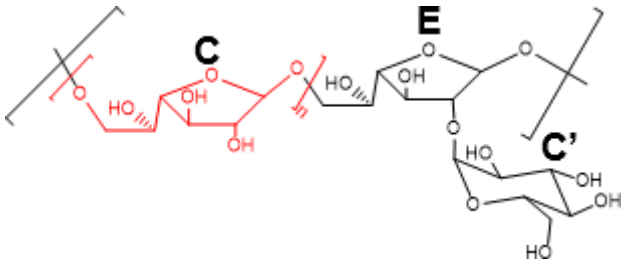

4.10 Conclusion

In conclusion, it was earlier reported that the bacterial strain *Lactobacillus fermentum* LF2 synthesises two populations of polysaccharides of different molecular masses, a high molecular mass (HMw) fraction of 1.23 x 10^6 $gmol^{-1}$ and a medium molecular mass (MMw) fraction of 8.80 x 10^4 $gmol^{-1}$. The two populations of polysaccharides were successfully separated using preparative size exclusion chromatography and the HMw polysaccharide was fully characterised. In this chapter, analysis of the fractions containing the population of the MMw polysaccharide by SEC-MALLS and ^{1}H-NMR were undertaken which suggested the presence of two MMw polysaccharides, one with an average weight molecular mass of 8.80 x 10^4 $gmol^{-1}$, and the other with an average weight molecular mass of 6.49 x 10^4 $gmol^{-1}$ both were accompanied by UV absorbing molecules. Unfortunately, all attempts to purify and separate the two MMw polysaccharides using a smaller pore-size column, mild acid hydrolysis, treatment with proteinase and DNase, failed. It was then decided to attempt to directly characterise the two polysaccharides as a mixture. Monomer analysis performed on the mixture by GC-MS and HPAEC-PAD revealed the presence of glucose and galactose as the main components accompanied by and trace levels of mannose, glucosamine and galactosamine. The retention times of the peaks generated by the mixture during the determination of absolute configuration by GC-MS corresponded to those generated by standards D-Glucose and D-Galactose, which confirmed that both glucose and galactose that make up the repeating unit of the MMw polysaccharide mixture are of D-absolute configuration. Linkage analysis using per-methylated alditol acetates performed also generated two large peaks and three small peaks. The two large peaks corresponded to a non-reducing terminal hexose derivative and to a 1,2,6-linked hexofuranose. The three remaining small peaks were identified as being a 1,3-linked hexopyranose, a 1,6-linked hexofuranose and a 1,3-linked hexofuranose.

The structures of the two MMw polysaccharides were further investigated by subjecting the MMw polysaccharide mixture to Smith degradation. Monomer analysis of the Smith degraded products revealed the presence of arabinose, glucose and galactose as a large peak. The number and the sequence in which these sugars occur in the repeating unit of the Smith degraded MMw polysaccharide mixture was determined by NMR spectroscopy. A combination of ^{1}H-^{1}H-COSY, ^{1}H-^{1}H-TOCSY,

edited ^{1}H-^{13}C-HSQC, ^{13}C-HSQC-TOCSY, ^{1}H-^{13}C-HMBC and ^{1}H-^{1}H-ROESY and comparison of chemical shift data in the literature was used in identifying the chemical shifts of the protons and carbons of each sugar residue and the order of the residues in the repeating unit. The combination identified one of the MMw polysaccharides (MMwa) as having a repeating unit with sugar residues in the sequence:

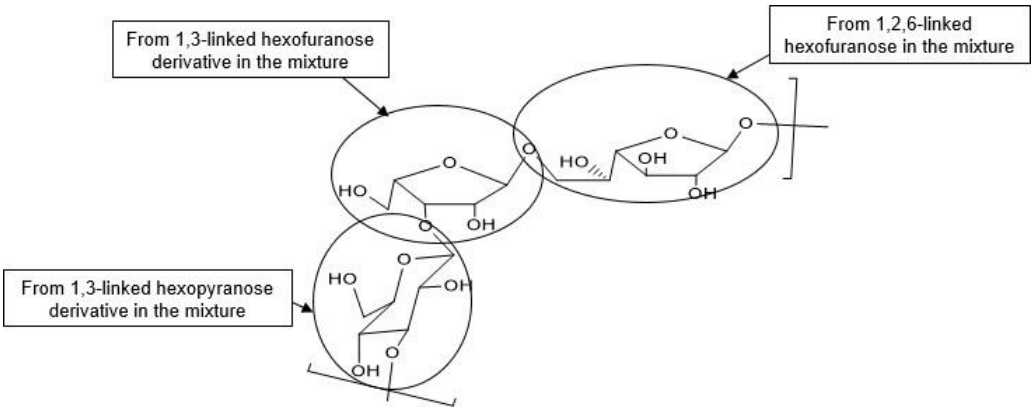

The combination also identified the other MMw polysaccharide (MMwb) as having a repeating unit comprising of mostly a 1,6-linked-β-D-galactofuranoside. This residue was identified in both the dialysis water and the dialysis bag, indicating that different molecular masses are present, of which the lower molecular weight passes through the dialysis bag and the medium molecular mass is retained. This is only possible with the suggestion whereby the native polysaccharide which generates this repeating unit has a main chain containing a 1,2,6-linked galactofuranose and a small number of Smith degradable 1,6-linked galactofuranose (identified in the linkage analysis of the mixture), which when subjected to Smith degradation, will form oligosaccharides of different molecular weights depending on where the 1,6-linked galactofuranose occurs.

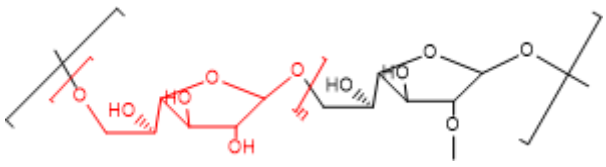

As was the case for the Smith degraded MMw polysaccharides, a combination of ^{1}H-^{1}H-COSY, ^{1}H-^{1}H-TOCSY, edited ^{1}H-^{13}C-HSQC, ^{13}C-HSQC-TOCSY, ^{1}H-^{13}C-HMBC

and ^{1}H-^{1}H-ROESY and comparison of literature chemical shift data identified the sugar residues, their individual chemical shifts and the sequence in which they occur in the repeating unit. The structure of the MMwa was determined to be:

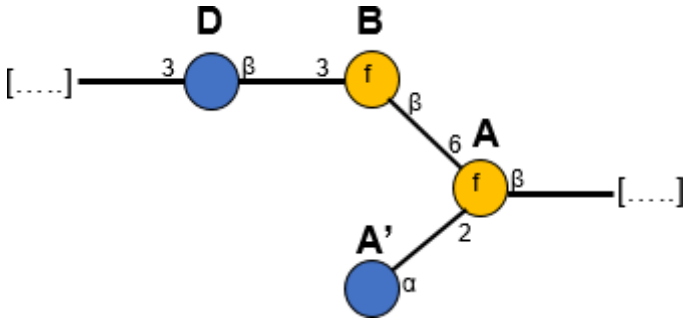

And finally, the structure of MMwb was found to be:

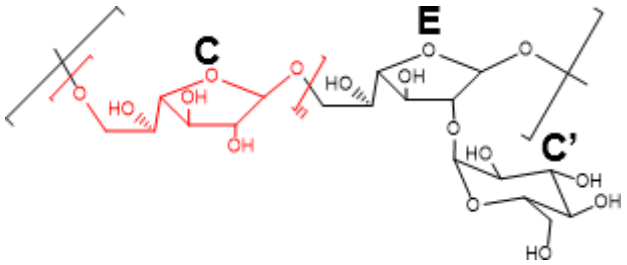

The extent to which the 1,6-linked-β-D-galactofuranoside is substituted at the 2-position is very dependent on the conditions under which the fermentation is performed. The 1,6-linked-β-D-galactofuranoside was found to be substituted at the 2-position greater than 80% under optimized fermentation conditions.

The structures of the two MMw EPSs synthesised by *L. fermentum* LF2 were compared with those in the scientific literature and structural data base of bacterial exopolysaccharide, and suggests that the two MMw EPSs have novel structures. The literature search also revealed that the non-stoichiometric glucose substitution at 2-position of a 1,6-linked-β-D-galactofuranoside has been seen in the structure of LPS isolated from *Acetobacter pasteurianus* CIP103108 (Pallach et al., 2018). However, in this case, the LPS has a repeat unit which contains the B, A, A' structural elements.

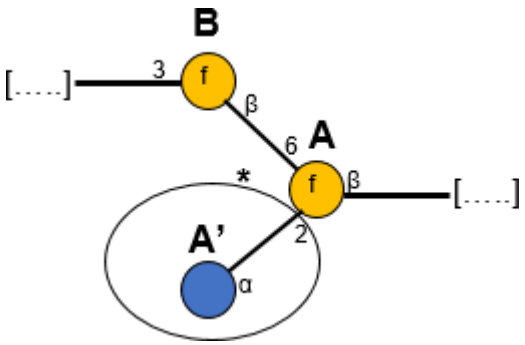

Provisional studies of the biological activity of the MMw polysaccharide mixture have shown that the polysaccharides are able to stimulate the release of the inflammatory cytokine TNF-α from PBMC. However, because the activity was checked on the MMw polysaccharide mixture, at this point, it is not possible to say which of the polysaccharides is responsible for the biological activity.

5 Isolation and structural characterisation of a novel EPS produced by *Lactobacillus mucosae* VG1

5.1 Introduction

As mentioned earlier in the introduction, *Lactobacillus mucosae* are interesting potential candidates for use as probiotics as they are acid and bile tolerant, have the capacity to adhere to the host's intestinal epithelial cells and possess the ability to inhibit pathogens, which would facilitate their survival in the GIT. These potentials of *L. mucosae* could be attributed to their EPS production, but unfortunately, very little is known about the EPS. In this chapter, the isolation and structural characterisation of a polysaccharide produced by a novel strain of *L*. *mucosae* (*L. mucosae* VG1), isolated from a faecal sample of a vegetarian who had been on a strict vegetarian diet for nine years, will be discussed. The strain was found to have a ropy phenotype amongst others, which is considered as a characteristic signifying EPS production and was therefore selected and identified using 16SrRNA sequencing performed by Omololu Fagunwa, a PhD student at the University of Huddersfield. The strain which was found to be a *Gram-positive* bacterium that grew as rods and the 16SrRNA sequencing revealed that it is a novel strain of *L mucosae*, which was here after called *L. mucosae* VG1. The strain was grown on MRS-c agar plates and HBM broth containing glucose as the carbon source using the procedure outlined in section **2.2.4**.

5.2 Isolation of EPS produced by *L*. *mucosae* VG1

The EPS was isolated from the HBM broth using the procedure described in section **2.2.6.1**. After exhaustive dialysis and freeze-drying, the EPS yield was found to be 62 mg/L. This yield is relatively low when compared to that which is produced by other LAB strains, which is usually higher (Slazar *et al*., 2016).

5.3 Structural characterisation of the EPS produced by *L. mucosae* VG1

5.3.1 Determination of weight average molecular mass by SEC-MALLS

The weight average molecular mass of the EPS was determined by SEC-MALLS using the procedure described in section **2.2.7.1**. Before any measurements were made, the instrument was assessed for its ability and accuracy to determine the actual molecular mass of macromolecules using pullulan as control as described in section **3.20**.

With the accuracy of the instrument confirmed, the weight average molecular mass of the *L. mucosae* VG1-EPS was determined. Analysis of the SEC-MALLS chromatogram (Fig 5.1) revealed the presence of three light scattering detector peaks at different retention times (27.7, 34.5 and 37.3 min) indicating the presence of potentially three different molecular mass polysaccharides. The main peak with the highest detector response being the 37.3 min peak. Analysis of the RI detector trace, which is concentration dependent, revealed that the first two peaks are small amounts of contaminants of macromolecules with no significant RI response, suggesting that the light scattering trace at 37.3 min which is accompanied by a significant RI trace is the most significant EPS peak. Analysis of UV trace suggest that the single polysaccharide isolated from *L. mucosae* VG1 is free from UV absorbing species.

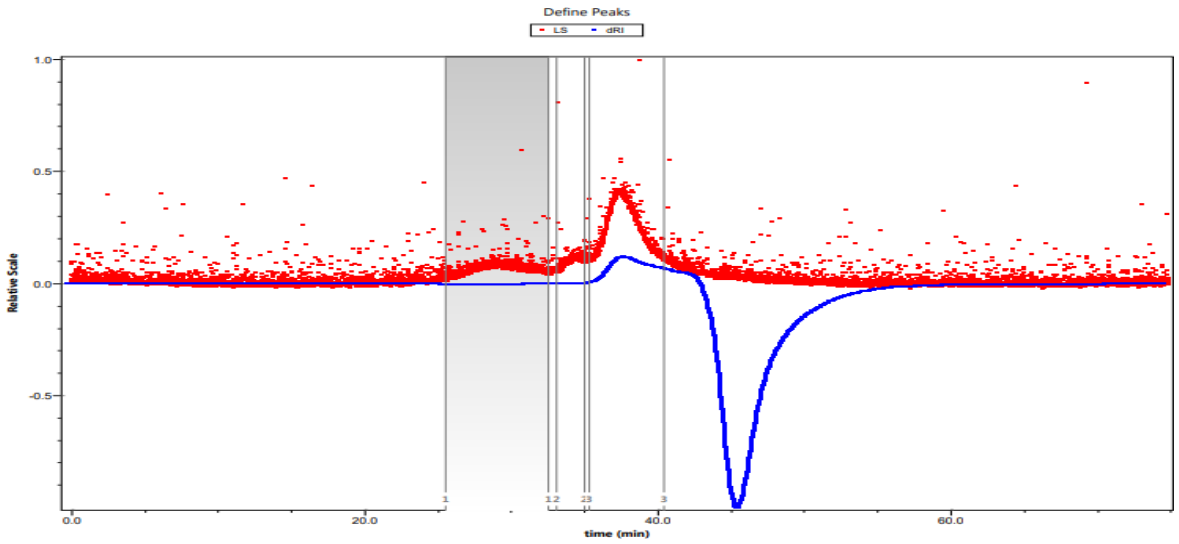

Figure 5.1: SEC-MALLS chromatogram of EPS produced by *L. mucosae* VG1.

Analysis of the single polysaccharide peak at RT = 37.3 min revealed a weight average molecular weight of the EPS to be 1.51 × 10^4 $gmol^{-1}$, with measured polydispersity (M_w/M_n) of 1.18. The size of EPS produced by LAB in terms of weight average molecular mass have been described as a broad range which varies depending on the producing strain from 10^4 to 10^7. The weight average molecular mass of the EPS produced by *L. mucosae* VG1 can be said to be relatively low when compared with those produced by other LAB (Ruas-Madiedo & De Los Reyes-Gavilán, 2005; Salazar *et al*., 2016).

5.3.2 Monomer analysis by HPAEC-PAD

Monomer analysis of the *L. mucosae* VG1-EPS was performed using the procedure described in section **2.2.8.1**. A single peak was obtained at RT = 15.984 min and was identified by matching the retention time with that of the sugar standards (fucose, rhamnose, galactose, glucose, xylose, mannose, fructose, *N*-acetyl glucosamine, *N*-acetyl galactosamine, glucosamine, and galactosamine).

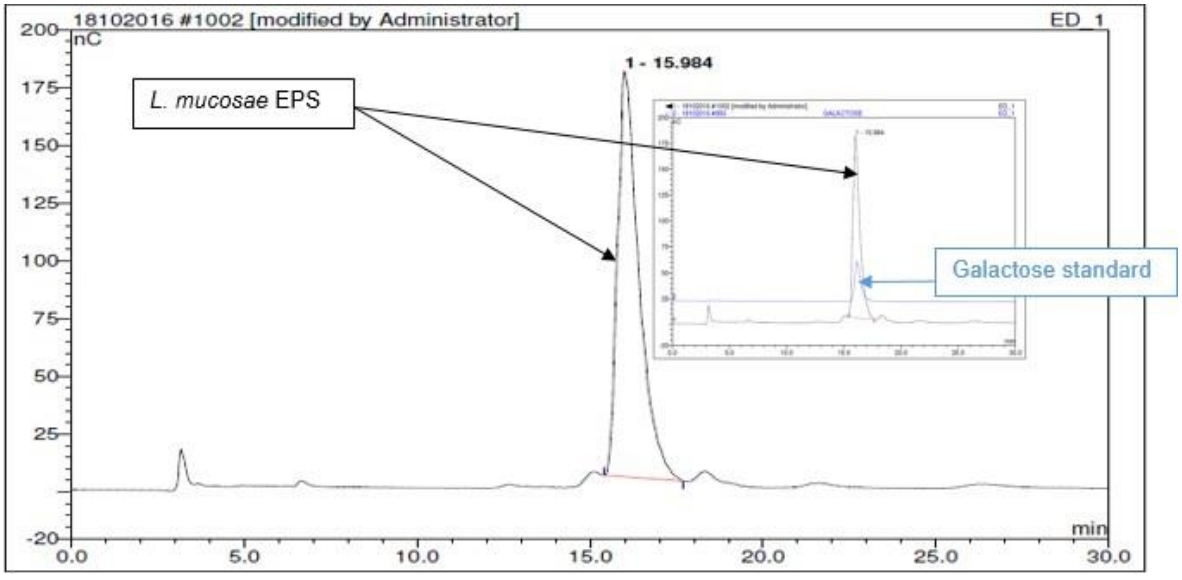

Figure 5.2: HPAEC-PAD chromatogram of the hydrolysed *L. mucosae* VG1- EPS and an overlaid chromatogram of the hydrolysed EPS with that of a galactose standard (on the right).

Analysis of the retention times of the sugar standards with that of the *L. mucosae* VG1 EPS revealed that, the retention time of the monosaccharide released from the EPS (15.98 min) corresponded to that of galactose (16.15 min), an overlay of the two peaks confirms this to be the case (Fig 5.2).

5.3.3 Monomer analysis by GC-MS

Monomer analysis of the EPS was also performed by GC-MS after hydrolysing and converting the monosaccharides present in the EPS into thier alditol acetates using the procedure described in section **2.2.8.2**. A single peak was obtained with a retention time (RT = 13.19 min) which was compared with the retention times of the alditol acetates mixture standard containing peracetylated inositol, mannitol, glucitol and galactitol purchased from Sigma Aldrich, UK.

Table 5.1: Retention times of the alditol acetates mixture standard containing inositol, mannitol, glucitol and galactitol purchased from Sigma Aldrich, UK

Standard (sugar alditol acetates)	**Retention time (min)**
Inositol	12.28
Mannitol	12.69
Glucitol	13.07
Galactitol	**13.27**
***L mucosae* EPS**	**13.19**

Analysis of the retention times obtained from running the alditol acetates mixture and that which is obtained from *L. mucosae* VG1-EPS as shown in table 5.1 revealed that the closest retention time to that of the *L. mucosae* VG1-EPS was that of galactose standard. This was further confirmed by preparing the alditol acetates of mannose, glucose and galactose and their retention times compared with that which was obtained by *L. mucosae* VG1-EPS. Analysis of the retention times of the sugar alditol acetates obtained (mannose; 14.49, glucose; 12.85 and galactose 13.14 min) further confirmed that the *L. mucosae* EPS is a galactan as indicated in Fig 5.3.

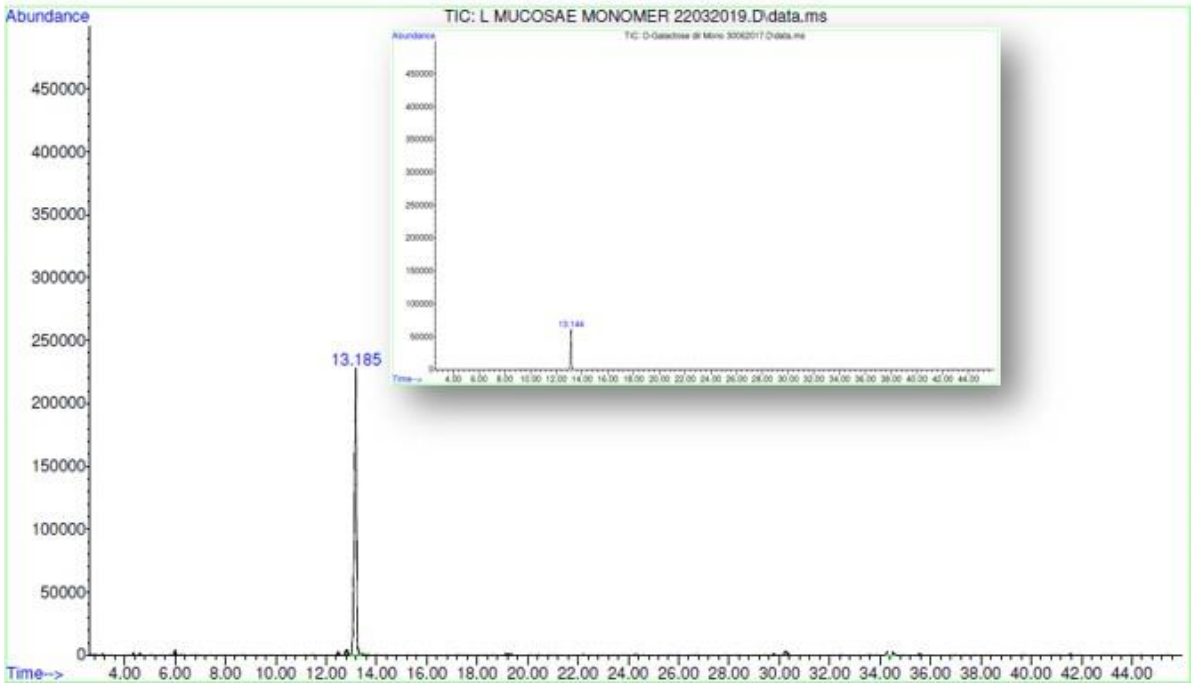

Figure 5.3: GC trace of monomer analysis performed on the *L. mucosae* VG1-EPS and that of the galactose sugar alditol acetate standard (top right).

5.3.4 Absolute configuration analysis by GC-MS

The absolute configuration of the galactose that forms the repeating unit of *L. mucosae* VG1-EPS was assessed using the procedure described in section **2.2.8.3.** Recognition of its absolute configuration was performed by comparison of the retention time obtained by the t-butyl glycosides generated from the reaction of *L. mucosae* VG1-EPS with those obtained from D- and L-galactose standards.

Table 5.2: Retention times generated by D- and L-galactose standards and that which was generated by *L. mucosae* VG1-EPS.

Sample	Retention time of the 1st peak (min.)	Retention time of the 2nd peak (min.)	Retention time of the 3rd peak (min.)
L-galactose	11.21	11.56	12.10
D-galactose	**11.28**	**11.60**	**12.29**
L mucosae VG1-EPS	**11.28**	**11.60**	**12.30**

Comparison of the retention times generated by D- and L-galactose standards and that which was generated by *L*. *mucosae* VG1-EPS revealed that the galactose that

forms the repeating unit of *L. mucosae* VG1-EPS is of the D-absolute configuration and as such, the *L*. *mucosae* VG1-EPS is a D-galactan.

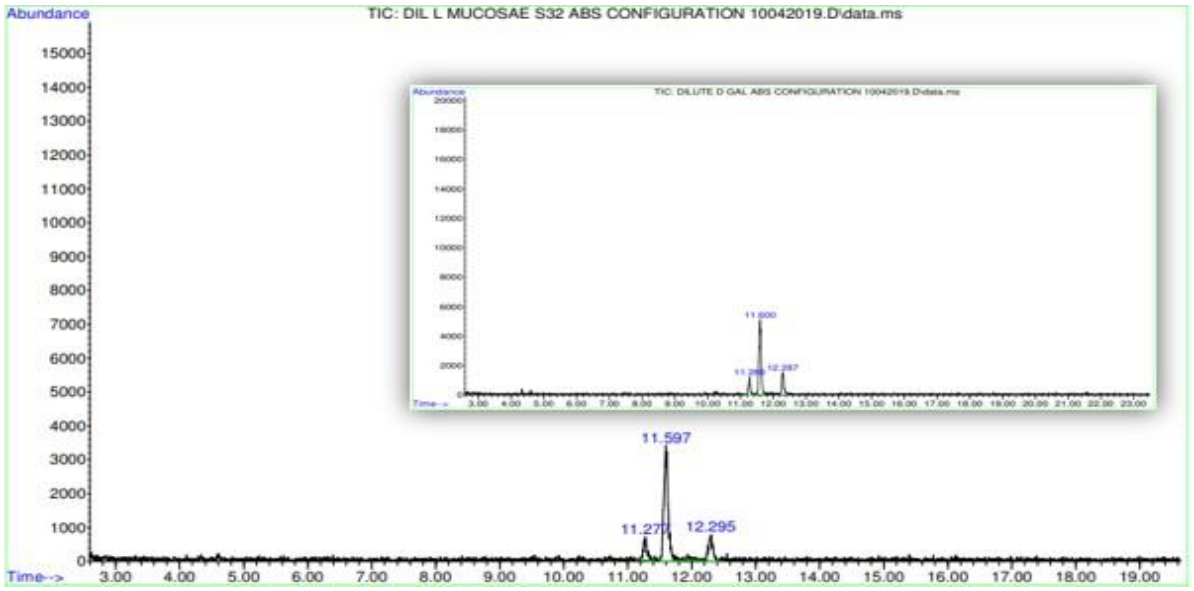

Figure 5.4: GC trace of absolute configuration analysis performed on the *L. mucosae* VG1-EPS and that of the D-galactose standard (top right).

5.3.5 Linkage analysis by GC-MS

The linkage positions between the galactose moieties present in the repeating unit of the galactan was performed by preparing per-methylated alditol acetates as described in section **2.2.8.4**. The GC trace (Fig 5.5) showed five distinct peaks, with the 16.811 min peak being the most abundant (27.22 %).

Table 5.3: Retention times of the linkage analysis peaks deduced for EPS produced by *L. mucosae* VG1 and their relative percentages.

S/N	RETENTION TIME (min)	CORRECTED AREA	PERCENTAGE (%)
1	12.75	174944	11.37
2	15.71	350120	22.76
3	16.81	418630	27.22
4	17.04	342542	22.27
5	20.18	251966	16.38
		TOTAL: 1538202	

Analysis of the mass spectra of each peak revealed the presence of a 1,5-di-*O*-acetyl-(1-deuterio)-2,3,4,6-tetra-*O*-methyl hexitol derived from a non-reducing terminal hexose, a 1,3,5-tri-*O*-acetyl-(1-deuterio)-2,4,6-tri-*O*-methyl hexitol derived from a 1,3-linked hexopyranose, a 1,4,6-tri-*O*-acetyl-(1-deuterio)-2,3,5-tri-*O*-methyl hexitol derived from a 1,6-linked hexofuranose, a 1,5,6-tri-*O*-acetyl-(1-deuterio)-2,3,4-tri-*O*-methyl hexitol derived from a 1,6-linked hexopyranose and a 1,3,5,6-tetra-*O*-acetyl-(1-deuterio)-2,4-di-*O*-methyl hexitol derived from a 1,3,6-linked hexopyranose at 12.75, 15.71, 16.81, 17.04 and 20.18 min respectively.

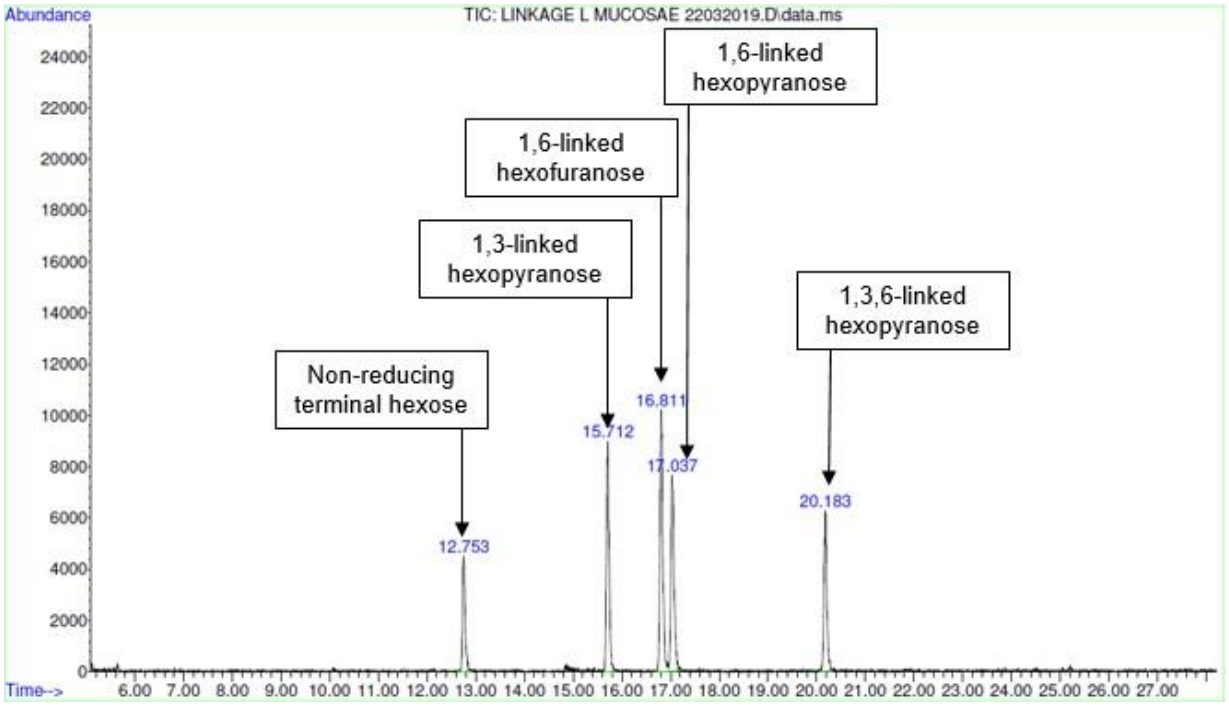

Figure 5.5: Retention times of the linkage analysis peaks deduced for EPS produced by *L. mucosae* VG1.

5.3.6 1D-NMR

The anomeric region of ^{1}H NMR spectra of the native EPS gave signals for the anomeric proton of each monosaccharide present in the repeating unit of the galactan produced by *L. mucosae* VG1. The ^{1}H NMR spectra was recorded using the procedure described in section **2.2.8.5**.

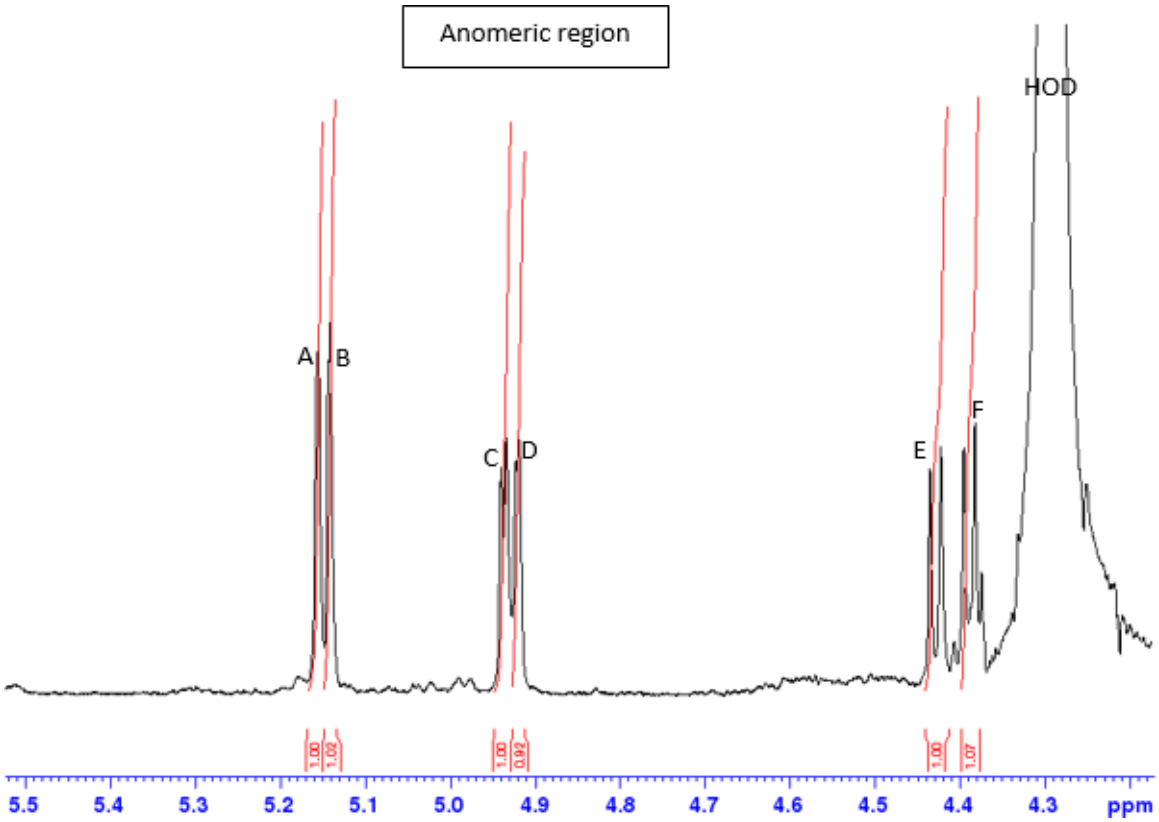

Figure 5.6: ^{1}H-NMR spectra recorded at 70 ^{o}C on the EPS produced by *L. mucosae* VG1.

Inspection of the anomeric region of the ^{1}H-NMR spectra recorded for the *L. mucosae* VG1-EPS revealed the presence of six sets of signals, labelled in order of decreasing chemical shift as A, B, C, D, E and F with integral ratios of 1.0:1.0:1.0:0.9:1.0:1.1 (Fig 5.6). The very similar integrals of 1 is an indicator of the presence of six monosaccharides in the repeating unit. The appearance of the anomeric protons of E and F at a higher field at δ 4.43 and 4.39 ppm with $^{3}J_{1,2}$ coupling constants of 7.72 and 7.84 Hz respectively, indicates that the sugars are D-hexopyranoses in their β-anomeric configuration. On the other hand, the appearance of the anomeric protons of sugars C and D at a lower field δ 4.94 and 4.92 ppm with $^{3}J_{1,2}$ coupling constant values of 3.76 and 2.10 Hz, indicate that the sugars are D-hexopyranoses in their α-anomeric configurations (Harding *et al.*, 2005). The appearance of the anomeric protons of A and B at an unusually low field (δ 5.15 and 5.14 ppm) is an indication that the sugars are either α-D-galacturonic acids or β- D-galactofuranoses or a combination of both (Bock & Pedersen, 1983).

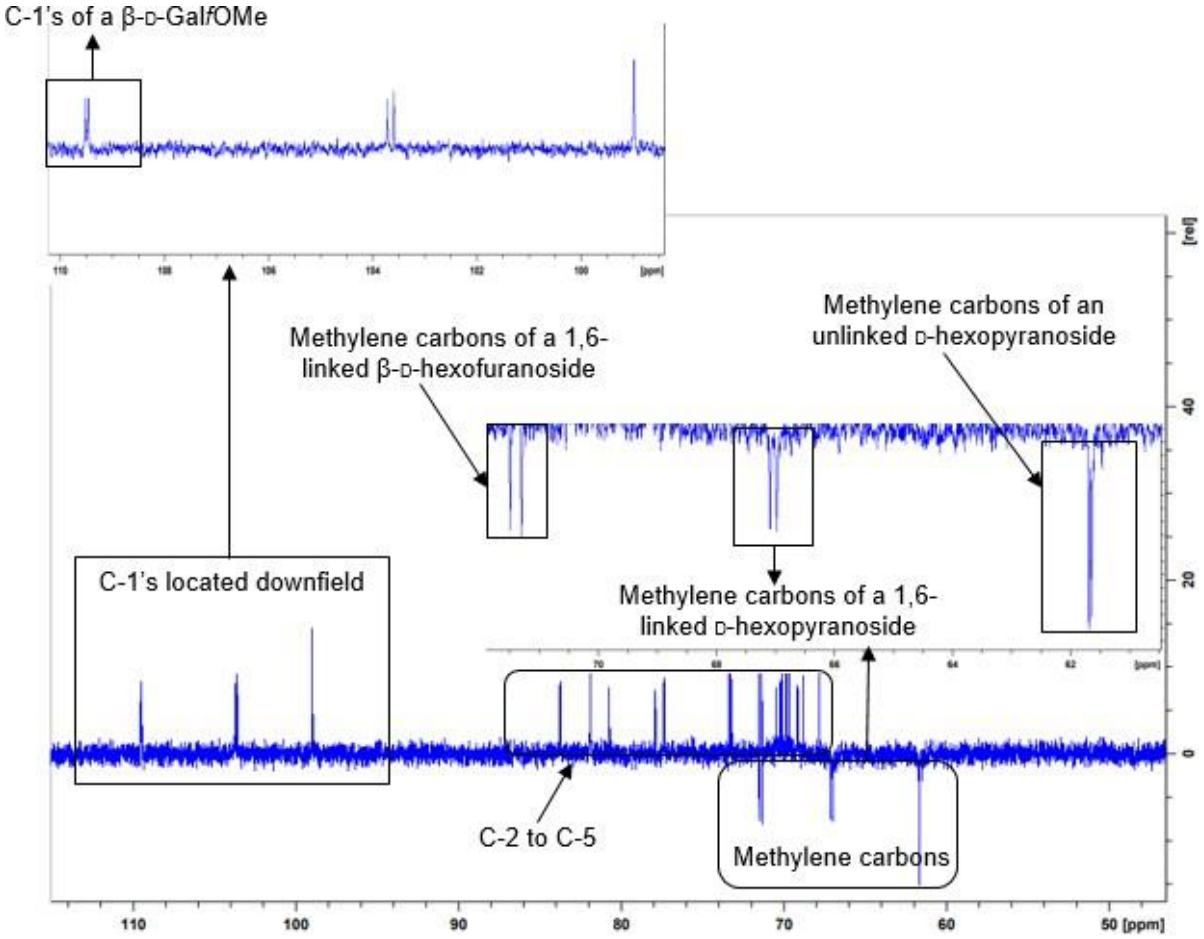

Figure 5.7*:* DEPT 135 ^{13}C-NMR spectra of EPS produced by *L. mucosae* VG1*.*

A DEPT 135 ^{13}C-NMR spectrum recorded on the *L. mucosae* VG1-EPS (Fig 5.7) indicated the presence of two downfield positive peaks at 109.52 and 109.47 ppm, which is what is expected for the anomeric carbons of a β-D-Gal*f*OMe. This implies that, two out of the six sugars that form the repeating unit of the *L. mucosae* VG1-EPS are β-D-galactofuranosides. It can therefore be deduced that, the two anomeric carbons are from the β-D-galactofuranoses of A and B of which their anomeric protons appeared at an unusually low field (δ 5.15 and 5.14 ppm) in the ^{1}H-NMR (see later discussion). The other remaining anomeric carbons occurred as positive peaks between 98.99 to 103.73 ppm and are from the remaining four D-galactopyranose sugars that form the repeating unit of the *L. mucosae* VG1-EPS.

The appearance of two methylene carbon (negative) peaks at 71.31 and 71.49 ppm are characteristic of those expected for the methylene carbons of a 1,6-linked β-D-

galactofuranose. This confirms the most abundant peak identified in the linkage analysis to be composed of the two 1,6-linked β-D-galactofuranose (A and B).

The two methylene peaks located at 66.98 and 67.10 ppm is an indication of the presence of 6-substituted D-hexopyranosides and therefore these must be from the 1,6-linked D-galactopyranose and 1,3,6-linked D-galactopyranose earlier identified in the linkage analysis. The other two methylene peaks located at 61.65 and 61.70 are characteristic of those expected for monosaccharides that are not involved in glycosidic linkages via their C-6, and therefore these must be from the remaining two peaks identified in the linkage analysis as non-reducing terminal galactose and 1,3-linked galactopyranose.

5.3.7 2D-NMR

Starting from the anomeric proton, the scalar coupling to the H-2 protons of A to F were tracked using a ^{1}H-^{1}H-COSY spectrum (Fig 5.8). The contours were distinct and each has a unique chemical shift, these were labelled as A_{H-2} (4.13 ppm), B_{H-2} (4.12 ppm), C_{H-2} (3.88 ppm), D_{H-2} (3.77 ppm), E_{H-2} (3.61 ppm) and F_{H-2} (3.50 ppm).

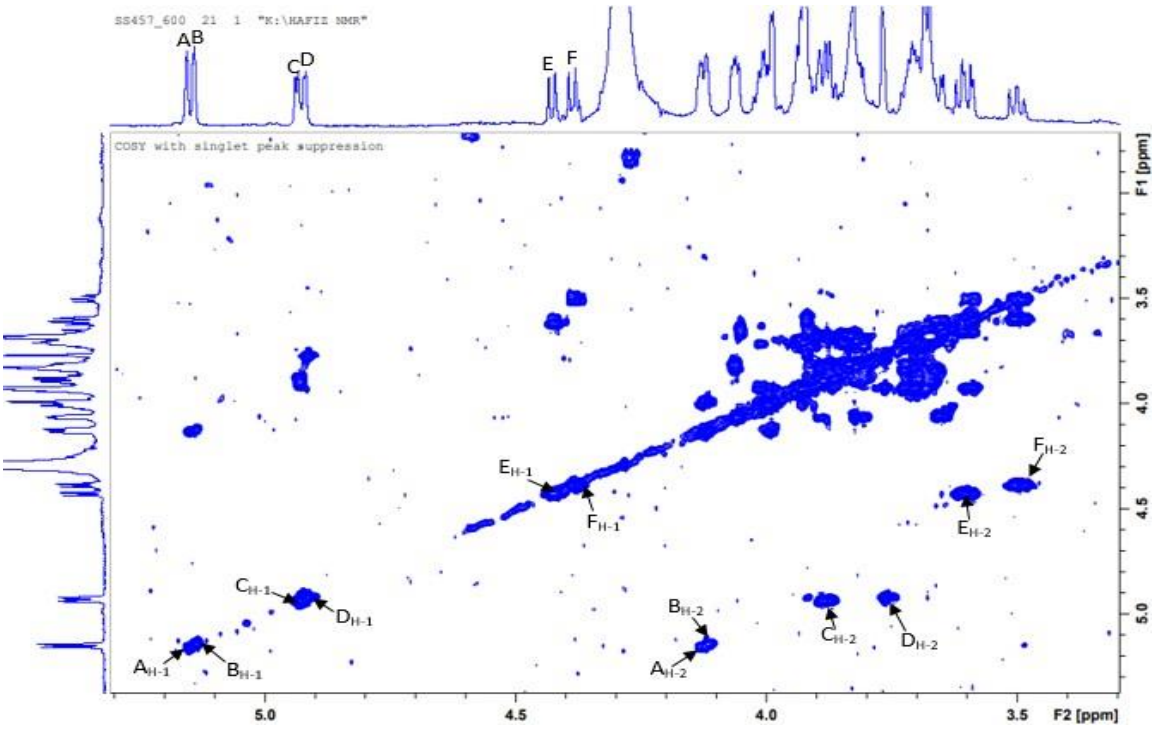

Figure 5.8: ^{1}H-^{1}H-COSY spectrum for the EPS produced by *L. mucosae* VG1 recorded at 70 °C on a Bruker 600 MHz spectrometer.

The chemical shifts of the remaining ring protons were determined and assigned by following the transmission of scalar coupling (H2 to H6) on the ^{1}H-^{1}H-TOCSY spectrum. As such, by using a combination of ^{1}H-^{1}H-COSY (blue contours in Fig 5.9) and ^{1}H-^{1}H-COSY spectrum (black contours in Fig 5.10), the scalar coupling of protons H-1 to H-4 in A to F were tracked from the anomeric protons to the remaining ring protons. It was not possible to assign the exact signals of each of the ring protons on all the sugars due to presence of some overlapping signals, as such, the overlapped signals were assigned with the help of related references (Ahrazem *et al*., 2007; Duus, Gotfredsen, & Bock, 2000; V. M. Marshall *et al*., 2001).

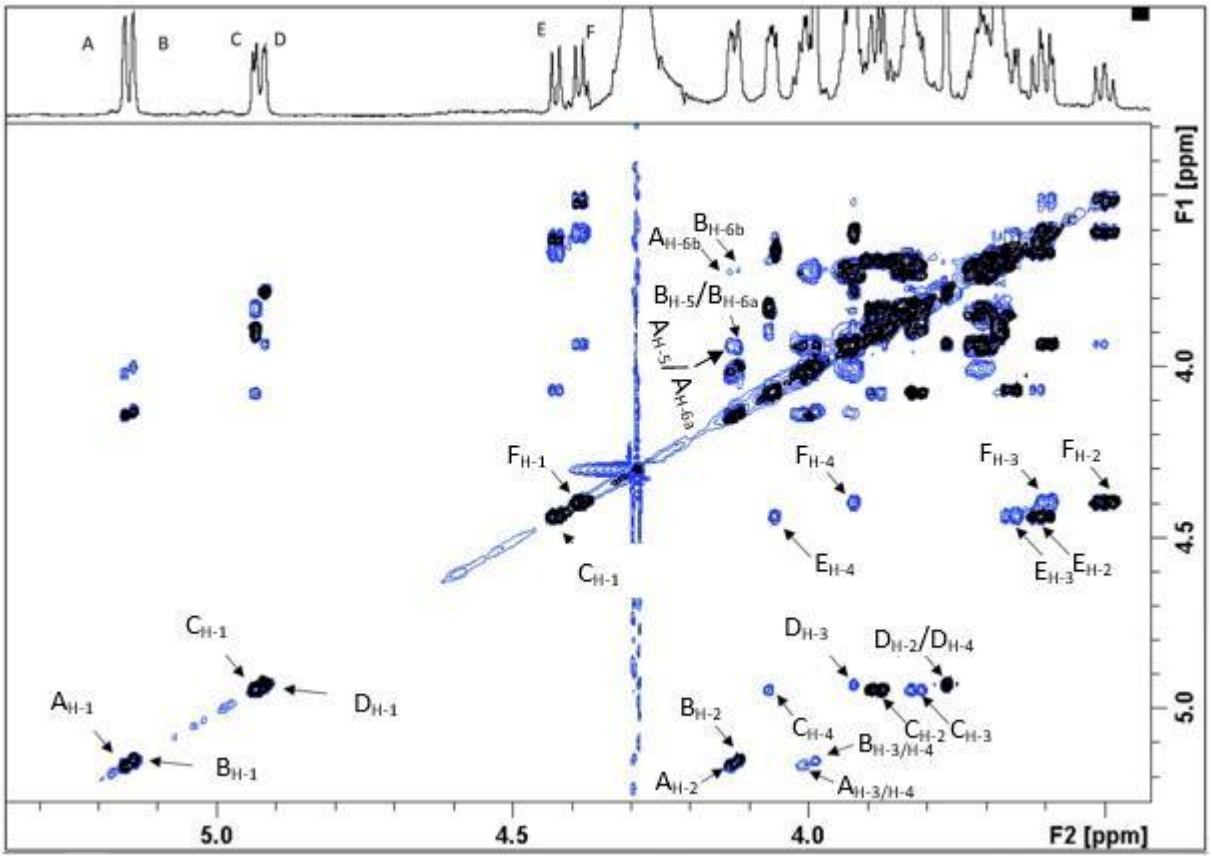

Figure 5.9: Overlaid ^{1}H-^{1}H-COSY (blue contours) and ^{1}H-^{1}H-TOCSY (black contours) spectra for the EPS produced by *L. mucosae* VG1 recorded at 70 °C on a Bruker 600 MHz spectrometer.

From the combination of ^{1}H-^{1}H-COSY and ^{1}H-^{1}H-TOSCY spectra, Fig 5.9 (above), it can be deduced that the H-4s of all the six sugars are located in the range of that which is expected for a galactan (3.90-4.35 ppm) (Harding *et al*., 2005).

A combination of an edited ^{1}H-^{13}C-HSQC spectrum (pink contours for CH and red contours for CH_2) and a ^{1}H-^{13}C-HSQC-TOCSY spectrum (blue contours) (Fig 5.10)

was used to identify the location of the carbon resonances (Bock & Pedersen, 1983). The resonance positions for the hydrogens and carbons for the EPS produced by *L. mucosae* VG1 are listed in table 5.7.

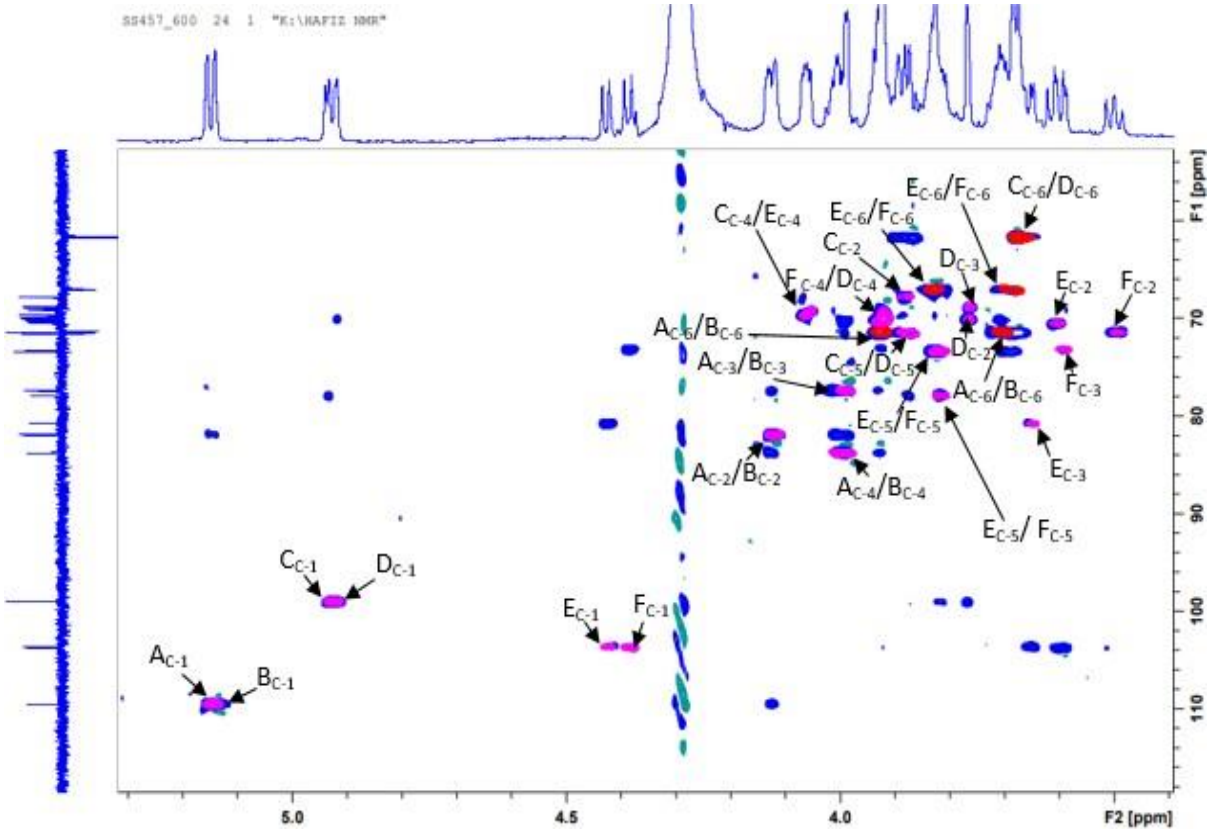

Figure 5.10: Edited ^{1}H-^{13}C-HSQC spectrum (pink contours for CH and red contours for CH_2) and a ^{1}H-^{13}C-HSQC-TOCSY spectrum (blue contours) spectrum recorded at 70 °C on a Bruker 600 MHz spectrometer.

As stated earlier, the occurrence of A_{C-1} and B_{C-1} at higher chemical shifts (109.52 and 109.47 ppm respectively) are characteristics of those which occur in β-D-galactofuranosides (109.9 ppm) (Bock & Pedersen, 1983). This further confirms that the two residues (A and B) are the 1,6-linked β-D-galactofuranoses in the repeating unit. The chemical shifts of the anomeric carbons of sugars C, D, E and F that were earlier identified as D-galactopyranoses were compared with those for a D-galactopyranoside reported in the literature. The comparison revealed that the two overlapping signals of C and D at 98.99 ppm is similar to that of the anomeric carbon of an α-D-galactopyranoside (100.1 ppm) whereas that of E and F which occur at 103.60 ppm and 103.73 ppm respectively are similar to that of a β-D-galactopyranoside (104.5 ppm) (Bock & Pedersen, 1983). This further confirms the result obtained from ^{1}H-NMR which identified A and B as the 1,6-linked β-D-galactofuranoses, C and D as α-D-galactopyranosides and E and F as β-D-galactopyranosides.

The chemical shifts of C_{C-3} and E_{C-3} were shifted downfield to 77.86 and 80.71 ppm respectively from the normal C-3 at 70.5 and 73.8 ppm for an α- and a β-galactopyranoside respectively (Bock & Pedersen, 1983). This implies that, the two sugar residues are linked at their 3-positions, one will be the 1,3-linked D-galactopyranose and the other will be 1,3,6-linked D-galactopyranose earlier identified in the linkage analysis. By a process of elimination, this leaves D and F, one of which must be the non-reducing terminal D-galactopyranose and the other must be the 1,6-linked D-galactopyranose.

Table 5.4: Information deduced for the sugar moieties present in the repeating unit of *L. mucosae* VG1-EPS.

Sugar residue	Deductions from linkage analysis, ^{1}H NMR, ^{1}H-^{13}C-HSQC and ^{13}C-HSQC-TOCSY
A and B	1,6-linked β-D-galactofuranoses
C (α-) and E (β-)	One is a 1,3-linked D-galactopyranose and the other is a 1,3,6-linked D-galactopyranose
D (α-) and F (β-)	One is a non-reducing terminal D-galactopyranose and the other must be the 1,6-linked D-galactopyranose

The resonance positions of C-1 to C-6 for D are those expected for a non-reducing terminal α-D-galactopyranose and as such D was identified as the non-reducing terminal α-D-galactopyranose in the repeating unit, which leaves F as the 1,6-linked-β-D-galactopyranose.

Table 5.5: Updated from table 5.4; information deduced for the sugar moieties present in the repeating unit of *L. mucosae* VG1-EPS.

Sugar residue	Deductions from linkage analysis, ^{1}H NMR, ^{1}H-^{13}C-HSQC and ^{13}C-HSQC-TOCSY
A	1,6-linked β-D-galactofuranose
B	1,6-linked β-D-galactofuranose
C (α-) and E (β-)	One is a 1,3-linked D-galactopyranose and the other is a 1,3,6-linked D-galactopyranose
D	Non-reducing terminal α-D-galactopyranose
F	1,6-linked-β-D-galactopyranose

5.3.7.1 Identifying the locations of H-5s for the galactopyranoses C, D, E and F

On the HMBC spectrum, the two methylene peaks located at 61.65 and 61.69 ppm earlier identified as non-reducing terminal α-D-galactopyranose (D) and 1,3-linked D-galactopyranose (C or E), show strong intra-residue coupling to protons resonating between 3.85 to 3.90 ppm.

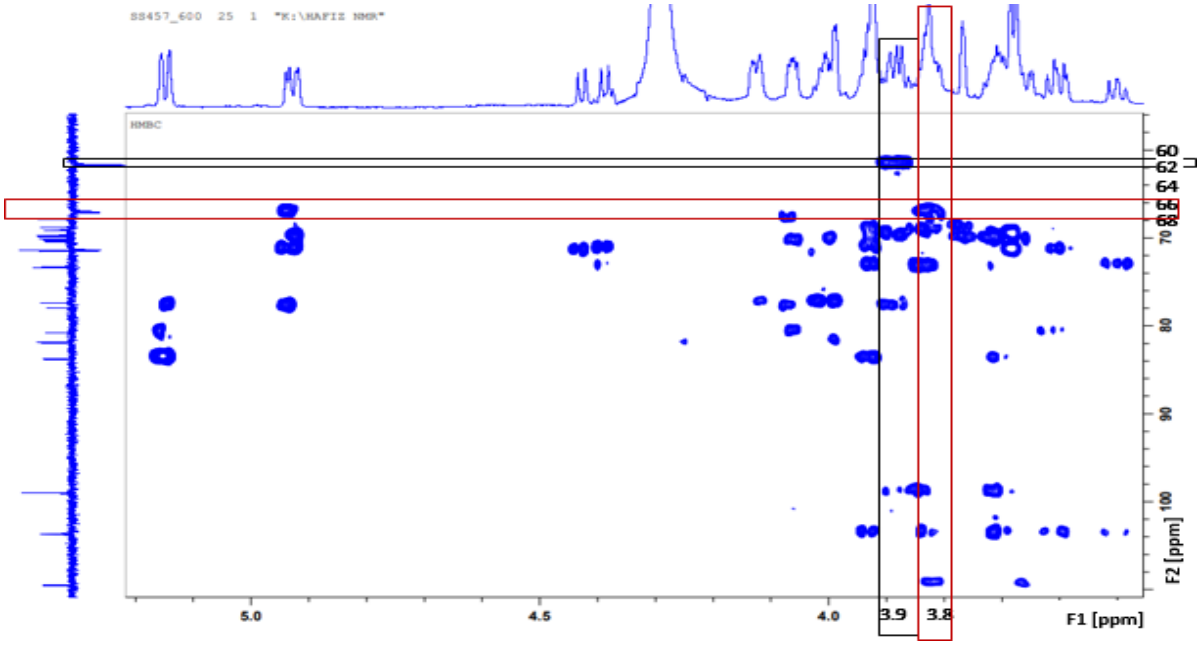

Figure 5.11: HMBC spectrum recorded at 70 °C on a Bruker 600 MHz spectrometer, highlighting the regions of intra-residue correlations.

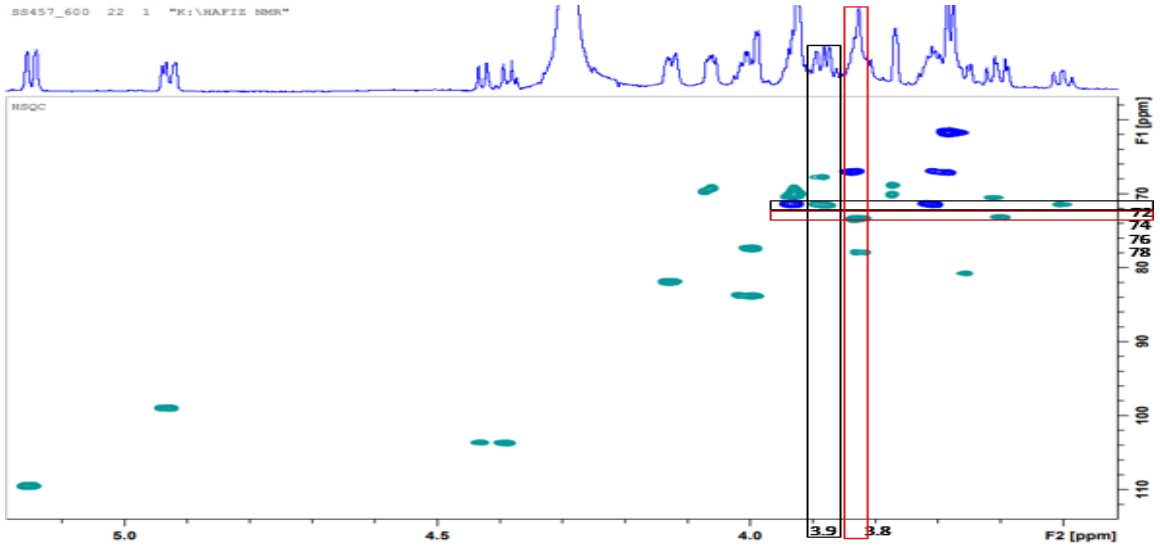

Figure 5.12: Edited ^{1}H-^{13}C-HSQC spectrum (green contours for CH and blue contours for CH_2) recorded at 70 °C on a Bruker 600 MHz spectrometer highlighting the scalar coupling of protons resonating between 3.85 to 3.90 ppm to carbons at 71.37 and 71.51 ppm.

On the HSQC spectrum, these protons resonating between 3.85 to 3.90 ppm are scalar coupled to carbons at 71.37 and 71.51 ppm. The chemical shifts of these carbons (71.37 and 71.51 ppm) are very close to the literature value observed for C-5s in α-D-galactopyranoside (71.6 ppm) as opposed to the C-5s in β-D-galactopyranoside (76.0 ppm). This indicate that these C-5s and their corresponding C-6s belong to the residues D earlier identified as non-reducing terminal α-D-galactopyranose and C which was earlier identified as having an α-anomeric configuration. C can now be identified as the α-1,3-linked D-galactopyranose and E as the β-1,3,6-linked D-galactopyranose by process of elimination. This was confirmed by locating the intra-residue scalar coupling observed between the methylene carbons at 66.98 and 67.09 ppm, and the H-5 protons at 3.81 to 3.85 ppm which, on HSQC spectrum, are scalar coupled to the two overlapping carbon signals at 73.33 ppm. Inspection of the carbon chemical shifts for residues F and E revealed that E, with a downfield shift for both C-3 and C-6 is the β-1,3,6-linked D-galactopyranose.

Table 5.6: Information deduced for the sugar moieties present in the repeating unit of *L. mucosae* VG1-EPS.

Sugar residue	**Deductions from linkage analysis, ^{1}H NMR, ^{1}H-^{13}C-HSQC and ^{13}C-HSQC-TOCSY**
A	1,6-linked β-D-galactofuranose
B	1,6-linked β-D-galactofuranose
C	α-1,3-linked D-galactopyranose
E	β-1,3,6-linked D-galactopyranose
D	Non-reducing terminal α-D-galactopyranose
F	1,6-linked-β-D-galactopyranose

Table 5.7: ^{1}H and ^{13}C NMR chemical shifts (δ, ppm) of the EPS from *L. mucosae* VG1 recorded in D_2O at 70 °C. Signals labelled with * or # could not be assigned definitively and should be considered as interchangeable.

Residue	**C-1**	**C-2**	**C-3**	**C-4**	**C-5**	**C-6**
	H-1	***H-2***	***H-3***	***H-4***	***H-5***	***H-6s***
→6)-β-D-Gal*f*-(1→ A	109.52	81.87	77.35	83.77	70.06*	71.32*
	5.155	*4.131*	*4.014*	*4.012*	*3.939*	*3.71, 3.93#*
→6)-β-D-Gal*f*-(1→ B	109.47	81.89	77.38	83.73	70.14*	71.51*
	5.141	*4.119*	*3.997*	*3.995*	*3.936*	*3.72, 3.94#*
→3)-α−D-Gal*p*-(1→ C	98.99	67.80	**77.86**	69.79	71.37	61.65
	4.935	*3.877*	*3.817*	*4.066*	*3.85/3.90*	*3.66, 3.72*
α−D-Gal*p*-(1→ D	98.99	68.82	70.05	69.17	71.51	61.69
	4.919	*3.767*	*3.767*	*3.923*	*3.85/3.90*	*3.66, 3.72*
→3,6)-β−D-Gal*p*-(1→ E	103.60	70.54	**80.71**	69.07	73.33	66.98
	4.426	*3.607*	*3.658*	*4.057*	*3.808*	*3.69,3.83*
→6)-β−D-Gal*p*-(1→ F	103.73	71.37	73.17	69.19	73.33	67.09
	4.387	*3.500*	*3.598*	*3.924*	*3.851*	*3.69,3.83*

5.3.7.2 Determining the sequence of monosaccharides in the repeating unit

The sequence in which the different linked sugars occur in the repeating sugar units was determined by the examination and identification of inter-residue correlations on both HMBC and ROESY spectra. The inter-residue correlations of the anomeric protons of a sugar residue to the neighbouring proton of another sugar residue via through space coupling, visible on the ROESY spectrum, were determined and are shown on Fig 5.13 and listed in table 5.8.

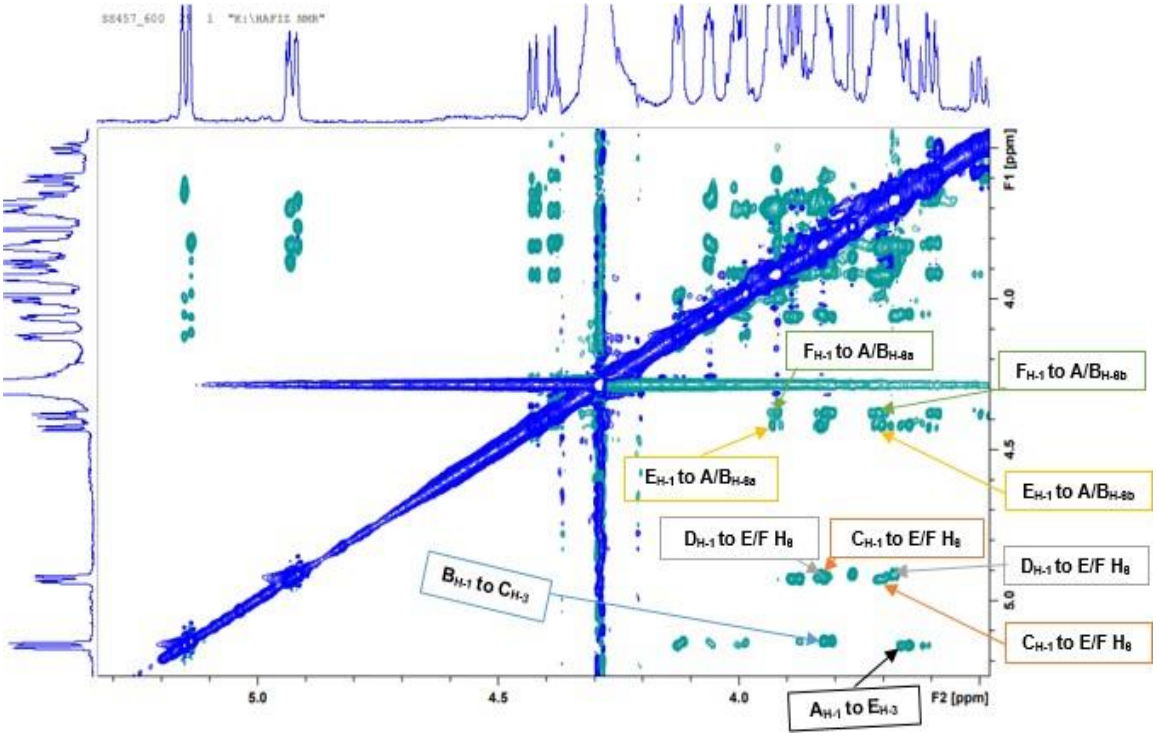

Figure 5.13: ROESY spectrum for the *L. mucosae* VG1-EPS recorded at 70 °C on a Bruker 600 MHz spectrometer showing the H-1 inter-residue correlations of A; black, B; blue, C:orange, D; ash, E; yellow and F; green.

Table 5.8: H-1 inter-residue correlations to the neighbouring proton via through space coupling for A to F in the ROESY spectrum recorded for *L. mucosae* VG1-EPS

Anomeric proton in sugar residue (δ)	Correlations to protons neighbouring residues (δ)
A$_{H-1}$ (5.16)	**E**$_{H-3}$ (3.66)
B$_{H-1}$ (5.14)	**C**$_{H-3}$ (3.82)
C$_{H-1}$ (4.94)	**E/F**$_{H-6}$ (3.83/3.69)
D$_{H-1}$ (4.92)	**E/F**$_{H-6}$ (3.83/3.69)
E$_{H-1}$ (4.43)	**A/B**$_{H-6a}$ (3.94), **A/B**$_{H-6b}$ (3.72)
F$_{H-1}$ (4.39)	**A/B**$_{H-6a}$ (3.93), **A/B**$_{H-6b}$ (3.71)

On the HMBC spectrum, the cross peaks showing the scalar coupling of the anomeric proton of a sugar residue through to the carbon of another sugar residue linked via a glycosidic bond was determined and are shown in Fig 5.14 and listed in table 5.9.

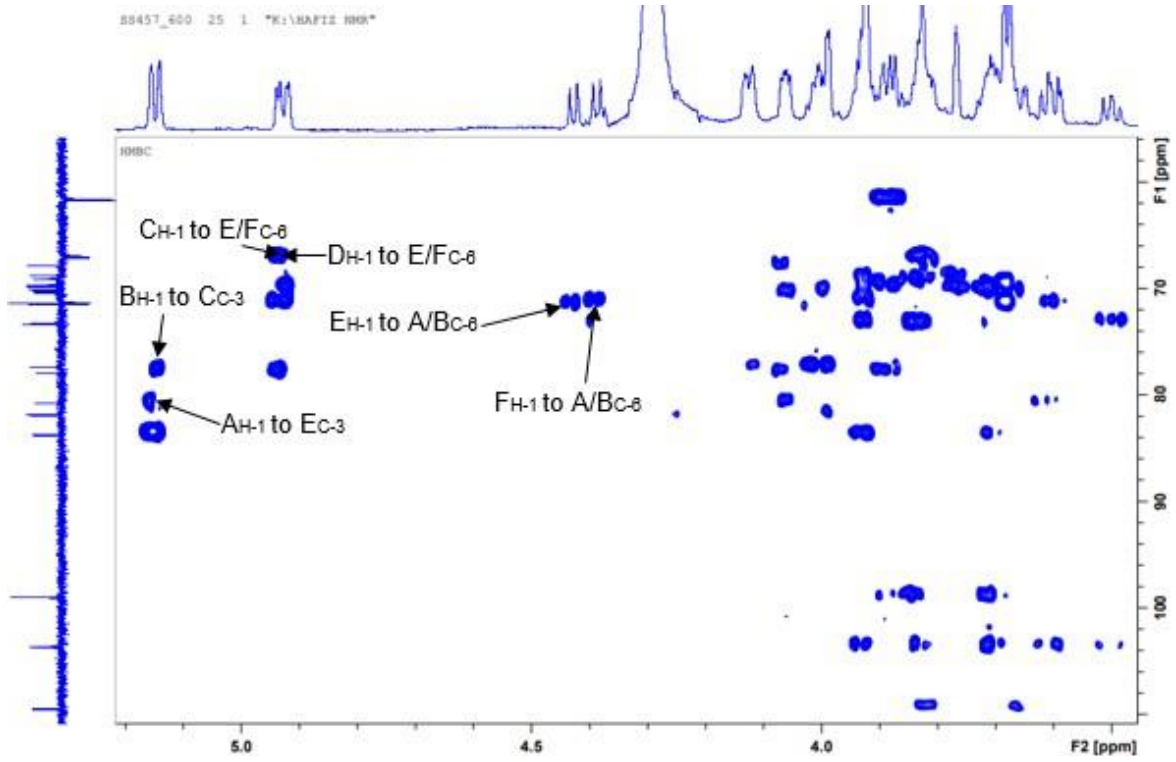

Figure 5.14: HMBC spectrum of the *L. mucosae* VG1-EPS recorded at 70 °C on a Bruker 600 MHz spectrometer showing the cross peaks derived from anomeric protons and carbons based on inter-residue coupling via glycosidic bond for A to F.

Table 5.9: H-1 inter-residue correlations to neighbouring carbons connected via glycosidic bond for A to F in the HMBC spectrum for *L. mucosae* VG1-EPS

Anomeric proton in sugar residue (δ)	Correlations to carbons neighbouring residues (δ)
A$_{H-1}$ (5.16)	**E**$_{C-3}$ (80.71)
B$_{H-1}$ (5.14)	**C**$_{C-3}$ (77.86)
C$_{H-1}$ (4.94)	**E/F**$_{C-6}$ (66.98/67.09)
D$_{H-1}$ (4.92)	**E/F**$_{C-6}$ (66.98/67.09)
E$_{H-1}$ (4.43)	**A/B**$_{C-6}$ (71.32/71.51)
F$_{H-1}$ (4.39)	**A/B**$_{C-6}$ (71.32/71.51)

From the ROESY spectrum, cross-peaks were observed between A_{H-1} to E_{H-3} and B_{H-1} to C_{H-3} which were matched by the presence of cross-peaks observed between A_{H-1} to E_{C-3} and B_{H-1} to C_{C-3} on the HMBC spectrum. These results confirm that A (1,6-linked β-D-galactofuranose) is 1,3 linked to E (1,3,6-linked β-D-galactopyranose) and B (1,6-linked β-D-galactofuranose) is 1,3-linked to C (α-1,3-linked D-galactopyranose):

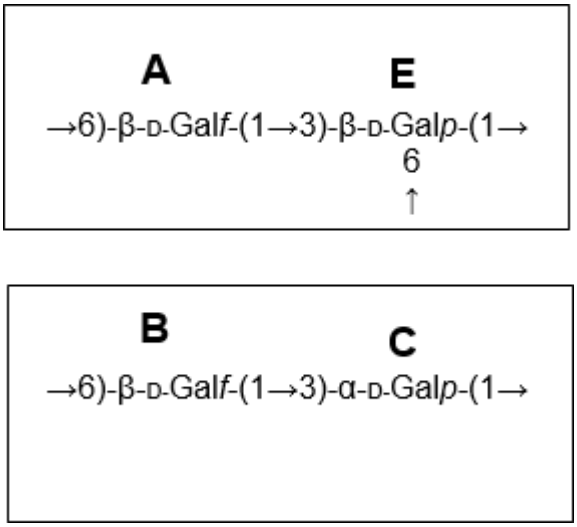

On the ROESY spectrum, there are cross-peaks between E_{H-1} and F_{H-1} to either the H-6 protons of A or B which were matched by the presence of cross-peaks observed between E_{C-1} and F_{C-1} to either the H-6 protons of A or B on the HMBC spectrum. One possible structure (structure 1) would have F (1,6-linked-β-D-galactopyranose) 1,6 linked to A (1,6-linked β-D-galactofuranose), then E would have to be 1,6-linked to B (1,6-linked β-D-galactofuranose) with the terminal sugar D (non-reducing terminal α-D-galactopyranose) 1,6-linked to E.

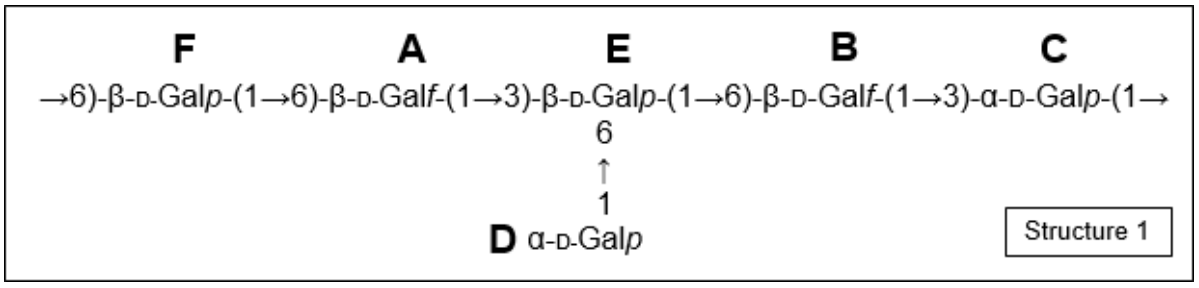

Alternatively, the main chain could have a structure containing EBC with a branch at E containing DFA in which D is 1,6-linked to F (structure 2).

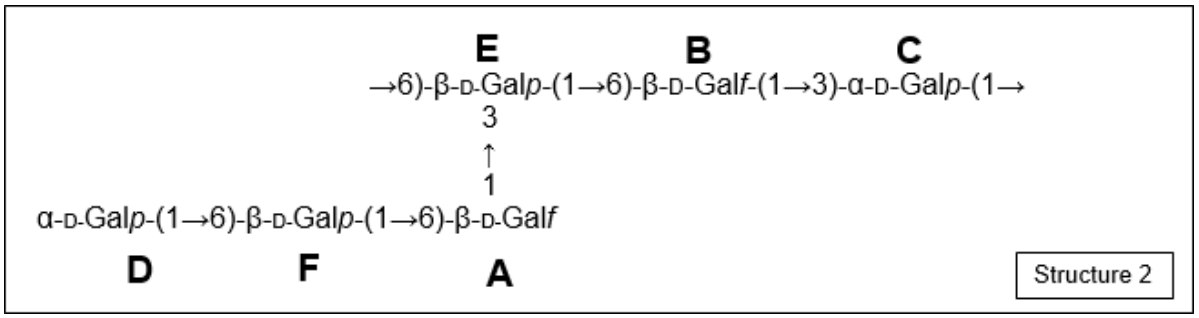

The data is also consistent with a third structure; structure 3. From the ROESY spectrum, as inter-residue NOEs were observed between $E_{H\text{-}1}$ and $F_{H\text{-}1}$ to either the H-6 protons of A or B which matched the presence of cross-peaks observed between $E_{C\text{-}1}$ and $F_{C\text{-}1}$ to either the H-6 protons of A or B on the HMBC spectrum, these also suggests that, if E (1,3,6-linked β-D-galactopyranose) is 1,6 linked to A (1,6-linked β-D-galactofuranose), then F (1,6-linked-β-D-galactopyranose) would have to be 1,6-linked to B (1,6-linked β-D-galactofuranose) with the terminal sugar D (non-reducing terminal α-D-galactopyranose) 1,6-linked to F. The main chain would then have a structure containing AE with a branch at E containing DFBC in which C is 1,6-linked to E (structure 3).

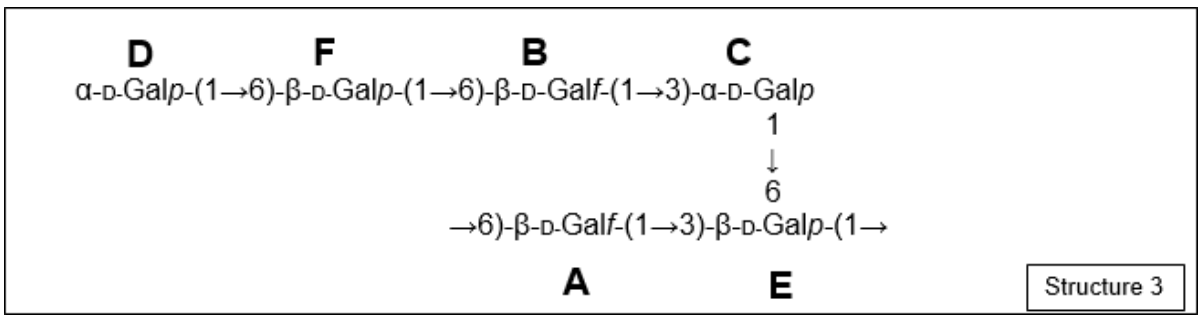

It was not possible to determine which amongst the three possible structures, was the structure of the *L. mucosae* VG1-EPS using the NMRs available. As such, the EPS was subjected to Smith degradation which has been frequently used to determine a structure within similar possible structures (Abdel-Akher, Hamilton, Montgomery, & Smith, 1952).

5.3.8 Smith degradation

In order to differentiate between the three possible structures suggested by analysing the results from HPAEC-PAD, GC-MS and NMRs generated by *L. mucosae* VG1-EPS, the EPS was subjected to Smith degradation using the procedure described in section **2.2.8.6**. In structures 2 and 3, it is expected that C and E, which are 1,3-linked will not undergo oxidation, C is α-1,6-linked to A, as such, oxidation of any of the structures would be expected to generate a disaccharide [α-D-Gal*p*-(1→6)-β-D-Gal*p*-(1→Gro)], as well as a number of small aliphatic acids and alditols as illustrated in Fig 5.18 and 5.19 for structures 2 and 3 respectively.

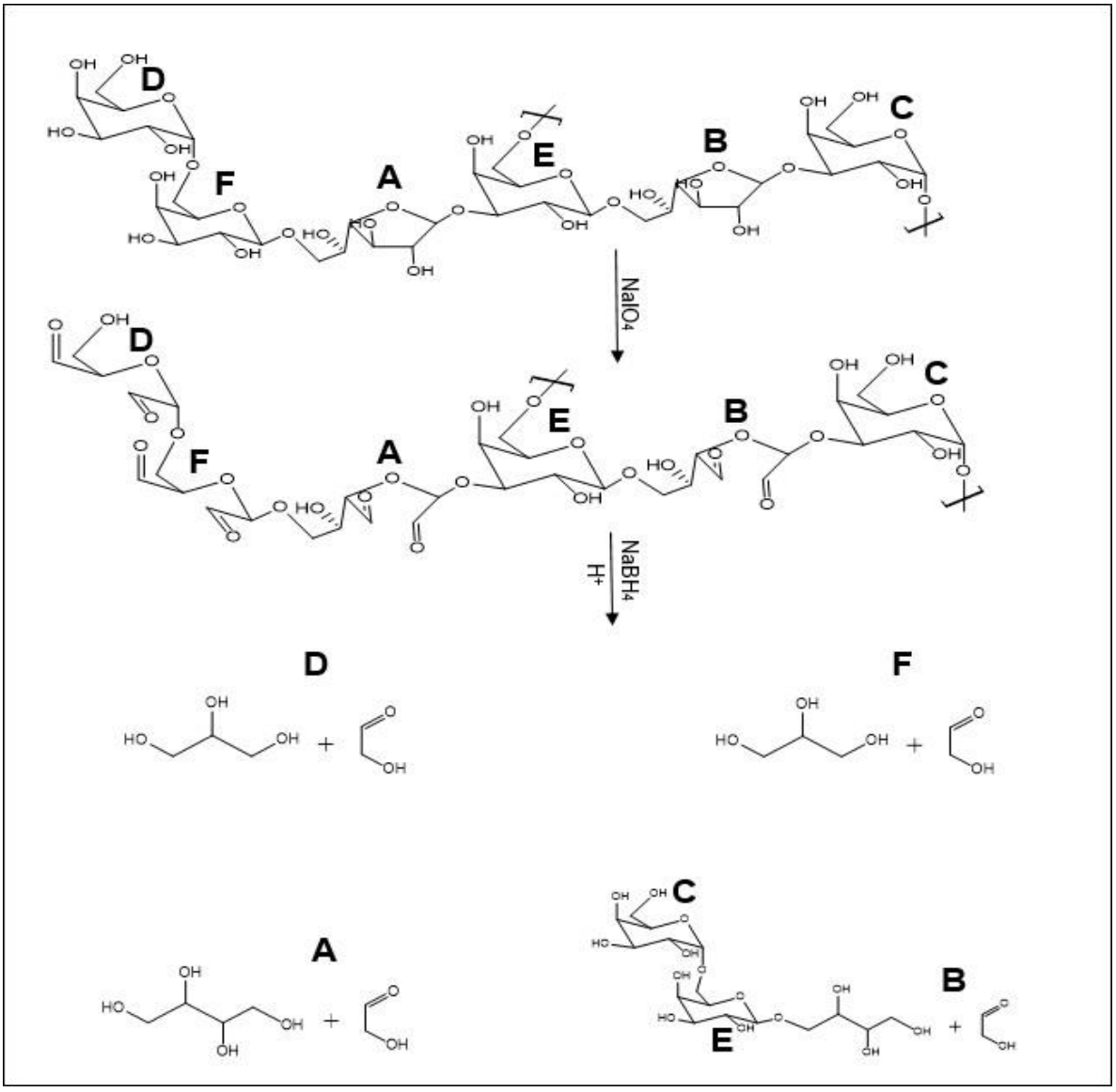

Figure 5.15: A complete Smith degradation for structure 2.

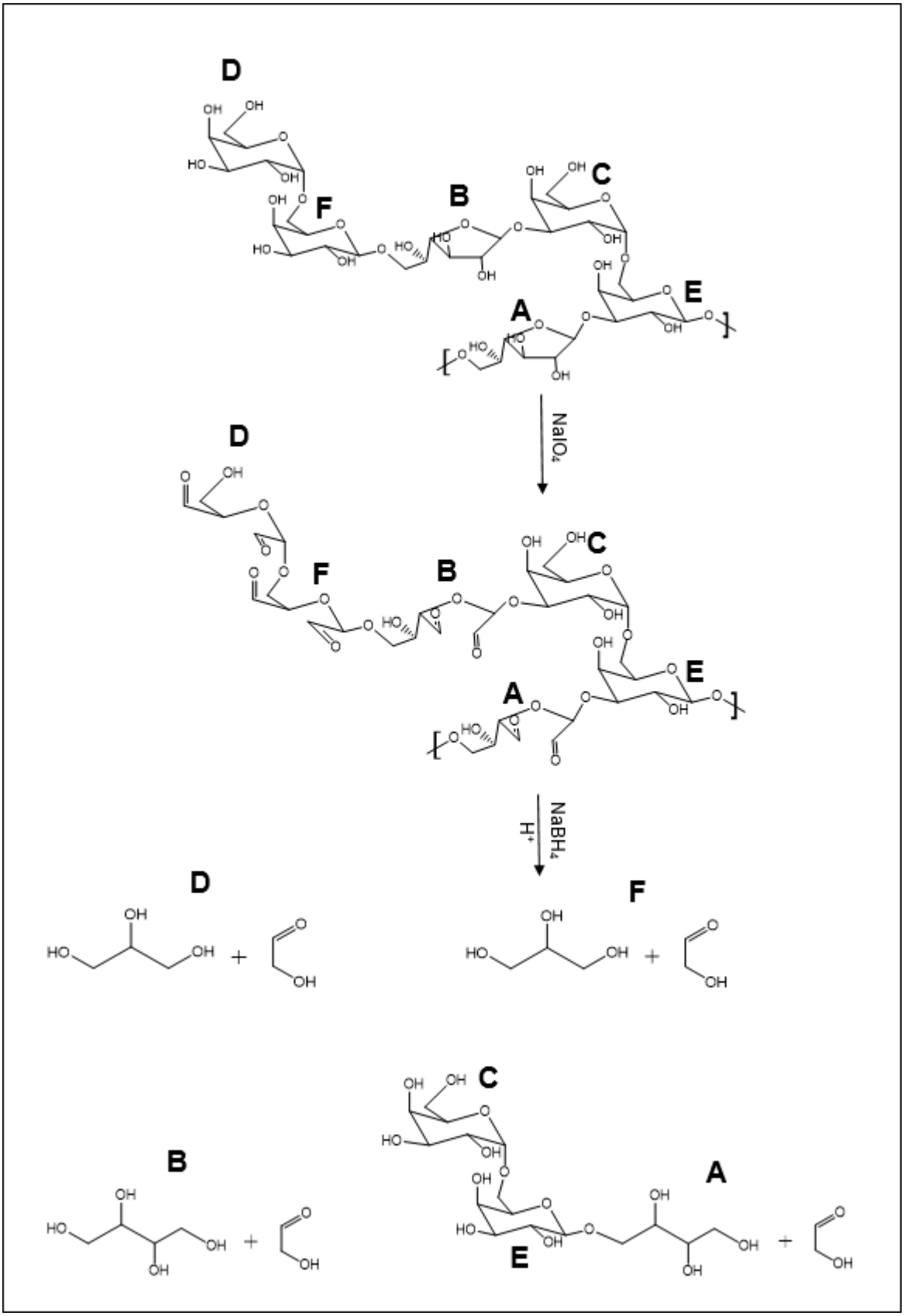

Figure 5.16: A complete Smith degradation for structure 3.

In structure 1, it is expected that C and E, which are 1,3-linked will not undergo oxidation. As the C and E are not adjacent to each other in this structure, C which is α-1,6-linked to F, would be expected to generate a monosaccharide that is α-linked to glycerol and E that is β-1,3-linked to B would be expected to generate a monosaccharide that is β-linked to D-threitol.

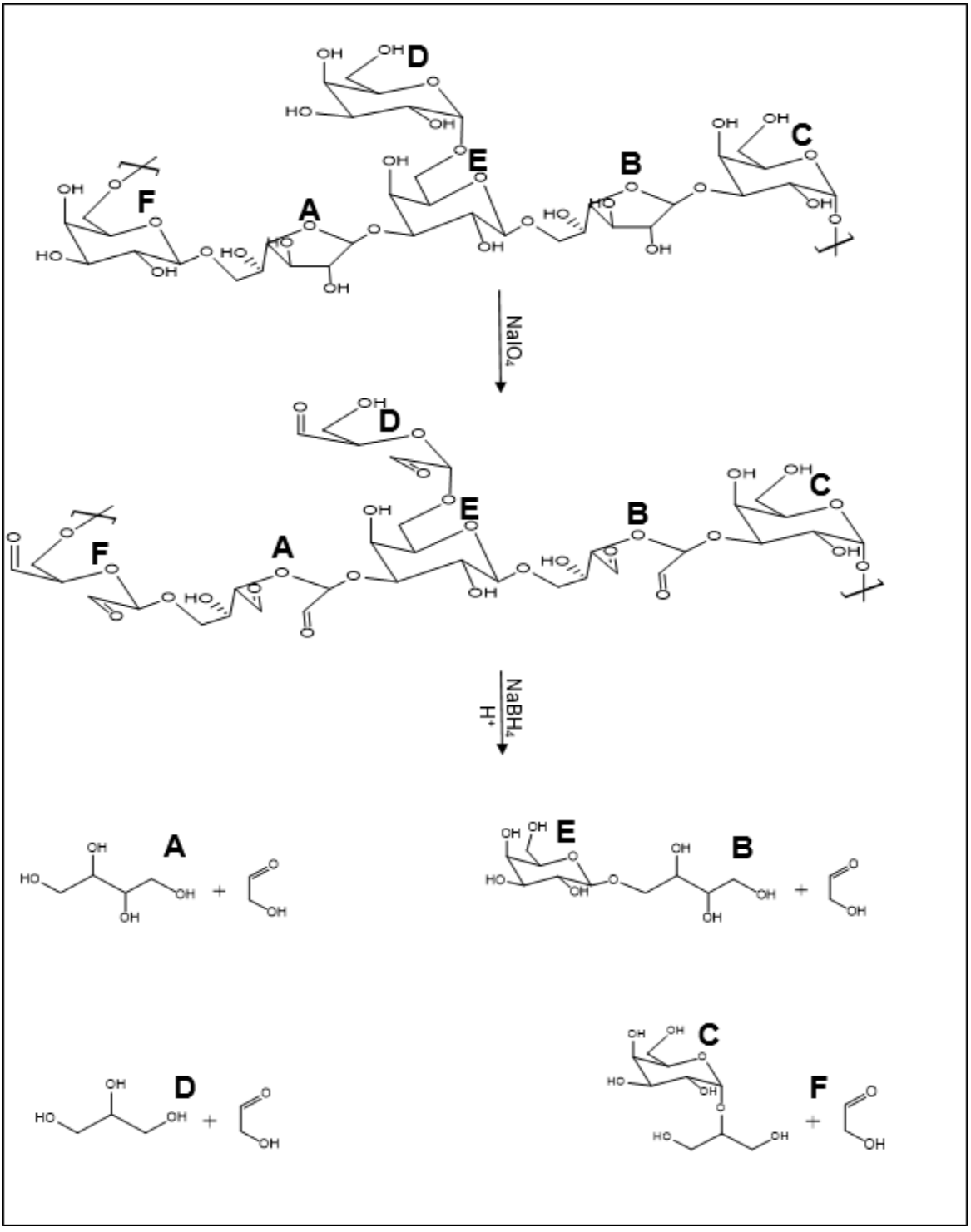

Figure 5.17: A complete Smith degradation for structure 1.

5.3.8.1 Linkage analysis on Smith degraded products derived from *L. mucosae* VG1-EPS

Linkage analysis of the Smith degraded products was performed by analysing the per-methylated alditol acetates generated using the procedure described in section **2.2.8.4**. It is expected that, linkage analysis of structures 2 and 3 would generate two peaks, of which their MS fragmentation pattern would be similar to a non-reducing terminal galactose from C and a 1,6-linked galactopyranose from E. In contrast, linkage analysis of structure 1 would be expected to generate a single peak, of which its MS fragmentation pattern would be similar to a non-reducing terminal galactose from C and E. The GC trace (Fig 5.18) of the Smith degraded products contained a single peak at 12.747 min (100.00 %).

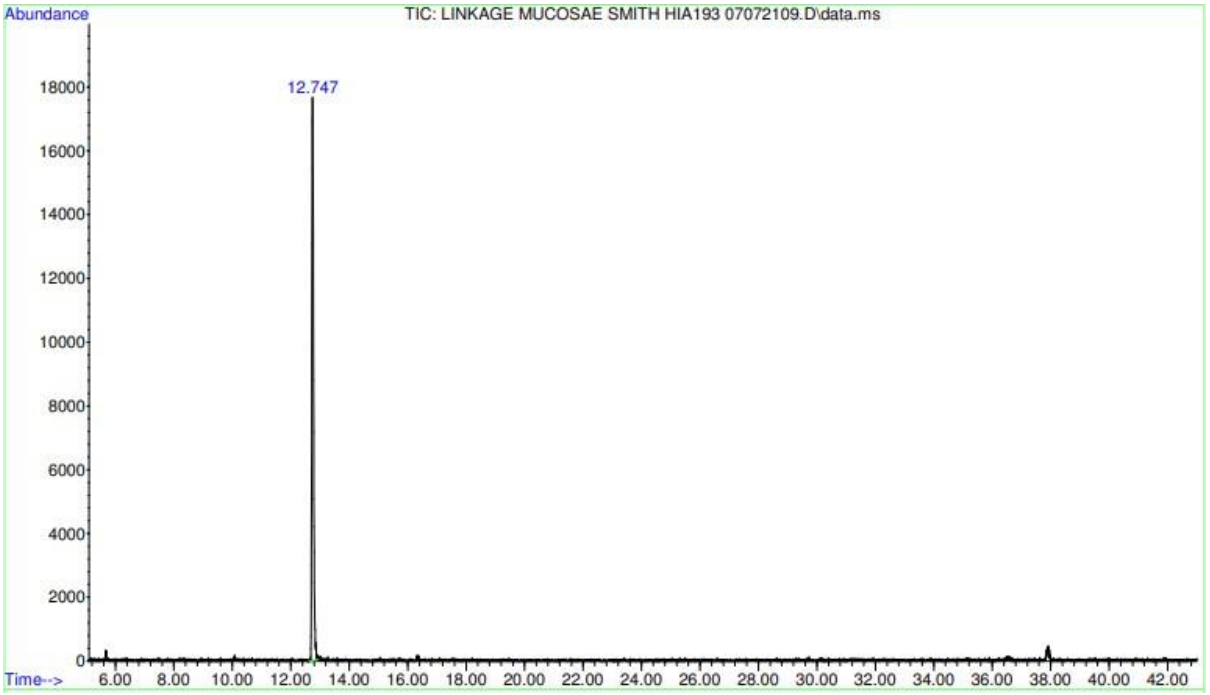

Figure 5.18: GC trace of linkage analysis performed on the hydrolysed partially methylated alditol acetate Smith degraded products derived from *L. mucosae* VG1-EPS.

The MS spectra of the 12.747 min peak was identical to that expected for a non-reducing terminal hexopyranoside (Fig 5.19).

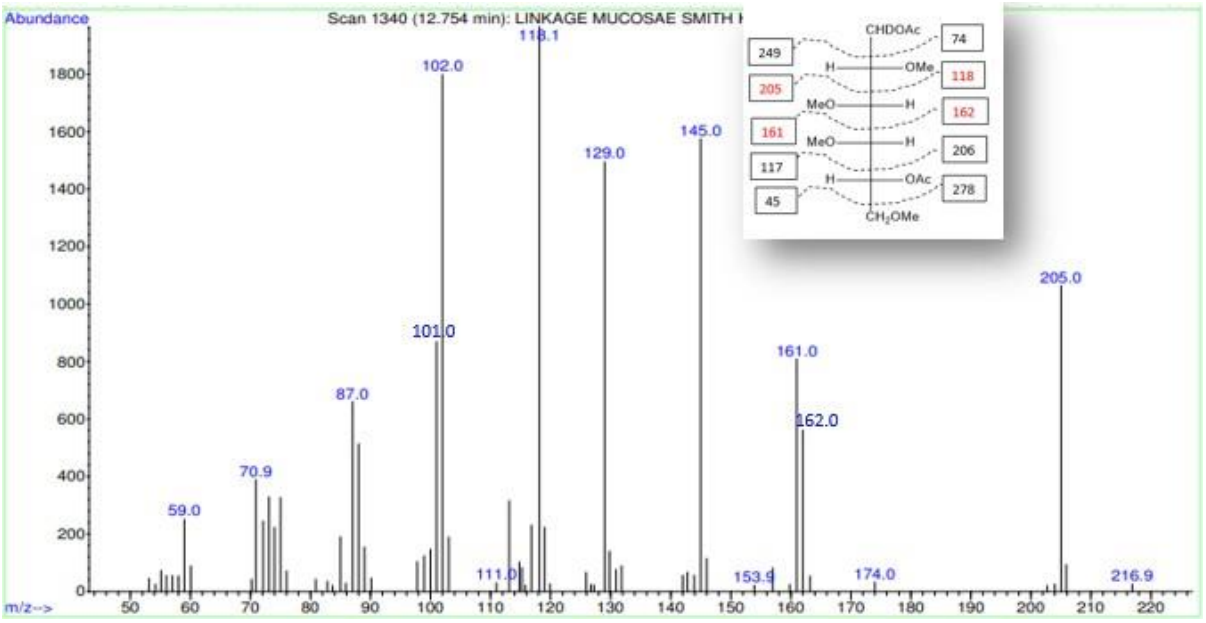

Figure 5.19: MS fragmentation pattern generated by the 12.474 min peak of the hydrolysed partially methylated alditol acetate Smith degraded products derived from *L. mucosae* VG1-EPS.

5.3.8.2 Edited HSQC NMR on Smith degraded products derived from *L. mucosae* VG1-EPS

The number of sugar moieties present in the Smith degraded products, their anomeric configurations and their linkage patterns were determined by inspecting the edited-^{1}H-^{13}C-HSQC spectrum generated by the Smith degraded products derived from *L mucosae* VG1-EPS using the procedure described in section **2.2.8.5**. The signals generated in response to the anomeric proton and carbon of each sugar present was inspected. Two protons and carbons were spotted within the anomeric region. As expected for the three structures, comparison with the literature values revealed that, one is α-D-galactopyranoside (H-1 4.82 ppm, C-1 98.8 ppm) derived from C and other is β-D-galactopyranoside (H-1 4.29 ppm, C-1 103.8 ppm) derived from E (Bock & Pedersen, 1983).

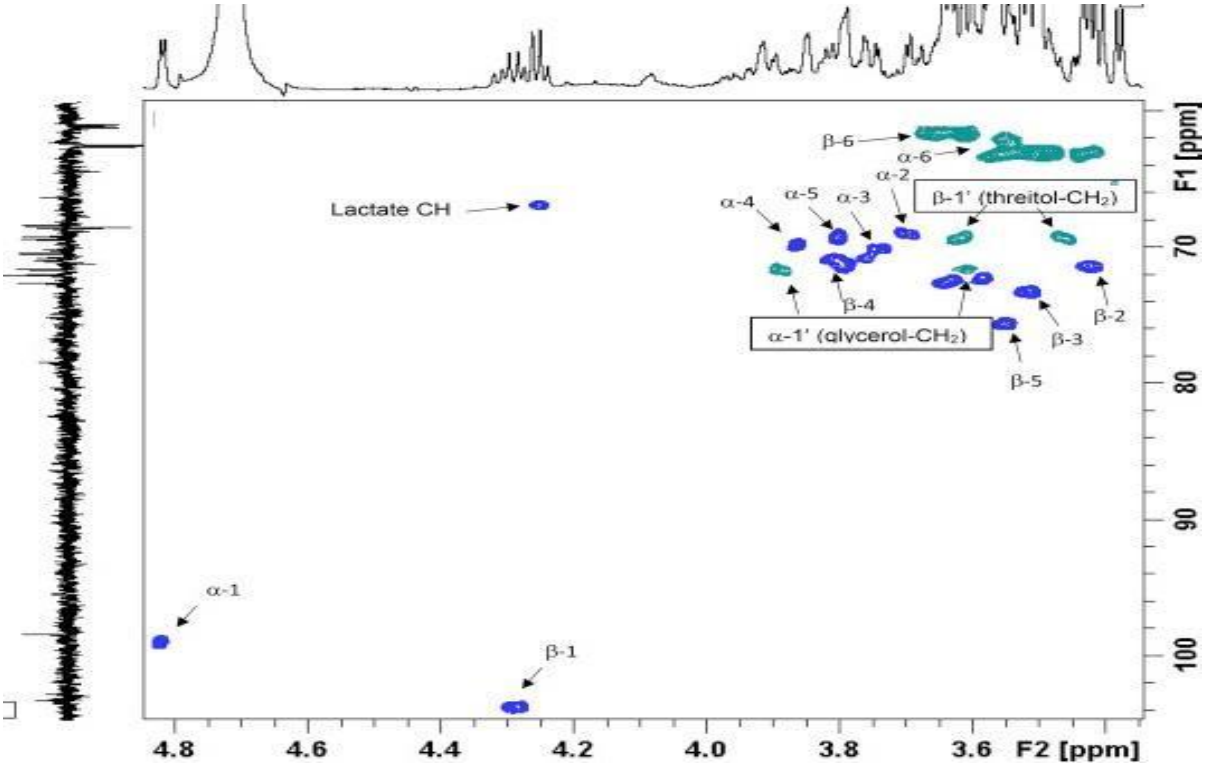

Figure 5.20: Edited ^{1}H-^{13}C-HSQC spectrum recorded at room temperature (blue contours = CH; green contours = CH_2) for the products generated after Smith oxidation of the *L. mucosae* VG1-EPS.

The appearance of two methylene carbon peaks at 61.50 ppm and 63.10 ppm are characteristic of those expected for a hexoses that are not linked at the C-6 position; unlinked β-D-galactopyranoside (62.0 ppm) and an unlinked α-D-galactopyranoside (62.2 ppm) (Bock & Pedersen, 1983). This result is consistent with the linkage analysis that identified no 1,6-linked galactopyranose. It can thus be concluded that the absence of a 1,6-linked galactopyranose eliminates the chance of the EPS having either structure 2 or 3, therefore the structure of the *L. mucosae* VG1-EPS must be structure 1.

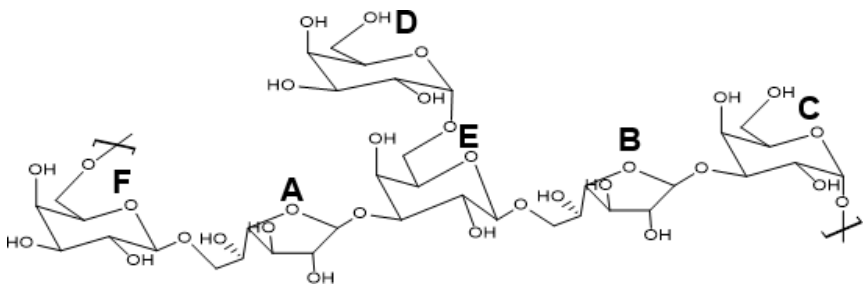

A number of bacterial species have been reported to produce EPS having D-galactose repeating units but none reported have the same structure as that which

was produced by *L. mucosae* VG1 (Gruter *et al*., 1992; Nagaoka *et al*., 1996; Svensson, Zhang, Huttunen, & Widmalm, 2011; Vinogradov *et al*., 2013).

Gruter *et al*., (1992) isolated an EPS *from Lactococcus lactis* subsp*. cremoris* H414 that was found to be a galactan with the following structure:

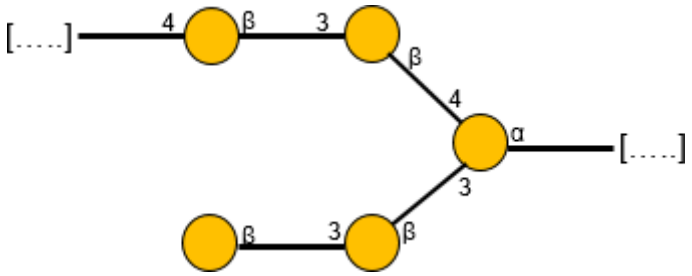

Nagaoka *et al*., (1996) isolated a CPS from *Bifidobacterium catenulatum* YIT4016 which was determined to be a galactan having the following structure:

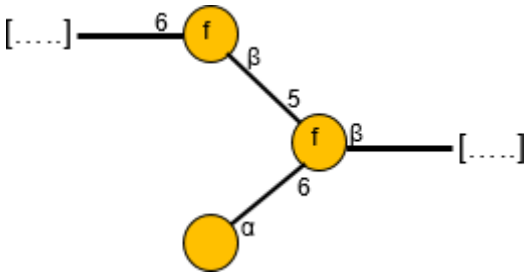

Svensson *et al*., (2011) also isolated a CPS from *Leuconostoc mesenteroides* ssp. cremoris PIA2 which was characterised and determined to be composed of a linear pentasaccharide repeating unit having the following structure:

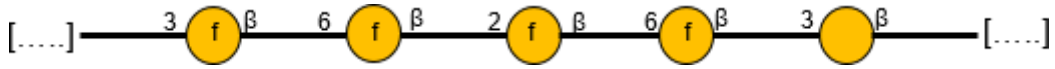

Vinogradov *et al*., (2013) isolated and purified the CPS of *L. helveticus* BROI, which was found to be composed of a linear hexasaccharide repeating unit with the following structure:

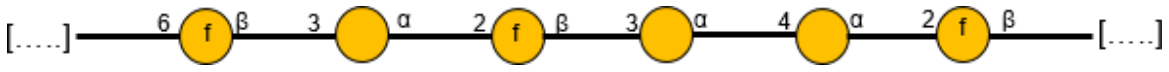

After the search of the literature and the bacterial Carbohydrate Structure Database (http://csdb.glycoscience.ru/bacterial/), it can therefore be concluded that, the *L. mucosae* VG1-EPS is a novel D-galactan and the first ever EPS from a *L. mucosae* strain to be fully characterised.

5.4 Conclusion

To conclude, in this research, a novel EPS produced by a novel strain of *L. mucosae* VG1, has been fully characterised. The native EPS yield (62 mg/L) and its weight average molecular mass (1.51×10^4 $gmol^{-1}$) were relatively low compared to that which is produced by other LAB. Monomer analysis performed by both HPAEC-PAD and GC-MS identified the presence of galactose as the sole monosaccharide present in the *L. mucosae* VG1-EPS. Absolute configuration analysis performed by GC-MS revealed that the galactose present in the *L. mucosae* VG1-EPS was of the D-configuration and as such the EPS is a D-galactan. Linkage analysis of the native EPS revealed the presence of non-reducing terminal galactopyranose, a 1,3-linked galactopyranose, a 1,6-linked galactopyranose, a 1,6-linked galactopyranose and a 1,3,6-linked galactopyranose. ^{1}H NMR spectra generated by the EPS revealed the presence of six anomeric protons having very similar integral ratios of 1, indicating the presence of six monosaccharides in the repeating unit. A DEPT 135 ^{13}C-NMR spectrum performed on the EPS produced by *L. mucosae* VG1 confirmed the presence of a 1,6-linked β-D-galactofuranose, a 1,6-linked D-galactopyranose, a 1,3,6-linked D-galactopyranose, a non-reducing terminal galactose and 1,3-linked galactopyranose. A combination of ^{1}H-^{1}H-COSY, ^{1}H-^{1}H-TOSCY, edited ^{1}H-^{13}C-HSQC,^{13}C-HSQC-TOCSY, ^{1}H-^{13}C-HMBC and comparison of the chemical shifts data with the literature was used in identifying the chemical shifts and the protons and carbons of the sugar moieties A to F. The combination also identified A and B as 1,6-linked β-D-galactofuranoses, D as non-reducing terminal α-D-galactopyranose, F as a 1,6-linked-β-D-galactopyranose, C as α-1,3-linked D-galactopyranose, and E as β-1,3,6-linked D-galactopyranose. From the combination of inter-residue NOEs observed between anomeric protons of a sugar residue to the neighbouring proton of another sugar residue through space on a ROESY spectrum which were matched by the presence of cross-peaks observed between the anomeric proton of a sugar residue through to the carbon of another sugar residue linked via glycosidic bond on

the HMBC spectrum revealed the presence of three possible structures for the *L. mucosae* VG1-EPS.

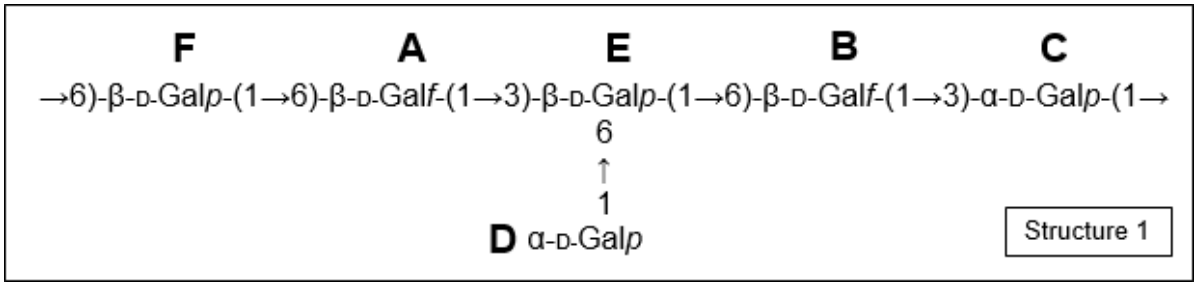

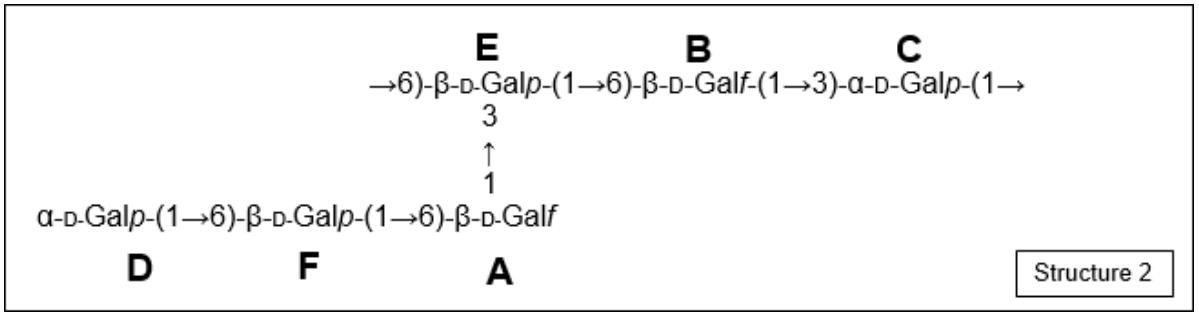

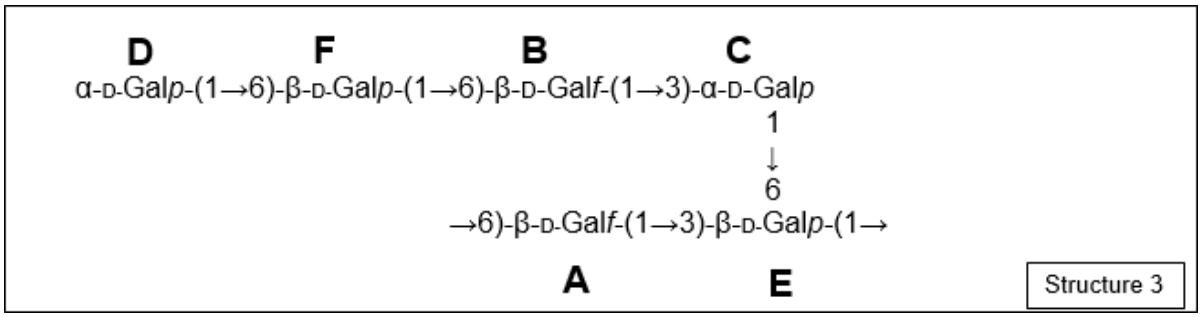

The three similar structures obtained were differentiated by subjecting the *L. mucosae* VG1-EPS to Smith degradation. Linkage analysis of the Smith degraded products generated a single peak, whose MS fragmentation pattern was similar to a non-reducing terminal galactose. Analysis of the edited ^{1}H-^{13}C-HSQC spectrum generated by the Smith degraded *L. mucosae* VG1-EPS revealed the presence of two methylene carbon peaks at 61.50 ppm and 63.10 ppm which are characteristic of those expected for C-6s that are not involved in glycosidic linkages. It was then concluded that the absence of a 1,6-linked galactopyranose eliminates the chance of the EPS having either structure 2 or 3 which were expected to generate a disaccharide [α-D-Gal*p*-(1→6)-β-D-Gal*p*-(1→Gro)], therefore the structure of the *L. mucosae* VG1-EPS must be structure 1, which was expected to generate two monosaccharides, one

which is α-linked to glycerol and the other β-1,3-linked to D-threitol. With the *L. mucosae* VG1-EPS fully characterised, future work will focus on its biological activity.

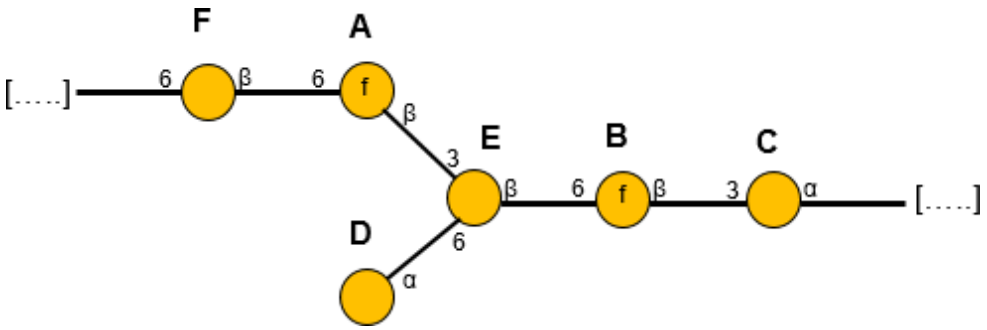

6 Production, isolation and characterisation of polysaccharides from *Lactobacillus salivarius* 702343

6.1 Introduction

As mentioned earlier in section **1.5.3**, *L. salivarius* are present in the GIT, they have been found to inhibit the growth of pathogens and are being gradually employed as probiotics, with EPS believed to responsible for the health benefits imparted to their hosts.. Previous research performed on the species has focused mainly on the genes responsible for EPS synthesis (Ahrne *et al*., 1998; Neville & O'Toole, 2010; Sarkar & Mandal, 2016). This chapter will discuss the findings on the production, isolation and characterisation of the EPSs synthesised by the strain *L. salivarius* 702343.

6.2 Bacterial growth measurements

The first set of experiment was performed to determine the optimal conditions for the growth of the strain *L. salivarius* 702343. The growth of *L. salivarius* 702343 in broth was monitored at two hourly intervals by measuring the turbidity of the broth media, after which time a graph of the absorbance measured was plotted against time.

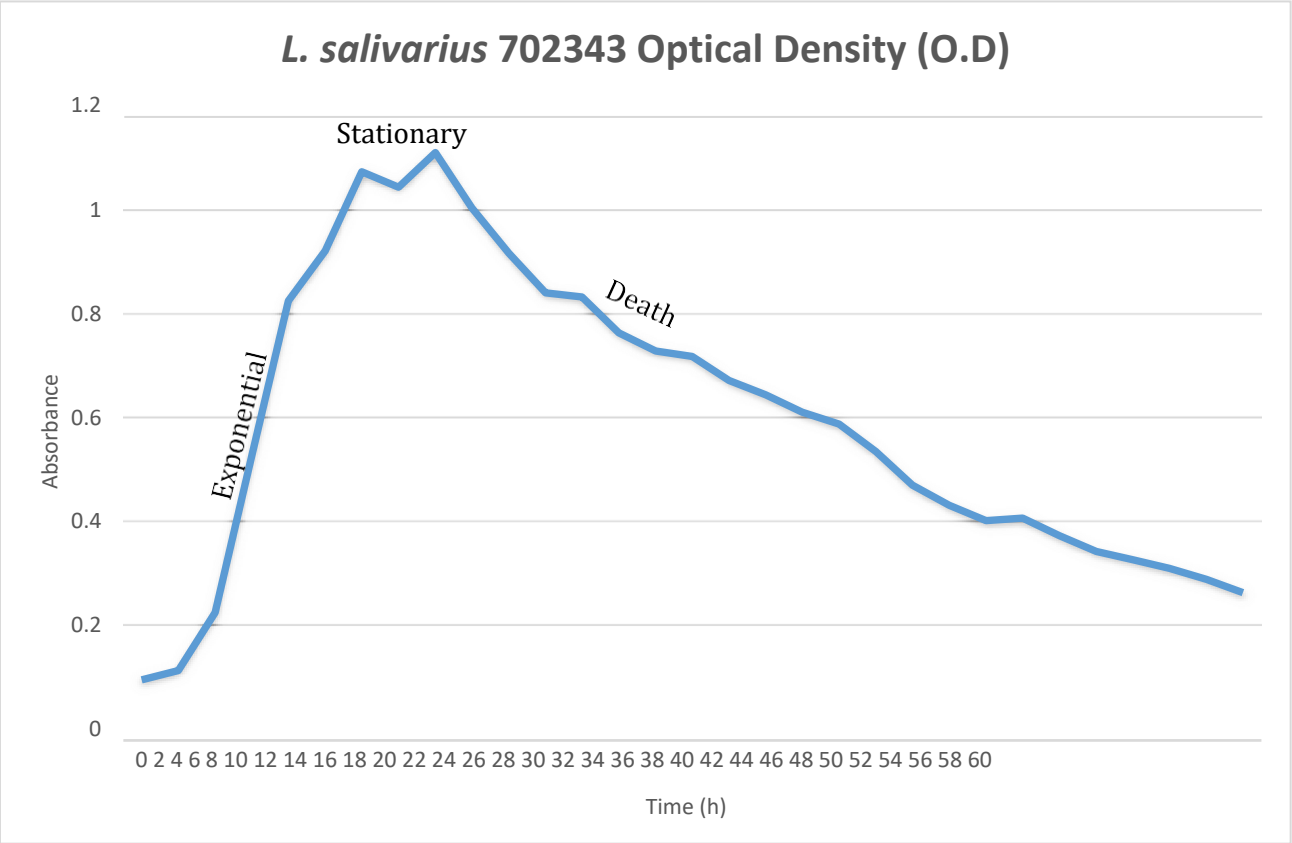

Figure 6.1: Growth curve for *L. salivarius* 702343.

The growth curve for *L. salivarius* 702343 (Fig 6.1) had an extremely short Lag phase and exponential growth began after 2 h. This was because as outlined in section **2.2.5**, the bacteria was taken from an exponentially growing culture (second 20 mL), under the same growth conditions, into a 500 mL broth of the same medium (HBM).

From the determination of the optical density of the broth, *L. salivarius* 702343 growth was monitored, it can be seen that the turbidity of the broth media rose for the first 16 h and then fell until 60 h, at which point the media became less turbid, which suggested that growth had reduced to a minimum. Because EPS production is normally associated with exponential growth, the choice for 72 h fermentation in the 500 mL broth was sufficient for maximum production of EPSs. Although the fermentation was not pH-controlled, the pH of the fermentation broth was also monitored.

At two hourly intervals, pH of the fermentation broth was monitored using the procedure outlined in section **2.2.5**. A graph of pH of the broth was plotted against the time interval.

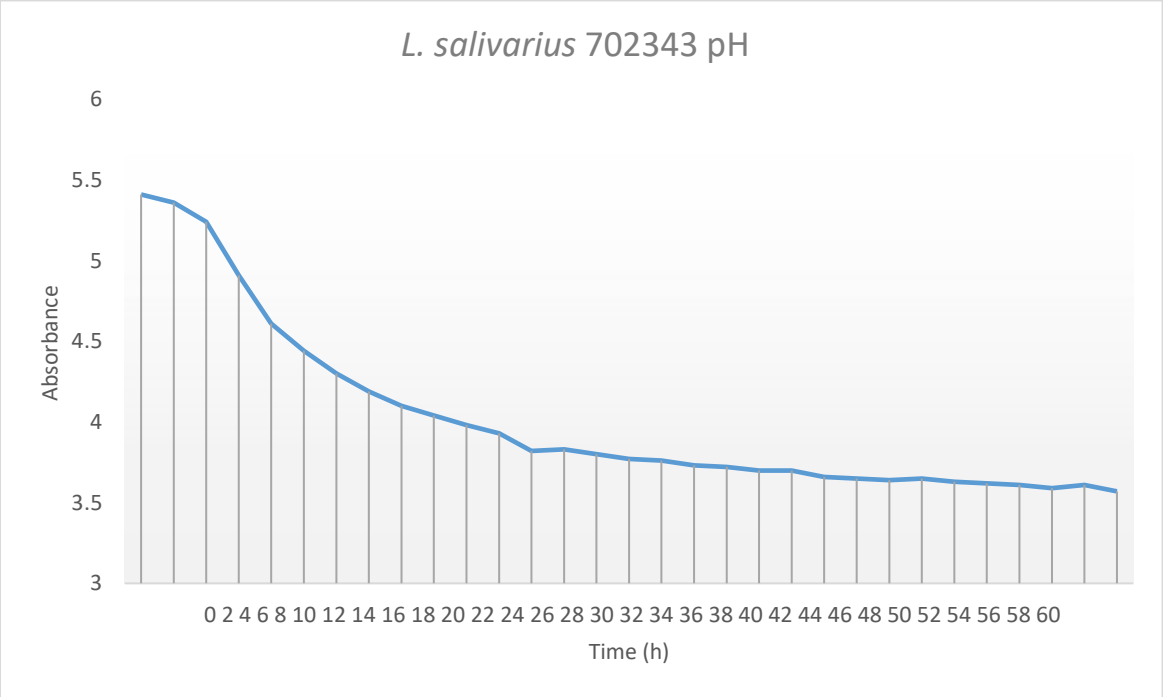

Figure 6.2: A graph of pH against time for *L. salivarius* 702343.

A significant drop in pH, from about 5.5 to 4.1 was observed between 0-12 h, which coincided with the exponential phase in the growth curve (Fig 6.1). This implies that, the drop in pH in the broth media was a result of bacterial cell division and production of lactic acid as the end product of their fermentation. Between 12-24 h, which coincides with the stationary phase in the growth curve (Fig 6.1) where the cell functions including energy metabolism and biosynthetic processes may continue, a continuation in drop of pH can be noticed (4.1 to 3.7), which implies that, lactic acid production continued at a much slower rate. Between 24-60 h, is the death phase in the growth curve, where the broth medium starts to become less turbid as the cells die, until eventually the medium becomes clear and a slight decrease in pH was noticed.

6.3 Study of EPS production and influence of carbon source

The influence of carbon source on bacterial growth and exopolysaccharide production was studied. *L. salivarius* 702343 was grown on HBM supplemented with glucose and a second set of fermentations were carried out using a galactose-supplemented medium.

Table 6.1: Recovered EPSs in a galactose and glucose supplemented medium expressed in mg/ 500 mL culture.

STRAIN	EPS yield (mg) in galactose supplemented medium (500 mL)	EPS yield (mg) in glucose supplemented medium (500 mL)
L. salivarius 702343	5.82	6.74
L. salivarius 702343	6.40	8.50

In both systems, the amount of EPS recovered was small, however, marginally more EPS was recovered when the medium was supplemented with glucose when compared with that which was supplemented with galactose.

Further fermentations were carried out in glucose-supplemented medium in an attempt to maximise recovery of EPSs. The concentration of glucose used in the HBM was doubled, and the EPS recovered was compared, to study the influence of glucose concentration in the medium and to make sure that the bacteria were not starved for maximum EPS recovery.

Table 6.2: Recovered EPSs in a glucose medium supplemented with 10 g and 20 g/ 500 mL.

STRAIN	S2 (mg) in HBM (500 mL) supplemented with 10 g glucose	S2 (mg) in HBM (500 mL) supplemented with 20 g glucose
L salivarius 702343	10.2	8.2

It can be seen that an increase in glucose concentration above 10 g/ 500 mL did not increase the EPS yield. As such, subsequent fermentations were carried out in HMB supplemented with 10 g/ 500 mL glucose. The concentration of glucose was also checked by Dubois method to determine the total glucose content before and after the fermentation to check for the availability of the carbon source at the end of the fermentation process.

Table 6.3: Dubois method results of glucose concentrations in HBM before and after fermentation.

STRAIN	Glucose concentration in HBM before fermentation (mg/ 500 mL)	Glucose concentration in HBM after fermentation (mg/ 500 mL)
L salivarius 702343	10.0	4.9

It can be seen that, the glucose concentration in HBM dropped from 10.0 mg/ 500 mL to 4.9 mg / 500 mL, which showed that the bacteria, for optimum growth, used the

glucose. This also suggests that there is sufficient amount of glucose present after the fermentation. As such, the bacteria were not starved.

6.4 Characterisation of the crude CPSs recovered from *L. salivarius* 702343.

The tightly bound CPSs (C_1 and C_2) recovered by extraction with NaOH from cells and subsequent precipitation with 1 volume of ethanol and 2 volumes of ethanol respectively were isolated from the HBM broth using the procedure described in section **2.2.6.2**. After exhaustive dialysis and freeze-drying, the CPSs yield were found to be 32.12 mg/ L and 1.61 mg/ L for C_1 and C_2 respectively. After collecting three batches from the fermentation broth, ^{1}H-NMR experiment was performed on the recovered CPSs.

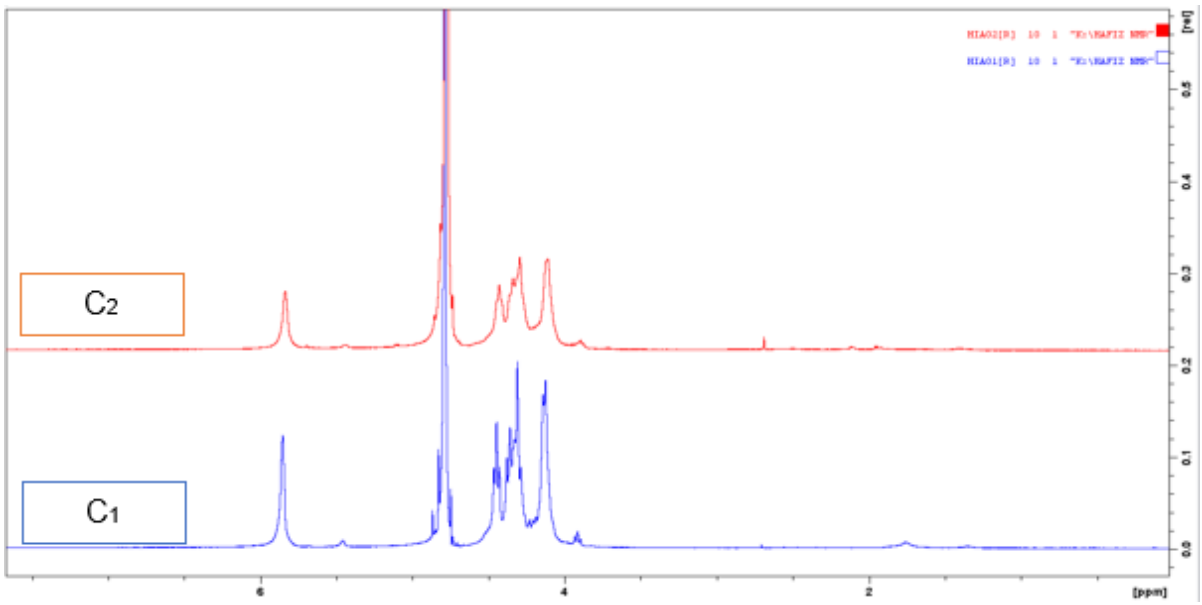

Figure 6.3: Overlaid ^{1}H-NMR spectra of crude CPSs (C_1 and C_2) for *L. salivarius* 702343.

From observation of the anomeric regions of the ^{1}H NMR spectrum of the CPSs produced by *L. salivarius* 702343, it can be seen that the structure of the repeating oligosaccharide unit of the CPS is from a single monosaccharide (homopolymeric) as a single peak is produced in the anomeric region (Fig 6.3). Also from observation of the ring protons as well as the anomeric region, it can be seen that the C_1 and C_2

fractions have the same pattern of peaks, which suggest that they contain the same repeating oligosaccharide unit.

Monomer, linkage and absolute configuration analysis performed using GC-MS and HPAEC using the procedure described in section **2.2.8** suggests that the CPSs synthesised by *L. salivarius* 702343 are composed of repeating unit of a 1,4-linked D-glucose (appendix 4,5 and 6). ^{1}H-NMR spectra previously performed on starch was compared with the ^{1}H-NMR of crude CPSs (C_1 and C_2). The results confirmed that C_1 and C_2 are made up of bacterial glycogen (appendix 3). This bacterial glycogen may have been produced internally and extracted from lysed cells present at the end of the fermentation.

6.5 Characterisation of the crude EPSs recovered from *L. salivarius* 702343.

After exhaustive dialysis and freeze-drying, the native EPS synthesised by *L. salivarius* 702343 which was recovered from the supernatant was analysed by ^{1}H-NMR spectroscopy using the procedure described in section **2.2.8.5**.

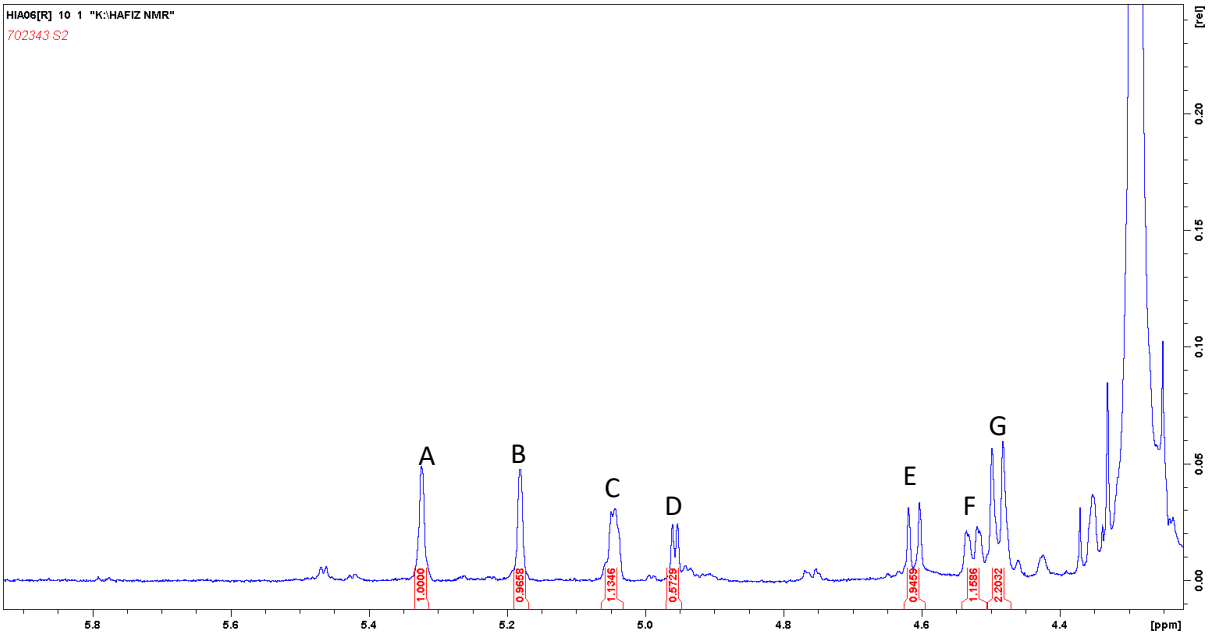

Figure 6.4: ^{1}H-NMR spectra recorded at 70 ^{o}C on the crude EPS produced by *L. salivarius* 702343.

Inspection of the anomeric region of the ^{1}H-NMR spectrum (Fig 6.4) recorded for the *L. salivarius* 702343 EPS revealed a number of signals which suggests a number of sugar residues are present in the repeating unit. These are labelled A to G in order of decreasing chemical shift. The same pattern of peaks were observed in the anomeric region for two batches of samples recovered from different fermentations and the integral ratios of A, B, C and E remained within error, as 1.0, whereas the ratio of D, E and F to A varies within batches: 0.5:1.0:2.0 in the first batch and 1.0:1.6:2.6 in the second batch respectively. This suggests the presence of more than one polysaccharide in the population.

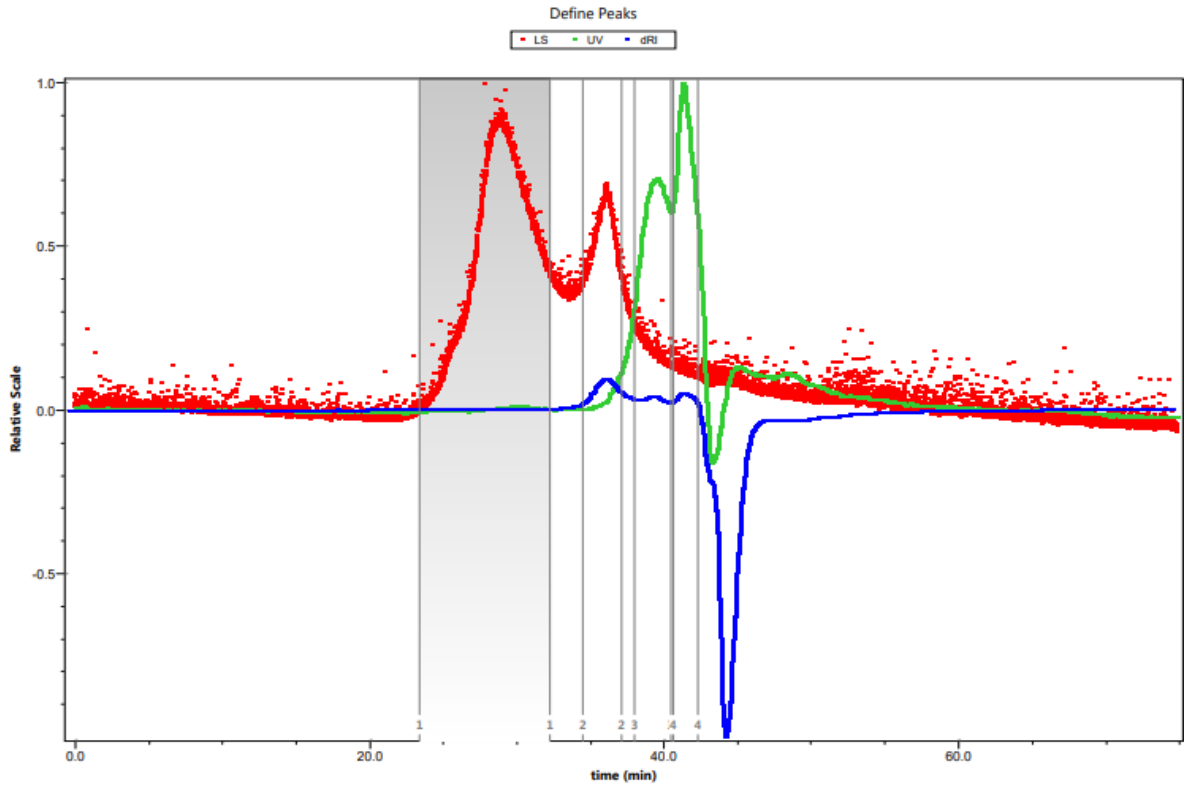

Figure 6.5: SEC-MALLS chromatogram of EPS from *L. salivarius* 702343

Inspection of the SEC-MALLS chromatogram (Fig 6.5) obtained from analysing the EPS synthesised by *L. salivarius* 702343 revealed the presence of two light scattering fractions (red trace) at RT = 25.8 min and 35.9 min. The first light scattering trace (RT = 25.8 min) was accompanied by a very small response of the refractive index trace indicating the presence of small amount of HMw polysaccharide (4.73×10^{5} gmol^{-1}). The second peak in the light scattering trace at RT = 35.9 min was accompanied by a

significant RI peak, suggesting that the polysaccharide present, whose weight average weight molecular mass was determined to be 2.59 x 10^4 $gmol^{-1}$, is more concentrated. Two small late eluting peaks were also observed on the RI trace which were associated with a UV response at RT = 39.5 min and 41.5 min which suggests the potential presence of proteins.

An attempt was made to separate the different polysaccharides using a preparative size exclusion chromatography (S-500 HR) employing the procedure described in section **2.2.7.2**.

6.5.1 Separation of the polysaccharides using Sephacryl S500HR column

The fractions collected from the preparative size exclusion column were assayed for their sugar content by Dubois method as described in section **2.2.7.3**. Fractions 26-34 were identified as containing carbohydrates and were combined in three groups and freeze-dried (fractions 26, 27 and 28), (fractions 29 and 30) and (fractions 31, 32, 33 and 34) respectively. The quantity of the freeze-dried samples are displayed in Figure 6.6 below:

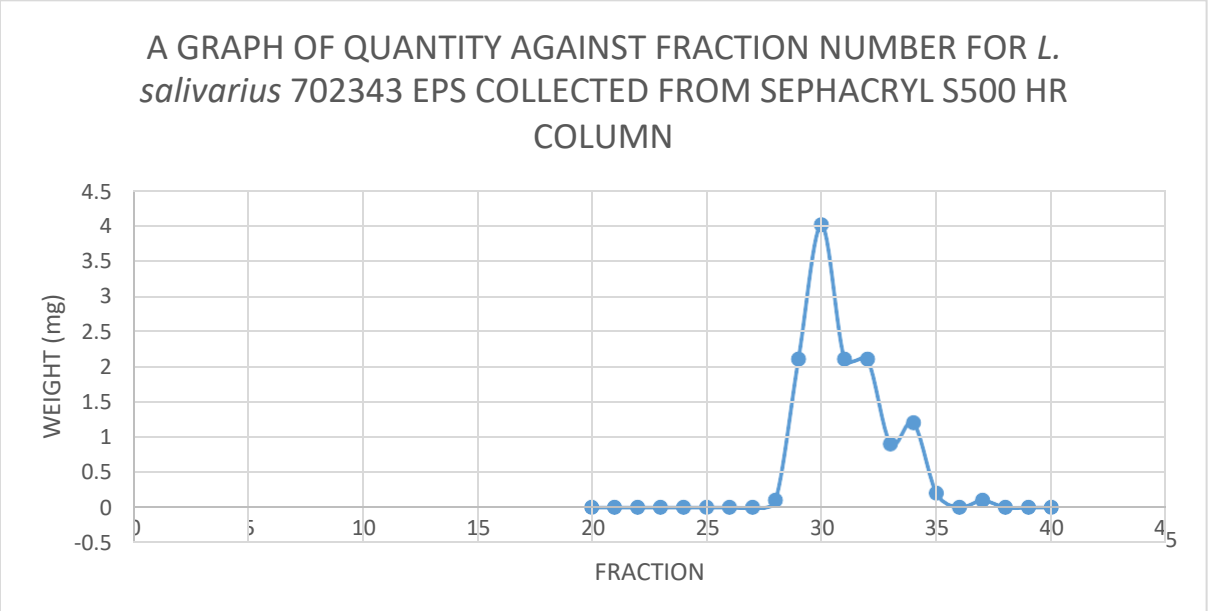

Figure 6.6: Quantity of freeze-dried samples collected from Sephacryl S500 HR column.

The freeze-dried fractions were analysed using ^{1}H-NMR spectroscopy. The ^{1}H-NMR spectra (Fig 6.7) showed that, the Sephacryl S500 HR column could not separate the two polysaccharides: as the anomeric region contains the same set of signals in all the fractions.

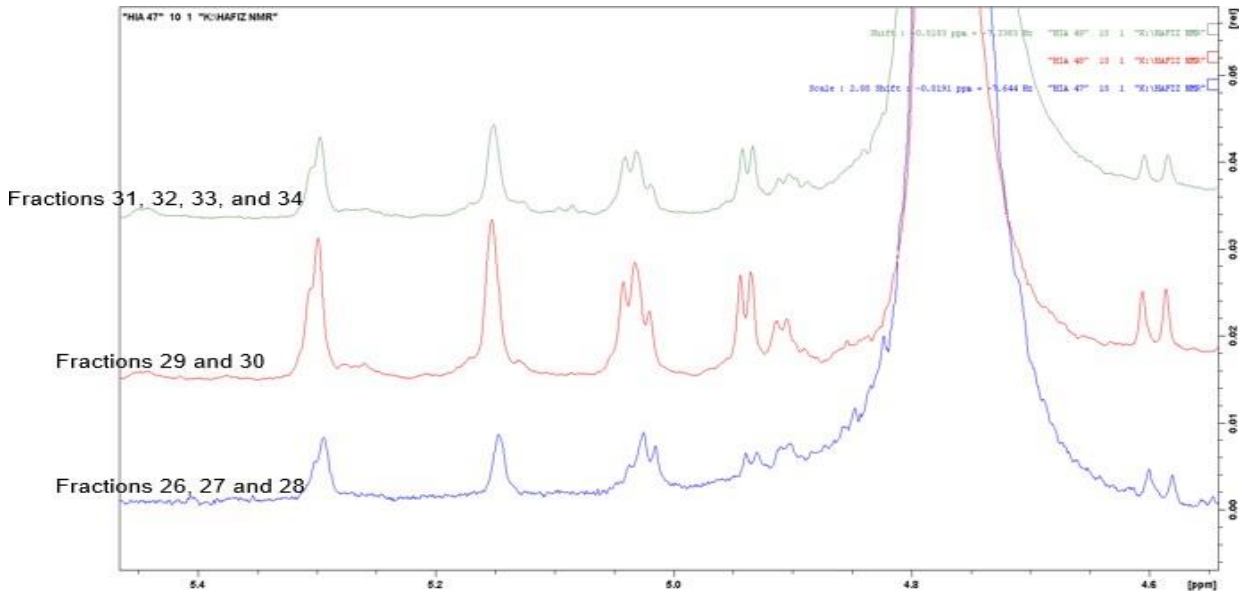

Figure 6.7: Overlaid ^{1}H-NMR spectra of the combined fractions collected from the Sephacryl S500 HR column.

Due to the fact that no visible change was observed in the anomeric region of the combined fractions containing the EPS mixture, a lower flow rate was employed to give the sample a longer time to equilibrate within the column.

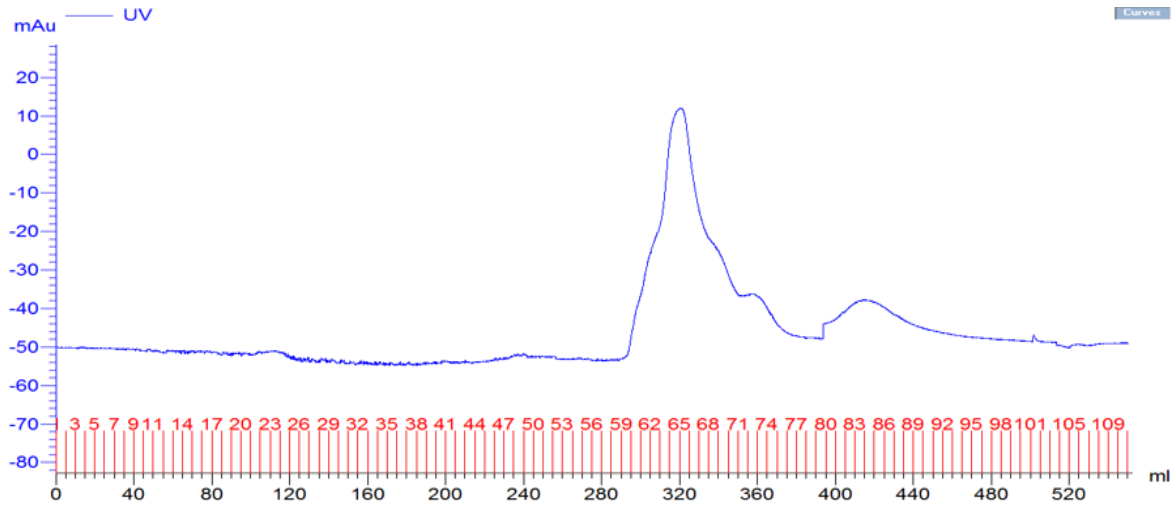

Figure 6.8: UV trace of the Sephacryl S-500 HR column ran on the native EPS at a flow rate of 1.0 mL/ min.

Analysis of the UV trace (Fig 6.8) obtained from the AKTA PRIME system revealed the presence of a single peak which appeared within fractions 59-77 suggesting that the polysaccharides have eluted within two column volumes and the material was able to enter the pores of the stationary phase. Again, each fraction was also analysed for its total carbohydrate content using the Dubois method.

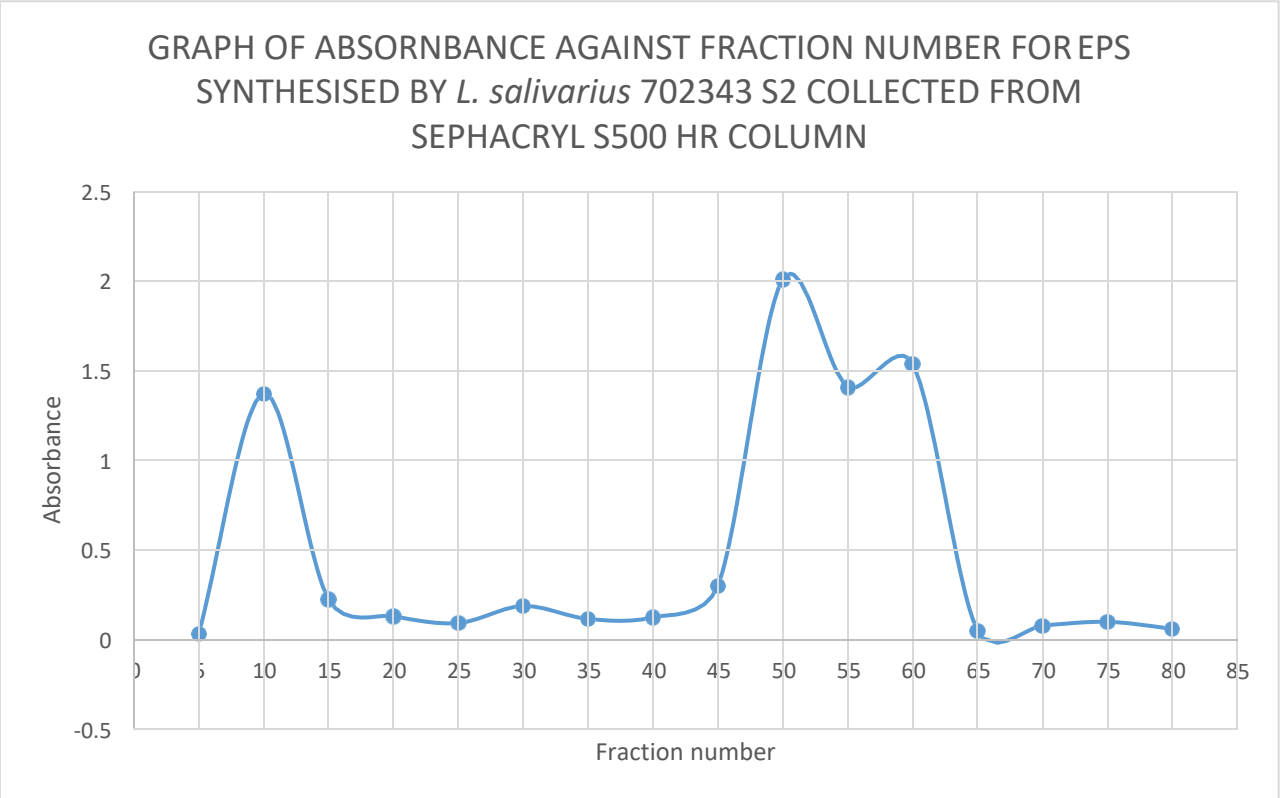

Figure 6.9: Carbohydrate concentration of fractions 1-80 from the Sephacryl S-500 HR column, at a flow rate of 1.0 mL/ min.

The graph of absorbance against fraction number plotted for the total carbohydrate in each fraction (Fig 6.9) suggested that the HMw polysaccharide eluted in the early fractions between fractions 5-15 and possibly two MMw polysaccharides eluted within fractions 45-55 and 55-60 respectively. Fractions were combined and lyophilised based on the Dubois results. No material was present in fractions 1-42, as such only the fractions containing substantial amount of the sample were analysed by ^{1}H-NMR.

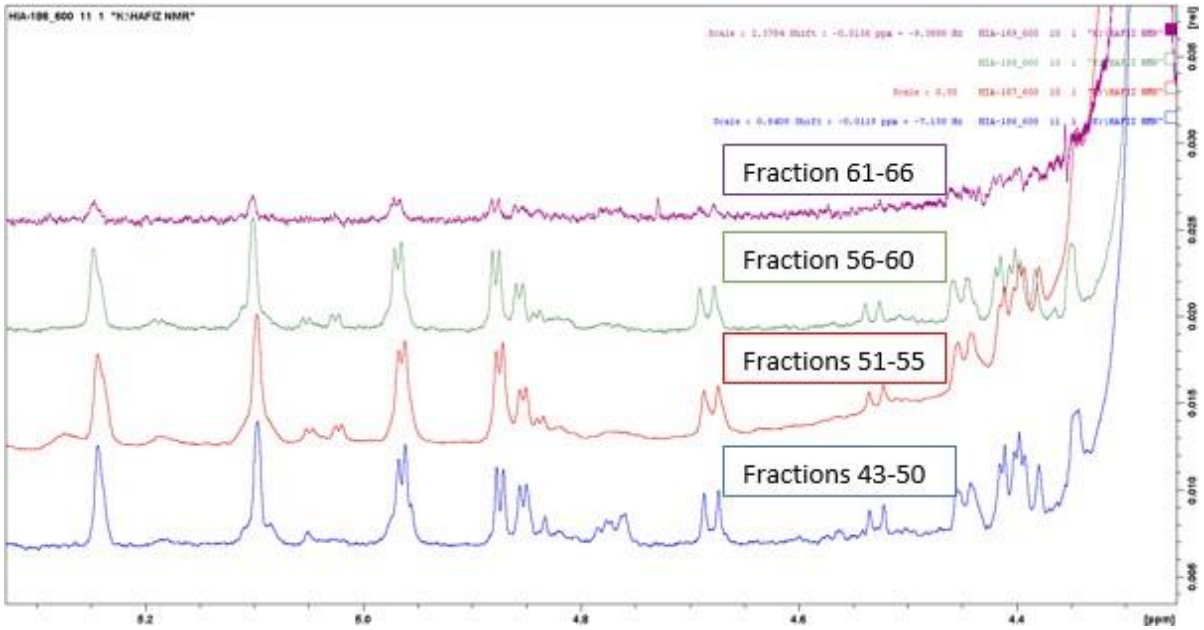

Figure 6.10: Overlaid ^{1}H-NMR spectra of the combined fractions collected from the Sephacryl S500 HR column at a flow rate of 1.0 mL/ min.

The overlaid ^{1}H-NMR spectra of the combined fractions collected from the Sephacryl S500HR column operating with a much lower flowrate (Fig 6.10) revealed that the combined fractions had the same pattern of peaks in their anomeric, which suggest that the polysaccharides had co-eluted. Visualising the anomeric regions of the fractions that had the EPS showed that, the proposed EPS mixture could not be separated by size exclusion chromatography using a Sephacryl S-500 HR column.

As was the case for the MMw polysaccharide mixture synthesised by *Lactobacillus fermentum* LF2, 2D-NMR spectra were recorded on the EPS mixture synthesised by *L salivarius* 702343. The ^{1}H-^{13}C-HSQC revealed the presence of C-1 resonances of A and B at unusually low field (δ 105.7 and 107.3 ppm) (Fig 6.11), this suggests that these resonances are derived from furanose sugars. As explained earlier in chapter 4, glycosidic bonds to furanoses are often acid labile and easily cleaved when subjected to a mild acid hydrolysis therefore, the EPS mixture synthesised by *L. salivarius* 702343 was subjected to mild acid hydrolysis.

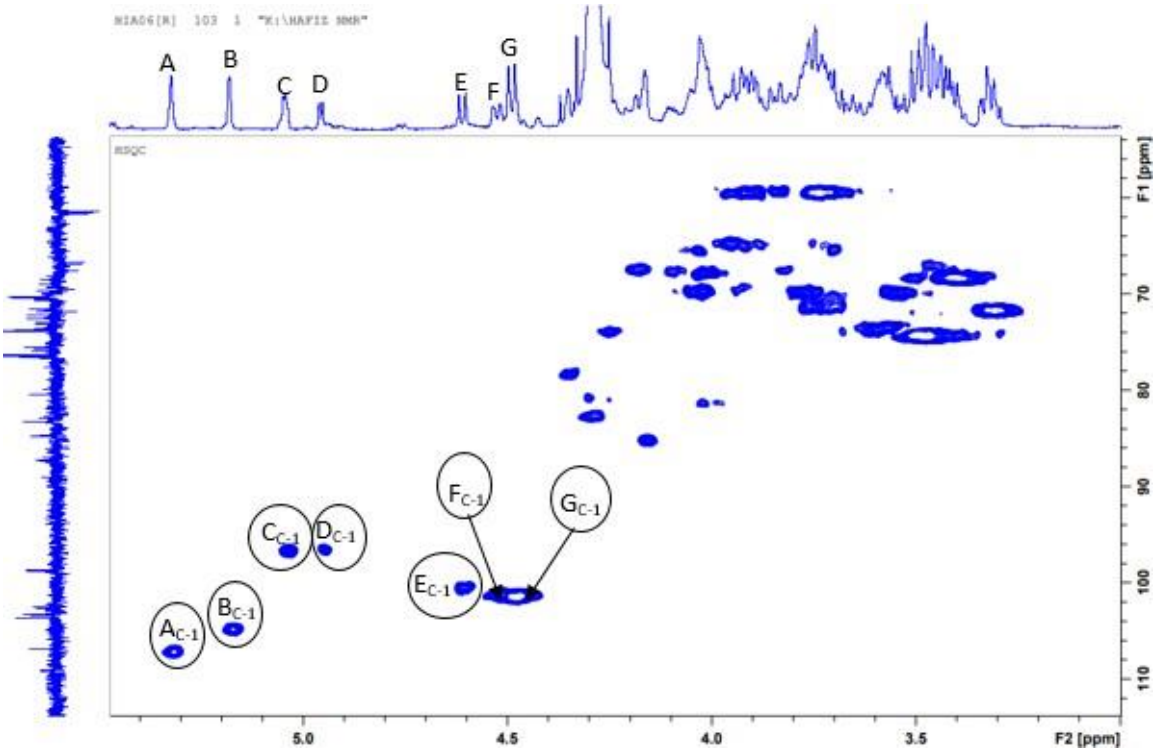

Figure 6.11: ^{1}H-^{13}C-HSQC spectrum recorded on the polysaccharide mixture.

6.5.2 Use of mild acid hydrolysis to separate the polysaccharide mixture

The polysaccharide mixture was treated with mild acid (0.5 M TFA, at room temperature) in an attempt to liberate oligosaccharides. The ^{1}H-NMR spectrum was recorded immediately and the sample was left at room temperature, with additional spectra being recorded at 24 hourly intervals for 3 days. After three days, the acid was removed by evaporation under a constant stream of nitrogen and an additional spectrum was recorded. Except for the shift of signals before and after removal of the acid, the set of anomeric protons present in the sample were the same and had a similar integral ratio before and after mild acid hydrolysis (Fig 6.12).

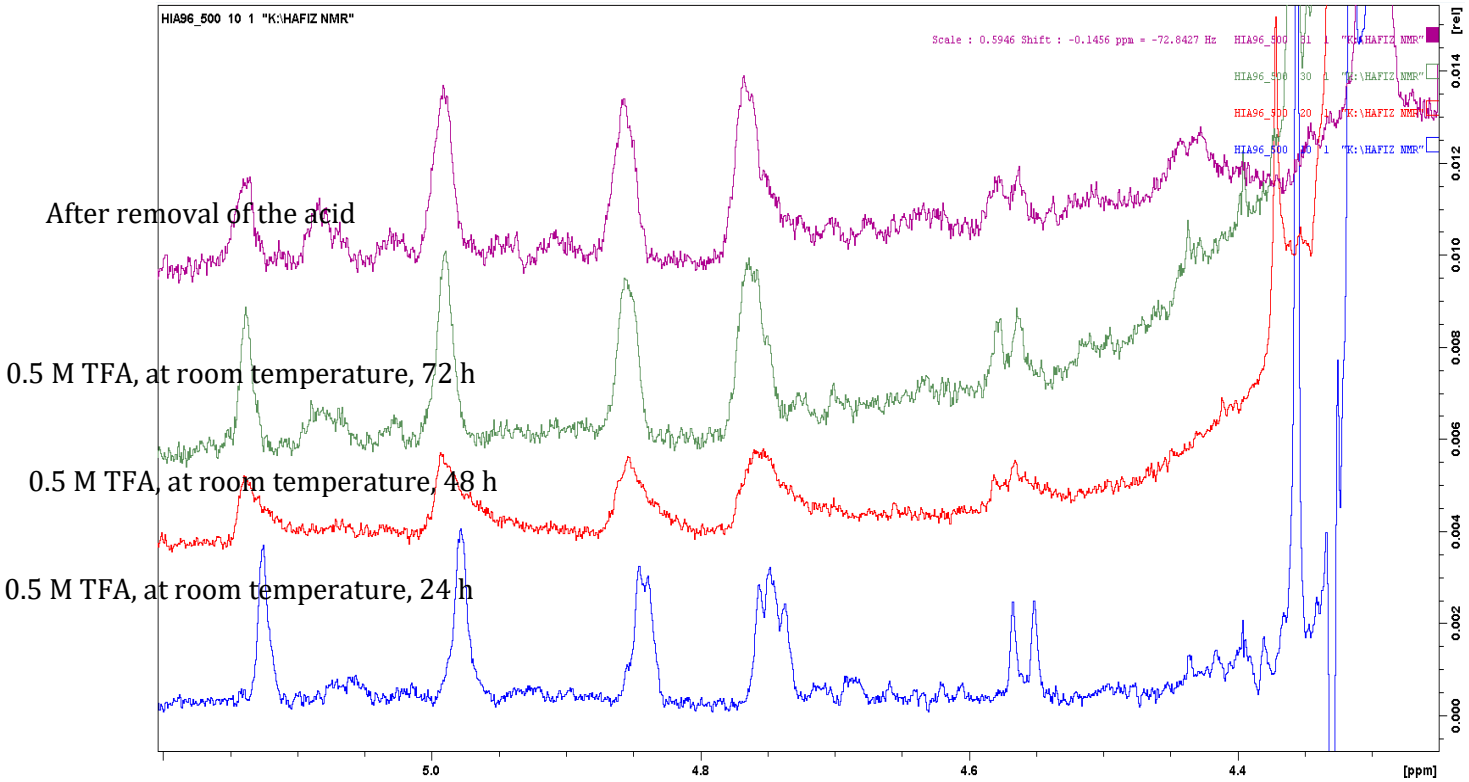

Figure 6.12: Overlaid ^{1}H-NMR spectra of EPS from *L. salivarius* 702343 after mild acid treatment.

The polysaccharide was also treated with mild acid (0.5 M TFA, at 100 ^{o}C), for 1 h, 2 h, 3 h, 4 h and 5 h respectively. This treatment did not generate oligosaccharides; however, further heating for several hours completely hydrolysed the polysaccharide. If the furanose sugars are present on the backbone of both polysaccharides, then both would be expected to degrade at a similar rate. However, it can be seen that, size exclusion chromatography or partial acid hydrolysis could not separate the two polysaccharide. Monomer analysis was performed on the crude polysaccharide to further understand its chemical composition and attempt to elucidate its structure.

6.5.3 Monomer analysis of EPS mixture synthesised by *L. salivarius* 702343

Monomer analysis of the EPS mixture was performed by GC-MS after converting them into their alditol acetates using the procedure described in section 2.2.2. The retention time of the peaks obtained for the sample were compared with that of a standard alditol acetate mixture. The MS fragmentation patterns generated by each peak was analysed and compared with those in the literature. Results of the monomer

analysis indicated that the polysaccharide mixture is composed of two hexoses, which were identified to be glucose and galactose in a ratio of 3:1.

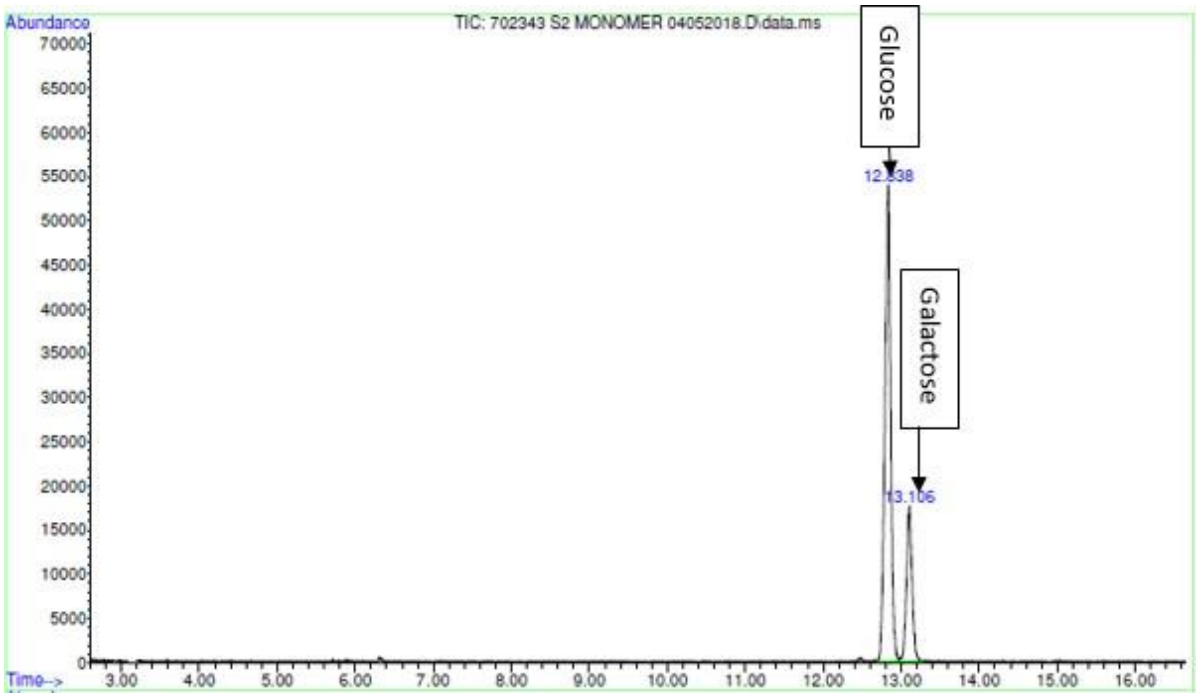

Figure 6.13: GC trace of monomer analysis performed on EPS mixture synthesised by *L. salivarius* 702343.

6.5.4 Linkage analysis of the EPS mixture synthesised by *L*. *salivarius* 702343

Results of methylation analysis of the polysaccharide performed by GC-MS revealed the presence of two large peaks at 12.047 and 15.934 min respectively. MS fragmentation pattern generated by the main peaks were analysed and compared with those in the literature (McGinnis & Biermann, 1989). The 12.047 min peak was identified as a 1,5-di-*O*-acetyl-2,3,4,6-tetra-*O*-methylhexitol derived from non-reducing terminal hexose, the retention time of the peak confirms the presence of non-reducing terminal glucose. The MS fragmentation of the 15.934 min peak revealed the presence of 1,4,6-tri-O-acetyl-(1-deuterio)-2,3,5-tri-*O*-methylhexitol derived from 1,6-linked hexofuranose.

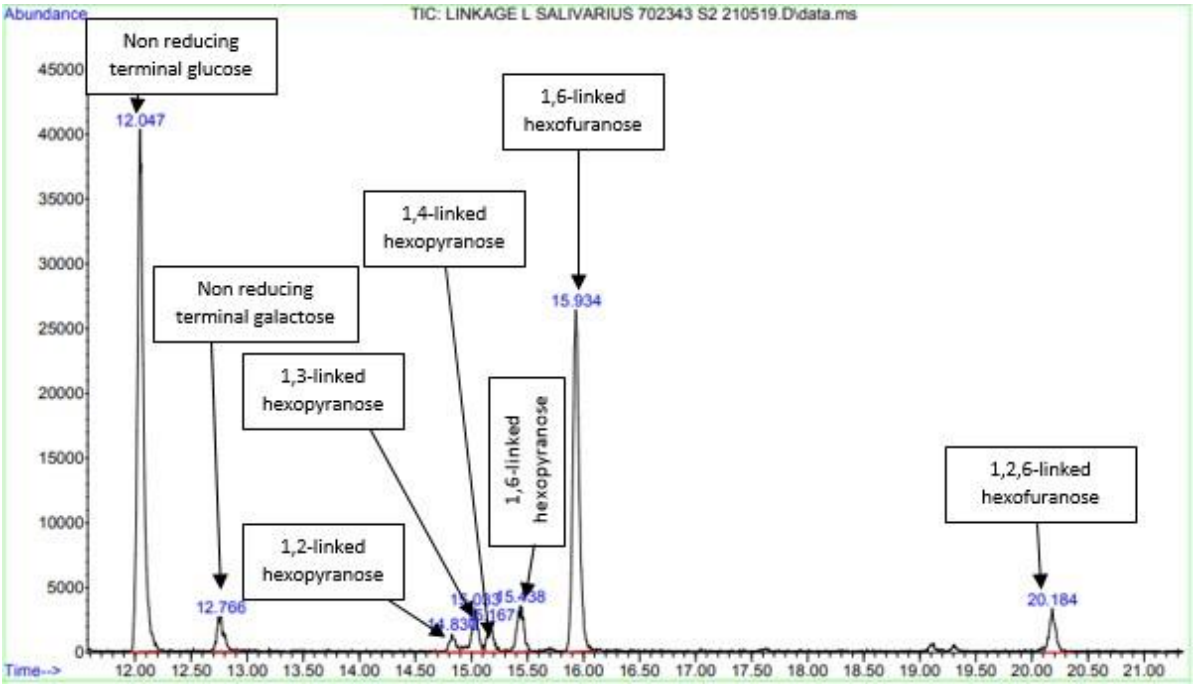

Figure 6.14: GC trace of linkage analysis performed on the EPS mixture synthesised by *L. salivarius* 702343.

Other peaks of low intensities observed at 12.77, 15.03, 15.17, 15.44 and 20.18 min revealed the presence of 1,5-di-*O*-acetyl-2,3,4,6-tetra-*O*-methylhexitol derived from a non-reducing terminal galactose, a 1,2,5-tri-*O*-acetyl-3,4,6-tri-*O*-methylhexitol derived from 1,2-linked hexopyranose, a 1,4,5-tri-*O*- acetyl-2,3,6-tri-*O*-methylhexitol derived from a 1,4-linked hexopyarose, a 1,4,5-tri-*O*-acetyl-2,3,6-tri-*O*-methylhexitol derived from 1,5-linked hexofuranose, a 1,4,6-tri-*O*- acetyl -2,3,6-tri-*O*-methylhexitol derived from a 1,6-linked hexofuranose and a 1,2,4,6-tetra-*O*-acetyl-3,5-di-*O*-methyl hexitol derived from a 1,2,6-linked hexofuranose respectively.

6.5.5 Smith degradation

The native EPS mixture was subjected to Smith degradation using the procedure described in section **2.2.8.6**. This was performed with the view that if the main backbone of any of the EPSs in the mixture is resistant to oxidation, then the oligosaccharide repeating unit would be retained in the dialysis bag. The linkage analysis performed on the native EPS mixture revealed that 75 % of the residues present in the repeating units are susceptible to oxidation, as such small oligosaccharides/monosaccharides are expected to be generated which would pass through the dialysis bag and thus would not be retained.

The identity of any sugar present in the repeating unit of the Smith degraded EPS mixture was determined by ^{1}H-NMR spectroscopy using the procedure described in section 2.2.8.5. No peaks were observed in the anomeric region of ^{1}H NMR spectra recorded for the dialysis bag content after Smith degradation. Inspection of the anomeric region of the freeze-dried dialysis water revealed the presence of small oligosaccharides/monosaccharides. This implies that, in all of the repeating units in the EPS mixture, neither was totally resistant to oxidation and as such, small oligosaccharides/monosaccharides were generated which passed through the dialysis bag and thus were not be retained.

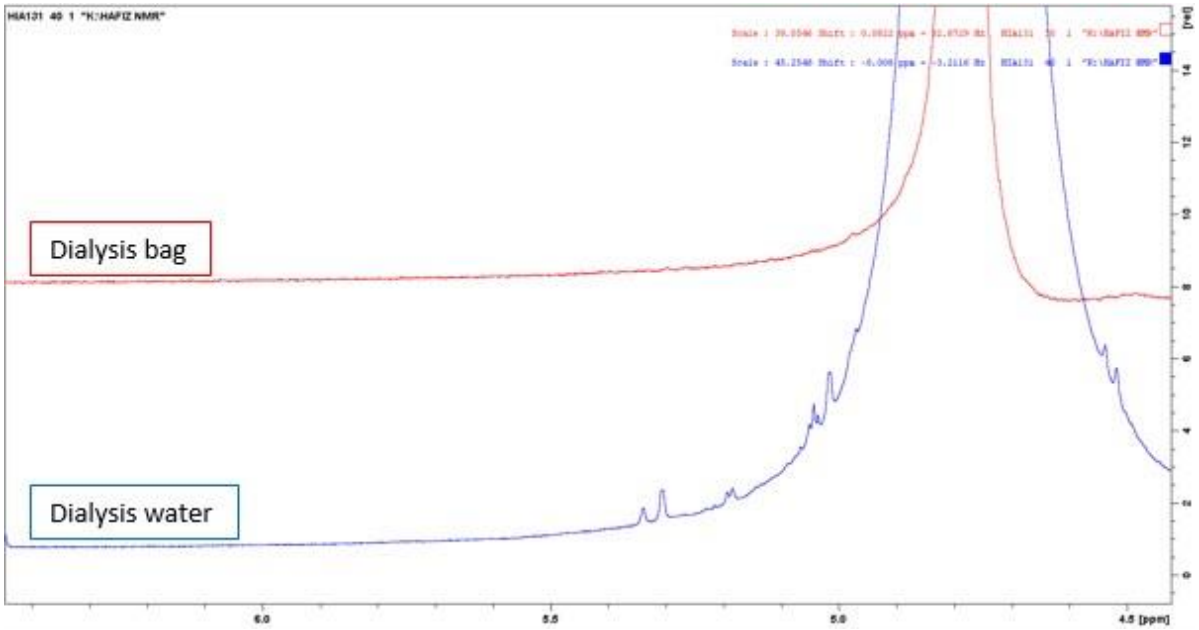

Figure 6.15: Overlaid ^{1}H-NMR of freeze-dried dialysis bag and dialysis water contents of the Smith degraded EPS mixture.

Given the limited amount of material available at this stage, it was decided to stop working with this particular culture.

6.6 Conclusion

To conclude, the growth of the strain *L. salivarius* 702343 was monitored in Huddersfield Broth Media. It was found out that the choice for 72 h fermentation in the 500 mL broth was sufficient for maximum production of exopolysaccharides and that a significant drop in pH, from about 5.5 to 4.1 was observed during the exponential growth. Following the isolation and purification procedures, both capsular and slime polysaccharides were recovered. The capsular polysaccharides (C_1 and C_2) were found to be composed of repeating unit of a 1,4-linked D-glucose and determined to be bacterial glycogen. Analysis of the EPS by SEC-MALLS and ^{1}H-NMR revealed the presence of more than one polysaccharide in the population. Unfortunately, use of mild acid hydrolysis, preparative size exclusion chromatography (Sephacryl S500 HR column) and Smith degradation, could not separate the polysaccharides present in the EPS mixture synthesised by *L. salivarius* 702343. However, monomer analysis performed on the EPS mixture revealed that the repeating units are composed of glucose and galactose residues. Linkage analysis of the EPS mixture revealed the presence of a non-reducing terminal glucose, a non-reducing terminal galactose, a 1,2-linked hexopyranose, a 1,4-linked hexopyarose, a 1,5-linked hexofuranose, a 1,6-linked hexofuranose, 1,6-linked hexopyranose and a 1,2,6-linked hexofuranose.

At the end of this work, the amount of EPS synthesised by *L. salivarius* 702343 was very small, future experiments should employ pH control to attempt to optimise the EPS yield. Moreover, it would be interesting if employing a smaller pore size column could separate the EPS mixture. 2D-NMR spectroscopy should be performed on the first dialysis water change after the mild acid hydrolysis step in Smith degradation, analysis of the small molecules might provide more information on the structure of the repeating units.

7 General conclusion

The first aim of this research was to separate and purify the polysaccharide mixture synthesised by *L. fermentum* LF2 and to elucidate the structure of each EPS in order to understand the relationship between their structures and their chemical, physical and biological activities. A high molecular mass polysaccharide was successfully separated, purified, and its structure elucidated. The high molecular mass polysaccharide was determined to possess a trisaccharide-repeating unit having the following structure:

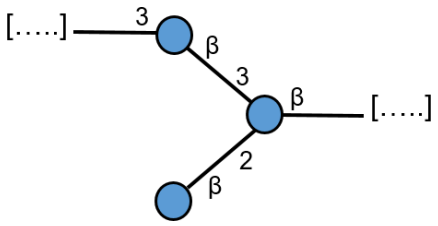

A search of the literature revealed that the structure of the high molecular mass polysaccharide produced by *L. fermentum* LF2 was found to be the same as that which was produced by three other strains of bacteria including *Pediococcus damnosus* 2.6, *Lactobacillus spp*. G-77 and *Oenococcus oeni* I4. Evaluation of immunomodulatory activity performed on the HMw polysaccharide looked very promising for use in the prevention of inflammatory bowel diseases such as Crohn's disease and ulcerative colitis. Microwave-assisted depolymerisation and ultrasonic disruption effectively decreased the molecular weight of the β-glucan in a controlled manner. Inspection of the ^{1}H-NMR of the depolymerised samples revealed that the decreases in molecular weight of the β-glucan does not alter its structure and in future work, studies should be undertaken if determine if the molecular mass of the polysaccharide influences the observed biological activity.

Analysis of the second population in the EPS mixture synthesised by *L. fermentum* LF2 suggested the presence of two MMw polysaccharides accounting for more than 75 % of the EPS mixture by weight. The structures of the two MMw polysaccharides were investigated by subjecting the MMw polysaccharide mixture to Smith degradation. Analysis of the EPS mixture with reference to the Smith degraded products revealed the structure of the repeating unit contained in MMwa to be:

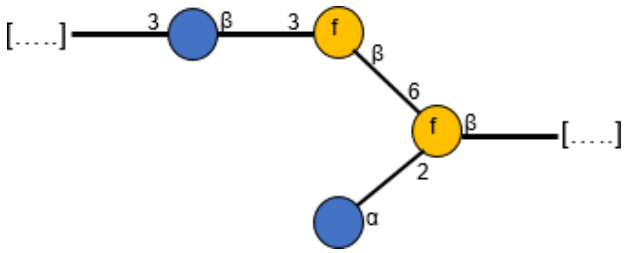

And that of MMwb to be:

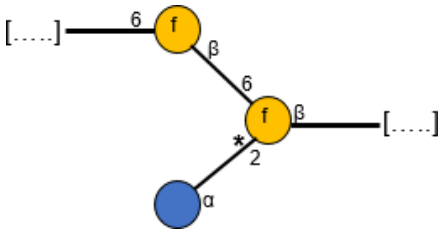

The extent to which the 1,6-linked-β-D-galactofuranoside in MMwb is substituted at the 2-position was very dependent on fermentation conditions. The 1,6-linked-β-D-galactofuranoside was found to be substituted at the 2-position greater than 80% under optimized fermentation conditions. A search of the literature suggests that the two MMw polysaccharides are novel.

The second aim of this research was to grow, isolate and characterise the EPS synthesised by a novel probiotic bacterial strain, *L. mucosae* VG1. The strain secretes a medium molecular mass D-galactan into the fermentation media during growth. Three possible structures of the repeating unit were proposed for the D-galactan after analysis with HPAEC, GC-MS, 1D- and 2D-NMR spectroscopy. The three structures obtained were differentiated by subjecting the D-galactan to Smith degradation. As was the case for the D-galactan, analysis of the Smith degraded products revealed that the D-galactan is composed of a repeating having the following novel structure:

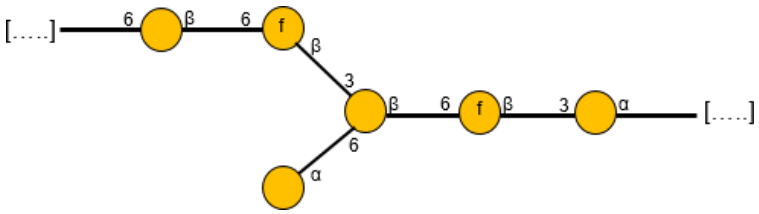

The third aim was to produce, isolate, purify and characterise polysaccharides synthesised by *L. salivarius* 702343. The strain produced 34 mgL^{-1} of capsular polysaccharides (CPSs) composed of repeating unit of a 1,4-linked D-glucose determined to be bacterial glycogen. The low yield 19 mgL^{-1} of EPS synthesised by the strain was determined to contain more than one polysaccharide in the population. Unfortunately, use of mild acid hydrolysis, preparative size exclusion chromatography (Sephacryl S500 HR column) and Smith degradation, could not separate the polysaccharides present in the EPS mixture. However, monomer analysis performed on the EPS mixture revealed that the repeating units are composed of glucose and galactose residues. Linkage analysis of the EPS mixture revealed the presence of a non-reducing terminal glucose, a non-reducing terminal galactose, a 1,2-linked hexopyranose, a 1,4-linked hexopyarose, a 1,5-linked hexofuranose, a 1,6-linked hexofuranose, 1,6-linked hexopyranose and a 1,2,6-linked hexofuranose.

7.1 Future work

In this study, the HMw β-glucan has been shown to impart immunotolerance in PBMC and is able to significantly influence the release of proinflammatory cytokines and as such curtail an excessive inflammatory response. Microwave-assisted de-polymerisation and ultrasonic disruption effectively decreased the molecular weight of the β-glucan in a controlled manner without altering its structure. It would be interesting to check the biological activity of the different molecular weights β-glucan formed during de-polymerisation in order to further understand the effect of molecular weight on biological activity. Moreover, provisional studies of the biological activity of the MMw polysaccharide mixture has also shown the polysaccharides mixture to be able to stimulate the release of the inflammatory cytokine TNF-α from PBMC. It would be interesting to employ a much smaller size preparative size exclusion column to attempt to separate the two polysaccharides and determine their biological activity individually. With the *L. mucosae* VG1-EPS fully characterised, future work should focus on determining its biological activity.

As for the bacterial strain *L. salivarius* 702343, some tests and experiments have also been left out due to time limitation. Since the amount of EPS synthesised by *L.*

salivarius 702343 is very small, future experiments should employ pH control to attempt to optimise the EPS yield. Moreover, it would be interesting if employing a smaller pore size column could separate the EPS mixture. 2D-NMR spectroscopy should be performed on the first dialysis water change after the mild acid hydrolysis step in Smith degradation, analysis of the small molecules might provide more information on the structure of the repeating units.

8 References

Abdel-Akher, M., Hamilton, J. K., Montgomery, R., & Smith, F. (1952). A new procedure for the determination of the fine structure of polysaccharides. *Journal of the American Chemical Society*, *74*(19), 4970-4971.

Abeygunawardana, C., Williams, T. C., Sumner, J. S., & Hennessey Jr, J. P. (2000). Development and validation of an NMR-based identity assay for bacterial polysaccharides. *Analytical biochemistry*, *279*(2), 226-240.

Ahrazem, O., Prieto, A., Leal, J. A., Giménez-Abián, M. I., Jiménez-Barbero, J., & Bernabé, M. (2007). Fungal cell wall polysaccharides isolated from Discula destructiva spp. *Carbohydrate research*, *342*(8), 1138-1143.

Ahrne, S., Nobaek, S., Jeppsson, B., Adlerberth, I., Wold, A. E., & Molin, G. (1998). The normal Lactobacillus flora of healthy human rectal and oral mucosa. *Journal of applied microbiology*, *85*(1), 88-94.

Albersheim, P., Nevins, D. J., English, P. D., & Karr, A. (1967). A method for the analysis of sugars in plant cell-wall polysaccharides by gas-liquid chromatography. *Carbohydrate Research*, *5*, 340-345.

Ale, E.C., Batistela, V.A., Correa Olivar, G., Ferrado, J.B., Sadiq, S., Ahmed, H.I., Reinheimer, J.A., Vera-Candioti, L., Laws, A.P., & Binetti, A. G. (2019). Statistical optimisation of the exopolysaccharide production by Lactobacillus fermentum Lf2 and analysis of its chemical composition. *International Journal of Dairy Technology*.

Ale, E. C., Perezlindo, M. J., Burns, P., Tabacman, E., Reinheimer, J. A., & Binetti, A. G. (2016). Exopolysaccharide from Lactobacillus fermentum Lf2 and its functional characterization as a yogurt additive. *Journal of Dairy Research, 83*(4), 487-492.

Alhudhud, M., Humphreys, P., & Laws, A. (2014). Development of a growth medium suitable for exopolysaccharide production and structural characterisation by Bifidobacterium animalis ssp. lactis AD011. *Journal of microbiological methods*, *100*, 93-98.

Amrouche, T., Boutin, Y., Prioult, G., & Fliss, I. (2006). Effects of bifidobacterial cytoplasm, cell wall and exopolysaccharide on mouse lymphocyte proliferation and cytokine production. *International Dairy Journal*, *16*(1), 70-80.

Arroyo, R., Martín, V., Maldonado, A., Jiménez, E., Fernández, L., & Rodríguez, J. M. (2010). Treatment of infectious mastitis during lactation: antibiotics versus oral administration of Lactobacilli isolated from breast milk. *Clinical Infectious Diseases, 50*(12), 1551-1558.

Axelsson, L., & Lindgren, S. (1987). Characterization and DNA homology of Lactobacillus strains isolated from pig intestine. *Journal of applied bacteriology*, *62*(5), 433-440.

Bahary, W. S., Hogan, M. P., Jilani, M., & Aronson, M. P. (1995). Size-exclusion chromatography of dextrans and pullulans with light-scattering, viscosity, and refractive index detection. *Advances in Chemistry Series*, *247*(1), 151-166.

Bajpai, V.K., Rather, I.A., Majumder, R., Shukla, S., Aeron, A., Kim, K., Kang, S.C., Dubey, R.C., Maheshwari, D.K., Lim, J. & Park, Y.H., (2016). Exopolysaccharide and lactic acid bacteria: Perception, functionality and prospects. *Bangladesh Journal of Pharmacology*, *11*(1), 1-23.

Balzaretti, S., Taverniti, V., Guglielmetti, S., Fiore, W., Minuzzo, M., Ngo, H.N., Ngere, J.B., Sadiq, S., Humphreys, P.N. & Laws, A.P. (2017). A novel rhamnose-rich hetero-exopolysaccharide isolated from Lactobacillus paracasei DG activates THP-1 human monocytic cells. *83*(3), e02702-02716.

Barnes, E. M., Despaul, J. E., & Ingram, M. (1963). The behaviour of a food poisoning strain of Clostridium welchii in beef. *Journal of Applied Bacteriology*, *26*(3), 415-427.

Barnes, E. M., & Ingram, M. (1956). The effect of redox potential on the growth of Clostridium welchii strains isolated from horse muscle. *Journal of Applied Bacteriology*, *19*(1), 117-128.

Barsanti, L., Passarelli, V., Evangelista, V., Frassanito, A. M., & Gualtieri, P. (2011). Chemistry, physico-chemistry and applications linked to biological activities of β-glucans. *Natural product reports*, *28*(3), 457-466.

Behare, P. V., Singh, R., Nagpal, R., & Rao, K. H. (2013). Exopolysaccharides producing Lactobacillus fermentum strain for enhancing rheological and sensory attributes of low-fat dahi. *Journal of food science and technology*, *50*(6), 1228-1232.

Betsy, T., & Keogh, J. E. (2005). *Microbiology demystified*: McGraw-Hill.

Beveridge, T. J. (1999). Structures of gram-negative cell walls and their derived membrane vesicles. *Journal of bacteriology*, *181*(16), 4725-4733.

Biermann, C. J., & McGinnis, G. D. (1988). *Analysis of Carbohydrates by GLC and MS*: CRC Press.

Blake, J. D., & Richards, G. N. (1970). A critical re-examination of problems inherent in compositional analysis of hemicelluloses by gas-liquid chromatography. *Carbohydrate Research*, *14*(3), 375-387.

Bock, K., & Pedersen, C. (1983). Carbon-13 nuclear magnetic resonance spectroscopy of monosaccharides. In *Advances in carbohydrate chemistry and biochemistry* (Vol. 41, pp. 27-66): Elsevier.

Boels, I. C., van Kranenburg, R., Hugenholtz, J., Kleerebezem, M., & De Vos, W. M. (2001). Sugar catabolism and its impact on the biosynthesis and engineering of exopolysaccharide production in lactic acid bacteria. *International Dairy Journal*, *11*(9), 723-732.

Brown, S., Santa Maria Jr, J. P., & Walker, S. (2013). Wall teichoic acids of gram-positive bacteria. *Annual review of microbiology*, *67*, 313-336.

Buysse, J. A. N., & Merckx, R. (1993). An improved colorimetric method to quantify sugar content of plant tissue. *Journal of Experimental Botany*, *44*(10), 1627-1629.

Calmon, C., & Kressman, T. R. E. (1957). *Ion exchangers in organic and biochemistry*. Retrieved from

Casey, P.G., Casey, G.D., Gardiner, G.E., Tangney, M., Stanton, C., Ross, R.P., Hill, C. & Fitzgerald, G.F. (2004). Isolation and characterization of anti-Salmonella lactic acid bacteria from the porcine gastrointestinal tract. *Letters in applied microbiology, 39*(5), 431-438.

Castro-Bravo, N., Wells, J. M., Margolles, A., & Ruas-Madiedo, P. (2018). Interactions of surface exopolysaccharides from Bifidobacterium and Lactobacillus within the intestinal environment. *Frontiers in microbiology*, *9*.

Cerning, J., Bouillanne, C., Desmazeaud, M. J., & Landon, M. (1986). Isolation and characterization of exocellular polysaccharide produced byLactobacillus bulgaricus. *Biotechnology Letters*, *8*(9), 625-628.

Cerning, J., Bouillanne, C., Landon, M., & Desmazeaud, M. J. (1990). Comparison of exocellular polysaccharide production by thermophilic lactic acid bacteria. *Sciences des aliments*, *10*(2), 443-451.

Cerning, J., Bouillanne, C., Landon, M., & Desmazeaud, M. (1992). Isolation and characterization of exopolysaccharides from slime-forming mesophilic lactic acid bacteria. *Journal of Dairy Science*, *75*(3), 692-699.

Cerning, J. C. M. C., Renard, C. M. G. C., Thibault, J. F., Bouillanne, C., Landon, M., Desmazeaud, M., & Topisirovic, L. (1994). Carbon source requirements for exopolysaccharide production by Lactobacillus casei CG11 and partial structure analysis of the polymer. *Appl. Environ. Microbiol.*, *60*(11), 3914-3919.

Cescutti, P. (2009). Bacterial capsular polysaccharides and exopolysaccharides. In *Microbial Glycobiology* (pp. 93-108): Elsevier.

Cipolla, L., Gabrielli, L., Bini, D., Russo, L., & Shaikh, N. (2010). Kdo: a critical monosaccharide for bacteria viability. *Natural product reports*, *27*(11), 1618-1629.

Ciucanu, I., & Kerek, F. (1984). A simple and rapid method for the permethylation of carbohydrates. *Carbohydrate research*, *131*(2), 209-217.

Corradini, C., Cavazza, A., & Bignardi, C. (2012). High-performance anion-exchange chromatography coupled with pulsed electrochemical detection as a powerful tool to evaluate carbohydrates of food interest: principles and applications. *International Journal of Carbohydrate Chemistry*, *2012*.

Corradini, C., Lantano, C., & Cavazza, A. (2013). Innovative analytical tools to characterize prebiotic carbohydrates of functional food interest. *Analytical bioanalytical chemistry, 405*(13), 4591-4605.

Cox, C. P., & BRIGGS, M. (1954). Experiments on growth media for lactobacilli. *Journal of Applied Bacteriology*, *17*(1), 18-26.

Cuesta, G., Suarez, N., Bessio, M. I., Ferreira, F., & Massaldi, H. (2003). Quantitative determination of pneumococcal capsular polysaccharide serotype 14 using a modification of phenol–sulfuric acid method. *Journal of Microbiological Methods*, *52*(1), 69-73.

De Man, J. C., Rogosa, D., & Sharpe, M. E. (1960). A medium for the cultivation of lactobacilli. *Journal of applied Bacteriology*, *23*(1), 130-135.

De Vuyst, L., & De Vin, F. (2007). Exopolysaccharides from lactic acid bacteria.

De Vuyst, L., De Vin, F., Vaningelgem, F., & Degeest, B. (2001). Recent developments in the biosynthesis and applications of heteropolysaccharides from lactic acid bacteria. *International Dairy Journal, 11*(9), 687-707.

De Vuyst, L., & Degeest, B. (1999). Heteropolysaccharides from lactic acid bacteria. *FEMS microbiology reviews*, *23*(2), 153-177.

Denham, W. S., & Woodhouse, H. (1913). CLXXXVI.—The methylation of cellulose. *Journal of the Chemical Society, Transactions*, *103*, 1735-1742.

Dertli, E., Mayer, M. J., Colquhoun, I. J., & Narbad, A. (2016). EpsA is an essential gene in exopolysaccharide production in Lactobacillus johnsonii FI9785. *Microbial biotechnology*, *9*(4), 496-501.

Dertli, E., Toker, O. S., Durak, M. Z., Yilmaz, M. T., Tatlısu, N. B., Sagdic, O., & Cankurt, H. (2016). Development of a fermented ice-cream as influenced by in situ exopolysaccharide production: Rheological, molecular, microstructural and sensory characterization. *Carbohydrate polymers*, *136*, 427-440.

Di, W., Zhang, L., Wang, S., Yi, H., Han, X., Fan, R., & Zhang, Y. (2017). Physicochemical characterization and antitumour activity of exopolysaccharides produced by Lactobacillus casei SB27 from yak milk. *Carbohydrate polymers, 171*, 307-315.

Dilna, S. V., Surya, H., Aswathy, R. G., Varsha, K. K., Sakthikumar, D. N., Pandey, A., & Nampoothiri, K. *M.* (2015). Characterization of an exopolysaccharide with potential health-benefit properties from a probiotic Lactobacillus plantarum RJF4. *LWT-Food Science and Technology*, *64*(2), 1179-1186.

Doco, T., Wieruszeski, J. M., Fournet, B., Carcano, D., Ramos, P., & Loones, A. (1990). Structure of an exocellular polysaccharide produced by Streptococcus thermophilus. *Carbohydrate research*, *198*(2), 313-321.

Döderlein, A. (1892). The vaginal transsudate and its significance for childbed fever. *Centralblatt für bacteriologie*, *11*, 699-700.

Duus, J. Ø., Gotfredsen, C. H., & Bock, K. (2000). Carbohydrate structural determination by NMR spectroscopy: modern methods and limitations. *Chemical Reviews*, *100*(12), 4589-4614.

Ewaschuk, J.B., Diaz, H., Meddings, L., Diederichs, B., Dmytrash, A., Backer, J., Looijer-van Langen, M., & Madsen, K. L. (2008). Secreted bioactive factors from Bifidobacterium infantis enhance epithelial cell barrier function. *American Journal of Physiology-Gastrointestinal and Liver Physiology*, *295*(5), G1025-G1034.

Faber, E. J., Zoon, P., Kamerling, J. P., & Vliegenthart, J. F. (1998). The exopolysaccharides produced by Streptococcus thermophilus Rs and Sts have the same repeating unit but differ in viscosity of their milk cultures. *Carbohydrate research*, *310*(4), 269-276.

Flemming, H. C., Neu, T. R., & Wozniak, D. J. (2007). The EPS matrix: the "house of biofilm cells". *Journal of bacteriology*, *189*(22), 7945-7947.

Freitas, F., Alves, V.D., Pais, J., Costa, N., Oliveira, C., Mafra, L., Hilliou, L., Oliveira, R., & Reis, M. A. (2009). Characterization of an extracellular polysaccharide produced by a Pseudomonas strain grown on glycerol. *Bioresource technology*, *100*(2), 859-865.

Fuller, R. (1989). Probiotics in man and animals. *The Journal of applied bacteriology*, *66*(5), 365-378.

Galle, S., & Arendt, E. K. (2014). Exopolysaccharides from sourdough lactic acid bacteria. *Critical reviews in food science and nutrition, 54*(7), 891-901.

Gancel, F., & Novel, G. (1994). Exopolysaccharide production by Streptococcus salivarius ssp. thermophilus cultures. 1. Conditions of production. *Journal of Dairy Science*, *77*(3), 685-688.

Garcia-Garibay, M., & Marshall, V. M. E. (1991). Polymer production by Lactobacillus delbrueckii ssp. bulgaricus. *Journal of applied bacteriology*, *70*(4), 325-328.

Gerwig, G. J., Dobruchowska, J. M., Shi, T., Urashima, T., Fukuda, K., & Kamerling, J. P. (2013). Structure determination of the exopolysaccharide of Lactobacillus fermentum TDS030603—A revision. *Carbohydrate research*, *378*, 84-90.

Gerwig, G. J., Kamerling, J. P., & Vliegenthart, J. F. (1978). Determination of the D and L configuration of neutral monosaccharides by high-resolution capillary GLC. *Carbohydrate Research, 62*(2), 349-357.

Gibson, G. R., & Roberfroid, M. B. (1995). Dietary modulation of the human colonic microbiota: introducing the concept of prebiotics. *The Journal of nutrition*, *125*(6), 1401-1412.

Górska-Frączek, S., Sandström, C., Kenne, L., Rybka, J., Strus, M., Heczko, P., & Gamian, A. (2011). Structural studies of the exopolysaccharide consisting of a nonasaccharide repeating unit isolated from Lactobacillus rhamnosus KL37B. *Carbohydrate research*, *346*(18), 2926-2932.

Górska, S., Hermanova, P., Ciekot, J., Schwarzer, M., Srutkova, D., Brzozowska, E., Kozakova, H., & Gamian, A. (2016). Chemical characterization and immunomodulatory properties of polysaccharides isolated from probiotic Lactobacillus casei LOCK 0919. *Glycobiology*, *26*(9), 1014-1024.

Grobben, G., Smith, M., Sikkema, J., & De Bont, J. (1996). Influence of fructose and glucose on the production of exopolysaccharides and the activities of enzymes involved in the sugar metabolism and the synthesis of sugar nucleotides in Lactobacillus delbrueckii subsp. bulgaricus NCFB 2772. *46*(3), 279-284.

Grootaert, C., Delcour, J. A., Courtin, C. M., Broekaert, W. F., Verstraete, W., & Van de Wiele, T. (2007). Microbial metabolism and prebiotic potency of arabinoxylan oligosaccharides in the human intestine. *Trends in Food Science & Technology, 18*(2), 64-71.

Gruter, M., Leeflang, B. R., Kuiper, J., Kamerling, J. P., & Vliegenthart, J. F. (1992). Structure of the exopolysaccharide produced by Lactococcus lactis subspecies cremoris H414 grown in a defined medium or skimmed milk. *Carbohydrate research*, *231*, 273-291.

Guo, M. Q., Hu, X., Wang, C., & Ai, L. (2017). Polysaccharides: structure and solubility. In *Solubility of Polysaccharides*: IntechOpen.

Halász, A. (2009). Lactic acid bacteria. *Food Quality and Standards, 3*, 70-82.

Han, X., Yang, Z., Jing, X., Yu, P., Zhang, Y., Yi, H., & Zhang, L. (2016). Improvement of the texture of yogurt by use of exopolysaccharide producing lactic acid bacteria. *BioMed research international*, *2016*.

Harding, L. P., Marshall, V. M., Hernandez, Y., Gu, Y., Maqsood, M., McLay, N., & Laws, A. P. (2005). Structural characterisation of a highly branched exopolysaccharide produced by Lactobacillus delbrueckii subsp. bulgaricus NCFB2074. *Carbohydrate research*, *340*(6), 1107-1111.

Hardy, H., Harris, J., Lyon, E., Beal, J., & Foey, A. D. (2013). Probiotics, prebiotics and immunomodulation of gut mucosal defences: homeostasis and immunopathology. *Nutrients, 5*(6), 1869-1912.

Hasler, C. M. (1998). Functional foods: their role in disease prevention and health promotion. *FOOD TECHNOLOGY-CHAMPAIGN THEN CHICAGO-*, *52*, 63-147.

Hassan, A. N. (2008). ADSA Foundation Scholar Award: Possibilities and challenges of exopolysaccharide-producing lactic cultures in dairy foods. *Journal of Dairy Science*, *91*(4), 1282-1298.

Hatzakis, E. (2019). Nuclear Magnetic Resonance (NMR) Spectroscopy in Food Science: A Comprehensive Review. *Comprehensive Reviews in Food Science Food Safety, 18*(1), 189-220.

Haworth, W. N. (1915). III.—A new method of preparing alkylated sugars. *Journal of the Chemical Society, Transactions*, *107*, 8-16.

Heritage, J., Evans, E. G. V., & Killington, R. (1996). *Introductory microbiology*: Cambridge University Press.

Hidalgo-Cantabrana, C., López, P., Gueimonde, M., Clara, G., Suárez, A., Margolles, A., & Ruas-Madiedo, P. (2012). Immune modulation capability of exopolysaccharides synthesised by lactic acid bacteria and bifidobacteria. *Probiotics and Antimicrobial Proteins*, *4*(4), 227-237.

Hidalgo-Cantabrana, C., Sánchez, B., Milani, C., Ventura, M., Margolles, A., & Ruas-Madiedo, P. (2014). Genomic overview and biological functions of exopolysaccharide biosynthesis in Bifidobacterium spp. *Appl. Environ. Microbiol.*, *80*(1), 9-18.

Hilmi, H. T. A., Surakka, A., Apajalahti, J., & Saris, P. E. (2007). Identification of the most abundant Lactobacillus species in the crop of 1-and 5-week-old broiler chickens. *Applied and environmental microbiology, 73*(24), 7867-7873.

Hirsch, A., & Grinsted, E. (1954). 543. Methods for the growth and enumeration of anaerobic spore-formers from cheese, with observations on the effect of nisin. *Journal of Dairy Research*, *21*(1), 101-110.

Hogg, S. (2013). *Essential microbiology*: John Wiley & Sons.

Holzapfel, W. H., Haberer, P., Geisen, R., Björkroth, J., & Schillinger, U. (2001). Taxonomy and important features of probiotic microorganisms in food and nutrition. *The American journal of clinical nutrition*, *73*(2), 365s-373s.

Horn, N., Wegmann, U., Dertli, E., Mulholland, F., Collins, S.R., Waldron, K.W., Bongaerts, R.J., Mayer, M.J., & Narbad, A. (2013). Spontaneous mutation reveals influence of exopolysaccharide on Lactobacillus johnsonii surface characteristics. *PloS one*, *8*(3), e59957.

Hutkins, R.W., Krumbeck, J.A., Bindels, L.B., Cani, P.D., Fahey Jr, G., Goh, Y.J., Hamaker, B., Martens, E.C., Mills, D.A., Rastal, R.A., & Vaughan, E. (2016). Prebiotics: why definitions matter. *Current opinion in biotechnology*, *37*, 1-7.

Johnson-Henry, K. C., Donato, K. A., Shen-Tu, G., Gordanpour, M., & Sherman, P. M. (2008). Lactobacillus rhamnosus strain GG prevents enterohemorrhagic Escherichia coli O157: H7-induced changes in epithelial barrier function. *Infection and immunity*, *76*(4), 1340-1348.

Jolly, L., Vincent, S. J., Duboc, P., & Neeser, J.-R. (2002). Exploiting exopolysaccharides from lactic acid bacteria. In *Lactic Acid Bacteria: Genetics, Metabolism and Applications* (pp. 367-374): Springer.

Kimmel, S. A., & Roberts, R. F. (1998). Development of a growth medium suitable for exopolysaccharide production by Lactobacillus delbrueckii ssp. bulgaricus RR. *International journal of food microbiology*, *40*(1-2), 87-92.

Klosterman, H., & Smith, F. (1952). Threitan and Erythritan and their Reaction with Periodate1. *Journal of the American Chemical Society*, *74*(21), 5336-5339.

Knapp, D. R. (1979). *Handbook of analytical derivatization reactions*. John Wiley & Sons.

Kranenburg, R. V., Marugg, J. D., Van Swam, I. I., Willem, N. J., & De Vos, W. M. (1997). Molecular characterization of the plasmid-encoded eps gene cluster essential for exopolysaccharide biosynthesis in Lactococcus lactis. *Molecular microbiology*, *24*(2), 387-397.

Landersjö, C., Yang, Z., Huttunen, E., & Widmalm, G. J. B. (2002). Structural Studies of the Exopolysaccharide Produced by Lactobacillus r hamnosus strain GG (ATCC 53103). *3*(4), 880-884.

Lee, J.H., Valeriano, V.D., Shin, Y.R., Chae, J.P., Kim, G.B., Ham, J.S., Chun, J., & Kang, D. K. (2012). Genome sequence of Lactobacillus mucosae LM1, isolated from piglet feces.

Lemoine, J., Chirat, F., Wieruszeski, J. M., Strecker, G., Favre, N., & Neeser, J. R. (1997). Structural characterization of the exocellular polysaccharides produced by Streptococcus thermophilus SFi39 and SFi12. *Appl. Environ. Microbiol.*, *63*(9), 3512-3518.

Lilly, D. M., & Stillwell, R. H. (1965). Probiotics: growth-promoting factors produced by microorganisms. *Science*, *147*(3659), 747-748.

Liu, D., Cole, R. A., & Reeves, P. R. (1996). An O-antigen processing function for Wzx (RfbX): a promising candidate for O-unit flippase. *Journal of bacteriology, 178*(7), 2102-2107.

London, L. E. E., Price, N. P. J., Ryan, P., Wang, L., Auty, M. A. E., Fitzgerald, G. F., ... & Ross, R. P. (2014). Characterization of a bovine isolate L actobacillus mucosae DPC 6426 which produces an exopolysaccharide composed predominantly of mannose residues. *Journal of applied microbiology*, *117*(2), 509-517.

Looijesteijn, P. J., Boels, I. C., Kleerebezem, M., & Hugenholtz, J. (1999). Regulation of Exopolysaccharide Production byLactococcus lactis subsp. cremoris by the Sugar Source. *Appl. Environ. Microbiol.*, *65*(11), 5003-5008.

Looijesteijn, P. J., Van Casteren, W. H., Tuinier, R., Doeswijk-Voragen, C. H. L., & Hugenholtz, J. (2000). Influence of different substrate limitations on the yield, composition and molecular mass of exopolysaccharides produced by Lactococcus lactis subsp. cremoris in continuous cultures. *Journal of Applied Microbiology*, *89*(1), 116-122.

Lynch, K. M., Zannini, E., Coffey, A., & Arendt, E. K. (2018). Lactic acid bacteria exopolysaccharides in foods and beverages: isolation, properties, characterization, and health benefits. *Annual review of food science and technology*, *9*, 155-176.

MacFaddin, J. J. V. I. W., & Wilkins, B. (1985). Media for Isolation-Identification-Cultivation-Maintenance of Medical Bacteria.

Madigan, M. T., Clark, D. P., Stahl, D., & Martinko, J. M. (2010). *Brock Biology of Microorganisms 13th edition*: Benjamin Cummings.

Madigan, M. T., Martinko, J. M., & Parker, J. (2017). *Brock biology of microorganisms* (Vol. 13): Pearson.

Maheshwari, G., Sowrirajan, S., & Joseph, B. (2019). β-Glucan, a dietary fiber in effective prevention of lifestyle diseases–An insight. *Bioactive Carbohydrates and Dietary Fibre*, 100187.

Margaritis, A., Pace, G., Blanch, H., Drewand, S., & Wang, D. (1985). Comprehensive Biotechnology. *J. Pergamon, 3*, 1005-1013.

Marshall, R. T. (1992). Standard methods for the examination of dairy products.

Marshall, V. M., Cowie, E. N., & Moreton, R. S. (1995). Analysis and production of two exopolysaccharides from Lactococcus lactis subsp. cremoris LC330. *Journal of Dairy Research*, *62*(4), 621-628.

Marshall, V. M., Dunn, H., Elvin, M., McLay, N., Gu, Y., & Laws, A. P. (2001). Structural characterisation of the exopolysaccharide produced by Streptococcus thermophilus EU20. *Carbohydrate research*, *331*(4), 413-422.

Martín, R., Jiménez, E., Olivares, M., Marín, M., Fernández, L., Xaus, J., & Rodríguez, J. (2006). Lactobacillus salivarius CECT 5713, a potential probiotic strain isolated from infant feces and breast milk of a mother–child pair. *International journal of food microbiology, 112*(1), 35-43.

Masuko, T., Minami, A., Iwasaki, N., Majima, T., Nishimura, S. I., & Lee, Y. C. (2005). Carbohydrate analysis by a phenol–sulfuric acid method in microplate format. *Analytical biochemistry*, *339*(1), 69-72.

Matias, V. R., & Beveridge, T. J. J. J. o. b. (2006). Native cell wall organization shown by cryo-electron microscopy confirms the existence of a periplasmic space in Staphylococcus aureus. *188*(3), 1011-1021.

McFaddin, J. F. (1985). *Media for isolation-cultivation-identification maintenance of medical bacteria*: Williams & Wilkins.

McGinnis, G. D., & Biermann, C. J. (1989). *Analysis of monosaccharides as per-O-acetylated aldononitrile (PAAN) derivatives by gas–liquid chromatography (GLC)*: CRC Press, Boca Raton, FL.

Mercan, E., İspirli, H., Sert, D., Yılmaz, M. T., & Dertli, E. (2015). Impact of exopolysaccharide production on functional properties of some Lactobacillus salivarius strains. *Archives of microbiology*, *197*(9), 1041-1049.

Metchnikoff, E., & Metchnikoff, I. (1908). The Prolongation of Life, GP Putnam's Sons. *New York, NY*, 234-301.

Mishra, A., & Jha, B. (2013). Microbial exopolysaccharides. In *The Prokaryotes* (pp. 179-192): Springer.

Mould, D. L., & Synge, R. L. M. (1954). Separations of polysaccharides related to starch by electrokinetic ultrafiltration in collodion membranes. *Biochemical journal*, *58*(4), 571.

Mozzi, F., Vaningelgem, F., Hébert, E. M., Van der Meulen, R., Moreno, M. R. F., de Valdez, G. F., & De Vuyst, L. (2006). Diversity of heteropolysaccharide-producing lactic acid bacterium strains and their biopolymers. *Applied and environmental microbiology, 72*(6), 4431-4435.

Mussatto, S. I., & Mancilha, I. M. (2007). Non-digestible oligosaccharides: a review. *Carbohydrate polymers*, *68*(3), 587-597.

Nagaoka, M., Hashimoto, S., Shibata, H., Kimura, I., Kimura, K., Sawada, H., & Yokokura, T. (1996). Structure of a galactan from cell walls of Bifidobacterium catenulatum YIT4016. *Carbohydrate research*, *281*(2), 285-291.

Neeser, J. R., & Schweizer, T. F. (1984). A quantitative determination by capillary gas-liquid chromatography of neutral and amino sugars (as O-methyloxime acetates), and a study on hydrolytic conditions for glycoproteins and polysaccharides in order to increase sugar recoveries. *Analytical biochemistry*, *142*(1), 58-67.

Neville, B., & O'Toole, P. (2010). Probiotic properties of Lactobacillus salivarius and closely related Lactobacillus species. *Future Microbiology, 5*(5), 759-774.

Nichols, C. M., Lardière, S. G., Bowman, J. P., Nichols, P. D., Gibson, J. A., & Guézennec, J. (2005). Chemical characterization of exopolysaccharides from Antarctic marine bacteria. *Microbial ecology*, *49*(4), 578-589.

Nikolic, M., López, P., Strahinic, I., Suárez, A., Kojic, M., Fernández-García, M., Topisirovic, L., Golic, N., & Ruas-Madiedo, P. (2012). Characterisation of the exopolysaccharide (EPS)-producing Lactobacillus paraplantarum BGCG11 and its non-EPS producing derivative strains as potential probiotics. *International journal of food microbiology*, *158*(2), 155-162.

Pallach, M., Di Lorenzo, F., Facchini, F.A., Gully, D., Giraud, E., Peri, F., Duda, K.A., Molinaro, A., & Silipo, A. (2018). Structure and inflammatory activity of the LPS isolated from Acetobacter pasteurianus CIP103108. *International journal of biological macromolecules*, *119*, 1027-1035.

Patel, R., & DuPont, H. L. (2015). New approaches for bacteriotherapy: prebiotics, new-generation probiotics, and synbiotics. *Clinical Infectious Diseases, 60*(suppl_2), S108-S121.

Patten, D., & Laws, A. P. (2015). Lactobacillus-produced exopolysaccharides and their potential health benefits: a review. *Beneficial microbes, 6*(4), 457-471.

Pool-Zobel, B. L., & Sauer, J. (2007). Overview of experimental data on reduction of colorectal cancer risk by inulin-type fructans. *The Journal of nutrition*, *137*(11), 2580S-2584S.

Postgate, J. (2000). *Microbes and man*: Cambridge University Press.

Poxton, I. R. (2015). Teichoic Acids, Lipoteichoic Acids and Other Secondary Cell Wall and Membrane Polysaccharides of Gram-Positive Bacteria. In *Molecular Medical Microbiology* (pp. 91-103): Elsevier.

Prechtl, R. M., Wefers, D., Jakob, F., & Vogel, R. F. (2018). Cold and salt stress modulate amount, molecular and macromolecular structure of a Lactobacillus sakei dextran. *Food Hydrocolloids*, *82*, 73-81.

Purdie, T., & Irvine, J. C. (1903). C.—The alkylation of sugars. *Journal of the Chemical Society, Transactions*, *83*, 1021-1037.

Raftis, E. J., Salvetti, E., Torriani, S., Felis, G. E., & O'Toole, P. W. (2011). Genomic diversity of Lactobacillus salivarius. *Applied and environmental microbiology, 77*(3), 954-965.

Roberfroid, M., Gibson, G.R., Hoyles, L., McCartney, A.L., Rastall, R., Rowland, I., Wolvers, D., Watzl, B., Szajewska, H., Stahl, B., & Guarner, F. (2010). Prebiotic effects: metabolic and health benefits. *British Journal of Nutrition*, *104*(S2), S1-S63.

Robijn, G. W., Gallego, R. G., van den Berg, D. J., Haas, H., Kamerling, J. P., & Vliegenthart, J. F. (1996). Structural characterization of the exopolysaccharide produced by Lactobacillus acidophilus LMG9433. *Carbohydrate Research, 288*, 203-218.

Rocklin, R. D., & Pohl, C. A. (1983). Determination of carbohydrates by anion exchange chromatography with pulsed amperometric detection. *Journal of Liquid Chromatography*, *6*(9), 1577-1590.

Rogosa, M., Wiseman, R. F., Mitchell, J. A., Disraely, M. N., & Beaman, A. J. (1953). Species differentiation of oral lactobacilli from man including descriptions of Lactobacillus salivarius nov spec and Lactobacillus cellobiosus nov spec. *Journal of Bacteriology*, *65*(6), 681.

Roos, S., Karner, F., Axelsson, L., & Jonsson, H. (2000). Lactobacillus mucosae sp. nov., a new species with in vitro mucus-binding activity isolated from pig intestine. *International Journal of Systematic and Evolutionary Microbiology*, *50*(1), 251-258.

Roseman, S. (1972). Carbohydrate transport in bacterial cells. In *Metabolic transport* (pp. 41-89): Elsevier.

Ruas-Madiedo, P., & De Los Reyes-Gavilán, C. G. (2005). Invited review: methods for the screening, isolation, and characterization of exopolysaccharides produced by lactic acid bacteria. *Journal of dairy science*, *88*(3), 843-856.

Ruas-Madiedo, P., Gueimonde, M., Margolles, A., de los REYES-GAVILÁN, C. G., & Salminen, S. (2006). Exopolysaccharides produced by probiotic strains modify the adhesion of probiotics and enteropathogens to human intestinal mucus. *Journal of food protection*, *69*(8), 2011-2015.

Ruas-Madiedo, P., Hugenholtz, J., & Zoon, P. (2002). An overview of the functionality of exopolysaccharides produced by lactic acid bacteria. *International Dairy Journal*, *12*(2-3), 163-171.

Ruas-Madiedo, P., Salazar, N., & Clara, G. (2009). *Biosynthesis and chemical composition of exopolysaccharides* (p. 279). Norfolk: Caister Academic Press.

Russo, P., López, P., Capozzi, V., De Palencia, P. F., Dueñas, M. T., Spano, G., & Fiocco, D. (2012). Beta-glucans improve growth, viability and colonization of probiotic microorganisms. *International journal of molecular sciences*, *13*(5), 6026-6039.

Ryan, P., Ross, R., Fitzgerald, G., Caplice, N., & Stanton, C. (2015). Sugar-coated: exopolysaccharide producing lactic acid bacteria for food and human health applications. *Food & function, 6*(3), 679-693.

Ryan, P.M., Stolte, E.H., London, L.E., Wells, J.M., Long, S.L., Joyce, S.A., Gahan, C.G., Fitzgerald, G.F., Ross, R.P., Caplice, N.M., & Stanton, C. (2019). Lactobacillus mucosae DPC 6426 as a bile-modifying and immunomodulatory microbe. *BMC microbiology*, *19*(1), 33.

Salazar, N., Gueimonde, M., de los Reyes-Gavilan, C. G., & Ruas-Madiedo, P. (2016). Exopolysaccharides produced by lactic acid bacteria and bifidobacteria as fermentable substrates by the intestinal microbiota. *Critical reviews in food science nutrition, 56*(9), 1440-1453.

Salminen, S., & Von Wright, A. (2004). *Lactic acid bacteria: microbiological and functional aspects*: CRC Press.

Sampath, V. (2018). Bacterial endotoxin-Lipopolysaccharide; structure, function and its role in immunity in vertebrates and invertebrates. *Agriculture Natural Resources*.

Sanchez-Muñoz, F., Dominguez-Lopez, A., & Yamamoto-Furusho, J. K. (2008). Role of cytokines in inflammatory bowel disease. *World journal of gastroenterology: WJG*, *14*(27), 4280.

Sarkar, A., & Mandal, S. (2016). Bifidobacteria—Insight into clinical outcomes and mechanisms of its probiotic action. *Microbiological research, 192*, 159-171.

Sartor, R. B. J. G. (2008). Microbial influences in inflammatory bowel diseases. *134*(2), 577-594.

Sasaki, T., Abiko, N., Sugino, Y., & Nitta, K. (1978). Dependence on chain length of antitumor activity of (1→ 3)-β-D-glucan from Alcaligenes faecalis var. myxogenes, IFO 13140, and its acid-degraded products. *Cancer research*, *38*(2), 379-383.

Sasikumar, K., Vaikkath, D. K., Devendra, L., & Nampoothiri, K. M. (2017). An exopolysaccharide (EPS) from a Lactobacillus plantarum BR2 with potential benefits for making functional foods. *Bioresource technology*, *241*, 1152-1156.

Saulnier, D. M., Spinler, J. K., Gibson, G. R., & Versalovic, J. (2009). Mechanisms of probiosis and prebiosis: considerations for enhanced functional foods. *Current opinion in biotechnology*, *20*(2), 135-141..

Schaechter, M., Ingraham, J. L., & Neidhardt, F. C. (2006). *Microbe*: ASM press.

Schmid, J., Sieber, V., & Rehm, B. (2015). Bacterial exopolysaccharides: biosynthesis pathways and engineering strategies. *Frontiers in microbiology*, *6*, 496.

Spinler, J. K., Taweechotipatr, M., Rognerud, C. L., Ou, C. N., Tumwasorn, S., & Versalovic, J. (2008). Human-derived probiotic Lactobacillus reuteri demonstrate antimicrobial activities targeting diverse enteric bacterial pathogens. *Anaerobe*, *14*(3), 166-171.

Stack, H. M., Kearney, N., Stanton, C., Fitzgerald, G. F., & Ross, R. P. (2010). Association of beta-glucan endogenous production with increased stress tolerance of intestinal lactobacilli. *Appl. Environ. Microbiol.*, *76*(2), 500-507.

Stearns-Kurosawa, D. J., Osuchowski, M. F., Valentine, C., Kurosawa, S., & Remick, D. G. (2011). The pathogenesis of sepsis. *Annual review of pathology: mechanisms of disease*, *6*, 19-48.

Stingele, F., Neeser, J. R., & Mollet, B. (1996). Identification and characterization of the eps (Exopolysaccharide) gene cluster from Streptococcus thermophilus Sfi6. *Journal of bacteriology*, *178*(6), 1680-1690.

Svensson, M. V., Zhang, X., Huttunen, E., & Widmalm, G. (2011). Structural studies of the capsular polysaccharide produced by Leuconostoc mesenteroides ssp. cremoris PIA2. *Biomacromolecules*, *12*(7), 2496-2501.

Swinbanks, D., & O'Brien, J. (1993). Japan explores the boundary between food and medicine. *Nature*, *364*(6434), 180-180.

Tallon, R., Bressollier, P., & Urdaci, M. C. (2003). Isolation and characterization of two exopolysaccharides produced by Lactobacillus plantarum EP56. *Research in Microbiology*, *154*(10), 705-712.

Tannock, G. W. (2005). New perceptions of the gut microbiota: implications for future research. *Gastroenterology Clinics, 34*(3), 361-382.

Tieking, M., Kaditzky, S., Valcheva, R., Korakli, M., Vogel, R. F., & Gänzle, M. G. (2005). Extracellular homopolysaccharides and oligosaccharides from intestinal lactobacilli. *Journal of applied microbiology*, *99*(3), 692-702.

Todar, K. (2006). Todar's online textbook of bacteriology. In: University of Wisconsin-Madison Department of Bacteriology Madison, Wis, USA.

Torino, M. I., Font de Valdez, G., & Mozzi, F. (2015). Biopolymers from lactic acid bacteria. Novel applications in foods and beverages. *Frontiers in microbiology, 6*, 834.

Valeriano, V. D. V., Oh, J. K., Bagon, B. B., Kim, H., & Kang, D. K. (2017). Comparative genomic analysis of Lactobacillus mucosae LM1 identifies potential niche-specific genes and pathways for gastrointestinal adaptation. *Genomics*.

Van Calsteren, M. R., Gagnon, F., Nishimura, J., & Makino, S. (2015). Structure determination of the neutral exopolysaccharide produced by Lactobacillus delbrueckii subsp. bulgaricus OLL1073R-1. *Carbohydrate research*, *413*, 115-122.

Van Geel-Schutten, G.H., Faber, E.J., Smit, E., Bonting, K., Smith, M.R., Ten Brink, B., Kamerling, J.P., Vliegenthart, J.F.G., & Dijkhuizen, L. (1999). Biochemical and Structural Characterization of the Glucan and Fructan Exopolysaccharides Synthesized by theLactobacillus reuteri Wild-Type Strain and by Mutant Strains. *Appl. Environ. Microbiol.*, *65*(7), 3008-3014.

van Hijum, S. A., Kralj, S., Ozimek, L. K., Dijkhuizen, L., & van Geel-Schutten, I. G. (2006). Structure-function relationships of glucansucrase and fructansucrase enzymes from lactic acid bacteria. *Microbiology and Molecular Biology Reviews, 70*(1), 157-176.

Vergin, F. (1954). Antibiotics and probiotics. *Hippokrates*, *25*(4), 116-119.

Vinogradov, E., Valence, F., Maes, E., Jebava, I., Chuat, V., Lortal, S., Grard, T., Guerardel, Y., & Sadovskaya, I. (2013). Structural studies of the cell wall polysaccharides from three strains of Lactobacillus helveticus with different autolytic properties: DPC4571, BROI, and LH1. *Carbohydrate research*, *379*, 7-12.

Vitlic, A., Sadiq, S., Ahmed, H.I., Ale, E.C., Binetti, A.G., Collett, A., Humpreys, P.N., & Laws, A. P. (2019). Isolation and characterization of a high molecular mass β-glucan from Lactobacillus fermentum Lf2 and evaluation of its immunomodulatory activity. *Carbohydrate research*, *476*, 44-52.

Wefers, D., Tyl, C. E., & Bunzel, M. (2014). Novel arabinan and galactan oligosaccharides from dicotyledonous plants. *Frontiers in chemistry*, *2*, 100.

Welman, A. D., & Maddox, I. S. (2003). Exopolysaccharides from lactic acid bacteria: perspectives and challenges. *Trends in biotechnology*, *21*(6), 269-274.

Whitfield, C. (1988). Bacterial extracellular polysaccharides. *Canadian Journal of Microbiology, 34*(4), 415-420.

Wyatt, P. J. (1993). Light scattering and the absolute characterization of macromolecules. *Analytica chimica acta*, *272*(1), 1-40.

Xu, Y., Cui, Y., Yue, F., Liu, L., Shan, Y., Liu, B., Zhou, Y., & Lü, X. (2019). Exopolysaccharides produced by lactic acid bacteria and Bifidobacteria: Structures, physiochemical functions and applications in the food industry. *Food hydrocolloids*.

Yadav, V., Prappulla, S. G., Jha, A., & Poonia, A. (2011). A novel exopolysaccharide from probiotic Lactobacillus fermentum CFR 2195: Production, purification and characterization. *Biotechnol Bioinf Bioeng, 1*, 415-421.

Yamamoto, Y., Harashima, A., Saito, H., Tsuneyama, K., Munesue, S., Motoyoshi, S., Han, D., Watanabe, T., Asano, M., Takasawa, S., & Okamoto, H. (2011). Septic shock is associated with receptor for advanced glycation end products ligation of LPS. *The Journal of Immunology*, *186*(5), 3248-3257.

Yasuda, E., Serata, M., & Sako, T. (2008). Suppressive effect on activation of macrophages by Lactobacillus casei strain Shirota genes determining the synthesis of cell wall-associated polysaccharides. *Appl. Environ. Microbiol.*, *74*(15), 4746-4755.

Yilmaz, M., Celik, G. Y., Aslim, B., & Onbasili, D. (2012). Influence of carbon sources on the production and characterization of the exopolysaccharide (EPS) by Bacillus sphaericus 7055 Strain. *20*(1), 152-156.

Yuksekdag, Z. N., & Aslim, B. (2008). Influence of different carbon sources on exopolysaccharide production by Lactobacillus delbrueckii subsp. bulgaricus (B3, G12) and Streptococcus thermophilus (W22). *Brazilian archives of Biology and Technology*, *51*(3), 581-585.

Zeidan, A. A., Poulsen, V. K., Janzen, T., Buldo, P., Derkx, P. M., Øregaard, G., & Neves, A. R. (2017). Polysaccharide production by lactic acid bacteria: from genes to industrial applications. *FEMS microbiology reviews, 41*(Supp_1), S168-S200.

Zhang, Y. U., Li, S., Zhang, C., Luo, Y., Zhang, H., & Yang, Z. (2011). Growth and exopolysaccharide production by Lactobacillus fermentum F6 in skim milk. *African Journal of Biotechnology*, *10*(11), 2080-2091.

Zhou, Y., Cui, Y., & Qu, X. (2018). Exopolysaccharides of lactic acid bacteria: Structure, bioactivity and associations: A review. *Carbohydrate polymers*.

9 Publications

1. Laws, A., Vitlic, A., Sadiq, S., **Ahmed, H.I**., Ale, E.C., Binetti, A.G., Collett, A., & Humphreys, P., (2018). Evidence for the Modulation of the Immune Response in Peripheral Blood Mononuclear Cells after Stimulation with a High Molecular Weight β-glucan Isolated from *Lactobacillus fermentum* Lf2. *bioRxiv*, 400267.
2. Vitlic, A., Sadiq, S., **Ahmed, H.I**., Ale, E.C., Binetti, A.G., Collett, A., Humpreys, P.N., & Laws, A.P., (2019). Isolation and characterization of a high molecular mass β-glucan from *Lactobacillus fermentum* Lf2 and evaluation of its immunomodulatory activity. *Carbohydrate research*, *476*, 44-52.
3. Ale, E.C., Batistela, V.A., Correa Olivar, G., Ferrado, J.B., Sadiq, S., **Ahmed, H.I**., Reinheimer, J.A., Vera-Candioti, L., Laws, A.P., & Binetti, A.G., (2019). Statistical optimisation of the exopolysaccharide production by *Lactobacillus fermentum* Lf2 and analysis of its chemical composition. *International Journal of Dairy Technology*.
4. Fagunwa, O., **Ahmed, H. I**., Sadiq, S., Humphreys, P. N., McLay, N., & Laws, A. P. (2019). Isolation and characterization of a novel exopolysaccharide secreted by *Lactobacillus mucosae* VG1. *Carbohydrate research*, *484*, 107781.

Submitted:

5. **Ahmed, H.I**., Ramson-Jones, E., Sadiq, S., Vitlic, A., McLay, N., Rojas, M.F., Ale, E.C., Binetti, A.G., Collett, A., Humpreys, P.N., & Laws, A.P., (2019). Structural characterisation of two medium molecular mass exopolysaccharides produced by the bacterium *Lactobacillus fermentum* Lf2. *Carbohydrate research*, *478*.

Appendices

Appendix 1: Selected regions of $^{13}C,^{1}H$-HSQC-TOCSY (black contours) superimposed on top of an $^{13}C,^{1}H$-ed-HSQC (Red contours = CH; Magenta contours =CH_2) spectrum for *L. fermentum* Lf2 SD-MMMP recorded at 70 ^{o}C on a Bruker 600 MHz spectrometer; labels (**A-E & A',C'**) identify the different monosaccharides and the numbers (**1-6**) identify the respective protons/carbons. Red labels (A-E & A',C'; 1-6) identify overlap of HSQC and HSQC-TOCSY signals. Imp=impurity; mainly spectral noise and often not correlated to either a carbon or hydrogen.

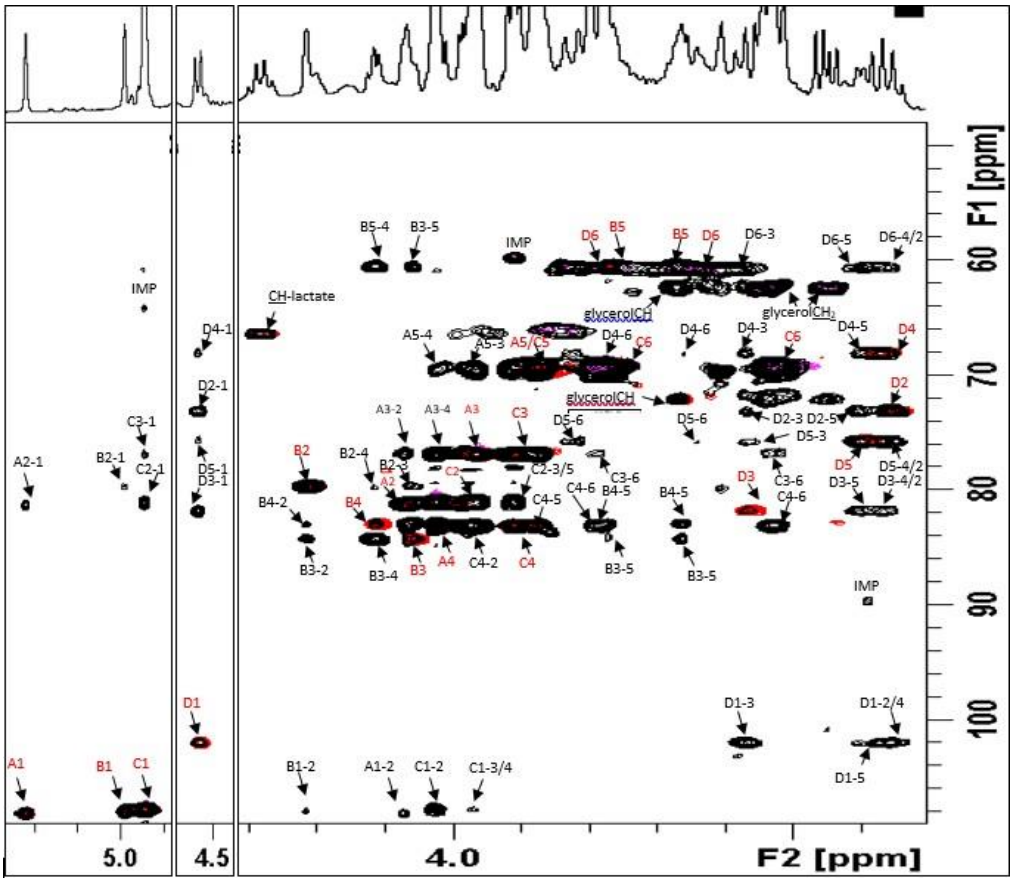

Appendix 2: Selected regions of $^{13}C,^{1}H$-HSQC-TOCSY (black contours) superimposed on top of an $^{13}C,^{1}H$-ed-HSQC (Red contours = CH; Magenta contours =CH_2) spectrum for *L. fermentum* Lf2 MMMP recorded at 70 ^{o}C on a Bruker 600 MHz spectrometer; labels (**A-E & A',C'**) identify the different monosaccharides and the numbers (**1-6**) identify the respective protons/carbons. Red labels (A-E & A',C'; 1-6) identify overlap of HSQC and HSQC-TOCSY signals. Imp=impurity; mainly spectral noise and often not correlated to either a carbon or hydrogen

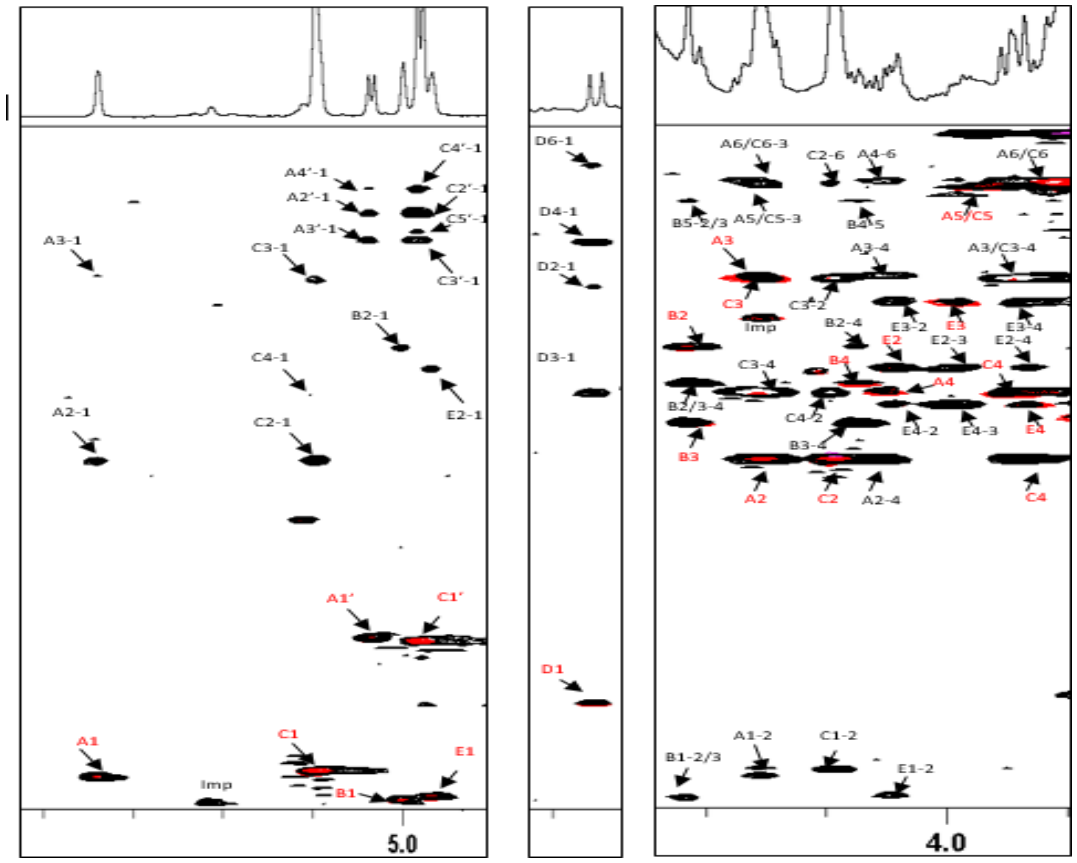

Appendix 3: ^{1}H-NMR spectra of starch

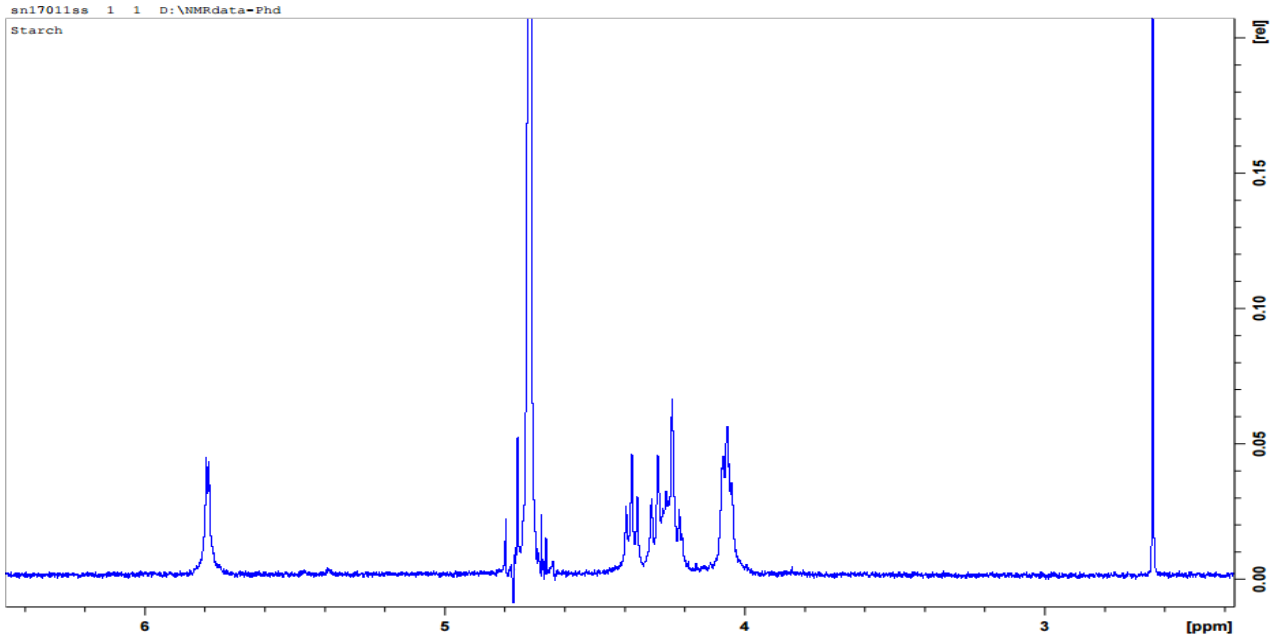

Appendix 4: GC trace of the monomer analysis performed on capsular polysaccharide synthesised by *L salivarius* 702343.

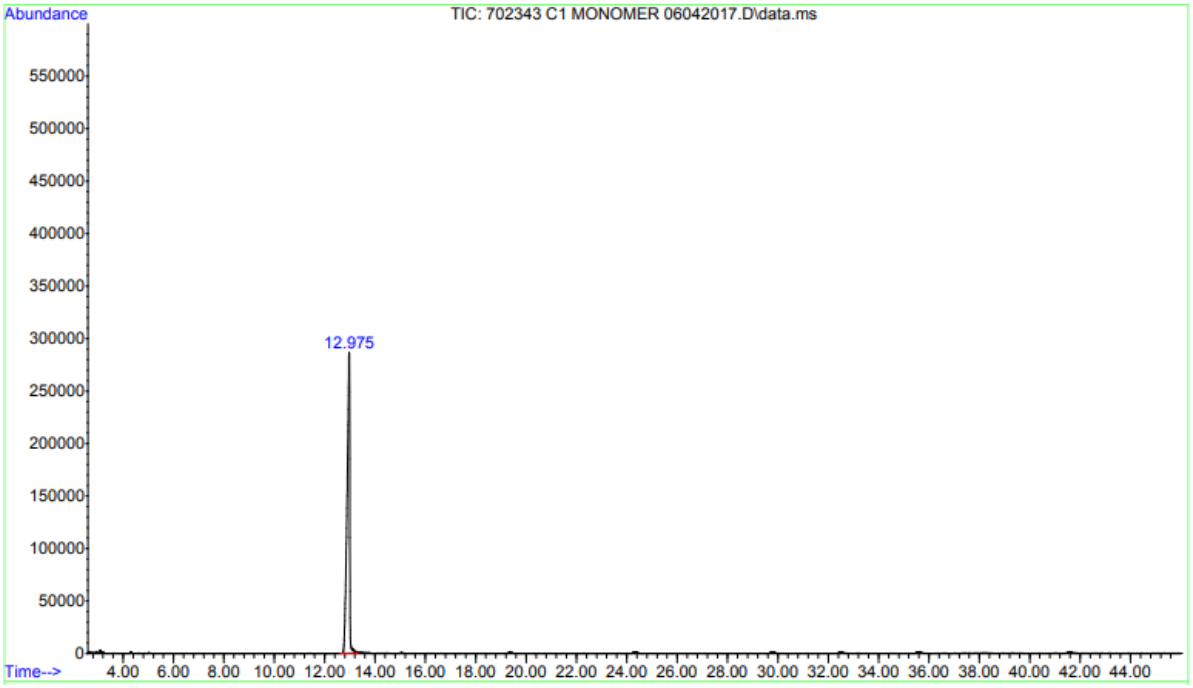

Appendix 5: GC trace and MS fragmentation pattern of the linkage analysis performed on capsular polysaccharide synthesised by *L salivarius* 702343.

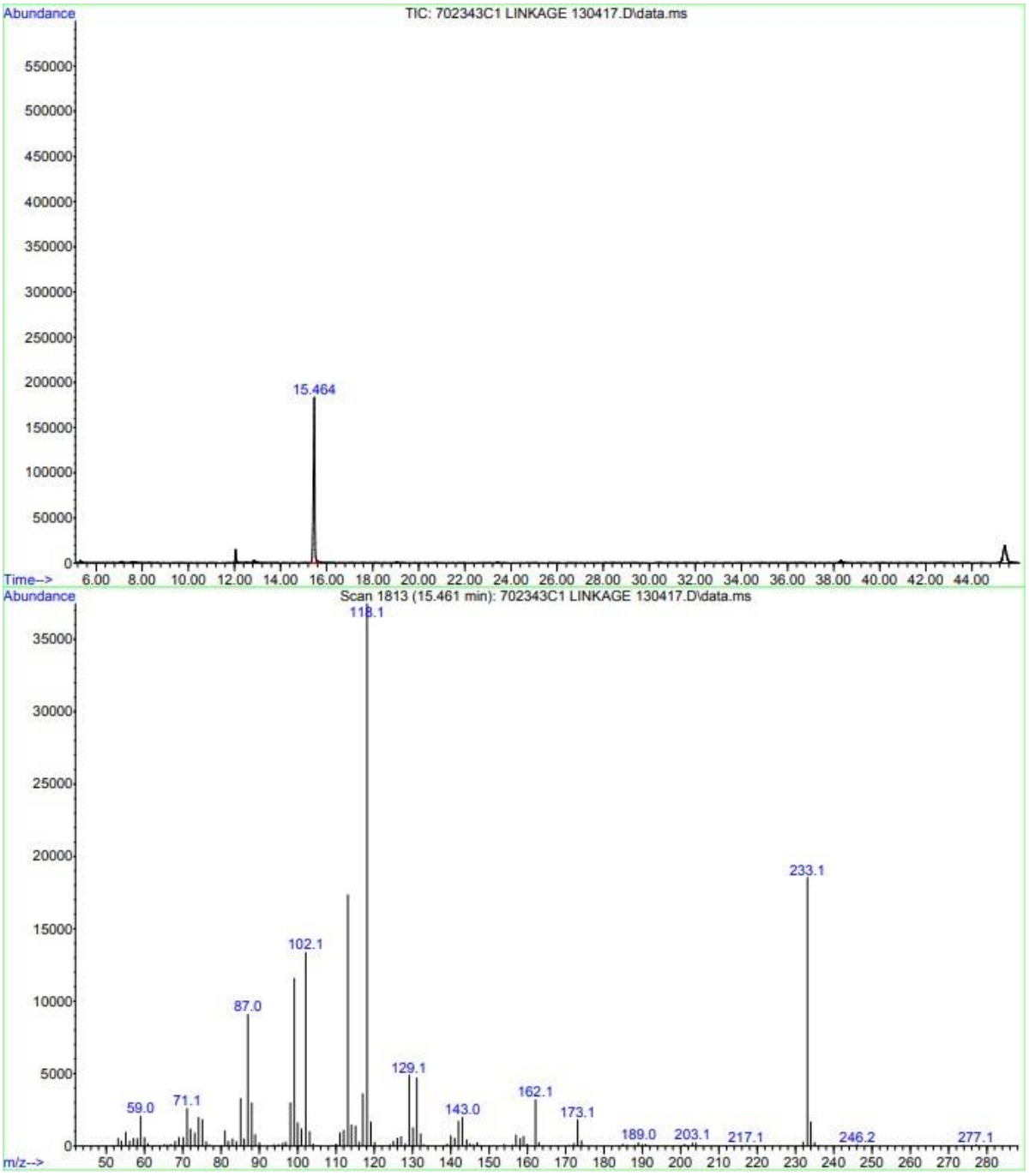

Appendix 6: GC trace of the absolute configuration analysis performed on capsular polysaccharide synthesised by *L salivarius* 702343.

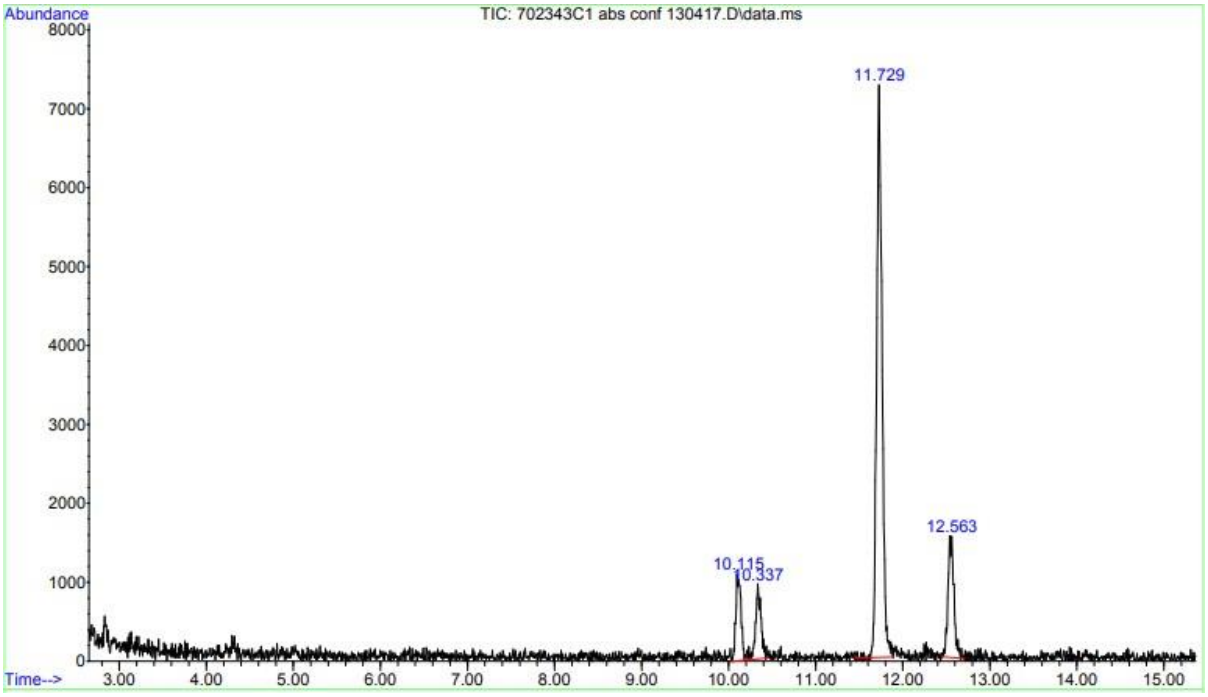

Appendix 7: EPS yield of *L fermentum* LF2 grown in HBM for 72 h under different conditions (Ale *et al*., 2016).

Media	Volume (mL)	Carbon source	Temperature (°C)	pH	Fermentation time (h)	~EPS yield (mg)
SDM	1000	Glucose	37	Uncontrolled	72	85.0
SDM	1000	Glucose	30	Uncontrolled	72	265.0
SDM	1000	Glucose	37	6.0	72	112.3

Appendix 8: Monosaccharide symbol nomenclature
(https://www.ncbi.nlm.nih.gov/glycans/snfg.html)

SHAPE	White (Generic)	Blue	Green	Yellow	Orange	Pink	Purple	Light Blue	Brown	Red
Filled Circle	Hexose	Glc	Man	Gal	Gul	Alt	All	Tal	Ido	
Filled Square	HexNAc	GlcNAc	ManNAc	GalNAc	GulNAc	AltNAc	AllNAc	TalNAc	IdoNAc	
Crossed Square	Hexosamine	GlcN	ManN	GalN	GulN	AltN	AllN	TalN	IdoN	
Divided Diamond	Hexuronate	GlcA	ManA	GalA	GulA	AltA	AllA	TalA	IdoA	
Filled Triangle	Deoxyhexose	Qui	Rha		6dGul	6dAlt		6dTal		Fuc
Divided Triangle	DeoxyhexNAc	QuiNAc	RhaNAc			6dAltNAc		6dTalNAc		FucNAc
Flat Rectangle	Di-deoxyhexose	Oli	Tyv		Abe	Par	Dig	Col		
Filled Star	Pentose		Ara	Lyx	Xyl	Rib				
Filled Diamond	Deoxynonulosonate		Kdn				Neu5Ac	Neu5Gc	Neu	Sia
Flat Diamond	Di-deoxynonulosonate		Pse	Leg		Aci		4eLeg		
Flat Hexagon	Unknown	Bac	LDmanHep	Kdo	Dha	DDmanHep	MurNAc	MurNGc	Mur	
Pentagon	Assigned	Api	Fru	Tag	Sor	Psi				